ORKUSTOFNUN
NATIONAL ENERGY AUTHORITY

THE UNITED NATIONS UNIVERSITY

GEOTHERMAL RESERVOIR ENGINEERING LECTURE NOTES

Snorri Páll Kjaran
and
Jónas Elíasson

UNU Geothermal Training Programme, Iceland.
Report 1983-2

GEOTHERMAL RESERVOIR ENGINEERING

Lecture notes

Snorri Páll Kjaran *
Jónas Elíasson **

* Present address: Vatnaskil h/f Consulting Engineers
** Present address: University of Iceland

ACKNOWLEDGEMENTS

The authors wish to express their special thanks to Dr. Ingvar Birgir Friðleifsson, resident coordinator at the United Nations University in Reykjavík, for his support and personal interest throughout the writing of this report.

Special thanks are due to Dr. Valgarður Stefánsson at the National Energy Authority, for reading the whole manuscripts and for his valuable comments.

Thanks are also expressed to Professor Sveinbjörn Björnsson for reading the final manuscript.

We would also like to thank Gísli Karel Halldórsson, reservoir engineer at Verkfræðistofan Vatnaskil for his advise and suggestions. Thanks are expressed to our colleagues at Verkfræðistofan Vatnaskil for encouragement and support.

For the preparation of the text we are indebted to Mr. Páll Ingólfsson at the National Energy Authority for his co-ordinating work.

Finally special thanks are expressed to Mrs. Kristín M. Westlund for typing the manuscript and Mrs. Edda Magnúsdóttir for the drafting.

Reykjavík, November 1982
Snorri Páll Kjaran
Jónas Elíasson

ACKNOWLEDGEMENTS

The authors wish to express their special thanks to Dr. [illegible], [illegible] Coordinator at the United Nations University in [illegible], for his support and personal interest throughout the writing of this report.

Special thanks are due to Dr. [illegible] of the National [illegible], for reading the whole manuscript and for his valuable comments.

Thanks are also extended to Professor [illegible] for reading the final manuscript.

We would also like to thank [illegible] for his advice and cooperation. Thanks are expressed to our colleagues at [illegible] for encouragement and support.

For the preparation of the text we are indebted to Mrs. [illegible] of the National [illegible] for the coordination work.

[illegible] thanks are extended to Mrs. [illegible] for typing the manuscript and Mrs. [illegible] for the graphics.

[illegible], [illegible]

[illegible]

[illegible]

L I S T   O F   C O N T E N T S

LIST OF FIGURES

Page

Page

LIST OF TABLES

LIST OF SYMBOLS

A : area $[m^2]$

A $= N^W/H_{20}{}^W/N^S/H_{20}{}^S$

a : heat transfer coefficient $[W/m\,^\circ K]$

B^2 : leakage coefficient $= \frac{Tb}{K}\ [m^2 s^2]$

B : coefficient for laminar pressure drop $[m/l/s]$

b : thickness of semipervious layer $[m]$

b : the ratio of total interval open to flow to the total thickness of the producing zone

BE : barometric efficiency

C : speed of sound $[m/sec]$

C : tidal efficiency

C : coefficient for turbulent pressure drop $[m/(l/s)^2]$

C : wellbore storage coefficient $[m^3/Pa]$

C_D : dimensionless wellbore storage coefficient

$C_{D_{x_f}}$: dimensionless wellbore storage coefficient for a fractured well

C_A : Dietz shape factor

c : specific heat $[J/kg\,^\circ C]$

c : total compressibility $[Pa^{-1}]$

D : well diameter $[m]$

D : thickness of rock matrix per fracture $[m]$

d_{10} : 10% sieve diameter in mm

$(\frac{dp}{dz})_{f_o}$: single phase pressure drop $[Pa/m]$

$(\frac{dp}{dz})_F$: two phase pressure drop $[Pa/m]$

Ei : exponential integral

erf : error function

F(t) : unit response function

F'_{c_D} : dimensionless fracture capacity

f : dimensionless friction factor

$f(t)$: instantaneous unit response function

G : mass flux [$kg/s\ m^2$]

g : acceleration of gravity [m/s^2]

H : piezometric head [m]

h : enthalpy [kJ/kg]

h : water level [m]

h : thickness [m]

h_o : tidal fluctuation [m]

h_p : piezometric head [m]

$h_{D_{r_f}}$: dimensionless thickness for a horizontally fractured well

h_t : flowing enthalpy [kJ/kg]

i : hydraulic gradient

J : Bessel function

K : coefficient of permeability [m/s]

K_o : Bessel function

K : bulk modulus [m/s]

k : ratio between the specific heat at constant pressure and the specific heat at constant volume

k : intrinsic permeability [m^2]

k_f : fracture permeability [m^2]

k_s : relative permeability for steam

k_w : relative permeability for water

k_{xx} : element of permeability tensor

k_{xy} : element of permeability tensor

k_{yy} : element of permeability tensor

k_z : vertical permeability [m^2]

L : latent heat of vaporization [kJ/kg]

M : molecular weight [g/mole]

M : Mach number [m/s^2]

m : slope of semilogarithmic straight line

Nu : Nusselt's number

N_w : number of moles of noncondensable gas in water

N_s : number of moles of noncondensable gas in steam

$N^w_{H_2O}$: number of moles of water in waterphase

$N^s_{H_2O}$: number of moles of water in steamphase

n_w : mass fraction of gas in water

n_s : mass fraction of gas in steam

Pc : partial pressure of carbon dioxide [Pa]

p_D : dimensionless pressure

p : pressure [Pa]

p_a : barometric pressure [Pa]

pe : pressure at the external boundary [Pa]

p_i : initial pressure [Pa]

PI : productivity index of a well [kg/s/Pa]

p_o : well head pressure [Pa]

p_s : saturation pressure [Pa]

Pw_D : dimensionless pressure for a vertically fractured well

p_{wf} : bottom hole flowing pressure [Pa]

p_{ws} : shut-in pressure [Pa]

Q : flow rate [l/s]

Q_H : recoverable heat energy [W s/m^2]

q : flow rate [l/s]

q_h : heat energy [W s/m^2]

q : heat flow [w]

R : gas constant [J/kg °K]

R_a : Rayleigh number

R' : universal gas constant = 8314 J/mole °K

r : radial distance [m]

r : recovery factor

r_B : dimensionless radius = $\frac{r}{B} = \frac{r}{\sqrt{Tb/K}}$

r_f : fracture radius [m]

r_D : dimensionless radius = r/r_w

r_d : diffusion radius [m]

r_{eD} : dimensionless radius = r_e/r_w

r_e : effective radius [m]

r_s : radius of skin zone [m]

r_w : wellbore radius [m]

S : storage coefficient

S : skin factor

S : slip factor = V_s/V_w

S' : specific storage coefficient [1/m]

S_l : volume fraction of liquid in pores

S_p : pseudoskin factor resulting from partial penetration

S_{swp} : pseudoskin factor resulting from a slanted well

S_{tr} : true skin factor caused by damage to the completed portion of the well

S_w : volume fraction of water in pores

s : drawdown [m]

s_w : drawdown in the flowing well [m]

T : temperature [°K]

T : transmissivity [m^2/s]

T_o : reference temperature [°K]

T_s : saturation temperature [°K]

t : time [s]

t_D : dimensionless time based on wellbore radius

t_{DA} : dimensionless time based on total drainage area

$t_{D_{x_f}}$: dimensionless time for a vertiacally fractured well

$t_{D_{r_f}}$: dimensionless time for a horizontally fractured well

t_o : tidal period [s]

Δt : time step [s]

t_L : time lag [s]

TE : tidal efficiency

U : mass flux [kg/s m^2]

U : reservoir capacity [kg]

U : internal energy [kJ/kg]

V : velocity [m/s]

V : volume [m^3]

V_o : actual seepage velocity [m/s]

V_T : speed of temperature front [m/s]

v : specific volume [m^3/kg]

W : mass flow rate [kg/s]

W_D : dimensionless mass flow rate

W_{sf} : sandface flow rate [kg/s]

W(x) : well function

w : fracture width [m]

x : mass fraction of steam

x : horizontal coordinate [m]

x_D : dimensionless distance

x_f : vertical fracture half length [m]

Y : Bessel function

y : horizontal coordinate [m]

Z : gas deviation factor

z : vertical coordinate [m]

z^* : location of flash level in the well [m]

α : volume fraction of steam

α $= \alpha(T)$ solubility of gas [Pa^{-1}]

α : chloride content

α : rock compressibility [Pa^{-1}]

α $= \dfrac{\rho_w C_w}{(1-\phi)\rho_r C_r + \phi\rho_w C_w}$

β : volume coefficient of thermal expansion

β : fluid compressibility [Pa^{-1}]

β : chloride content

β_c : compressibility resulting from dissolved carbon dioxide [Pa^{-1}]

β_s : two phase compressibility [Pa^{-1}]

γ : specific weight = ρg [kg/m^2s]

γ : Eulers constant

γ : chloride content

γ $= (1-S_w)\rho_s + \dfrac{n_w}{n_s} S_w\rho_w$

ϕ : porosity

ϕ_e : effective porosity

ϕ_{fo} : two phase flow multiplier

κ : exponent of Euler's constant

κ : thermal diffusivity [m^2/s]

λ : thermal conductivity [Watt/m°C]

λ_e : effective heat conduction coefficient

λ_d : dispersion heat conduction coefficient

η : horizontal coordinate [m]

ξ : horizontal coordinate [m]

ξ : similarity variable $= \dfrac{r^2}{4\kappa t}$

μ : dynamic viscosity [Pa s]

μ_t : flowing dynamic viscosity [Pa s]

ν : kinematic viscosity [m^2/s]

ν_t : flowing kinematic viscosity [m^2/s]

ω : angular velocity [s^{-1}]

ρ : density [kg/m^3]

ρ_o : reference density [kg/m^3]

ρ_t : flowing density [kg/m^3]

σ : total vertical stress [Pa]

σ_x : horizontal stress [Pa]

σ_y : horizontal stress [Pa]

σ_z : vertical stress, effective stress [Pa]

Subscripts

c : carbon dioxide

f : fracture

l : liquid

m : mixture

r : rock

s : steam

v : vapour

w : water

1 INTRODUCTION

All of us have many times heard about technological disciplines that are "more an art than a science". Most reservoir engineers working in geothermal sciences would surely agree that their field is more an art than a science. But what kind of art is reservoir engineering? Basically it is the art of striking water from rock, and coming to think of it we must admit that this is an art that nobody has been really good at since Moses. So the reservoir engineer is really an artist, that is trying to behave like a scientist in a job where you really need a prophet.

Some people prefer to think that reservoir engineering is a new field that is still in the maturing process. This is not the case. The physical process of fluid seepage through porous media is adequately described by partial differential equations of the parabolic type, the equation of heat conduction to be more precise, and the methods of analytical treatment have been known since Fourier. The theory was adapted to cold water reservoirs by Theis (1935) and Jacob (1946), later to oil reservoirs, and now to geothermal fluid reservoirs. Tens and hundreds of fine engineers and scientists have devoted themselves to reservoir engineering. If this field was to be judged by the amount of skilled efforts that has been put into it, the science should by now be so advanced, that predicting the yield from a geothermal well should be no more trouble than predicting the bending strength of a steel rod. But alas, there is more to it than that. There is the element of good luck. We never know for sure if the well we are drilling will turn out to be a good or a bad well. We can at the most predict the odds, for and against.

The first papers and articles written on geothermal reservoir engineering were concerned with predicting the energy content of the reservoir. This is natural, the first objective is to know the size of the resource. Lately people have turned more towards the capacity of the wells. How great is it now, how will it dwindle? Will our wells have sufficient capacity in the next year? In two years? In five years? In ten years?

So, instead of making the great prophecies of the resource energy that would come flowing up, by just drilling a few wells, the reservoir engineer must take on the role of the watchman. He must be on the constant lookout for everything that can indicate a change in the state of the reservoir, constantly observing and comparing the results with his previous knowledge. In this way he will steadily improve his capability of extrapolating his results into the future, until nothing in the behavior of the reservoir is of any surprise to him, and he can make fairly accurate predictions of the reservoir yield into the future.

The heart of this process is a carefully planned and skilfully executed observation program that starts as a geophysical exploration and continues as a reservoir research program and ends as a production supervision. Along the way the reservoir engineer must manage a steadily growing data file, and implement new methods to extract all relevant information from it.

This report is devoted to the latter part. It adapts the line of approach, that if you are able to calculate the decline of the reservoir pressure then you are able to predict the rundown of the wells. This is of course just one corner of the science, but in this one corner there are many things.

This report was written to meet the need for a textbook and a reference manual for the Geothermal Training Programme of the United Nations University (UNU) in Reykjavík, as well as a handbook for those working in the field of reservoir engineering. UNU Fellows who only attend the introductory tectures in reservoir engineering should get themselves acquainted with the material in sections 2, 3.5, 4.3 and 4.4. Those of the UNU Fellows specializing in reservoir engineering should cover sections 1, 2, 3.1, 3.2, 3.3, 3.4, 3.5 and 3.16 as well as sections 4 and 5. The rest of the report serves the purpose of a handbook.

The report contains fully worked exercises taken from actual reservoir engineering experience to illustrate the theory. The SI (Systѐme Internationale) unit system is used with a few exceptions, where the English technical system is used. This is done to make the reader familiar with this set of units, which is still used in the English reservoir engineering literature.

2 RESERVOIR PROPERTIES

In this section we discuss and define the rock and fluid properties which are of most interest to the reservoir engineer. The main topics discussed are, rock properties, fluid properties and state, aquifer properties, and reservoir characteristics.

2.1 Rock properties

Rock properties of interest to the reservoir engineer are general properties defining the flow resistance and fluid storage capacity of the rock mass. To obtain this information one has mainly to rely on geological and geophysical evidence brought about by field investigations. These properties are mainly function of the distribution of fractures and pores within the rock mass, which is very inhomogeneous in this respect, there are usually great variations from point to point (microscale variation) so information obtained by testing of small samples in the laboratory is usually of limited value.

The rock properties of greatest interest are the following: Coefficient of permeability, K, intrinsic permeability, k, porosity, ϕ, and compressibility, α.

Coefficient of permeability, K, is defined according to Darcy's law:

$$V = Ki = K\frac{h_L}{L} \tag{2.1}$$

where the symbols are defined in Fig. 2.1, and V is the mean velocity with respect to the total flow area, that is:

$$V = \frac{Q}{A}$$

where Q is the flow rate, and A the total flow area.

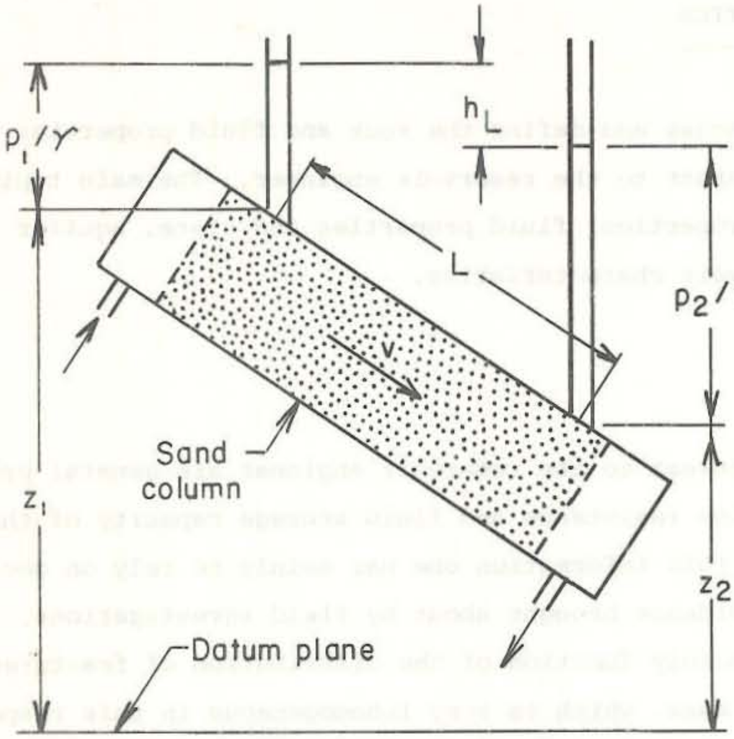

Fig. 2.1 Explanation of terms in eq. 2.1

K has the dimension of velocity. It depends on the viscosity and density of the fluid and geometrical properties of the rock. As we see in the following the viscosity is very temperature dependent, the coefficient of permeability is therefore also very temperature dependent. Another definition of permeability which is independent of fluid properties is the intrinsic permeability, k.

$$k = \frac{\mu}{\rho g} K \tag{2.2}$$

μ: dynamic viscosity of the fluid

ρ: density of the fluid

g: acceleration of gravity

k has the dimension of area, frequently expressed in DARCY

$$1 \text{ DARCY} = 0.987 \cdot 10^{-12} m^2 = 1.062 \cdot 10^{-11} ft^2$$

k varies within wide limits. Engelund (1953) gives for homogeneous sand:

$$k = cd_{10}^{2} \frac{\phi^2}{(1-\phi)^3} \tag{2.3}$$

d_{10}: 10% sieve diameter in mm, that is the diameter of sieve net through which goes 10% of the material in sieve analysis

ϕ : porosity

c is a constant for individual formations, but varies by a factor of up to 5 between different formations.

In rock formations the permeability is more or less due to cracks and fissures. Local k values show great variation. The reservoir as a whole has a gross average permeability which is more than all other factors responsible for the thermodynamical characteristics of the reservoir and its production capacity.

Field	Permeability in millidarcy		Reference
	Horizontal	Vertical	
Broadlands, N.Z. average		1	Donaldsson (1970)
Broadlands, central 1 km^2		100	Donaldsson (1970)
Lardarello, Italy	10	10	Donaldsson (1970)
Olkaria, Kenya	19	13	Sveco and Virkir (1976)
Wairakei, N.Z.	100	10	Wooding (1963)
Svartsengi, Iceland	200	100	Kjaran et al. (1980)

Table 2.1 Permeability of various reservoirs

The figures in Table 2.1 are estimates of overall values by various researchers. Overall permeability coefficients may be estimated by natural heat output studies, see section 4, and pumping test analysis, see section 3. There are two different well testing methods. Interference tests, which give the permeability between an observation well and a flowing well and are thus good estimates of overall permeability values. The other method is local well testing, which includes injection tests, step drawdown tests (well completion tests) and pressure build-up tests. Permeability values determined with such tests may be affected by skin effects, which are local alterations in the flow field in the immediate vicinity of the well. These alterations may be due to natural fractures or to disturbances of the rock during drilling, or concentrated inflow into the well where turbulence is developed and Darcy's law is no longer valid. These tests are also complicated by wellbore storage effects as will be discussed in detail in section 3.

Porosity, ϕ, is actually the void fraction of the rock mass, i.e.:

$$\phi = \frac{\text{total pore volume}}{\text{total volume}}$$

All the pores are filled with fluid (liquid or gas), but some of the pores are closed, and some fluid is bounded to the rock minerals, so when water is flowing within the reservoir, only a part of the water in storage is actually in motion. If we define:

$$\phi_e = \phi \cdot \frac{\text{fluid free to move (volume)}}{\text{fluid in storage (volume)}}$$

then ϕ_e may be referred to as the effective porosity. This is usually much smaller than the real porosity, especially when all the reservoir is liquid saturated.

Porosity can be estimated from various logging methods like resistivity, neutron-neutron, gamma-gamma, and sonic, and on core samples.

Estimations of effective porosity are more difficult. It is obvious that it is the effective porosity rather than the total porosity that defines the volume of fluid available for harnessing.

Compressibility, α. The coefficient of bulk compressibility is defined as fractional changes in bulk volume per unit change in effective stress. The stress tensor in a porous medium is three dimensional given by σ_x, σ_y, σ_z. Because only the vertical deformations are of interest we restrict ourselves to the vertical stress in the following:

$$\alpha = -\left(\frac{1}{V}\frac{dV}{d\sigma_z}\right) \tag{2.4}$$

The total vertical stress, σ, at any point in a confined reservoir may as a rule be treated as a constant equal to total weight of overburden.

Total vertical stress is composed of effective stress (grid stress in the rock mass) and fluid pressure.

$$\sigma = \sigma_z + p \tag{2.5}$$

which defines σ_z, as p is usually equal to the hydrostatic fluid pressure.

The compressibility, α, is constant as long as the rock responds to changes in stresses as an elastic medium, and in that stage the compression and stress changes are reversible. For larger changes in stress the compression becomes plastic and irreversible. Plastic deformations are much larger than elastic deformations and can reduce the effective porosity irreversibly so the permeability may be permanently decreased.

2.2 Fluid properties and state

The fluid properties which will be discussed in the following are, density, ρ, viscosity, μ, ν, and enthalpy, h.

Fluid density, ρ, defined as the mass of unit volume of the fluid, generally depends on pressure and temperature:

$$\rho = \rho\ (p,T) \tag{2.6}$$

In reservoir engineering the fluid we are in general dealing with is compressed water, saturated steam and superheated steam, also of great interest due to the change in behaviour of the reservoir fluid is the case of reservoir fluid with dissolved gases and free gases. For compressed water the density can be taken as independent of pressure, except when calculating fluid storage, so we have $\rho = \rho\ (T)$. Expanding, we get:

$$\rho = \rho_{T=T_o} + (T-T_o)\left.\frac{d\rho}{dT}\right|_{T=T_o} + \frac{1}{2}\,(T-T_o)^2\left.\frac{d^2\rho}{dT^2}\right|_{T=T_o} + \ldots.. \tag{2.7}$$

Retaining the two first terms we get the equation of state:

$$\rho = \rho_o \ (1 - \beta(T-T_o)) \tag{2.8}$$

where $\rho_o = \rho(T_o)$, $\beta = - \left.\frac{d\rho}{dT}\right|_{T=T_o} / \rho_o$ is the volume coefficient of thermal expansion.

For saturated steam, pressure and temperature are dependent variables and the density can then be taken as a function of either of the two. The equation of state is given in steam tables.

For superheated steam the density is both a function of pressure and temperature. The equation of state is given in steam tables and can be written as:

$$\rho = \frac{p}{ZRT} \tag{2.9}$$

where Z is the gas deviation factor and R is the gas constant.

Fluid viscosity, μ, ν: Distinction must be made between dynamic viscosity, μ, and kinematic viscosity, ν. We have:

$$\nu = \frac{\mu}{\rho} \tag{2.10}$$

The dynamic viscosity is given in Fig. 2.2.

$$1 \text{ centipoise (cp)} = 10^{-3} \frac{Ns}{m^2}$$

The figure shows that the viscosity depends heavily on the temperature, but variation with fluid pressure is less important. From eq. 2.10 we see that the kinematic viscosity is dependent on the density which is a function of both temperature and pressure.

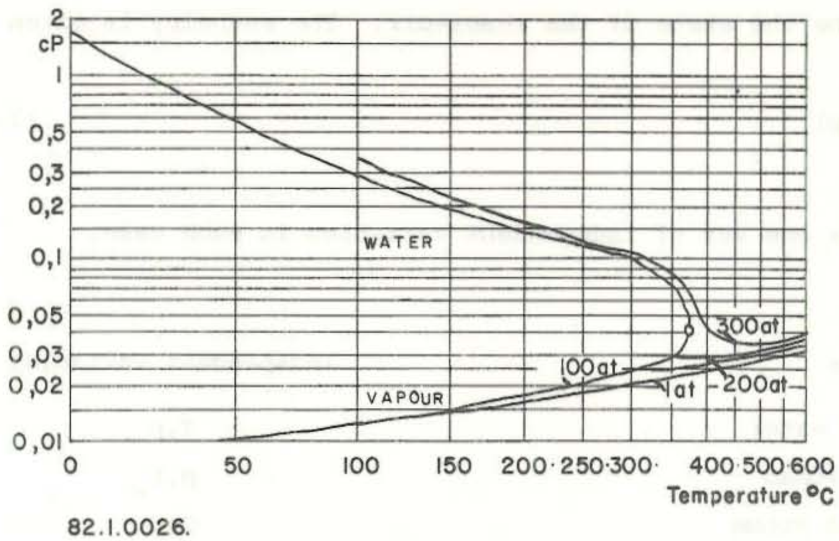

Fig. 2.2 Dynamic viscosity for water, and steam in centipoise (cp)

Fluid enthalpy, h, is a thermodynamical property of great interest to the reservoir engineer. In a compressed water reservoir the total fluid enthalpy is given by the water enthalpy, which is a function of temperature and pressure given by:

$$h = h_w \ (T,p) \qquad (2.11)$$

where h_w is the water enthalpy.

In the case of saturated steam reservoir temperature and pressure are no longer independent variables and we have:

$$p = p_s \ (T) \qquad (2.12)$$

In that case the pressure and temperature cannot be used as two independent variables to describe the state of the reservoir. Instead we could choose e.g. pressure and water saturation, S_w, which is defined as the volume fraction of water in pores. At a point in the reservoir where x is the mass fraction of steam in pores we can calculate the total enthalpy:

$$h = xh_s + (1 - x) \ h_w \qquad (2.13)$$

In a superheated steam reservoir, temperature and pressure can again be used to describe the state of the reservoir. The enthalpy is given by:

$$h = h_s\ (T,p) \tag{2.14}$$

Table 2.2 gives one set of independent variables in each case.

Fluid state	Independent variables
Compressed water	T,p
Saturated steam	p,S_w
Superheated steam	T,p

Table 2.2 Independent variables to calculate reservoir state

From the reservoir engineering point of view the fluid chemistry is a fluid property. Of main interest are the dissolved solids and noncondensable (dissolved and free) gases. The dissolved solids and gases interact with the rock. These reactions are functions of pressure, temperature, and time. The silica thermometer and other chemical thermometers are examples of the practical use of the water-rock interaction.

When all fluid properties are known within a reservoir the complete state of the reservoir is defined. Above we said that knowledge of two parameters can define the state. To understand this, and the meaning of it for reservoir engineering we take two idealized (unrealistic) examples. Visualize two reservoirs filled with ideal fluid, composed partly of ideal frictionless liquid, and ideal frictionless vapour. The two reservoirs are two extremes, one is static (no fluid flow) the other dynamic (fluid constantly flowing). Both are isolated.

In the static reservoir the temperature distribution will be uniform, the temperature is the same everywhere, say equal to T. The pressure will be hydrostatic. The vapour phase will be separated from the liquid phase and we get a picture of the state of the reservoir as shown in Fig. 2.3.

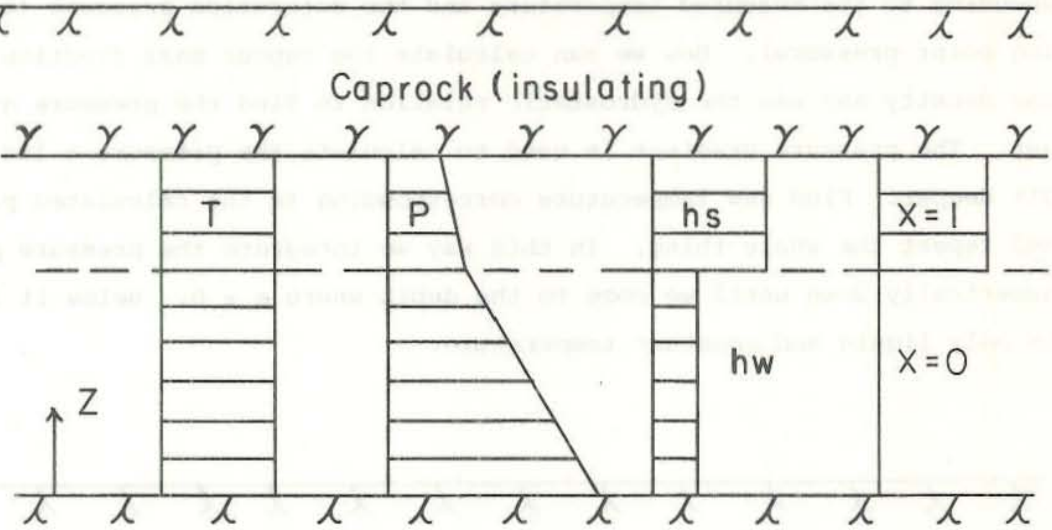

82.1.0027.

Fig. 2.3 State of an ideal static reservoir

We measure the temperature and pressure at the top of the reservoir just beneath the caprock. We find that $T > T_s(p)$ (boiling point at the measured pressure). From thermodynamical tables we find the density of steam, calculate the pressure downwards by the hydrostatic pressure relation.

$$\frac{dp}{dz} = - \rho g \tag{2.15}$$

At a certain depth we find:

$$T = T_s(p) \tag{2.16}$$

from there and down we have liquid and steeper rise in pressure. The enthalpy is easily calculated. For ideal fluids it is a function of temperature alone.

In the dynamic reservoir the fluid is flowing. Ideal fluids flow with constant enthalpy so the enthalpy is constant everywhere. The flow is frictionless, so the pressure distribution is still hydrostatic. Let us assume that the temperature and enthalpy is known just beneath the caprock. From thermodynamical tables we get the specific enthalpies corresponding to the measured temperature and the saturation pressure (boiling point pressure). Now we can calculate the vapour mass fraction x and the density and use the hydrostatic relation to find the pressure gradient. The pressure gradient is used to calculate the pressure a little bit deeper. Find new temperature corresponding to the calculated pressure and repeat the whole thing. In this way we integrate the pressure profile numerically down until we come to the depth where $x = 0$. Below it there is only liquid and constant temperature.

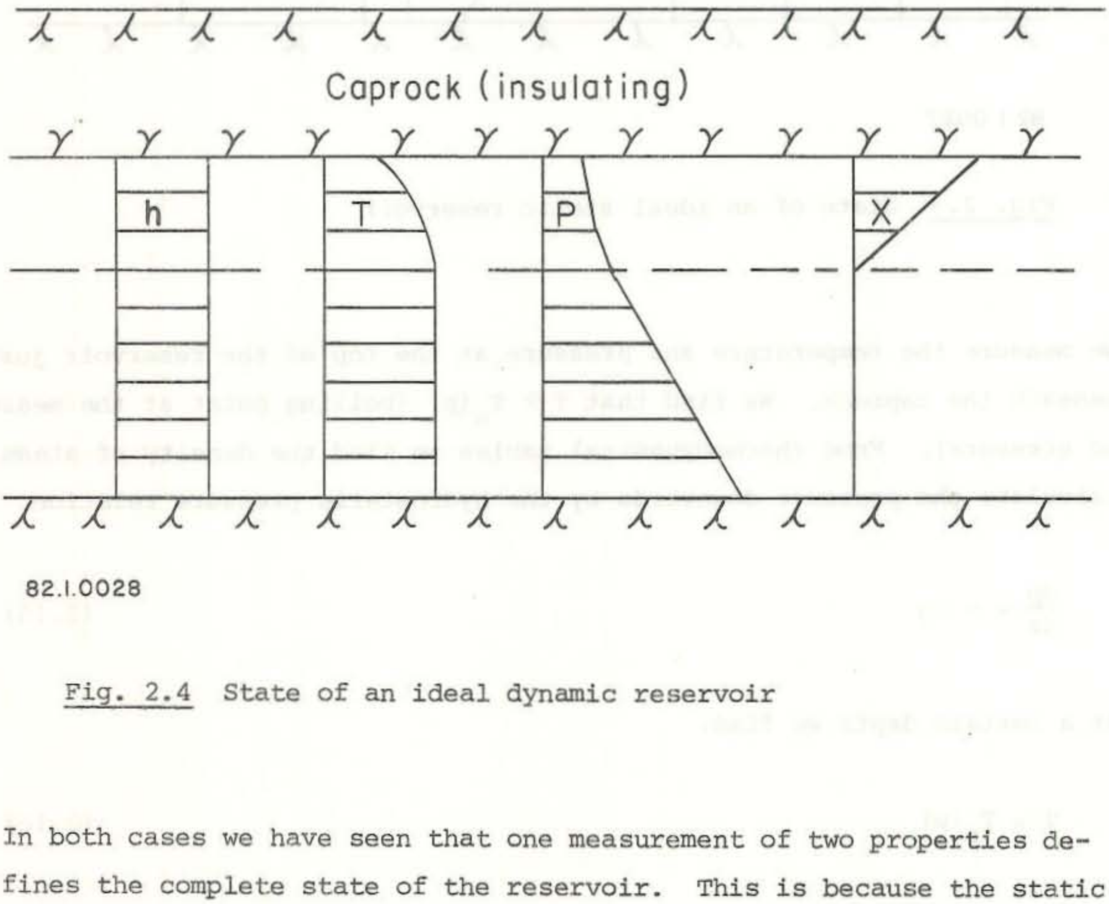

Fig. 2.4 State of an ideal dynamic reservoir

In both cases we have seen that one measurement of two properties defines the complete state of the reservoir. This is because the static reservoir is isothermal and the dynamic reservoir is isenthalpic in the thermodynamical sense of definition. Real reservoirs are neither isothermal nor isenthalpic, but the isothermal and isenthalpic approximations may be used to calculate the state of certain regions within them. These small examples also demonstrate the main purpose of reservoir engineering: To calculate the state of the reservoir from minimum of information, in order to find the most feasible method to exploit the energy.

Fluid compressibility, β, is defined as changes in fluid volume per unit change in fluid pressure, and can be written as:

$$\beta = -\frac{1}{V}\left(\frac{dV}{dp}\right)_{h\,=\,\text{constant}} \tag{2.17}$$

taking $v = \frac{1}{\rho}$ we get:

$$\beta = \frac{1}{\rho}\left(\frac{d\rho}{dp}\right)_{h\,=\,\text{constant}} \tag{2.18}$$

2.3 Aquifer properties

Aquifer properties are of course defined when rock and fluid properties are separately defined. But in the literature several parameters are defined which are combined quantities. Those of them discussed in the following are the storage coefficient, S, transmissivity, T, barometric efficiency, BE, tidal efficiency, TE, relative steam and water permeabilities, k_s, k_w, thermal conductivity, λ, specific heat, c, diffusivity, κ, and dispersions coefficient, λ_d.

Storage coefficient, S, is defined as the volume of water released by unit volume of reservoir for unit drop in pressure head. The storage coefficient is very different for single phase and two phase reservoirs. The storage coefficient for single phase fluids is defined in section 3.2 and for two phase fluids in section 3.16. In order to give an example the single phase storage coefficient of an elastic aquifer is defined as:

$$S' = \rho g\,(\alpha + \phi\beta) \tag{2.19}$$

where ρ is the density of the single phase fluid.

In horizontal flow studies, a storage coefficient that depends on the aquifer thickness is used for aquifers with hydrostatic pressure:

$$S = S' \cdot h \tag{2.20}$$

where h is the aquifer thickness. It represents the volume of water released from storage per unit area. It is therefore a dimensionless quantity per m drop in pressure head.

Transmissivity, T, is usually denoted by T and is defined as:

$$T = K \cdot h \tag{2.21}$$

Barometric efficiency, BE. Changes in reservoir storage due to pumping and recharge are reflected by corresponding changes in the water table. Factors other than pumping, such as barometric pressure changes, and ocean tides also influence water levels. An appreciation for the water level fluctuations induced by these factors is required, otherwise observed changes in water level may be erroneously interpreted.

The elevation of the piezometric surface in confined aquifers is indicated by the water level in piezometers. Let us study the change in the piezometric level associated with a change in barometric pressure. Consider the situation in Fig. 2.5 and suppose that the barometric pressure p_a increases by dp_a. The increase of atmospheric pressure is transmitted directly to the water surface in the piezometer, tending to displace water from the piezometer into the aquifer. On the other hand, the increased atmospheric pressure also increases the load on the confined aquifer which tends to displace water from the aquifer into the piezometer. Part of the increased load is born by the aquifer skeleton, however, and the net result of the increase in barometric pressure is to decrease h_p. The absolute value of the ratio of dh_p to $dp_a/\rho g$ is the barometric efficiency, BE, given by:

$$BE = \left| \frac{dh_p}{dp_a/\rho g} \right| \tag{2.22}$$

The barometric efficiency of a confined aquifer depends upon the compressibility of the aquifer and its contained water.

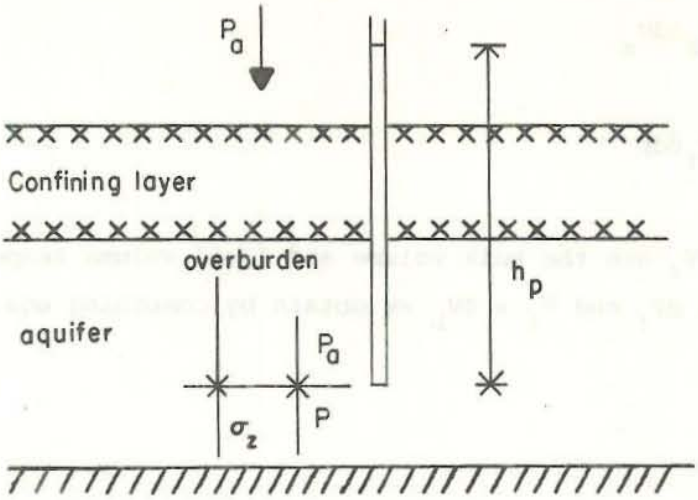

82.01.0029.

Fig. 2.5 Stress balance in the aquifer

Taking stress balance we get:

$$\sigma_z + p = \text{overburden pressure} + p_a \qquad (2.23)$$

and

$$p = \rho g h_p + p_a \qquad (2.24)$$

The total derivatives of eqs. 2.23 and 2.24 are:

$$dp = dp_a - d\sigma_z \qquad (2.25)$$

$$dp = \rho g dh_p + dp_a \qquad (2.26)$$

Equations 2.25 and 2.26 are combined to yield:

$$\frac{dh_p}{\frac{1}{\rho g}\, dp_a} = - \frac{d\sigma_z/dp}{1 + d\sigma_z/dp} \qquad (2.27)$$

Eqs. 2.4 and 2.17 give respectively:

$$dV_b = - V_b \alpha d\sigma_z \tag{2.28}$$

$$dV_f = - V_f \beta dp \tag{2.29}$$

where V_b and V_f are the bulk volume and fluid volume respectively. As we have $dV_b = dV_f$ and $V_f = \phi V_b$ we obtain by combining eqs. 2.28 and 2.29:

$$\frac{d\sigma_z}{dp} = \frac{\beta\phi}{\alpha} \tag{2.30}$$

and by inserting into eq. 2.27 we obtain:

$$\frac{dh_p}{dp_a/\rho g} = - \frac{1}{1 + \frac{\alpha}{\beta\phi}} \tag{2.31}$$

and from the definition of barometric efficiency we have:

$$BE = \left| \frac{dh_p}{dp_a/\rho g} \right| = \frac{1}{1 + \frac{\alpha}{\beta\phi}} \tag{2.32}$$

By using the definition of the storage coefficient, eq. 2.19, the barometric efficiency can be written as:

$$BE = \frac{\rho\phi g\beta}{S'} \tag{2.33}$$

If the barometric efficiency of an aquifer is known, eq. 2.33 can be used to estimate the storage coefficient.

$$S' = \frac{\rho g \phi \beta}{BE} \tag{2.34}$$

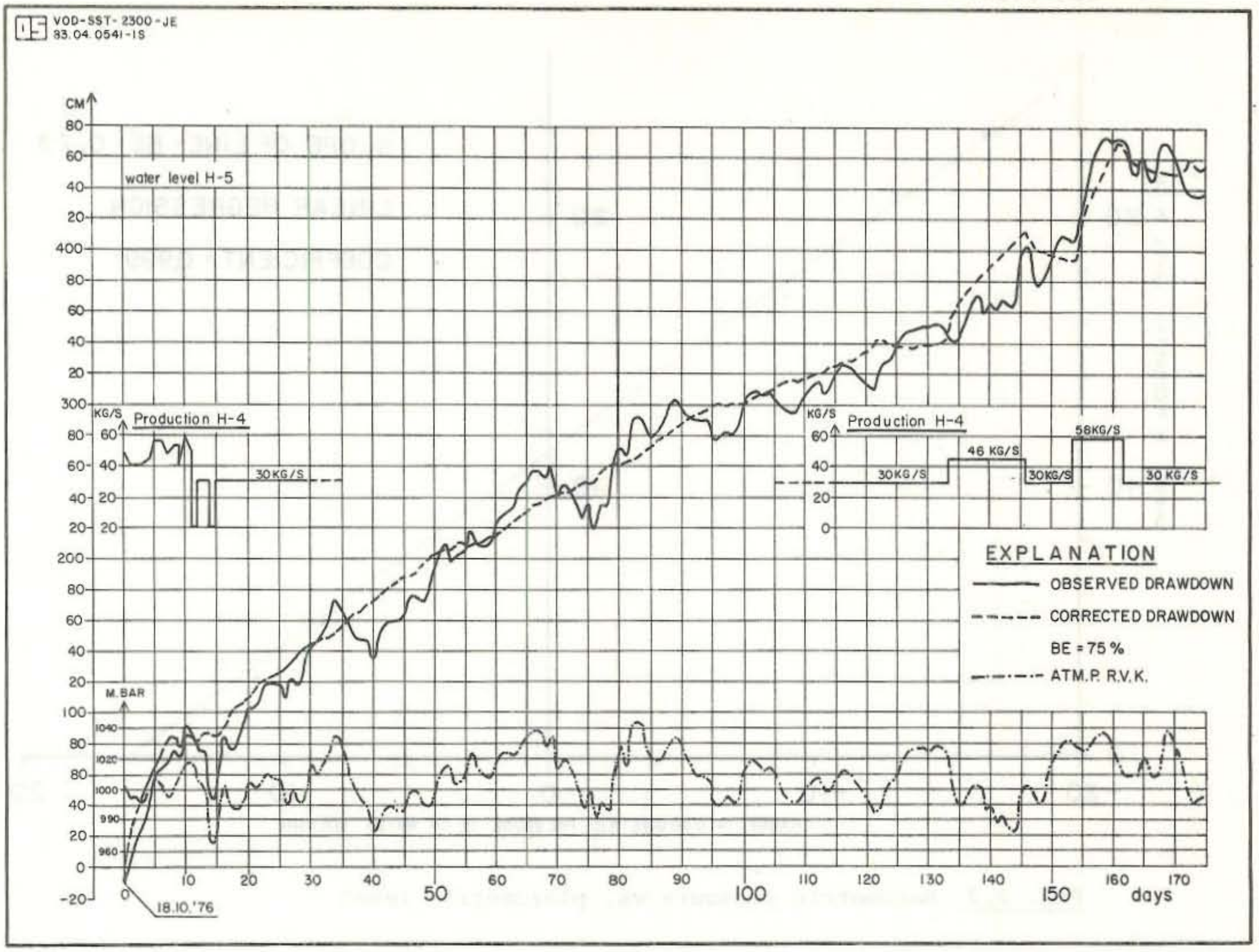

Fig. 2.6 Water level changes, well H-5, Svartsengi (Elíasson et al. 1977)

Fig. 2.6 shows observed water level fluctuations in a 1500 m deep well, 240°C hot in the Svartsengi geothermal field in Iceland. When water level fluctuations due to barometric pressure changes are subtracted from the observed drawdown values, the true drawdown due to production is obtained. To do this, the BE value has to be used. Fig. 2.7 shows how it is found by analysing a short period where drawdown due to production is small compared to barometric water level changes.

Finally it should be noted from equation 2.31 that water levels h_p decrease when the barometric pressure increases and the water levels increase when the barometric pressure decreases.

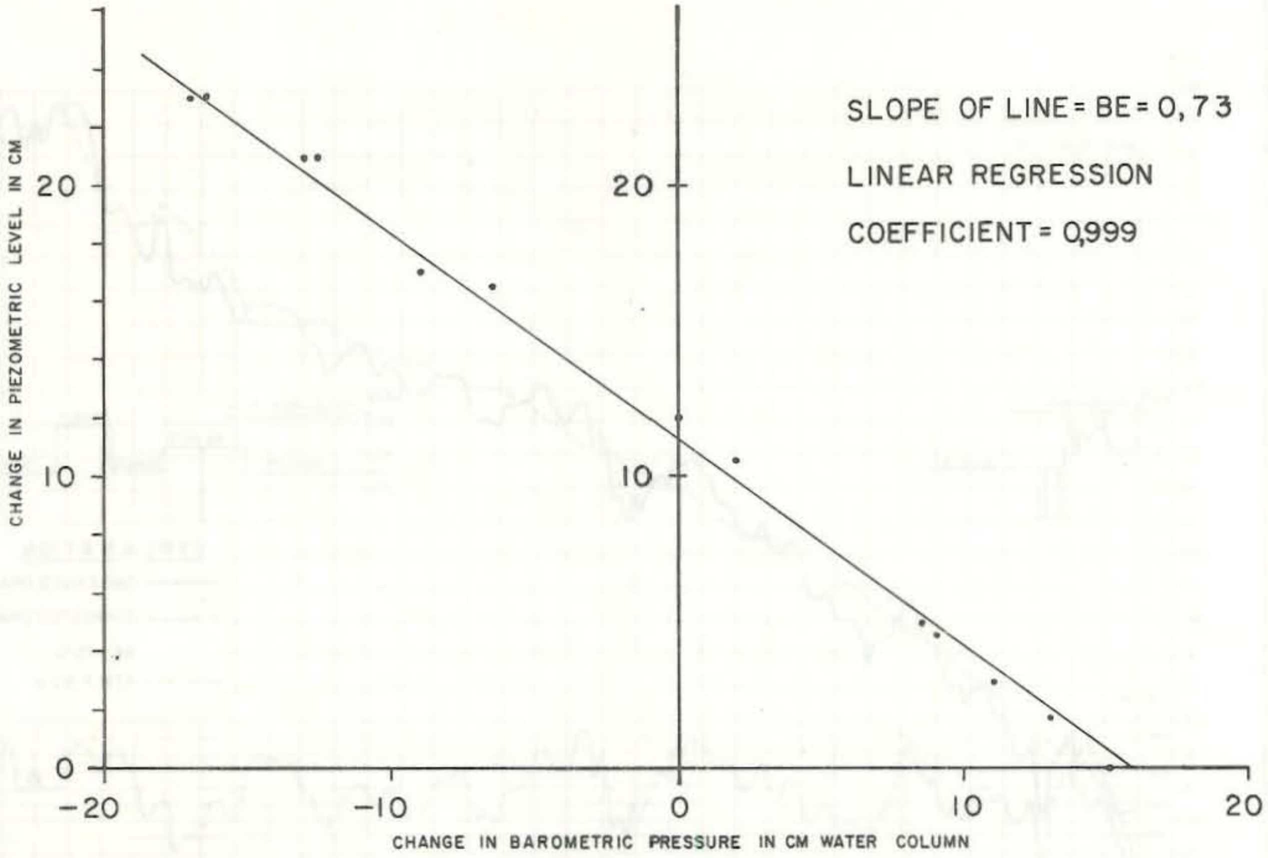

Fig. 2.7 Barometric pressure vs. piezometric level

Tidal efficiency, C: The water level in wells and piezometers responds to external loads other than atmospheric pressure. Because the change in load due to fluctuating tides are applied only to the aquifer and not to the water surface in the piezometer, the water level response is opposite that observed for changes in barometric pressure. In other words, the increased load produces a rise in water levels. The response of water levels to slowly changing external loads can be analysed in a manner similar to that for barometric loading. For example, consider a confined aquifer extending beneath the ocean floor or beneath a river or estuary in which the water stage, H, changes with the tide. Provided that the entire change in pressure ρgdH is transmitted to the confined aquifer.

$$\frac{dh_p}{dH} = \frac{1}{1 + \frac{d\sigma_z}{dp}} \qquad (2.35)$$

From eq. 2.30 the tidal efficiency, C, is:

$$C = \frac{dh_p}{dH} = \frac{\alpha}{\alpha + \phi\beta} \tag{2.36}$$

From eqs. 2.32 and 2.36 we see that:

$$BE + C = 1 \tag{2.37}$$

Relative permeabilities of steam and water, k_s, k_w: When steam and water are flowing in mixture through rock, studies of wellfluid enthalpy have indicated different permeabilities for the steam and the water flow from those observed in a single phase flow. The ratio between these permeabilities and the intrinsic permeability values are called relative permeabilities, and are usually listed as functions of water saturation. See section 3.16 for discussion of relative permeabilities.

It is possible to find physical arguments for the relative permeabilities, but the numerical values of relative permeabilities are still uncertain. Considerable research is being done on this subject throughout the world (Kruger and Ramey, 1978).

Thermal conductivity, λ, of a medium is the proportionality factor between the heat flux and the temperature gradient. In Table 2.3 some values of the thermal conductivity are given for different materials together with other thermal properties. The thermal conductivity of an isotropic aquifer can be written as:

$$\lambda = \phi\lambda_1 + (1-\phi)\lambda_r , \tag{2.38}$$

where subscripts 1 and r denote liquid and rock respectively. Here we have assumed a parallel conduction model in which heat conduction occurs simultaneously but separately through the liquid and rock. Sometimes a series conduction model is used:

$$1/\lambda = \phi/\lambda_1 + (1-\phi)/\lambda_r . \tag{2.39}$$

In anisotropic media λ is a second rank tensor (Bear, 1972) and in isotropic media a scalar. Thermal conductivity decreases with increasing temperature, but the variation is small and without importance within our temperature range.

An average value of λ for Icelandic rocks is believed to be 1.7 watt/°C m (Pálmason and Saemundsson 1979).

Specific heat, c, for both liquid and rock in aquifers varies insignificantly with temperature. For a single phase water reservoir the heat capacity ρc is commonly written:

$$\rho c = \phi \rho_l c_l + (1-\phi)\rho_r c_r \tag{2.40}$$

Some values of the specific heat for volcanic rocks are given in Table 2.3.

Material	Density kg/m^3	Specific heat J/kg°C	Conductivity Watt/m°C	Diffusivity m^2/s
Basalt	2800	890	1.7	$6.8 \cdot 10^{-7}$
Dolerit	3800	-	1.6	-
Gabbro	2800	-	2.0	-
Granit	2600	820	3.0	$14.1 \cdot 10^{-7}$

Table 2.3 Thermal properties of some volcanic rocks (adapted from Kappelmeyer and Haenel 1974)

Thermal diffusivity, $\kappa = \lambda/\rho c$, with dimension m^2/s accounts for the transport of energy by conduction due to the exchange of kinetic energy between the molecules. Molecular diffusion is independent of fluid velocities and is usually considered constant in saturated porous media. Some values are given in Table 2.3.

Dispersion in porous media is the mechanism of spreading of a solute due to the random flow and resulting macroscopic mixing in the pores. Originally the coefficient of dispersion was considered to be a scalar, but later experiments have shown, that even in isotropic media longitudinal and transversal dispersion are different. Bear (1972) discusses the nature of the coefficient of dispersion with reference to numerous articles on the subject and shows that the coefficient of dispersion is a second order tensor, which depends on a fourth order tensor, the latter being a function of the porous medium alone (the dispersivity tensor).

The effective heat conduction coefficient can be written as the sum of the ordinary heat conduction coefficient and the dispersion coefficient:

$$\lambda_e = \lambda + \lambda_d \tag{2.41}$$

where λ_e and λ_d are the effective and dispersion heat conduction coefficient respectively. For a geothermal reservoir in its natural state, the velocities are very small and the dispersion coefficient, which is velocity dependant becomes insignificant and the heat conduction process is governed by molecular diffusion.

2.4 Reservoir characteristics

Geothermal reservoirs have been classified in many different ways. A certain terminology and certain phrases are in use in the literature and it is useful to know the definition of them. In the following we will define some of these phrases which are: Liquid and vapour-dominated reservoirs, low temperature and high temperature reservoirs and the boiling curve.

Liquid-dominated and vapour-dominated reservoirs. Geothermal reservoirs are conveniently categorized as either vapour-dominated or liquid-dominated. In each case the name refers to the phase which controls the pressure in the reservoir in its undisturbed state. The other phase may also be present and partly mobile. Thus, vapour-dominated systems contain immobile or slightly mobile liquid and liquid-dominated systems may either contain liquid water only, or a steam-water mixture.

Most reservoirs contain either liquid or a mixture of liquid and vapour. Vapour-dominated reservoirs are characterized by having a vertical pressure gradient equal to the hydrostatic pressure of vapour. Boiling water that flows through a rock mass towards a well, is cooled off due to the boiling and thereby the water can draw heat from the rock. The wells can thus discharge dry steam, (or high enthalpy fluid) although the reservoir is not vapour-dominated in the undisturbed state. Important to note is, that steam will seek upwards in the reservoir driven by a strong buoyancy force due to its large specific volume.

The same reservoir can have different characteristics at different times as the exploitation continues. Let us consider a single phase liquid reservoir in its natural undisturbed state. After production has started boiling may occur in the reservoir due to pressure drop and we now have a two phase liquid-dominated reservoir. When the boiling becomes very pronounced we might have steam as the dominant mobile phase. Finally it is possible around production wells to have superheated steam and thus a single phase fluid again.

Low temperature and high temperature reservoirs: This is a classification according to base temperature, originally proposed by Böðvarsson (1961).

Low temperature fields have base temperatures lower than 150°C, and high temperature fields have higher base temperatures. This classification has special significance in Iceland because most low temperature geothermal resources in the country yield water of good quality (low content of dissolved solids). This is not the case elsewhere. E.g. low temperature geothermal brines are exploited in France.

Boiling curve. This feature is often seen in the literature, in most cases it is a pre-calculated curve (Fig. 2.8) but as shown in Fig. 2.8, the boiling curve is the boiling point for actual reservoir pressure at the corresponding height so in fact it is a real reservoir characteristic.

In this respect it must be mentioned that well pressure and temperature logs do usually not show actual reservoir pressures or temperatures at all depths. It is only at those depths where the well is open to the reservoir where measured values can be the same as the actual reservoir parameters.

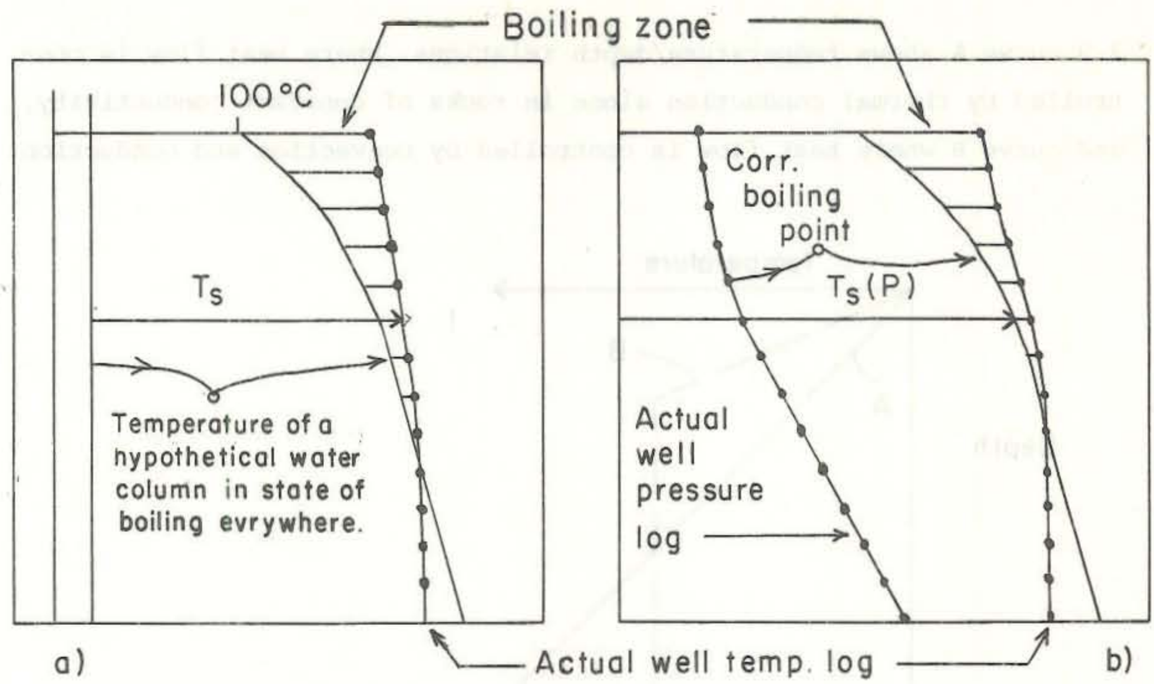

82.01.0032.

Fig. 2.8 a) wrong, and b) correct, boiling curve

2.5 Heat transfer in the reservoir

According to the preceding chapter heat is transported by dispersion, conduction (or diffusion) and convection. In the fluid, heat is transferred by all three mechanisms, whereas in the solid phase heat is transferred by conduction. Finally heat is transported between the fluid and the solid. Dispersion and conduction have been described in the preceding chapter.

Heat transport by convection is due to the fact that the flowing fluid carries its own heat content from one part of the field to another. If the convective motion is due to external means, for instance injection of a hot fluid into an aquifer we speak of forced convection. Convective flow due to density variations resulting from temperature differences within the field is known as free or natural convection. Natural convection may occur when the bottom plane of an aquifer is heated, thus creating buoyancy forces that may onset convective motion.

Let us now take two examples of these heat transfer mechanisms. In Fig.

2.9 curve A shows temperature/depth relations, where heat flow is controlled by thermal conduction alone in rocks of constant conductivity, and curve B where heat flow is controlled by convection and conduction.

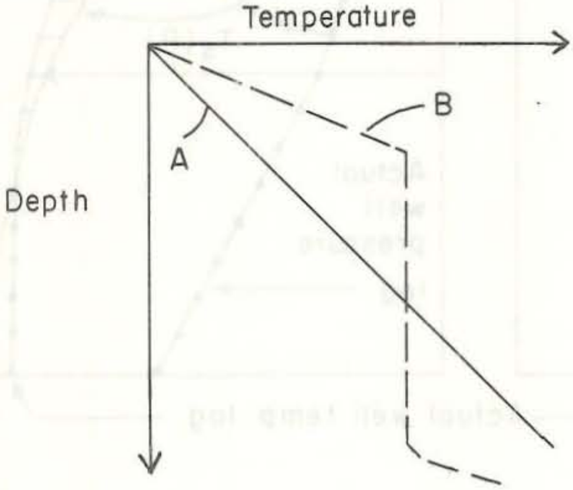

82.1.0033

Fig. 2.9 Temperature/depth relation

Let us for the second example take the movement of a temperature front. When water is injected into a geothermal reservoir cold water will spread away from the well. Fig. 2.10 shows a schematic picture of the temperature front.

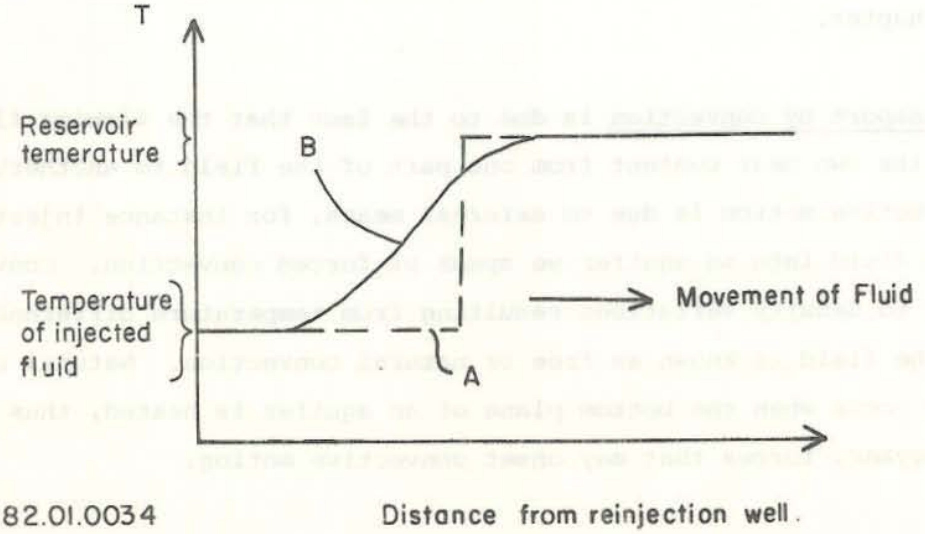

82.01.0034

Fig. 2.10 Schematic picture of a temperature front

If we just take convective heat transfer into account, that is the bulk movement of the fluid, but neglect both conduction and dispersion effects, the profile A in the figure would be the resulting temperature front. If conduction and dispersion are taken into account that would result in the S shaped profile B in the figure.

Heat transfer between liquid and rock is commonly described as a linear process:

$h = a(T_r - T_l)$, where

a is a heat transfer coefficient, and T_l and T_r denote the temperature of liquid and rock respectively. Including this mechanism in the equations describing the heat transport results in serious complications in solving the equations since we get an extra unknown (T_r) and the heat balance equations for liquid and rock are coupled. For relatively low flow velocities the temperature difference between liquid and rock is always small and consequently neglected by taking $T_l = T_r$ which corresponds to $a = \infty$.

In the following we neglect any heat transfer between liquid and rock by setting $T_l = T_r$.

2.6 Conceptual reservoir models

The construction of a conceptual model of a geothermal reservoir, consists of gathering all available hydrogeological information into one picture where all the elements are compatible with each other. A conceptual model should show:

1) A hydrogeological section with aquifers and aquicludes separately designated.

2) Natural discharge and recharge areas.

3) Direction of flow in aquifers.

4) Impervious boundaries.

Such a model is a great help in planning further investigations, and it is a necessary basis for all reservoir calculations.

Conceptual models are often speculative in the details, and for that reason difficult to work with. Therefore it is necessary to use all available information to construct them.

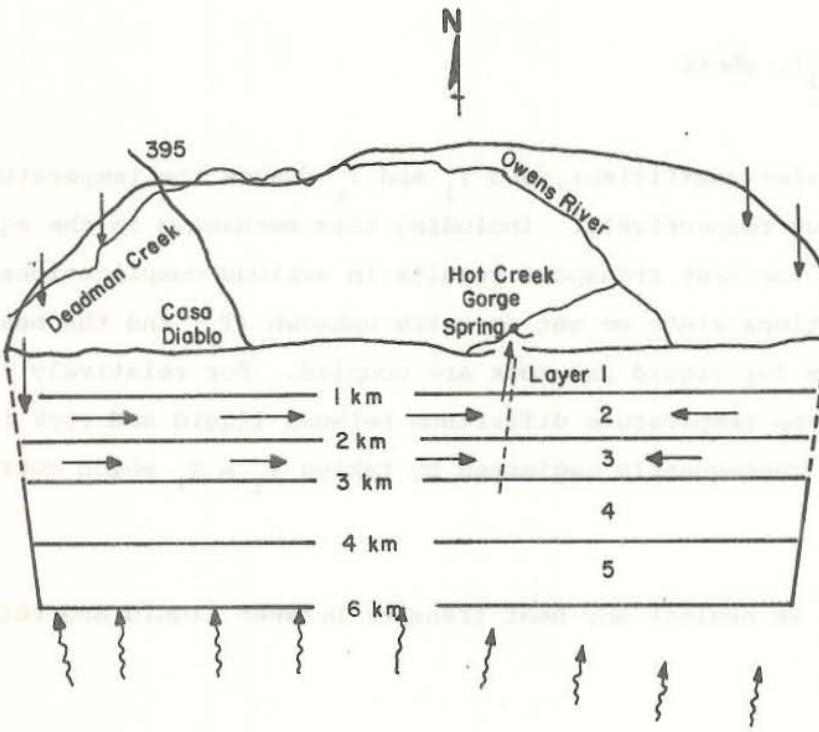

Fig. 2.11 The Long Valley model (Sorey, 1976)

Fig. 2.11 shows a conceptual model of the Long Valley hydrothermal system, California U.S.A. (Sorey 1976). It shows a 450 km^2 caldera with a multi-layered aquifer. Recharge is along the caldera boundary, discharge is all in the Hot Creek Gorge. The model is used for numerical calculation of the temperature and pressure pattern. From such calculations one can e.g. estimate if reservoir pressure drop from exploitation causes increased recharge.

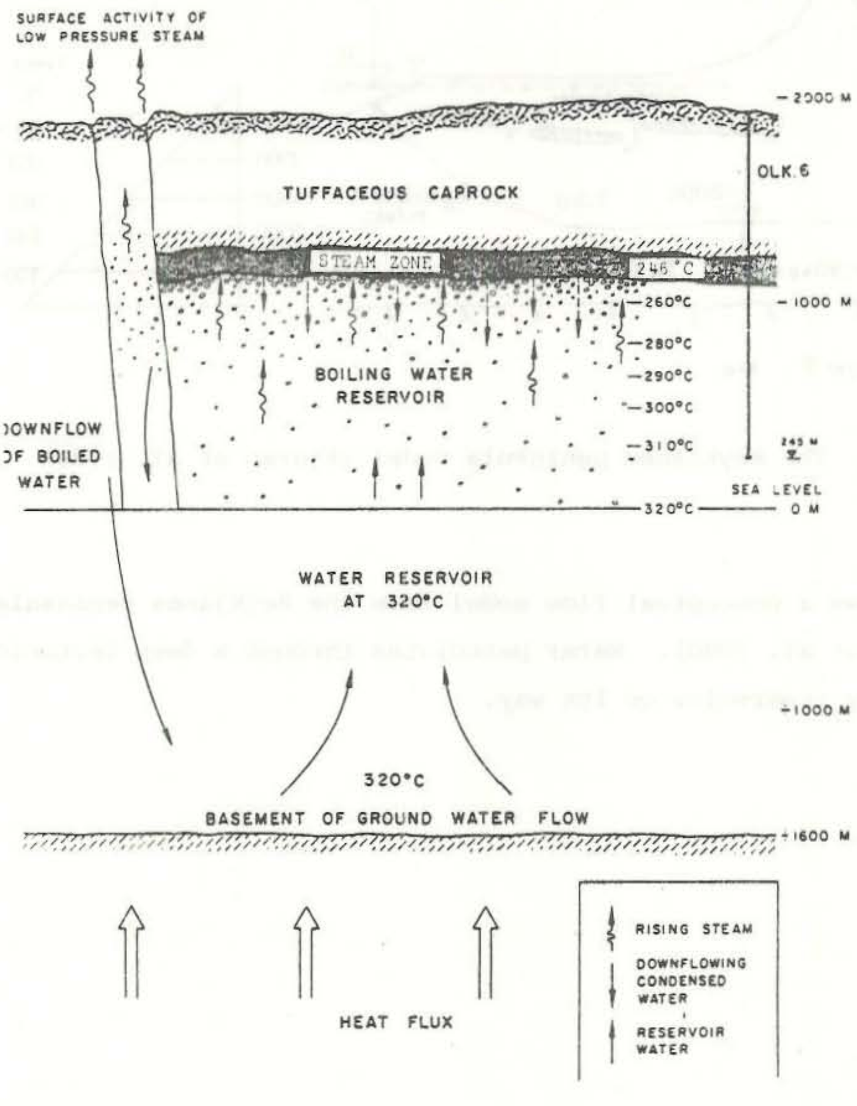

Fig 2.12 The Olkaria model (Sveco and Virkir 1976)

Fig.2.12 shows a conceptual model of the Olkaria Geothermal field, Kenya (Sveco and Virkir 1976). It shows a vapour-dominated reservoir overlying a liquid-dominated zone. Heating is from an unidentified heat source below, steam escapes through a fault zone. Note the complicated steam-waterflow picture.

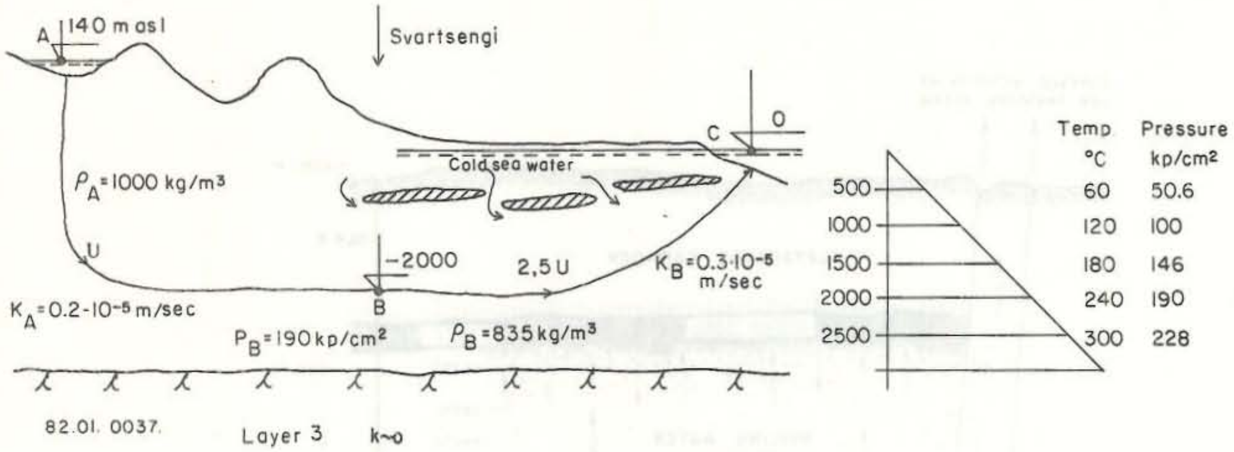

<u>Fig. 2.13</u> The Reykjanes peninsula model (Kjaran et al. 1980)

Fig. 2.13 shows a conceptual flow model from the Reykjanes peninsula Iceland (Kjaran et al. 1980). Water percolates through a deep tectonic fault and feeds many reservoirs on its way.

3 WELL TESTING

3.1 Introduction

Well testing is conducted in order to evaluate the condition of the well and flow capacity of the well. Parameters of interest include formation permeability, compressibility, the presence of barriers and leaky boundaries, extent of well bore damage, the presence of prominent fractures close to the well, the mixing of vertically separated producing zones, and so on. Closely related to well testing is well stimulation, where the well testing methods are used to evaluate the well improvement.

Hydraulic well testing consists of producing from or injecting into one or more wells at controlled rates and over periods ranging from a few hours to a few weeks and monitoring changes in pressure within the producing well itself or nearby observation wells. It should be noted here that the same formulas apply for production and injection wells with just the mass flow with reversed sign in the equations. Geothermal well testing and analysis is more difficult than more conventional well testing techniques of hydrology and petroleum engineering. The flow in geothermal reservoirs is generally two-phase flow under non-isothermal conditions, and methods of interpretation of data for such situations are complicated. A large amount of literature is available on testing isothermal single phase systems because of the investigation of petroleum engineers and hydrologists over the past five decades. However, there is in general lack of experience in testing non-isothermal flow in single and two phase reservoirs. Nevertheless, under certain conditions, it is possible to use isothermal techniques for non-isothermal situations. As mentioned in chapter 2 a single-phase reservoir may either be vapour-dominated or liquid-dominated. The dynamics of a vapour-dominated reservoir is similar to that of a gas reservoir and some of the techniques from petroleum industry have been applied in such cases. In the case of liquid-dominated systems the methods from groundwater well technology and petroleum industry have been applied.

In this chapter the differential equation for horizontal, isothermal flow will be derived. Well testing methods for liquid-dominated reservoirs will be described and finally necessary corrections are made for the use in vapour-dominated reservoirs. In all the methods the reservoir will be considered homogeneous and isotropic and the flow will be considered horizontal, except for partial-penetration of wells, where corrections will be made to account for vertical flow components. Both the production well itself and observation wells will be used for the well testing methods and in the case of the production well itself near well characteristics will be described.

3.2 The differential equation for isothermal, horizontal flow

The basic differential equation will be derived in radial form thus simulating the flow of fluids in the vicinity of a well. Analytical solutions of the equation can then be obtained under various boundary and initial conditions for use in the description of well testing and well inflow, which have considerable practical application in reservoir engineering. The radial cell geometry is shown in Fig. 3.1 and initially the following simplifying assumptions will be made.

1) The flow is considered isothermal.

2) The reservoir is considered homogeneous and isotropic.

3) The producing well penetrates the entire formation thickness.

4) The formation is completely saturated with a single fluid.

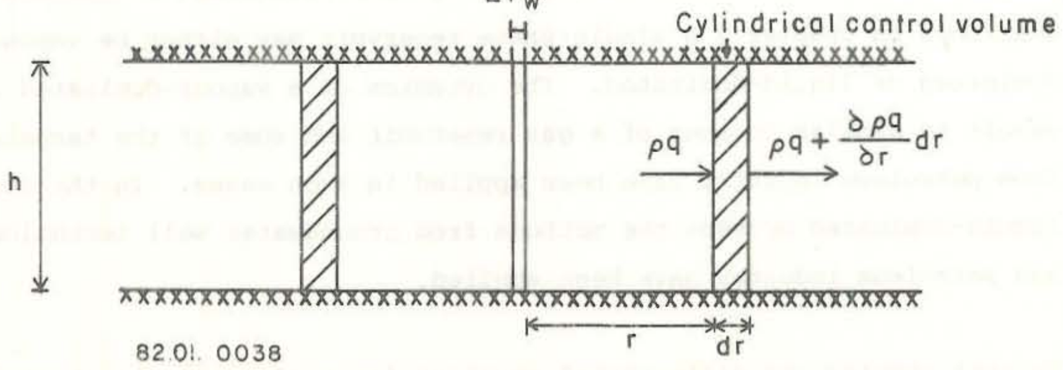

Fig. 3.1 Radial flow of a single phase fluid in the vicinity of a producing well

Consider the flow through a volume of thickness, dr, situated at a distance, r, from the centre of the radial cell. Then applying the principle of mass conservation.

Mass flow in - Mass flow out = Rate of change of mass within the control volume

$$\rho q \qquad - (\rho q + \frac{\partial \rho q}{\partial r} dr) = \qquad 2\pi r dr \frac{\partial(\phi\rho h)}{\partial t}$$

which simplifies to:

$$-\frac{\partial(\rho q)}{\partial r} = 2\pi r \frac{\partial(\rho\phi h)}{\partial t} \tag{3.1}$$

By applying Darcy's law, see eq. 2.1, for radial, horizontal flow it is possible to substitute for the flow rate, q, in eq. 3.1 since;

$$q = -\frac{2\pi r h k}{\mu}\frac{\partial p}{\partial r}$$

giving:

$$\frac{\partial}{\partial r}\left(\frac{2\pi r h k}{\mu}\rho\frac{\partial p}{\partial r}\right) = 2\pi r \frac{\partial(\phi h\rho)}{\partial t}$$

or

$$\frac{1}{r}\frac{\partial}{\partial r}\left(\frac{k\rho}{\mu} r \frac{\partial p}{\partial r}\right) = \frac{1}{h}\frac{\partial(\phi h\rho)}{\partial t} \tag{3.2}$$

The right hand side of eq. 3.2 can be written:

$$\frac{1}{h}\frac{\partial(\phi h\rho)}{\partial t} = \phi\frac{\partial\rho}{\partial t} + \rho \cdot \frac{1}{h}\frac{\partial(\phi h)}{\partial t}$$

By using eq. 2.18 we can write:

$$\phi\frac{\partial\rho}{\partial t} = \phi\rho\beta\frac{\partial p}{\partial t} \tag{3.3}$$

and by applying eq. 2.4 and just considering vertical deformations and constant total stress we get:

$$\rho \frac{1}{h} \frac{\partial(\phi h)}{\partial t} = \rho\alpha \frac{\partial p}{\partial t} \tag{3.4}$$

By defining:

$$c = (\beta + \frac{\alpha}{\phi}) \tag{3.5}$$

and inserting in eq. 3.2 we get:

$$\frac{1}{r} \frac{\partial}{\partial r} (\frac{k\rho}{\mu} r \frac{\partial p}{\partial r}) = c\rho\phi \frac{\partial p}{\partial t} \tag{3.6}$$

The coefficient defined by:

$$S = c\phi h\rho g \tag{3.7}$$

is according to eqs. 2.19 and 2.20 called the storage coefficient and is the weight of fluid released from storage per unit surface area of the reservoir per unit change in pressure. The coefficient defined by:

$$T = \frac{kg\rho}{\mu} h \tag{3.8}$$

is called the transmissivity coefficient. See eqs. 2.2 and 2.21.

Eq. 3.6 is the basic differential equation for the isothermal, radial flow of any single phase fluid in a porous medium. The equation is non-linear because of the implicit pressure dependence of the density, compressibility and viscosity appearing in the coefficients $k\rho/\mu$ and $\phi c\rho$. Because of this it is not possible to find simple analytical solutions of the equation without first linearizing it so that the coefficients somehow lose their pressure dependence. For that purpose we expand the left hand side of eq. 3.6, using the chain rule for differentiation gives:

$$\frac{1}{r} (\frac{\partial}{\partial r} (\frac{k}{\mu}) \rho r \frac{\partial p}{\partial r} + \frac{k}{\mu} \frac{\partial \rho}{\partial r} r \frac{\partial p}{\partial r} + \frac{k\rho}{\mu} \frac{\partial p}{\partial r} + \frac{k\rho}{\mu} r \frac{\partial^2 p}{\partial r^2}) = c\rho\phi \frac{\partial p}{\partial t} \tag{3.9}$$

Using eq. 2.18 for the compressibility of the fluid gives:

$$\beta\rho \frac{\partial p}{\partial r} = \frac{\partial \rho}{\partial r} \tag{3.10}$$

which when substituted into eq. 3.9 gives:

$$\frac{1}{r} \left(\frac{\partial}{\partial r} \left(\frac{k}{\mu}\right) \rho r \frac{\partial p}{\partial r} + \frac{k}{\mu} \beta\rho r \left(\frac{\partial p}{\partial r}\right)^2 + \frac{k\rho}{\mu}\frac{\partial p}{\partial r} + \frac{k\rho}{\mu} r \frac{\partial^2 p}{\partial r^2}\right) = c\rho\phi \frac{\partial p}{\partial t} \tag{3.11}$$

In the case of liquid-dominated reservoirs with isothermal flow the term $\frac{\partial}{\partial r}\left(\frac{k}{\mu}\right) = 0$, and if we assume that the pressure gradients are small, then terms of the order $(\partial p/\partial r)^2$ can be neglected. Eq. 3.11 then reduces to:

$$\frac{1}{r}\frac{\partial}{\partial r}\left(r \frac{\partial p}{\partial r}\right) = \frac{\phi\mu c}{k}\frac{\partial p}{\partial t} \tag{3.12}$$

If this flow equation had been derived using vector notations the resulting equation would have been:

$$\Delta p = \frac{\phi\mu c}{k}\frac{\partial p}{\partial t} \tag{3.13}$$

Eq. 3.12 is the basic equation for well test analysis. Different well testing methods are just solutions of the differential equation 3.12 for various boundary and initial conditions. Equations 3.12 and 3.13 are the diffusivity equations in which the coefficient $\frac{k}{\phi\mu c}$ is called the diffusivity constant. These equations are also identical with the heat equations, and therefore the solutions to heat conduction problems can be modified to be used in well testing. The book "Conduction of Heat in Solids", by Carslaw and Jaeger (1959) gives solutions of the diffusivity equation for a large variety of boundary and initial conditions and is, therefore, a helpful reference text in reservoir engineering.

It should be emphasized that due to the isothermal, horizontal flow approximations, the pressure distribution in the vertical direction is hydrostatic. Because we are using pressure as a dependent variable in the differential equation, pressure values of the same elevation must be compared at different times to calculate the pressure decline.

In some liquid-dominated reservoirs the watertable is measured instead of pressure. Because of the hydrostatic pressure distribution we can define piezometric head thus:

$$H = z + p/\gamma = \text{constant}, \tag{3.14}$$

where z is the elevation and γ is defined as $\gamma = \rho g$. Then pressure can be calculated from eq. 3.14. For example we have for a pressure drop Δp along a horizontal streamline:

$$\Delta p = \gamma \Delta H \tag{3.15}$$

where ΔH is the drawdown of the water table. We have neglected $\Delta\rho$ which is small in liquids. If we insert the pressure from eq. 3.14 into eq. 3.12 we get:

$$\frac{1}{r}\frac{\partial}{\partial r}\left(r\,\frac{\partial H}{\partial r}\right) = \frac{\phi\mu c}{k}\frac{\partial H}{\partial t} \tag{3.16}$$

When analysing well testing data, the watertable measurements can therefore either be changed into pressure according to eqs. 3.14 or 3.15 or we can make use of eq. 3.16. The appropriate initial and boundary conditions must of course be formulated either in pressure or elevation of the water table. Most of the following equations will be formulated in pressure units, but the examples given will both be watertable and pressure measurements data. Bearing the above in mind, the use of either watertable or pressure data should cause no confusion.

3.3 Dimensionless variables and qualitative characteristics of the pressure decline for producing reservoirs

Dimensionless parameters will be introduced and the differential-equation 3.12 will be presented in dimensionless form. The characteristic of the solution to the differential equation will then be discussed qualitatively.

The dimensionless time is defined as:

$$t_D = \frac{kt}{\phi\mu c\, r_w^2} \tag{3.17}$$

when based on wellbore radius, r_w, or

$$t_{DA} = \frac{kt}{\phi \mu c A} = t_D \frac{r_w^2}{A} \tag{3.18}$$

when based on total drainage area, A.

The dimensionless radial distance from the producing well is defined as:

$$r_D = r/r_w \tag{3.19}$$

The dimensionless pressure drop is defined as:

$$P_D\ (r_D,\ t_D) = \frac{2\pi k h \rho}{W\mu}\ (p_i - p(r,t)) \tag{3.20}$$

Substitution of these variables into the radial diffusivity equation 3.12 gives:

$$\frac{1}{r_D} \frac{\partial}{\partial r_D} (r_D \frac{\partial P_D}{\partial r_D}) = \frac{\partial P_D}{\partial t_D} \tag{3.21}$$

This demensionless diffusivity equation can then be solved for the appropriate initial and boundary conditions.

The qualitative behaviour of the solution to eq. 3.21 is shown in Fig. 3.2 for constant dimensionless radius r_D. The flow regime A is the infinite reservoir period, where the pressure decline at some distance, r_D, from the producing well is not affected by the boundary conditions and the reservoir behaves as it was infinite in the areal extent.

As will be shown later the P function is linear with the logarithm of time after certain time has elapsed. The solution to the diffusivity equation in this case is called the Theis solution or the exponential integral solution.

The flow regime B is the transition between the long term pressure decline and the initial pressure decline. It is the behaviour of the reservoir

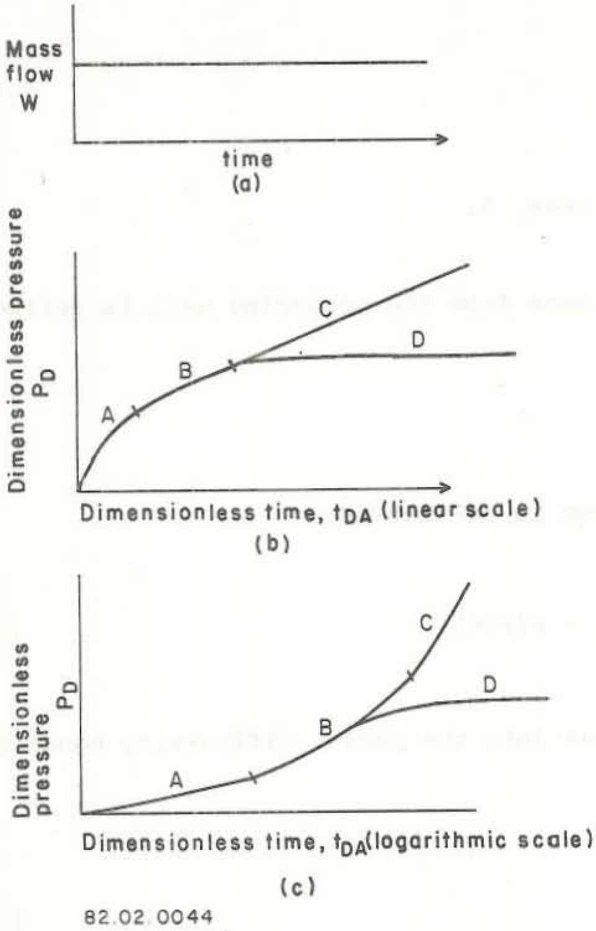

Fig. 3.2 Transient flow regimes:

A - infinite reservoir period

B - transition period

C - pseudosteady state

D - steady state

when it can no longer be looked upon as infinite. In the case that the pressure decline has struck impermeable boundaries at some distance from the well, but is still spreading to other sides, B soon becomes a straight line in the lin-log plot with a steeper slope than A.

The flow regime C is called pseudosteady state where pressure decline is proportional to time. This means that the pressure decline has struck impermeable boundaries all around the producing well and the reservoir is being depleted at a constant rate.

The flow regime D is called steady state. Then the pressure does not drop any more and we have constant pressure with time. The pressure decline has produced new inflow which is equal to the mass outflow and thus producing steady state pressure conditions.

The solutions to the diffusivity equation are relatively simple for cases A, C and D, but for many problems the transition state B gives more complex solutions. The fact that the full solution is so complex is rather unfortunate since the constant terminal rate solution of the radial diffusivity equation can be regarded as the basic equation in reservoir analysis. As will be shown later, the pressure response can be theoretically described by superposing such solutions.

Finally it should be noted, that in case of waterlevel observations the dimensionless equations remain the same except eq. 3.20, which changes to:

$$P_D\ (r_D,\ t_D) = \frac{2\pi kh\rho}{W\mu}\gamma\ (H_i - H\ (r,t)) \tag{3.22}$$

or by using T from equation 3.8:

$$P_D\ (r_D,\ t_D) = \frac{2\pi T\rho}{W}\ (H_i - H\ (r,t)) \tag{3.23}$$

3.4 Steady state and semisteady state solutions

When the pressure decline has produced new inflow, recharge, which is equal to the mass outflow, we have steady state conditions. For steady state conditions eq. 3.21 reduces to Laplace's equation:

$$\nabla P_D = 0 \tag{3.24}$$

with the appropriate boundary conditions. The steady state solution can be determined directly without first solving the timedependent problem. A special type of steady state solutions will be presented in section 3.10. Let us here take an example of a single well producing in a homogeneous aquifer with constant pressure boundaries located at the radial distance r_e from the well. Fig. 3.3 shows a schematic picture of the flow situation.

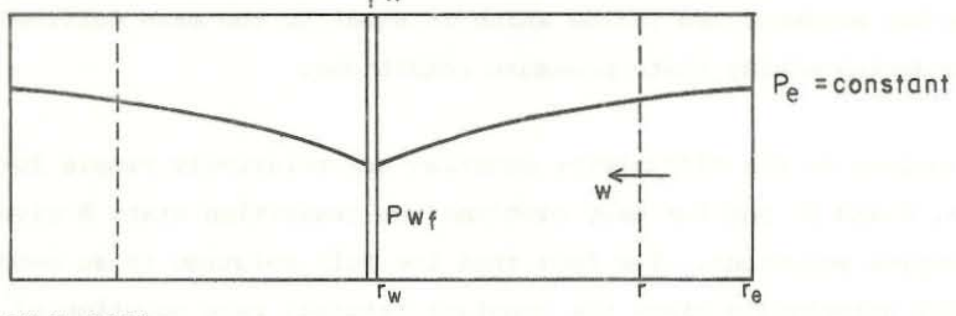

Fig. 3.3 Radial flow into a well under steady state conditions

Darcy's law can be expressed as:

$$W = \frac{2\pi rhk\rho}{\mu} \frac{\partial p}{\partial r}$$

and separating the variables and integrating:

$$\int_{p_{wf}}^{p} dp = \frac{W\mu}{2\pi hk\rho} \int_{r_w}^{r} \frac{dr}{r}$$

where p_{wf} is the conventional symbol for the bottom hole flowing pressure. The integration results in:

$$p - p_{wf} = \frac{W\mu}{2\pi hk\rho} \ln \frac{r}{r_w} \tag{3.25}$$

which shows that the pressure increases logarithmically with respect to the radius, as shown in Fig. 3.3, the pressure drop being consequently much larger close to the well than near the outer boundary. In particular, when $r = r_e$ then:

$$p_e - p_{wf} = \frac{W\mu}{2\pi hk\rho} \ln \frac{r_e}{r_w} \tag{3.26}$$

The solution is very simple in this case because of the radial symmetry.

In case of other geometries Laplace's equation has to be solved with more elaborate methods than the above. The solution e.g. for a rectangular constant pressure boundary with the producing well a line source is given by:

$$P_D = \frac{8}{\pi} \sum_{n=1}^{\infty} \sum_{m=1}^{\infty} \frac{\sin \frac{n\pi y}{\sqrt{A}} \sin \frac{m\pi x}{\sqrt{A}} \cdot \sin \frac{m\pi\xi}{\sqrt{A}} \sin \frac{n\pi\eta}{\sqrt{A}}}{m^2 + n^2} \tag{3.27}$$

where A is the rectangular area and (ξ,η) are the coordinates of the line source in a rectangular coordinate system, and (x,y) are the coordinates of the observed pressure decline. (x,y) = (0,0) is in one of the corners of the rectangular area.

Often there is a damaged zone in the vicinity of the wellbore, which reduces the permeability in the area. The situation is shown in Fig. 3.4, in which r_s represents the radius of this zone.

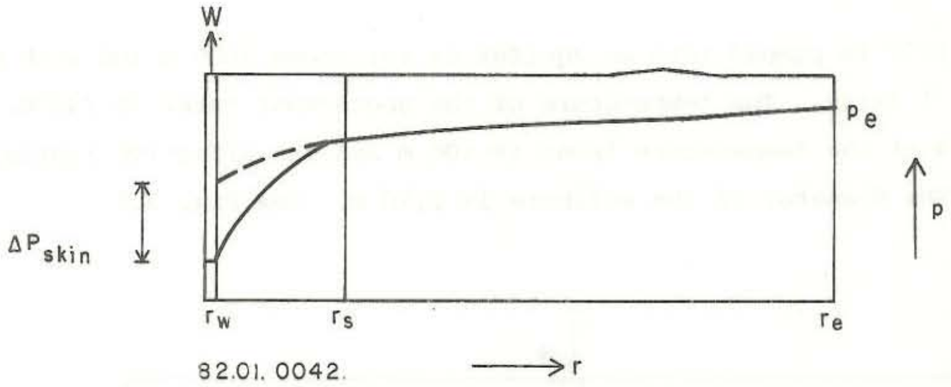

Fig. 3.4 Radial pressure profile for a damaged well

If the well were undamaged, the pressure profile for $r<r_s$ would be as shown by the dashed line, whereas due to the reduced permeability in the damaged zone, eq. 3.26 implies that the pressure drop will be larger than normal, or that P_{wf} will be reduced. According to van Everdingen (1953) the additional pressure drop close to the well is defined by:

$$\Delta p_{skin} = \frac{W\mu}{2\pi kh\rho} S \tag{3.28}$$

in which the ΔP_{skin} is attributed to a skin of reduced permeability around the well and S is a dimensionless skin factor, which can be determined from well testing methods, see chapter 3.14 for further discussion of the skin effect. Eq. 3.26 can now be expressed with the skin factor:

$$p_e - p_{wf} = \frac{W\mu}{2\pi hk\rho}\left(\ln\frac{r_e}{r_w} + S\right) \qquad (3.29)$$

The productivity index of a well is defined as the mass flow divided by wellbore pressure drop:

$$PI = \frac{W}{p_e - p_{wf}} = \frac{2\pi hk\rho}{\mu\left(\ln\frac{r_e}{r_w} + S\right)} \qquad (3.30)$$

PI is the productivity index of a well, expressed in $kg/s/N/m^2$, and is a measure of the well performance.

EXERCISE 3.1

Water of 10°C is pumped into an aquifer of thickness 1000 m and with permeability 1 darcy. The temperature of the geothermal water is 240°C. The radius of the temperature front is 100 m and the effective radius is 1000 m. The diameter of the wellbore is 0,20 m. See Fig. 3.5.

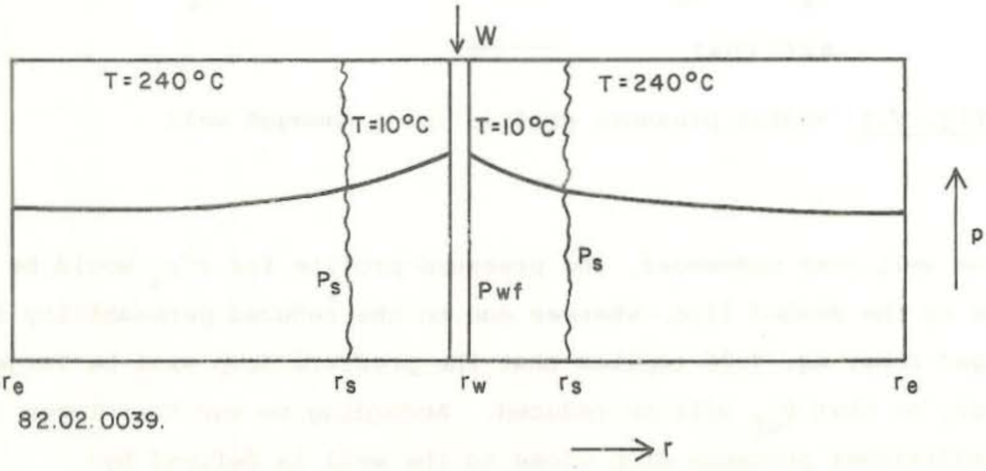

Fig. 3.5 Pressure profile during the pumping of cold water into a high temperature geothermal reservoir

1) What is the productivity index of the well under the above conditions?

2) If the cooled section of radius r_s is considered as skin effect zone, determine the skin factor.

Solution

From the data given we have:

$$\rho_{10^\circ C} = 999.7\ kg/m^3 \qquad \mu_{10^\circ C} = 1.307 \cdot 10^{-3}\ Ns/m^2$$

$$\rho_{240^\circ C} = 813.7\ kg/m^3 \qquad \mu_{240^\circ C} = 1.3 \cdot 10^{-4}\ Ns/m^2$$

From eq. 3.26 we get:

$$p_s - p_{wf} = \frac{W\mu_{10}}{2\pi hk\rho_{10}} \ln \frac{r_s}{r_w} \tag{3.31}$$

$$p_e - p_s = \frac{W\mu_{240}}{2\pi hk\rho_{240}} \ln \frac{r_e}{r_s} \tag{3.32}$$

Adding the two equations we get:

$$p_e - p_{wf} = \frac{W\mu_{240}}{2\pi hk\rho_{240}} \left(\frac{\mu_{10}}{\mu_{240}} \frac{\rho_{240}}{\rho_{10}} \cdot \ln \frac{r_s}{r_w} + \ln \frac{r_e}{r_s}\right) \tag{3.33}$$

1) The productivity index is given by eq. 3.30.

$$PI = \frac{W}{p_e - p_{wf}} = \frac{2\pi hk\rho_{240}}{\mu_{240} \left(\frac{\mu_{10}}{\mu_{240}} \frac{\rho_{240}}{\rho_{10}} \cdot \ln \frac{r_s}{r_w} + \ln \frac{r_e}{r_s}\right)} \tag{3.34}$$

$$= \frac{2 \cdot \pi \cdot 1000 \cdot 0.987 \cdot 10^{-12} \cdot 813.7}{1.3 \cdot 10^{-4} \left(\frac{1.3 \cdot 10^{-3}}{1.3 \cdot 10^{-4}} \frac{813.7}{999.7} \ln \frac{100}{0.1} + \ln \frac{1000}{100}\right)} \simeq 7 \cdot 10^{-4}\ kg/s/N/m^2$$

$\simeq$ 70 kg/s/bar

2) Following eq. 3.29 we write:

$$p_e - p_{wf} = \frac{W\mu_{240}}{2\pi hk\rho_{240}} (\ln \frac{r_e}{r_w} + S)$$

Eq. 3.33 can be written as:

$$p_e - p_{wf} = \frac{W\mu_{240}}{2\pi hk\rho_{240}} (\ln \frac{r_e}{r_w} + (\frac{\mu_{10}}{\mu_{240}} \frac{\rho_{240}}{\rho_{10}} - 1) \ln \frac{r_s}{r_w}) \qquad (3.35)$$

Comparing we see that S is given by:

$$S = (\frac{\mu_{10}}{\mu_{240}} \frac{\rho_{240}}{\rho_{10}} - 1) \ln \frac{r_s}{r_w}$$

$$= (\frac{1.3 \cdot 10^{-3}}{1.3 \cdot 10^{-4}} \cdot \frac{813.7}{999.7} - 1) \ln \frac{100}{0.1}$$

$$\simeq 49.3$$

If eq. 3.35 is used to estimate the permeability of the formation by measuring the pressure increase of the well when pumping cold water into the aquifer, we would have:

$$k = \frac{W\mu_{240}}{2\pi h\rho_{240}(p_e - p_{wf})} (\ln \frac{r_e}{r_w} + (\frac{\mu_{10}}{\mu_{240}} \frac{\rho_{240}}{\rho_{10}} - 1) \ln \frac{r_s}{r_w}) \qquad (3.36)$$

If the cooled section of the aquifer was not taken into account, the permeability of the formation would be estimated by eq. 3.26 getting:

$$k' = \frac{W\mu_{240}}{2\pi h\rho_{240}(p_e - p_{wf})} \ln \frac{r_e}{r_w} \qquad (3.37)$$

We then have:

$$\frac{k}{k'} = 1 + \frac{\left(\frac{\mu_{10}}{\mu_{240}} \cdot \frac{\rho_{240}}{\rho_{10}} - 1\right) \ln \frac{r_s}{r_w}}{\ln \frac{r_e}{r_w}}$$

$$= 1 + \frac{S}{\ln \frac{r_e}{r_w}} \approx 1 + \frac{49.3}{\ln \frac{1000}{0.1}} \cong \underline{\underline{6.4}}$$

Using eq. 3.37 to estimate the permeability under the above conditions would yield an estimate of the permeability almost one order of magnitude smaller than by using eq. 3.36. This effect is caused mainly by the viscosity which decreases by a factor of ten from 10°C to 240°C. In practice one would have to consider the warming up of the cold water due to heat exchange between the water and the rock. This is not done here for the sake of simplicity.

In vapour-dominated reservoirs and in liquid-dominated reservoirs with high permeability the velocity becomes sometimes so high, that the flow becomes turbulent and Darcy's law is no longer valid. In Fig. 3.6 we see that the highest velocities occur in the vicinity of the well where the pressure gradients are greatest.

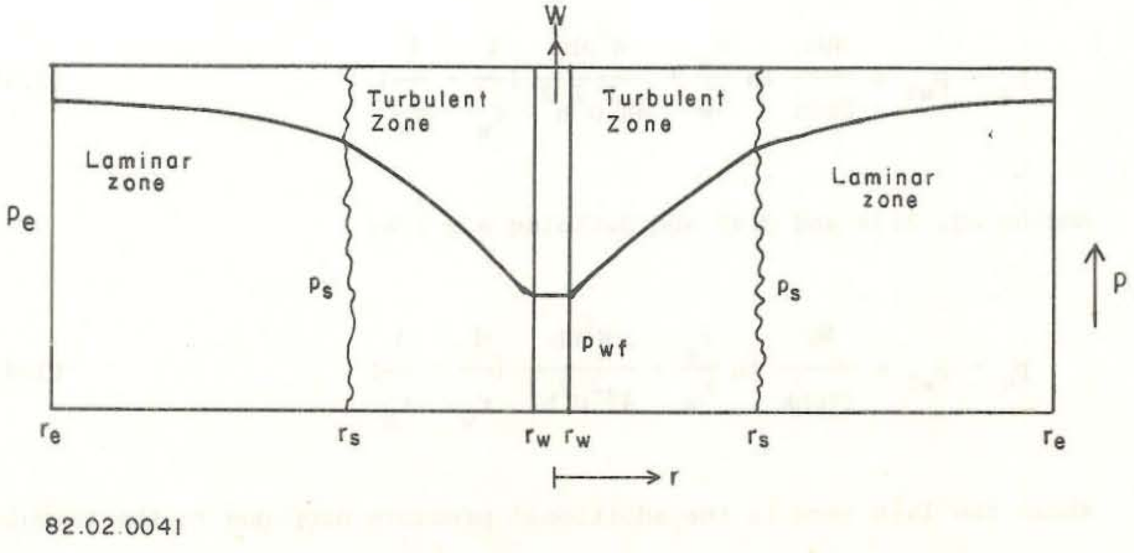

Fig. 3.6 Pressure profiles in laminar and turbulent flow zones

From eq. 3.26 we have for the pressure profile in the laminar zone:

$$p_e - p_s = \frac{W\mu}{2\pi hk\rho} \ln \frac{r_e}{r_s} \tag{3.38}$$

The pressure gradient in the turbulent zone can be expressed as:

$$\frac{\partial p}{\partial r} = \mu a V + \mu b V^2 \tag{3.39}$$

where V is the velocity given by the equation of continuity:

$$V = \frac{W}{\rho 2\pi rh} \tag{3.40}$$

combining eq. 3.39 and 3.40:

$$\frac{\partial p}{\partial r} = \frac{W\mu a}{2\pi\rho h} \cdot \frac{1}{r} + \frac{W^2\mu b}{4\pi^2\rho^2h^2} \frac{1}{r^2} \tag{3.41}$$

and separating the variables and integrating:

$$\int_{p_{wf}}^{p_s} dp = \frac{W\mu a}{2\pi\rho h} \int_{r_w}^{r_s} \frac{dr}{r} + \frac{W^2\mu b}{4\pi^2\rho^2h^2} \int_{r_w}^{r_s} \frac{dr}{r^2}$$

The integration results in:

$$p_s - p_{wf} = \frac{W\mu a}{2\pi\rho h} \ln \frac{r_s}{r_w} + \frac{W^2\mu b}{4\pi^2\rho^2h^2} \left(\frac{1}{r_w} - \frac{1}{r_s}\right) \tag{3.42}$$

Adding eq. 3.38 and 3.42 and defining $a = 1/k$:

$$p_e - p_{wf} = \frac{W\mu}{2\pi\rho hk} \ln \frac{r_e}{r_w} + \frac{W^2\mu b}{4\pi^2\rho^2h^2} \left(\frac{1}{r_w} - \frac{1}{r_s}\right) \tag{3.43}$$

Where the last term is the additional pressure drop due to the turbulent zone. If $r_s >> r_w$ eq. 3.43 reduces to:

$$p_e - p_{wf} = \frac{W\mu}{2\pi\rho hk} \ln \frac{r_e}{r_w} + \frac{W^2\mu b}{4\pi^2\rho^2h^2r_w}$$

which can be written as:

$$p_e - p_{wf} = \frac{W\mu}{2\pi\rho hk} (\ln \frac{r_e}{r_w} + \frac{Wbk}{2\pi\rho hr_w}) \quad (3.44)$$

We define:

$$C = \frac{bk}{2\pi\rho hr_w} \quad (3.45)$$

and inserting in eq. 3.44 gives:

$$p_e - p_{wf} = \frac{W\mu}{2\pi\rho hk} (\ln \frac{r_e}{r_w} + CW) \quad (3.46)$$

CW is the additional pressure drop at the wellbore due to turbulent flow conditions. The turbulent pressure drop will be discussed later in chapter 3.11 and 3.14.

The total pressure drop at the wellbore can now be expressed for steady state conditions.

$$p_e - p_{wf} = \frac{W\mu}{2\pi\rho hk} (\ln \frac{r_e}{r_w} + S + CW) \quad (3.47)$$

Estimation methods of the parameters S and C will be discussed later as mentioned above. The skin factor S should not be confused with the storage coefficient S.

The semisteady state or pseudosteady state solutions occur when the pressure decline is proportional to time. This means that the pressure decline curve has struck impermeable boundaries all around the producing well and the reservoir is being depleted at a constant rate. Using the storage coefficient, eq. 3.7 we have:

$$A dp c \phi h \gamma = - W dt g$$

where A is the drainage area.

$$\frac{dp}{dt} = - \frac{W}{c \phi h \rho A} \tag{3.48}$$

If we have a circular drainage area with drainage radius, r_e we get:

$$\frac{dp}{dt} = \frac{-W}{c \phi h \rho \pi r_e^2} \tag{3.49}$$

Eq. 3.12 now reduces to:

$$\frac{1}{r} \frac{\partial}{\partial r} (r \frac{\partial p}{\partial r}) = - \frac{W\mu}{h \rho k \pi r_e^2} \tag{3.50}$$

and integrating this equation:

$$r \frac{\partial p}{\partial r} = - \frac{W \mu r^2}{2 \pi r_e^2 k h \rho} + C,$$

where C, is a constant of integration.

At the outer, no flow boundary $\partial p/\partial r$ vanishes and hence the constant can be evaluated as $C, = \frac{W\mu}{2\pi k h \rho}$ which, when substituted in the last equation, gives:

$$\frac{\partial p}{\partial r} = \frac{W\mu}{2\pi k h \rho} (\frac{1}{r} - \frac{r}{r_e^2})$$

Integrating once again:

$$p_r - p_{wf} = \frac{W\mu}{2\pi kh\rho} \left(\ln \frac{r}{r_w} - \frac{r^2}{2r_e^2}\right) \tag{3.51}$$

in which the term $\frac{r_w^2}{r_e^2}$ is considered negligible. Eq. 3.51 is a general expression for the pressure as a function of the radius. In the particular case when $r = r_e$ then:

$$p_e - p_{wf} = \frac{W\mu}{2\pi kh\rho} \left(\ln \frac{r_e}{r_w} - \frac{1}{2}\right) \tag{3.52}$$

in which both the skin factor and the turbulent pressure drop could be included. See eq. 3.47.

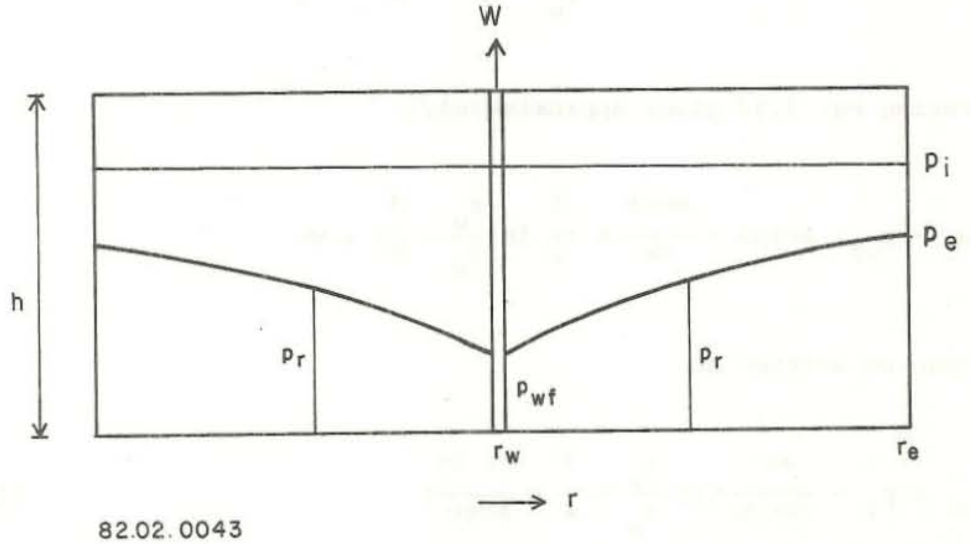

Fig. 3.7 Pressure distribution for the solution of the radial diffusivity equation under semi-steady state conditions

Fig. 3.7 shows the pressure situations after the well has been producing at a constant rate for some time t. The mass balance equation for the drainage volume is given by:

$$\int_{r_w}^{r_e} (p_i - p_r)\, 2\pi r dr c\phi h\rho = Wt \tag{3.53}$$

which can be simplified as:

$$p_i A c\phi h\rho - \int_{r_w}^{r_e} p_r \; 2\pi r c\phi h\rho dr = Wt$$

Inserting eq. 3.51 for p_r gives:

$$p_i A c\phi h\rho - p_{wf} A c\phi h\rho + p_{wf} \pi r_w^2 c\phi h\rho - \frac{W\mu c\phi}{k} \int_{r_w}^{r_e} r \; (\ln \frac{r}{r_w} - \frac{r^2}{2r_e^2}) \; dr = Wt$$

As $\pi r_w^2 << A$ this equation can be approximated by:

$$(p_i - p_{wf}) \; A c\phi h\rho - \frac{W\mu c\phi}{k} \int_{r_w}^{r_e} r \; (\ln \frac{r}{r_w} - \frac{r^2}{2r_e^2}) \; dr = Wt \qquad (3.54)$$

Integrating eq. 3.54 gives approximately:

$$(p_i - p_{wf}) \; A c\phi h\rho - \frac{W\mu c\phi}{\pi k} A \; (\frac{1}{2} \ln \frac{r_e}{r_w} - \frac{3}{8}) = Wt$$

Which can be written as:

$$p_{wf} = p_i - \frac{W\mu}{2\pi k\rho h} (\ln \frac{r_e}{r_w} - \frac{3}{4} + \frac{kt \; 2\pi}{A c\phi\mu}) \qquad (3.55)$$

Eq. 3.55 is identical to eq. 3.52 except that it is expressed in initial pressure, p_i, instead of boundary pressure, p_e. Eq. 3.55 can be written as:

$$p_{wf} = p_i - \frac{W\mu}{2\pi k\rho h} (\frac{1}{2} \ln \frac{4A}{\kappa C_A r_w^2} + 2\pi \frac{kt}{A c\phi\mu}) \qquad (3.56)$$

where κ is the exponential of Euler's constant, see eq. 3.65 and A is the drainage area, equal to πr_e^2 and C_A is called drainage shape factor. Eq. 3.56 was derived for circular geometry resulting in the factor C_A = 31.6. If eq. 3.50 is solved for any other geometry, then the solution can be expressed as eq. 3.56 with different C_A factors. As mentioned before the skin effect and the turbulent pressure drop can be included in eq. 3.56 similar to eq. 3.47. Eq. 3.56 expressed in dimensionless variables is given by:

$$P_D\ (1,t_D) = \frac{1}{2}\ln\frac{4A}{\kappa C_A r_w^{\ 2}} + 2\pi\ t_{DA} \tag{3.57}$$

If we assume that the transition regime in Fig. 3.2 is very short in duration, it is possible to determine approximate time at which the change from transient to semi-steady state conditions will occur, by equating eq. 3.57 for the semi-steady state and eq. 3.67 for the infinite reservoir case i.e.:

$$\frac{1}{2}\ln\left(\frac{4t_D}{\kappa}\right) \cong \frac{1}{2}\ln\frac{4A}{\kappa C_A r_w^{\ 2}} + 2\pi\ t_{DA}$$

which may be expressed as:

$$C_A\ t_{DA} \simeq e^{4\pi t_{DA}} \tag{3.58}$$

For the circular geometry, $C_A = 31.6$ and eq. 3.58 gives:

$$t_{DA} = \frac{kt}{\phi\mu cA} \simeq 0.1$$

Fig. 3.8 gives drainage shape factors C_A, together with this t_{DA} time limit for different geometries. For all of the geometrical figures in Fig. 3.8 the approximation of short transition time is very good. Care must be taken for other geometrical configuration, where the transition regime is very large, making the approximation by eq. 3.58 invalid. Necessary condition for eq. 3.58 to be valid is completely closed drainage area, as all the geometrical configurations in Fig. 3.8 are.

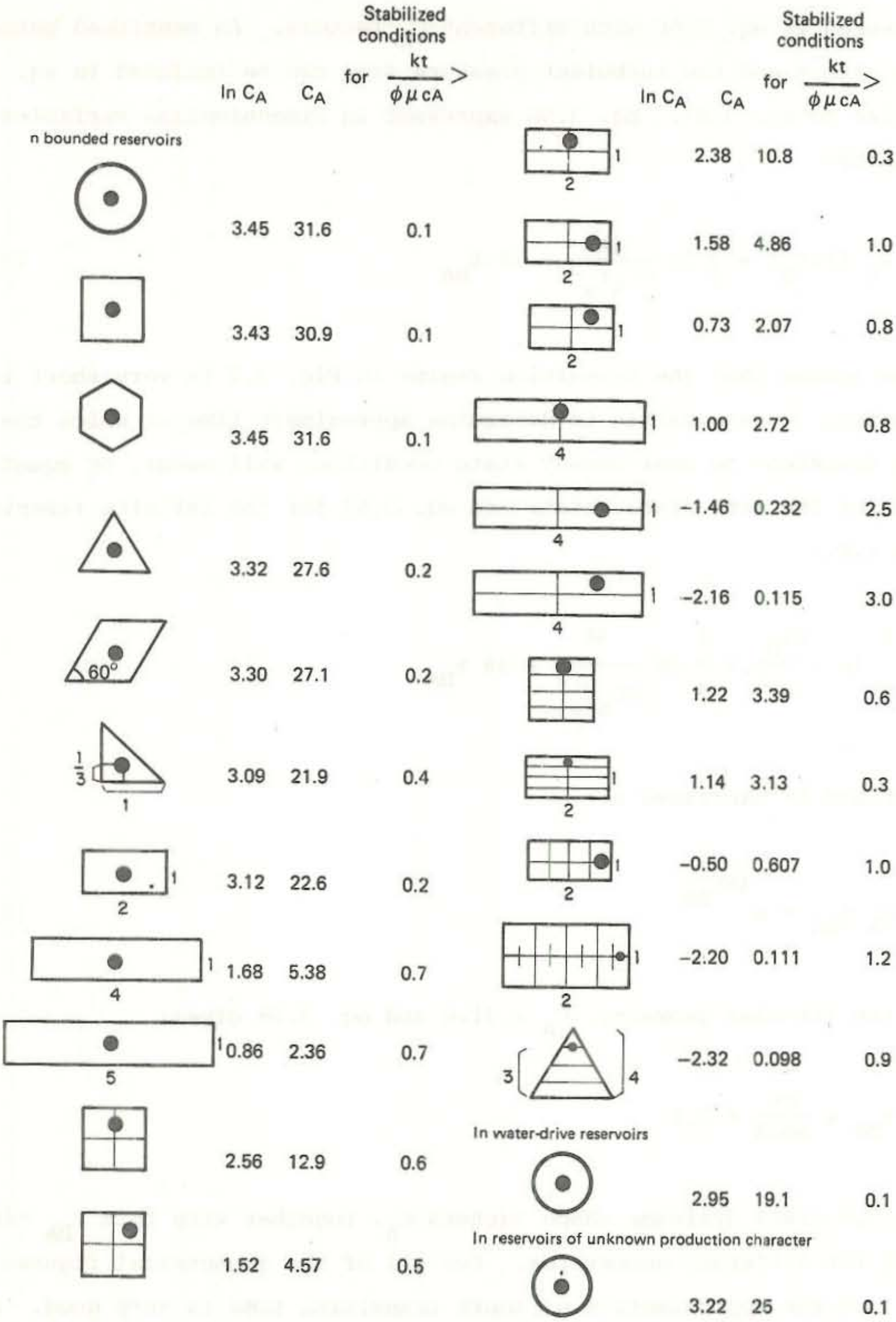

Fig. 3.8 Dietz shape factors for various geometries (Dietz, 1965)

3.5 The infinite reservoir case, Theis solution and interference tests

During the initial transient flow period, it has been found that the well can be approximated by a line source. This assumes that in comparison to the apparently infinite reservoir the wellbore radius is negligible and the wellbore itself can be treated as a line. This leads to a considerable simplification in the mathematics and for this solution the boundary and initial conditions may be stated as follows:

$$
\begin{array}{lll}
1) & P_D = 0 & \text{at} \quad t_D = 0, \text{ for all } r_D \\
2) & P_D = 0 & \text{at} \quad r_D = \infty, \text{ for all } t_D \\
3) & \lim\limits_{r_D \to 0} r_D \dfrac{\partial P_D}{\partial r_D} = 1. & \qquad t_D > 0
\end{array}
\tag{3.59}
$$

The solution to the radial diffusivity equation with these boundary and initial conditions is given by:

$$P_D\ (t_D, r_D) = -\frac{1}{2}\,\mathrm{Ei}\ \left(-\frac{r_D^2}{4t_D}\right) \tag{3.60}$$

This solution is the exponential integral solution. Where the exponential integral is defined by:

$$\mathrm{Ei}(-x) = -\int_x^{\infty} \frac{e^{-u}}{u}\,du \tag{3.61}$$

In groundwater hydrology the solution is known as Theis solution. The exponential integral eq. 3.61 is usually defined thus:

$$W(x) = -\ \mathrm{Ei}(-x) \tag{3.62}$$

$W(x)$ is known as the well function, it can be expanded as follows:

$$W(x) = \gamma + \ln x + \sum_{n=1}^{\infty} \frac{(-1)^n x^n}{n n!} \tag{3.63}$$

where $\gamma = 0.5772$, Eulers constant. If $x<0.01$ it can be approximated as:

$$W(x) \simeq \gamma + \ln x \tag{3.64}$$

If we define:

$$\kappa = e^{\gamma} = e^{0.5772} = 1.781 \tag{3.65}$$

Eq. 3.64 can be written as:

$$Ei(-x) = \ln \kappa x \tag{3.66}$$

Eq. 3.60 can now be approximated as:

$$P_D\ (t_D, r_D) = \frac{1}{2} \ln \frac{4t_D}{\kappa r_D^2} = \frac{1}{2} (\ln \frac{t_D}{r_D^2} + 0.8091) \tag{3.67}$$

provided that:

$$\frac{t_D}{r_D^2} > 25 \tag{3.68}$$

Eq. 3.67 is called the logarithmic approximation.

The exponential integral solution, eq. 3.60, is shown in Fig. 3.9.

As said before the exponential integral solution is a line source solution. If we take into account the radius of the wellbore, the initial and boundary conditions become:

$$\begin{aligned} &1)\quad P_D = 0 &&\text{at}\quad t_D = 0,\ \text{for all } r_D>1 \\ &2)\quad P_D = 0 &&\text{at}\quad r_D = \infty,\ \text{for all } t_D \\ &3)\quad \left(r_D \frac{\partial P_D}{\partial r_D}\right)_{r_D = 1} = 1 \end{aligned} \tag{3.69}$$

which can be compared with eq. 3.59.

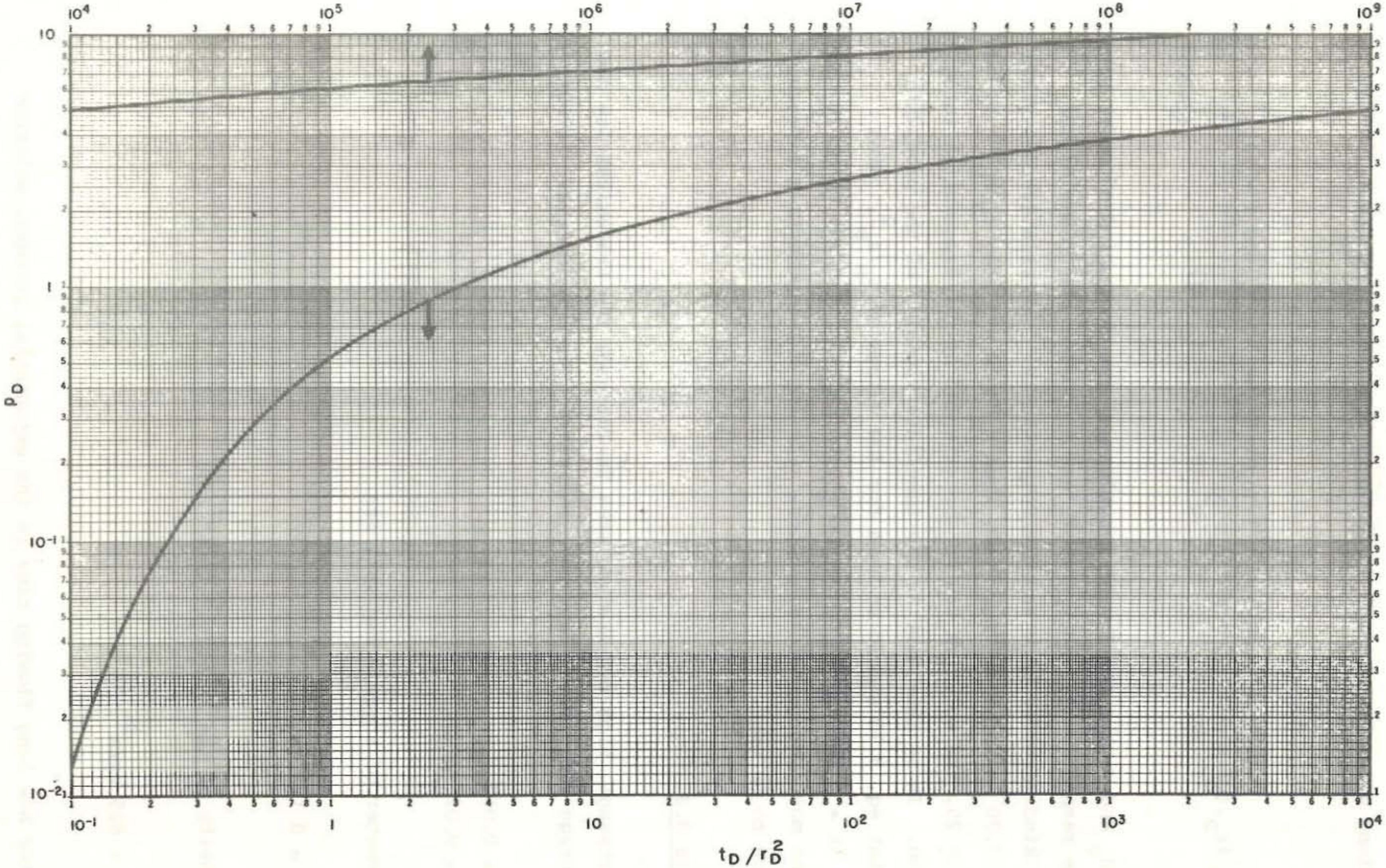

Fig. 3.9 Dimensionless pressure for a single well in an infinite system, no wellbore storage, no skin. Exponential-integral solution (Earlougher 1977)

The solution to the radial diffusivity equation with initial and boundary conditions given by eq. 3.69 is given by Everdingen and Hurst (1949):

$$P_D(r_D,t_D) = \frac{2}{\pi} \int_0^{\infty} \frac{(1-e^{-u^2 t_D}) \, (J_1(u)Y_o(ur_D) - Y_1(u)J_o(ur_D))}{u^2 \, (J_1^{\,2}(u) + Y_1^{\,2}(u))} du \tag{3.70}$$

where J_o and J_1 are the Bessel functions of the first kind of order zero and one respectively, and Y_o and Y_1 are the Bessel functions of the second kind of order zero and one respectively. The relationship given by eq. 3.70 is shown in Fig. 3.10, when $r_D \geq 20$ and when $t_D/r_D^{\,2} \geq 0.5$ or $t_D/r_D^{\,2} \geq 25$, the solution can be approximated by the exponential integral solution. It is thus just in the immediate vicinity of the producing well that eq. 3.70 should be used for low values of $t_D/r_D^{\,2}$. When $r_D = 1$ ($r = r_w$) then the above conditions become, $t_D \geq 25$, which is the case for most geothermal reservoirs, allowing the exponential integral solution to be used.

EXERCISE 3.2

In Svartsengi, high temperature area in Iceland, the transmissivity and the storage coefficient have been estimated, see Kjaran et al. (1980):

$S = 0.012$
$T = 0.012 \ m^2/s$

The diameter of a producing well is:

$d_w = 8 \ 1/2$ in.

The density of the reservoir fluid is:

$\rho_w = 825 \ kg/m^3$

1) After how long flowing time is the exponential integral solution valid for $r = r_w$?

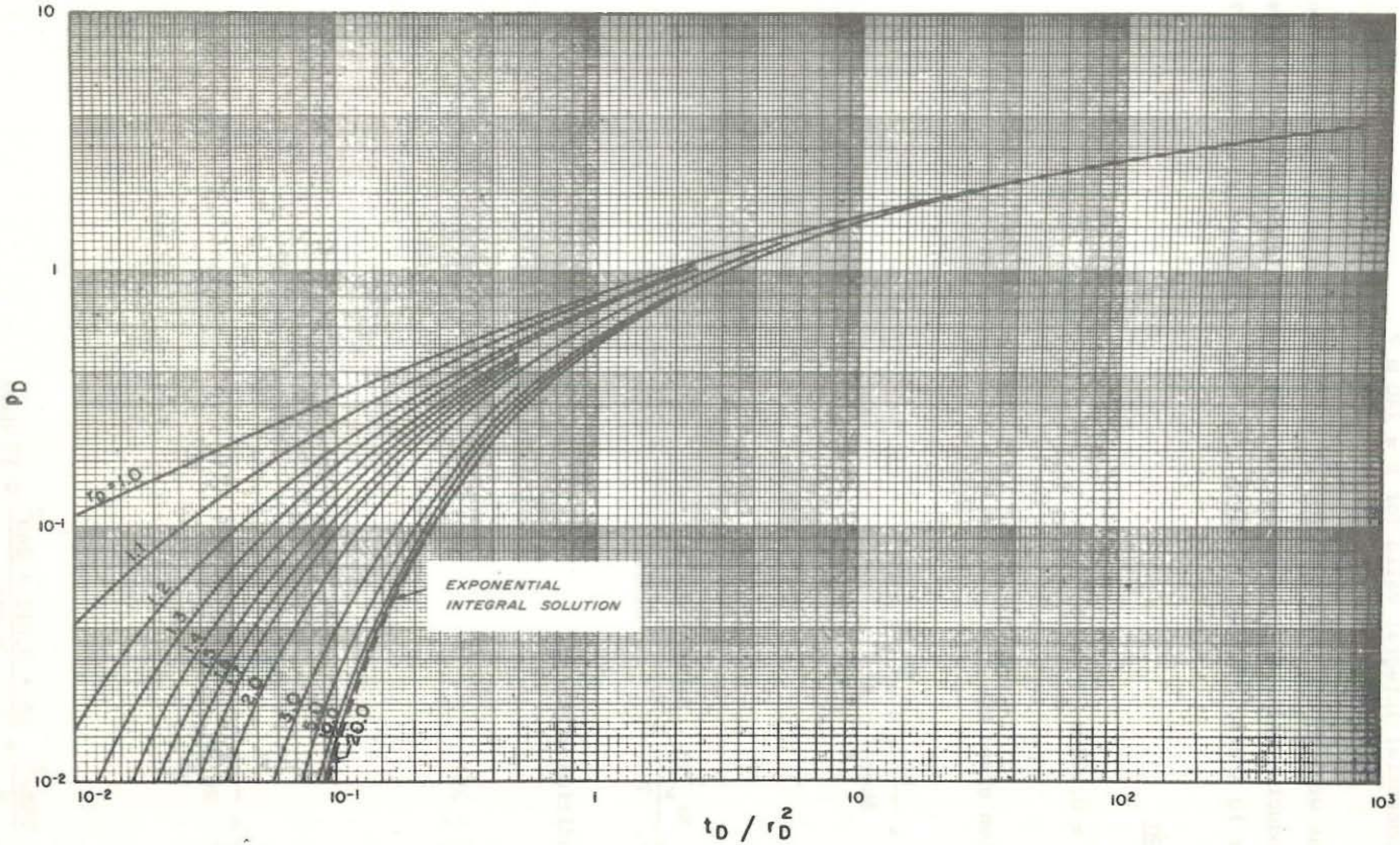

Fig. 3.10 Dimensionless pressure for single well in an infinite system, small r_D, short time, no wellbore storage, no skin. (Mueller and Witherspoon, 1965)

2) After how long flowing time is the logarithmic approximation to the exponential integral valid for $r = 240$ m ?

3) What will be the pressure drop at an observation well 240 m from the producing well, if it has been flowing at the steady rate of 60 kg/s for 10 hours, assuming infinite reservoir conditions still prevail ?

Solution

1) $r_w = 0.108$ m

Condition given by:

$$t_D = \frac{kt}{\phi\mu c r_w^2} = \frac{T}{S r_w^2} t \geq 25$$

or

$$t \geq \frac{S r_w^2 25}{T} = \frac{0.012 \cdot 0.108^2 \cdot 25}{0.012} \cong 0.3 \text{ sec.}$$

2) Condition given by:

$$\frac{t_D}{r_D^2} \geq 25$$

or

$$\frac{t_D}{r_D^2} = \frac{Tt}{S r_w^2 r_D^2} = \frac{Tt}{S r^2} \geq 25$$

or

$$t \geq \frac{25 S r^2}{T} = \frac{25 \cdot 0.012 \cdot 240^2}{0.012} \cong 17 \text{ days}$$

3) Eq. 3.60 and eq. 3.20 give:

$$P_D = \frac{2\pi kh\rho}{W\mu}\,\Delta p = -\frac{1}{2}\,\mathrm{Ei}\,\left(-\frac{r_D^{\,2}}{4t_D}\right)$$

$$\frac{2\pi T}{Wg}\,\Delta p = -\frac{1}{2}\,\mathrm{Ei}\,\left(-\frac{r_D^{\,2}}{4t_D}\right)$$

$$\frac{r_D^{\,2}}{4t_D} = \frac{r_D^{\,2} S r_w^{\,2}}{4Tt} = \frac{r^2 S}{4Tt}$$

$$= \frac{240^2 \cdot 0.012}{4 \cdot 0.012 \cdot 10 \cdot 3600} = 0.4$$

Fig. 3.9 gives:

$$-\mathrm{Ei}\,(-0.4) = 0.35$$

which gives: $P_D = \frac{1}{2} \cdot 0.35 = 0.175$

solving for: Δp

$$\Delta p = \frac{Wg}{2\pi T}\,P_D = \frac{60 \cdot 9.81 \cdot 0.175}{2 \cdot \pi \cdot 0.012} = 1366\ \mathrm{N/m^2}$$

$$\cong 0.014\ \mathrm{bar} = 0.17\ \mathrm{m}$$

The logarithmic approximation gives:

$$P_D = \frac{1}{2}\,\left(\ln \frac{t_D}{r_D^{\,2}} + 0.8091\right) = \frac{1}{2}\,(\ln 0.625 + 0.891) = 0.170$$

which can be compared with the exact value $P_D = 0.175$.

The most common use of the infinite reservoir period in well testing, is to estimate the reservoir parameters k and ϕc. The exponential integral and its logarithmic approximation is often used in the interference well testing analysis. The process of measuring pressure decline in an observation well while another well is producing at constant rate, is named interference test. Two methods are available, the match point method using the exponential integral, and the straight line method using the logarithmic approximation.

By combining eq. 3.20 and eq. 3.60 and taking logarithm of both sides we have:

$$\log \Delta p - \log \frac{W\mu}{2\pi kh\rho} = \log P_D$$

$$\log \frac{r^2}{t} - \log \frac{k}{\phi\mu c} = \log \left(\frac{t_D}{r_D^2}\right) \tag{3.71}$$

By selecting a match point on Fig. 3.9, eq. $P_D = \frac{r_D^2}{t_D} = 1$, we can solve eq. 3.71 with respect to k and ϕc:

$$k = \frac{W\mu}{2\pi h\rho\ \Delta p}$$

$$\phi c = \frac{kt}{\mu r^2} \tag{3.72}$$

or when S and T are used:

$$T = \frac{Wg}{2\pi\ \Delta p}$$

$$S = \frac{Tt}{r^2} \tag{3.73}$$

The match point method is illustrated on Fig. 3.11. It is not restricted to the exponential integral solution, but can be used with any dimensionless pressure function.

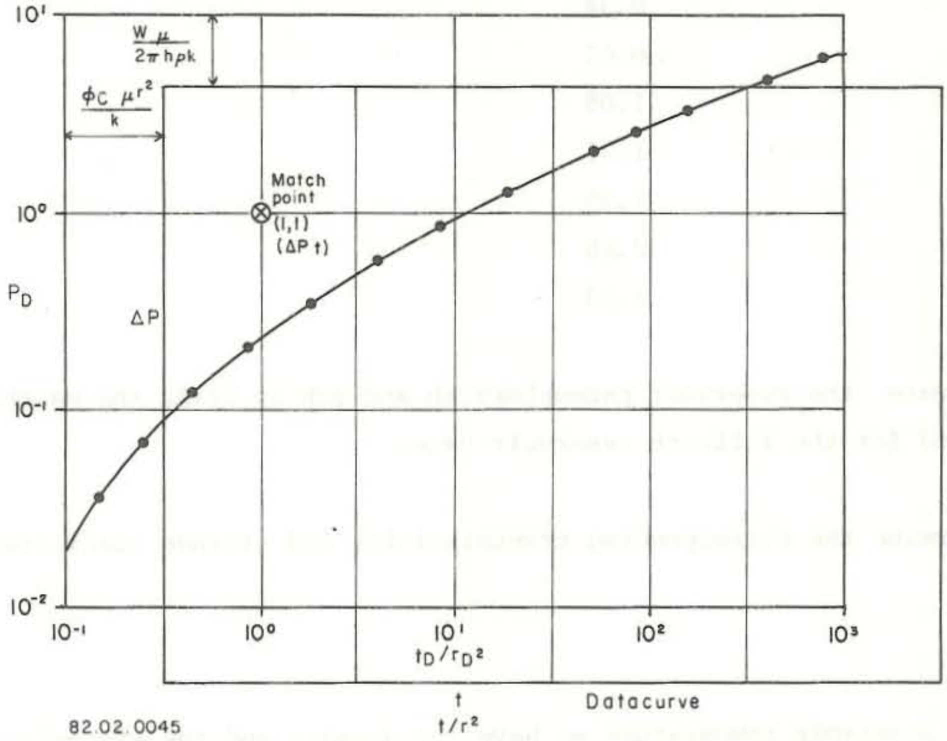

Fig. 3.11 Illustration of the match point method

EXERCISE 3.3

Following data is from an interference test from a geothermal reservoir at East Mesa, in the Imperial Valley, California. Data is taken from Witherspoon et al. (1976).

Reservoir temperature	:	T = 154°C
Distance between the observation well and the producing well	:	r = 1250 ft
Flow rate	:	Q = 130 gpm

The pressure response is given by:

Time hours	Pressure drop, psi
15	0.34
26	0.65
38	1.05
50	1.35
60	1.70
85	2.20
100	2.50

1) Estimate the reservoir parameters kh and ϕch by using the match point method for the infinite reservoir case.

2) Determine the corresponding transmissivity and storage coefficient.

Solution

From the reservoir temperature we have the density and the viscosity.

$$\rho = 913 \text{ kg/m}^3 = 1.77 \text{ slug/ft}^3$$
$$\mu = 0.17 \text{ cp} = 0.35 \cdot 10^{-5} \text{ lb}_f\text{s/ft}^2$$
$$Q = 130 \text{ gpm} = 0.29 \text{ ft}^3/\text{s}$$
$$\rho_{20^\circ C} = 1.94 \text{ slug/ft}^3$$
$$W = Q\rho_{20^\circ C} = 0.563 \text{ slug/s}$$

1) The pressure response is plotted on the datacurve on Fig. 3.12. According to the match point method it is compared with the dimensionless pressure on Fig. 3.9 and the match point is selected. The result for the matchpoint is $(P_D, t_D/r_D^2) = (1,1)$

$\Delta p = 3.8$ psi

$t = 77$ hours

The coefficients can now be calculated according to eq. 3.72.

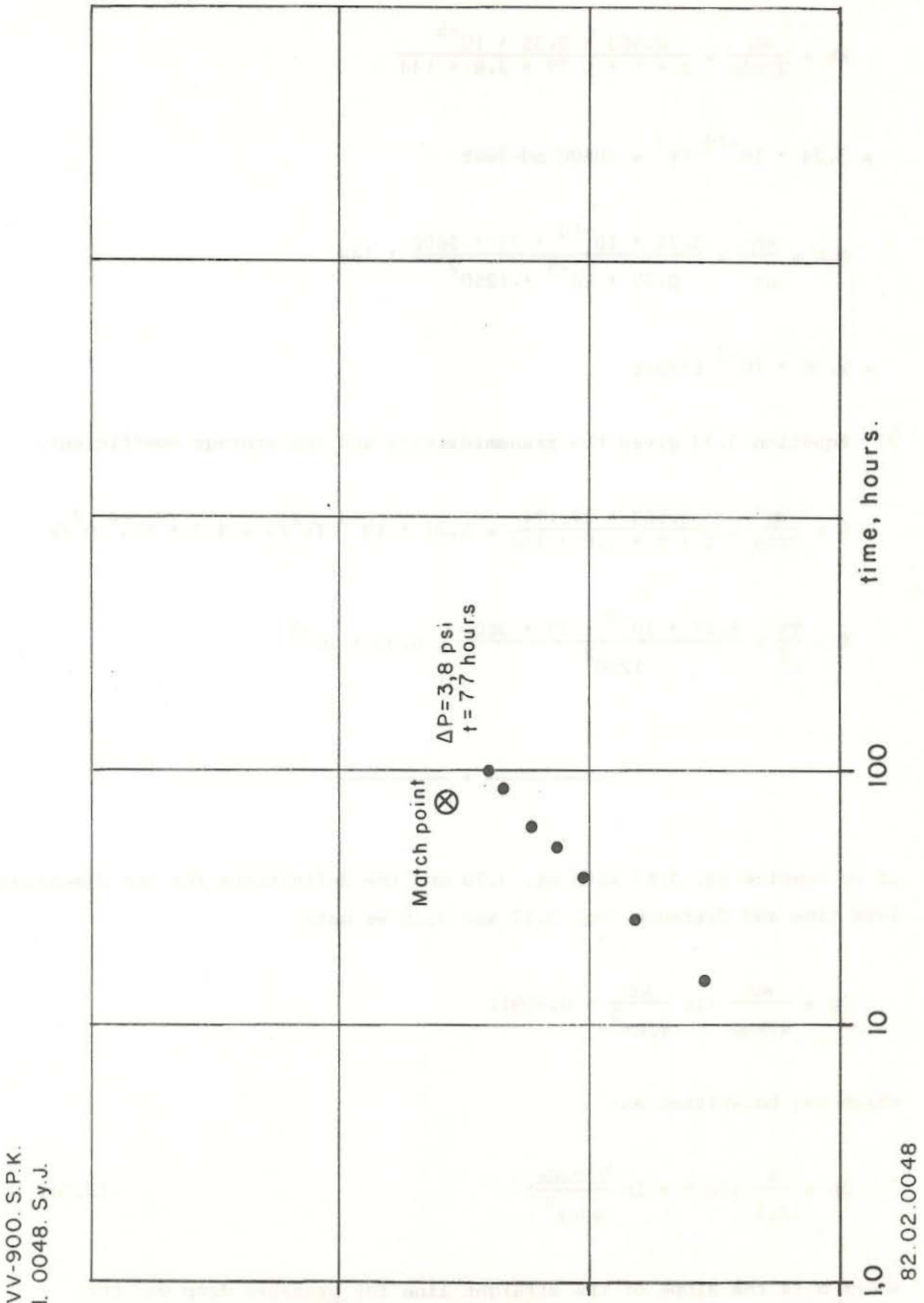

Fig. 3.12 Datacurve for interference test at East Mesa

$$kh = \frac{W\mu}{2\pi\rho\Delta p} = \frac{0.563 \cdot 0.35 \cdot 10^{-5}}{2 \cdot \pi \cdot 1.77 \cdot 3.8 \cdot 144}$$

$$= 3.24 \cdot 10^{-10}\ ft^3 = 30500 \text{ md-feet}$$

$$\phi ch = \frac{kht}{\mu r^2} = \frac{3.24 \cdot 10^{-10} \cdot 77 \cdot 3600}{0.35 \cdot 10^{-5} \cdot 1250^2} \cdot 144$$

$$= 2.36 \cdot 10^{-3}\ ft/psi$$

2) Equation 3.73 gives the transmissivity and the storage coefficient.

$$T = \frac{Wg}{2\pi\Delta p} = \frac{0.563 \cdot 32.174}{2 \cdot \pi \cdot 3.8 \cdot 144} = 5.27 \cdot 10^{-3}\ ft^2/s = 4.9 \cdot 10^{-4}\ m^2/s$$

$$S = \frac{Tt}{r^2} = \frac{5.27 \cdot 10^{-3} \cdot 77 \cdot 3600}{1250^2} = 0.93 \cdot 10^{-3}$$

If we combine eq. 3.67 with eq. 3.20 and the definitions for the dimensionless time and distance, eq. 3.17 and 3.19 we get:

$$\Delta p = \frac{W\mu}{4\pi kh\rho} \left(\ln \frac{kt}{\phi\mu cr^2} + 0.8091\right)$$

which can be written as:

$$\Delta p = \frac{m}{2.3} \left(\ln t + \ln \frac{2.246k}{\phi\mu cr^2}\right) \qquad (3.74)$$

where m is the slope of the straight line for pressure drop vs. the 10-logarithm of time. Eq. 3.74 is the basis for the straight line method mentioned before, but of course eq. 3.68 must be fullfilled for eq. 3.74 to be valid. If we plot the pressure drop vs. the logarithm of time we get an estimate of the permeability from the slope of the line as follows:

$$k = \frac{2.3W\mu}{4\pi h\rho m} \tag{3.75}$$

and expressed in transmissivity coefficient:

$$T = \frac{2.3Wg}{4\pi m} \tag{3.76}$$

If we put $\Delta p = 0$ in eq. 3.74 and define the corresponding time by t_o, eq. 3.74 gives:

$$\phi c = \frac{2.246kt_o}{\mu r^2} \tag{3.77}$$

and expressed in storage coefficient:

$$S = \frac{2.246Tt_o}{r^2} \tag{3.78}$$

EXERCISE 3.4

The following data is from an interference test at Reykir hydrothermal system in south west Iceland (Thorsteinsson, 1975). The temperature of the geothermal water is about 85°C. Well MG-4 was producing 25 l/s for about 17 hours, and the water table drawdown was measured in well MG-11 at a 300 m distance from the pumping well. The measured drawdown is given by:

Time s t	Drawdown m ΔH	Time s t	Drawdown m ΔH
180	0.018	5100	0.195
330	0.040	7200	0.220
510	0.060	10500	0.240
690	0.075	14400	0.265
1020	0.100	18600	0.280
1410	0.120	26400	0.320
1800	0.130	33600	0.330
3000	0.160	54000	0.380
3600	0.170		

1) Estimate the parameters S and T by using the semilog straight line method.

2) What would the drawdown at the pumping well be after ten days of operation if the pumping rate were 25 l/s. The wellbore diameter is 0.22 m.

Solution

The drawdown is plotted on Fig. 3.13 vs. the logarithm of time. According to eq. 3.68 we must have that:

$$t > \frac{25r^2S}{T}$$

When the straight line on Fig. 3.13 is drawn the above condition must be taken into account, thus giving the last points greatest weight, and accordingly the first points deviate from the straight line.

From the reservoir temperature we have the density and mass flow of well MG-4.

$$\rho = 968 \text{ kg/m}^3, \qquad W = \rho Q \cong 24.2 \text{ kg/s}$$

1) According to eq. 3.76 expressed in the slope for the drawdown vs. the logarithm of time we have:

$$T = \frac{2.3W}{4\pi m\rho} = \frac{24.2 \cdot \ln 10}{4 \cdot \pi \cdot 968 \cdot 0.17} \cong 2.69 \cdot 10^{-2} \ m^2/s$$

and eq. 3.78 gives for the storage coefficient:

$$S = \frac{2.246Tt_o}{r^2} = \frac{2.246 \cdot 2.69 \cdot 10^{-2} \cdot 310}{300^2} \simeq 2.08 \cdot 10^{-4}$$

Checking the condition for t we get:

$$t > \frac{25r^2S}{T} = \frac{25 \cdot 300^2 \cdot 2.08 \cdot 10^{-4}}{2.69 \cdot 10^{-2}} \simeq 17398 \text{ sec.}$$

Accordingly the straight line on Fig. 3.13 need not be corrected.

2) Ten days = 864,000 s and the logarithmic approximation can be used. Eq. 3.67 gives:

$$P_D = \frac{1}{2} (\ln \frac{t_D}{r_D^2} + 0.8091)$$

$$= \frac{1}{2} (\ln \frac{Tt}{Sr_w^2} + 0.8091)$$

$$= \frac{1}{2} (\ln \frac{2.69 \cdot 10^{-2} \cdot 864000}{0.11^2 \cdot 2.08 \cdot 10^{-4}} + 0.8091)$$

$$\cong 11.88$$

Eq. 3.23 then gives for the drawdown:

$$\Delta H = \frac{P_D W}{2\pi T\rho} = \frac{11.88 \cdot 24.2}{2 \cdot \pi \cdot 2.69 \cdot 10^{-2} \cdot 968} \simeq 1.76 \text{ m}$$

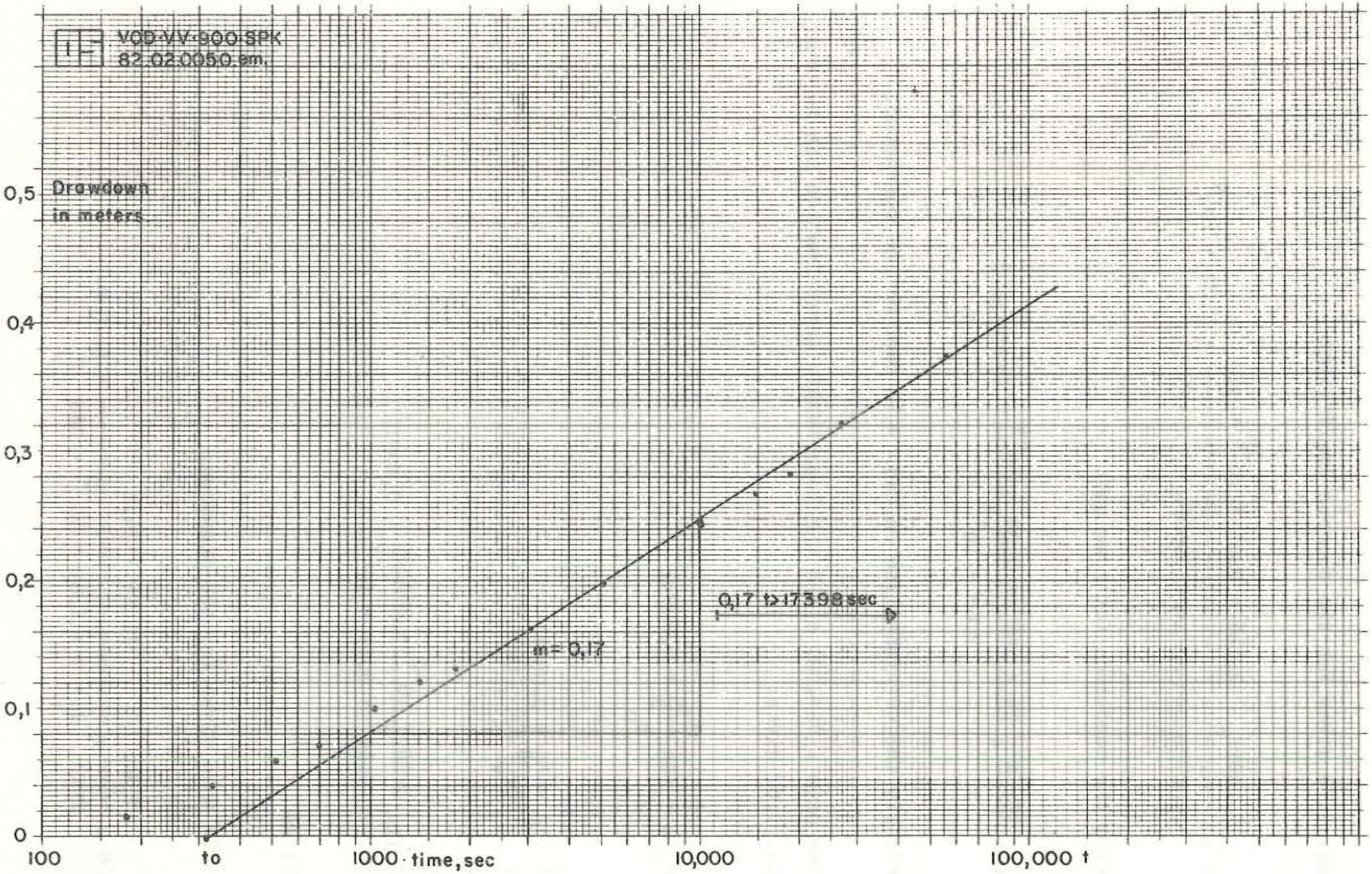

<u>Fig. 3.13</u> Data from an interference test at the Reykir geothermal field, Iceland

Finally two examples of the entire pressure drawdown history for two different reservoirs will be given. The first one is an actual example from the Svartsengi geothermal area in Iceland. Fig. 3.14 shows the pressure drawdown history and reservoir geometry. The pressure drawdown is given by the following equation, see Kjaran et al. (1980):

$$\Delta H = \frac{1}{\rho AS} \sum_{n=o}^{\infty} \sum_{m=o}^{\infty} C_{nm}\, \phi_{nm}(x,y)\phi_{nm}(\xi,\eta) \int_{o}^{t} W(\tau) e^{-(t-\tau)K_{mn}} d\tau \qquad (3.79)$$

where the coefficients are defined as:

$$C_{nm} = \begin{cases} 4 & n \neq 0,\ m \neq 0 \\ 2 & (n \neq 0 \text{ and } m = 0) \text{ or } (n = 0 \text{ and } m \neq 0) \\ 1 & n = 0 \text{ and } m = 0 \end{cases} \qquad (3.80)$$

$$K_{mn} = \frac{S}{\pi^2 T(\frac{m^2}{a^2} + \frac{n^2}{b^2})} \qquad (3.81)$$

$$\phi_{nm} = \cos \frac{m\pi x}{a} \cdot \cos \frac{n\pi y}{b} \qquad (3.82)$$

and other symbols are defined on Fig. 3.14.

Here the first part is as usual the infinite reservoir case and then comes the transition state, which is in this example very large and eq. 3.58 can not be used to estimate the beginning of the semi-steady state. For practical purposes this reservoir has no steady or semi-steady state. It is more like a narrow trench, open in one end but closed in the other end.

The second example is for a well draining from the centre of a circular, bounded drainage area. The variation of the pressure at the boundary with time is given by eqs. 3.55, 3.56 and 3.57. The full solution reads using dimensionless parameters:

$$P_D(t_D) = \frac{2t_D}{r_{eD}^2} + \ln r_{eD} - \frac{3}{4} + 2 \sum_{n=1}^{\infty} \frac{e^{-\alpha_n^2 t_D} J_1^2(\alpha_n r_{eD})}{\alpha_n^2 (J_1^2(\alpha_n r_{eD}) - J_1^2(\alpha_n))} \qquad (3.83)$$

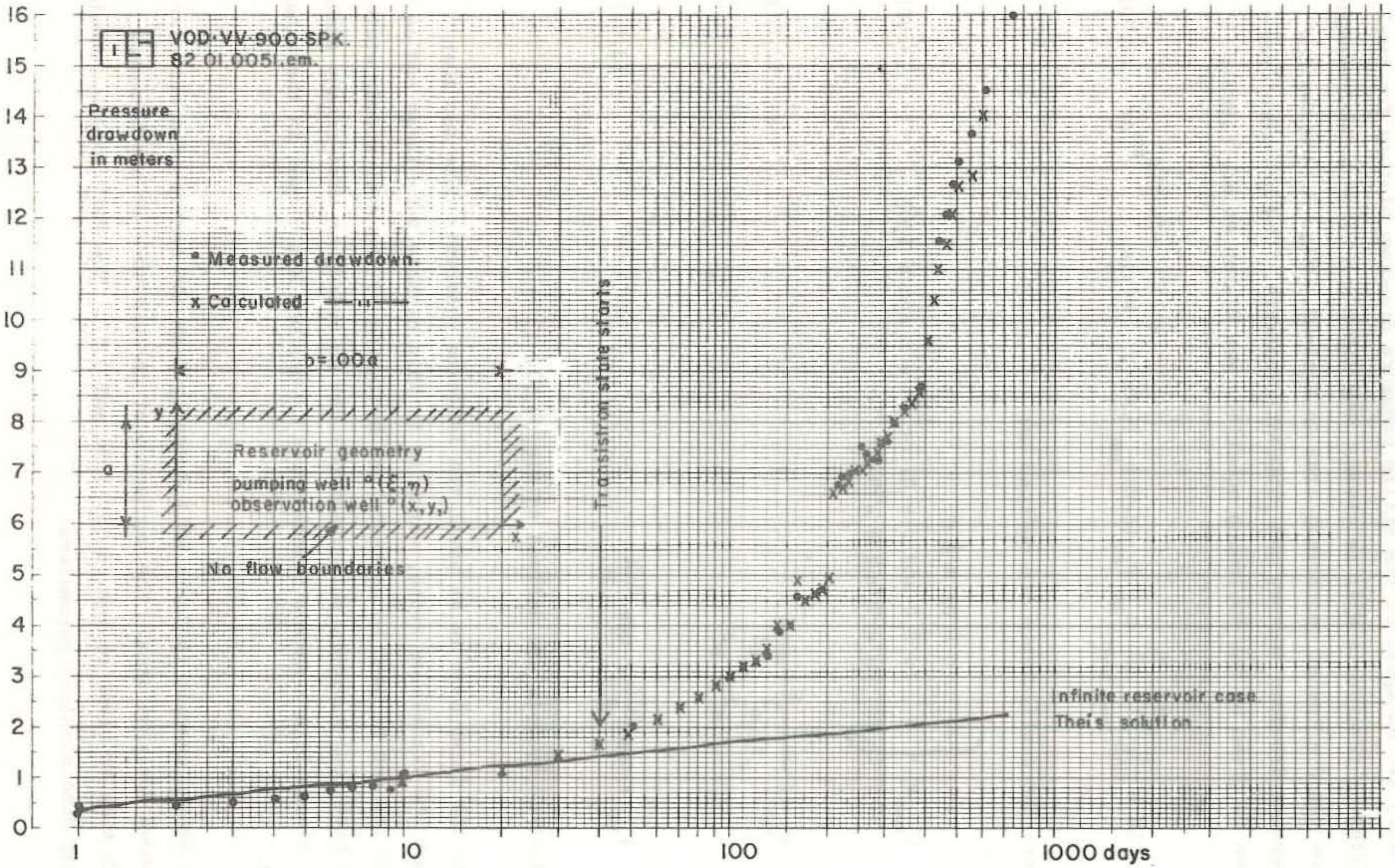

Fig. 3.14 Pressure drawdown history of a well at the Svartsengi geothermal field, Iceland

in which $r_{eD} = r_e/r_w$ and α_n are the roots of:

$$J_1(\alpha_n r_{eD})\ Y_1(\alpha_n) - J_1(\alpha_n)\ Y_1(\alpha_n r_{eD}) = 0 \tag{3.84}$$

J_1 and Y_1 are the Bessel functions of the first and second kind. One thing that can be observed immediately from this equation is that it is extremely complex, to say the least, and yet this is the expression for the case of simple radial symmetry. Fortunately there is a fairly abrupt change from transient to semi-steady state flow so the transient term of eq. 3.83 need never be used to generate the P_D functions. Instead eq. 3.60 can be used for small values of the flowing time and eq. 3.56 for large values, with the transition occurring, according to eq. 3.58, at $t_{DA} \simeq 0.1$.

These two examples are given to show, that sometimes the full solution must be used for the pressure behaviour and in other cases just the infinite reservoir solution and the semi-steady state (steady state) solution are satisfactory to describe the pressure distribution.

3.6 Constant pressure solution

The transient behaviour of a well operating at constant pressure is analogous to that of a well operating at a constant flow rate. In a constant pressure flow test, the well is assumed to produce at a constant bottom-hole pressure and flow rate is recorded with time. As will be discussed later the well flowing at constant rate is influenced by wellbore storage i.e. changes in the quantity of fluid contained in the well itself. The constant pressure well is there against not influenced by the wellbore storage effect. However, if the surface pressure is maintained constant, the frictional pressure drop in the wellbore may act in a manner similar to wellbore storage, causing bottom-hole pressure to vary during the test. Fig. 3.15 schematically represents pressure and rate behaviour in a constant-pressure drawdown test.

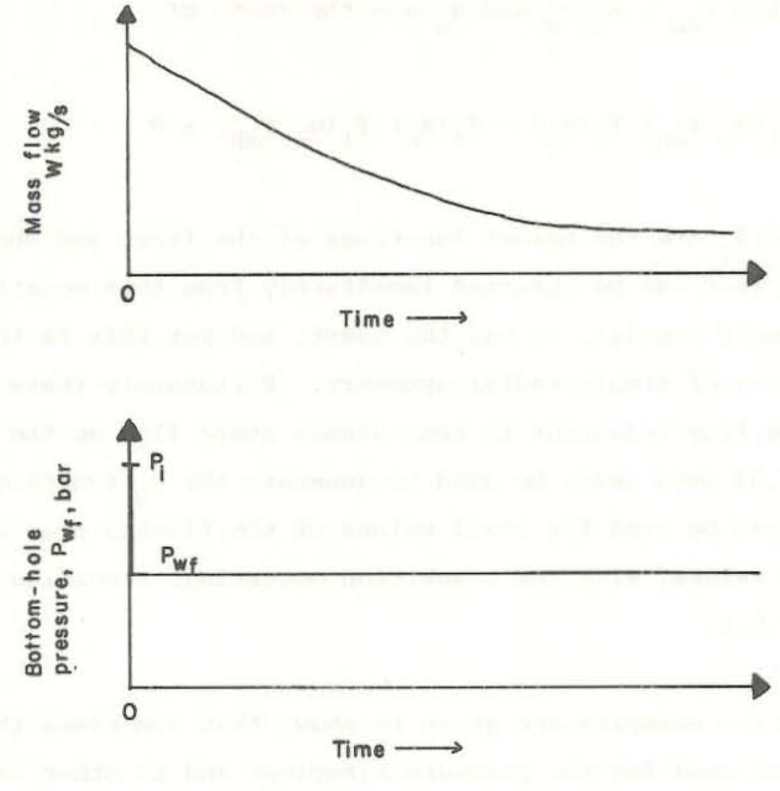

Fig. 3.15 Schematic representation of massflow and pressure histories during a constant pressure test

The differential equation for the flow situation is the same as before, the radial diffusivity equation, eq. 3.21. The initial and boundary conditions are given by:

$$
\begin{aligned}
&1)\quad P_D = 0 && \text{at} \quad t_D = 0, \text{ for all } r_D \\
&2)\quad P_D = 0 && \text{at} \quad r_D = \infty, \text{ for all } t_D > 0 \\
&3)\quad P_D = \frac{2\pi k h \rho}{W\mu}(p_i - p_{wf}) && \text{at} \quad r_D = 1, \text{ for all } t_D > 0
\end{aligned}
\tag{3.85}
$$

The solution is given by Jacob and Lohman (1952):

$$W_D(t_D) = \frac{4t_D}{\pi} \int_0^\infty x e^{-t_D x^2} \left\{\frac{\pi}{2} + \operatorname{arctg}\left(Y_o(x)/J_o(x)\right)\right\} dx \tag{3.86}$$

in which $J_o(x)$ and $Y_o(x)$ are Bessel functions of zero order of the first and second kinds, respectively, and:

	10^{-4}	10^{-3}	10^{-2}	10^{-1}	1	10	10^{2}	10^{3}
1	56.9	18.34	6.13	2.249	0.985	0.534	0.346	0.251
2	40.4	13.11	4.47	1.716	0.803	0.461	0.311	0.232
3	33.1	10.79	3.74	1.477	0.719	0.427	0.294	0.222
4	28.7	9.41	3.30	1.333	0.667	0.405	0.283	0.215
5	25.7	8.47	3.00	1.234	0.630	0.389	0.274	0.210
6	23.5	7.77	2.78	1.160	0.602	0.377	0.268	0.206
7	21.8	7.23	2.60	1.103	0.580	0.367	0.263	0.203
8	20.4	6.79	2.46	1.057	0.562	0.359	0.258	0.200
9	19.3	6.43	2.35	1.018	0.547	0.352	0.254	0.198
10	18.3	6.13	2.25	0.985	0.534	0.346	0.251	0.196
	10^{4}	10^{5}	10^{6}	10^{7}	10^{8}	10^{9}	10^{10}	10^{11}
1	0.1964	0.1608	0.1360	0.1177	0.1037	0.0927	0.0838	0.0764
2	0.1841	0.1524	0.1299	0.1131	0.1002	0.0899	0.0814	0.0744
3	0.1777	0.1479	0.1266	0.1106	0.0982	0.0883	0.0801	0.0733
4	0.1733	0.1449	0.1244	0.1089	0.0968	0.0872	0.0792	0.0726
5	0.1701	0.1426	0.1227	0.1076	0.0958	0.0864	0.0785	0.0720
6	0.1675	0.1408	0.1213	0.1066	0.0950	0.0857	0.0779	0.0716
7	0.1654	0.1393	0.1202	0.1057	0.0943	0.0851	0.0774	0.0712
8	0.1636	0.1380	0.1192	0.1049	0.0937	0.0846	0.0770	0.0709
9	0.1621	0.1369	0.1184	0.1043	0.0932	0.0842	0.0767	0.0706
10	0.1608	0.1360	0.1177	0.1037	0.0927	0.0838	0.0764	0.0704

Table 3.1 Values of W_D for values of t_D between 10^{-4} and 10^{12} (Jacob and Lohman 1952)

$$W_D = \frac{\mu W}{2\pi k \rho h (p_i - p_{wf})} \tag{3.87}$$

and t_D is defined by eq. 3.17. The dimensionless mass flow function, W_D, has been evaluated by Jacob and Lohman (1952) and is given in Table 3.1 and Fig. 3.16. The match point can be used as before to estimate the reservoir coefficients. By selecting the match point $W_D = t_D = 1$ on Fig. 3.16 we have:

$$k = \frac{W\mu}{2\pi\rho h (p_i - p_{wf})} \tag{3.88}$$

and

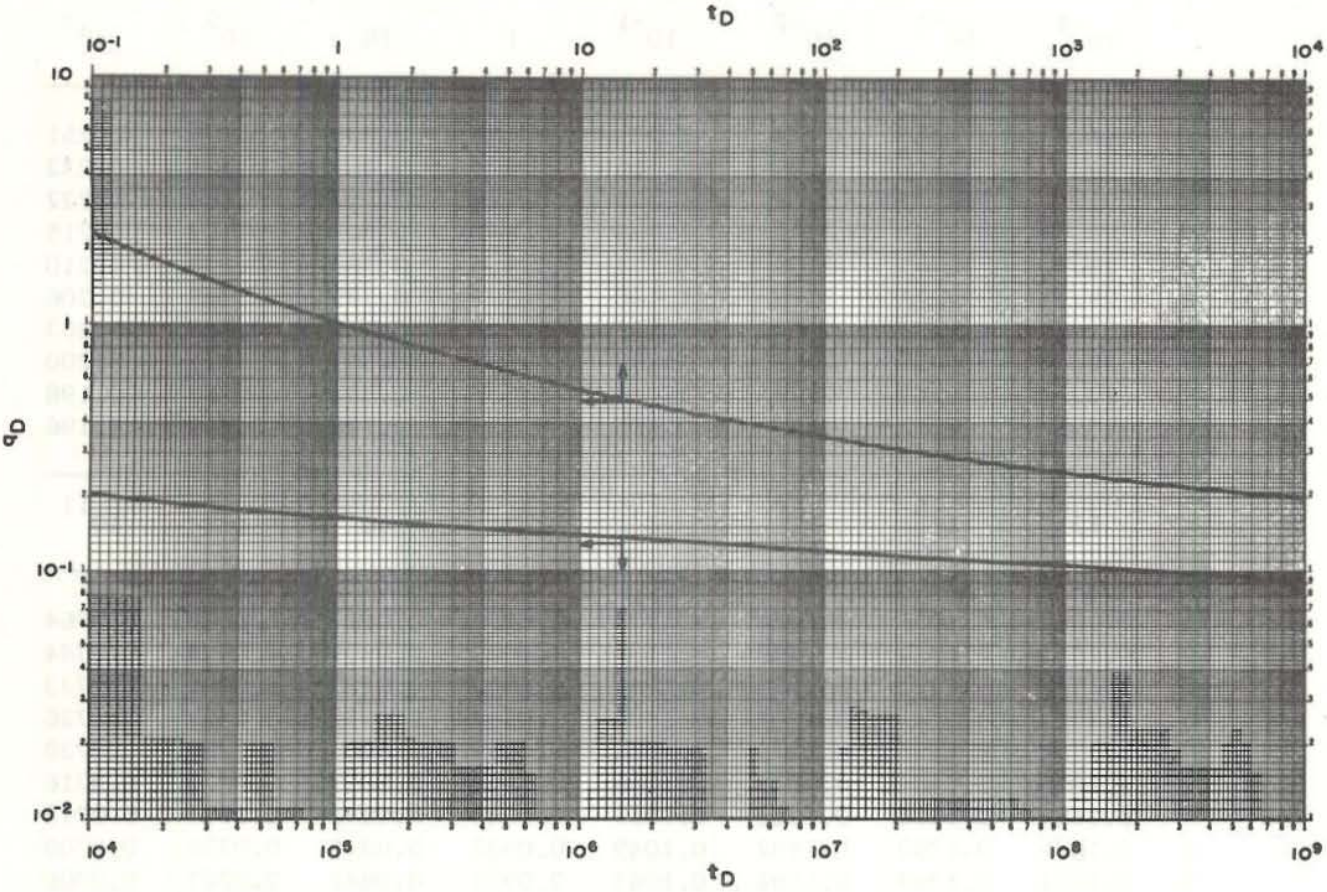

Fig. 3.16 Dimensionless mass flow function for a single well in an infinite system (Jacob and Lohman 1952)

$$\phi c = \frac{kt}{\mu r_w^2} \tag{3.89}$$

or when S and T are used:

$$T = \frac{Wg}{2\pi(p_i - p_{wf})} \tag{3.90}$$

$$S = \frac{Tt}{r_w^2} \tag{3.91}$$

According to Jacob and Lohman (1952) the function W_D can be approximated for large values of time by:

$$W_D \cong \frac{2}{W(\frac{1}{4t_D})} \tag{3.92}$$

According to eq. 3.62 and eq. 3.64 $W(\frac{1}{4t_D})$ can be approximated for large values of time, by:

$$W(\frac{1}{4t_D}) \cong \ln t_D + 0.8091 \tag{3.93}$$

and inserting in eq. 3.92 gives:

$$W_D \simeq \frac{2}{\ln t_D + 0.8091} \tag{3.94}$$

Eq. 3.94 is correct within 0.1 percent for $t_D \geq 5 \cdot 10^{11}$. The error is only 1 percent when $t_D \geq 8 \cdot 10^4$ and is 2 percent when $t_D \geq 5 \cdot 10^3$.

Inserting eq. 3.94 into eq. 3.87 results in:

$$\frac{1}{W} = \frac{\mu}{4\pi k\rho h(p_i - p_{wf})} (\ln \frac{kt}{\phi\mu c r_w^2} + 0.8091) \tag{3.95}$$

which can be written as:

$$\frac{1}{W} = m\ (\ln t + \ln \frac{2.246k}{\phi\mu c r_w^2}) \tag{3.96}$$

where m is the slope of the straight line for 1/W vs. the logarithm of time. From the slope we have as before an estimate for the permeability:

$$k = \frac{\mu}{4\pi h\rho(p_i - p_{wf})m} \tag{3.97}$$

and expressed in transmissivity and pressure head:

$$T = \frac{1}{4\pi\rho\Delta Hm} \tag{3.98}$$

If we put $\frac{1}{W} = 0$ in eq. 3.96 and define the corresponding time by t_o we have:

$$\phi c = \frac{2.246kt_o}{\mu r_w^2} \tag{3.99}$$

and expressed in storage coefficient:

$$S = \frac{2.246Tt_o}{r_w^2} \tag{3.100}$$

The skin factor can be included if necessary. See chapter 3.16 for discussion on the skin factor.

EXERCISE 3.5

The following data is from a constant pressure test in Seltjarnarnes low temperature area in Iceland (Thorsteinsson 1969). The temperature of the geothermal water is 77.5°C. The mass flow of well S-2 is given on Fig. 3.17 as a function of the logarithm of time. The recorded pressure drop due to the opening of the well was 1 bar. Estimate the transmissivity of the reservoir.

Solution

From the reservoir temperature we have, $\rho = 973\ kg/m^3$. We then have:

$$\Delta H = \frac{10^5}{973 \cdot 9.81} = 10.48\ m$$

By using Fig. 3.17 we have according to eq. 3.98:

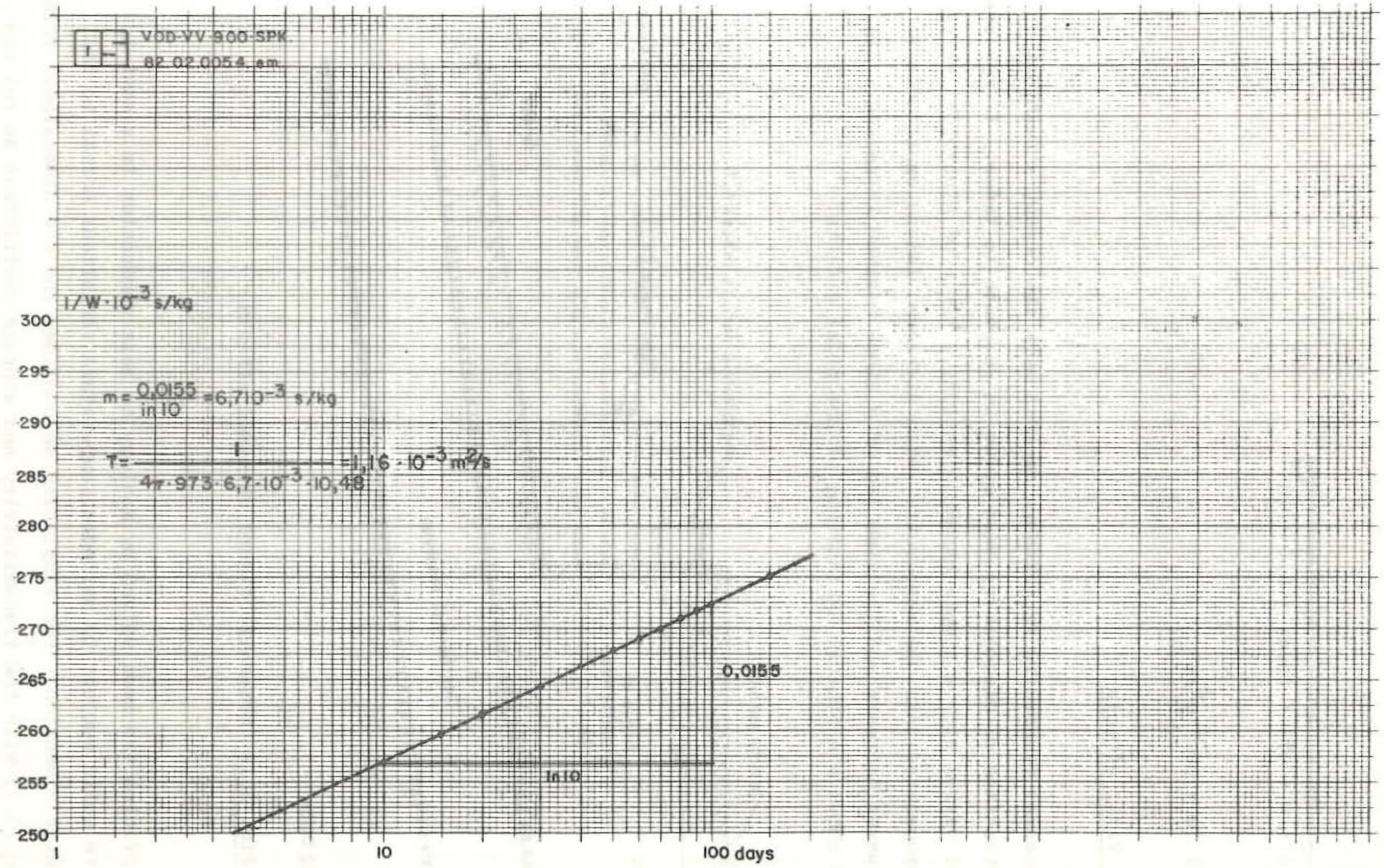

Fig. 3.17 Data from a constant pressure test in Seltjarnarnes, Iceland

$$T = \frac{1}{4\pi\rho\Delta Hm}$$

$$= \frac{1}{4 \cdot \pi \cdot 973 \cdot 10.48 \cdot 6.7 \cdot 10^{-3}}$$

$$\simeq 1.16 \cdot 10^{-3}\ m^2/s$$

3.7 Tidal effects

In coastal reservoirs in pressure contact with the ocean, sinusoidal fluctuations of piezometric head occur in response to tides. If the sea level varies with a simple harmonic motion, a train of sinusoidal waves is propagated into the reservoir. With distance, inland amplitudes of the waves decrease and the time lag of a given maximum increases. Fig. 3.18 shows a schematic explanation of the tidal effects.

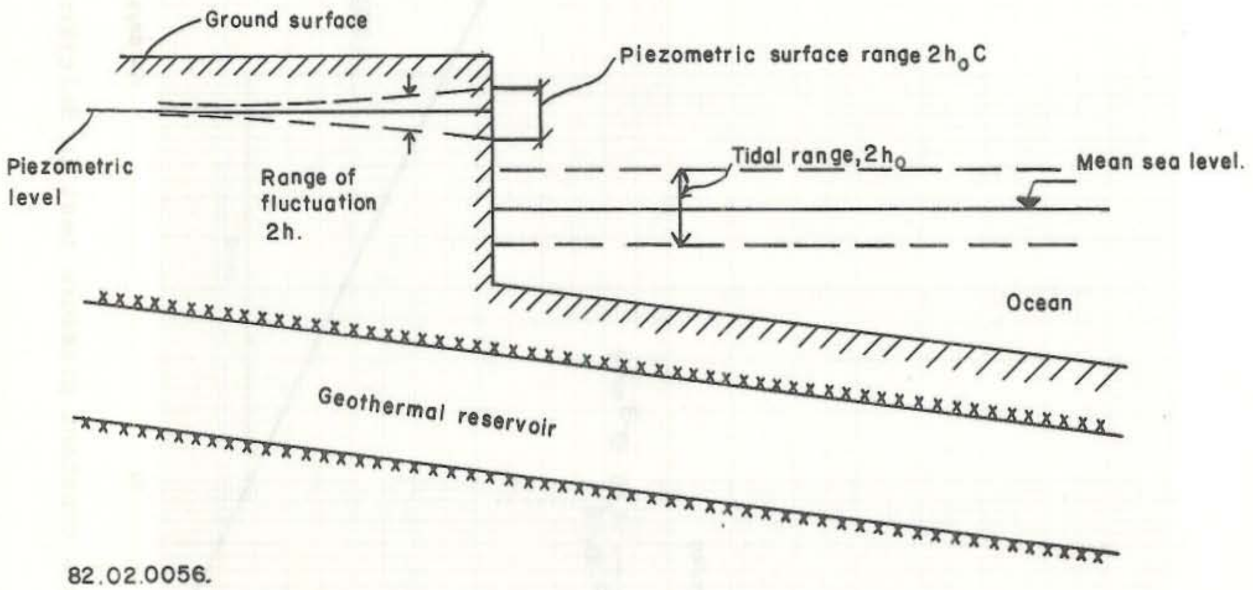

Fig. 3.18 Schematic figure of tidal effects

The problem has been solved by analogy to heat conduction in a semi-infinite solid subject to periodic temperature variations normal to the infinite dimension. For simplicity we consider the one dimensional form of eq. 3.13 with the transmissivity and storage coefficient as the reservoir parameters. The one dimensional equation is given by:

$$\frac{\partial^2 h}{\partial x^2} = \frac{S}{T}\frac{\partial h}{\partial t} \tag{3.101}$$

The boundary conditions are given by:

$$\begin{aligned} h &= h_o \sin wt & x &= o \\ h &= o & x &= \infty \end{aligned} \tag{3.102}$$

The angular velocity is ω for a tidal period t_o:

$$\omega = \frac{2\pi}{t_o} \tag{3.103}$$

The solution is given by, see Carslaw and Jaeger (1959):

$$h = h_o\, e^{-x\sqrt{\frac{\pi S}{t_o T}}} \sin\left(\frac{2\pi t}{t_o} - x\sqrt{\frac{\pi S}{t_o T}}\right) \tag{3.104}$$

The amplitude of the piezometric level is then given by:

$$h_x = h_o\, e^{-x\sqrt{\frac{\pi S}{t_o T}}} \tag{3.105}$$

This eq. can be written as:

$$x = \sqrt{\frac{t_o T}{\pi S}}\, \ln\left(\frac{h_o}{h_x}\right) \tag{3.106}$$

If m_1 is the slope of the straight line for x vs. the logarithm of the range ratio we have from eq. 3.106:

$$\frac{T}{S} = \frac{m_1^2 \pi}{t_o} \tag{3.107}$$

The time lag t_L of a given maximum or minimum after it occurs in the ocean can be obtained by solving the quantity within the parentheses of eq. 3.104 for t, so that:

$$t_L = x\sqrt{\frac{t_o S}{4\pi T}} \tag{3.108}$$

If m_2 is now the slope of the straight line for x vs. the time lag, t_L we have from eq. 3.108:

$$\frac{T}{S} = \frac{m_2 t_o}{4\pi} \tag{3.109}$$

Eq. 3.107 and eq. 3.109 can be used to estimate the ratio between the transmissivity and storage coefficient. If the ocean is not in direct contact with the aquifer, but acts as a loading of the reservoir, the situation is as described in Fig. 3.19.

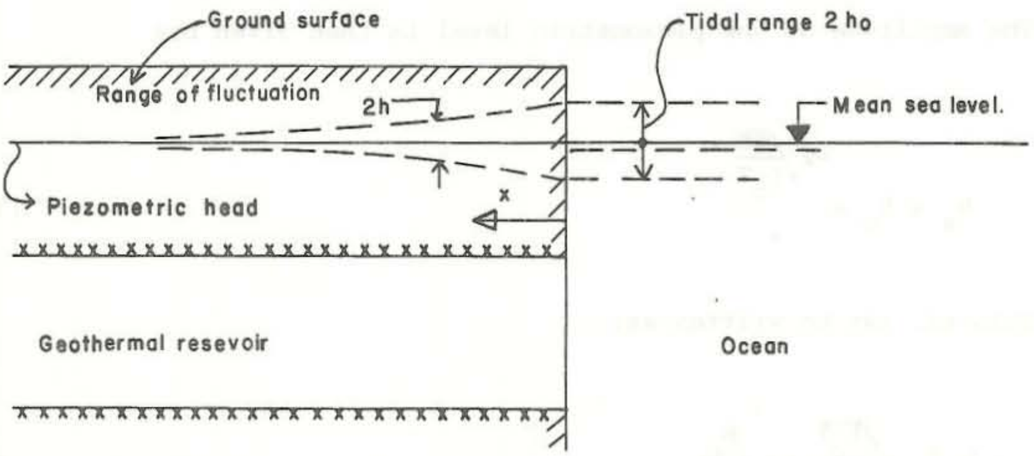

82.02.0055.

Fig. 3.19 Schematic figure of tidal loading of reservoir

C is the tidal efficiency as explained in chapter 2. Eq. 3.105 now becomes:

$$h_x = Ch_o\, e^{-x\sqrt{\frac{\pi S}{t_o T}}} \tag{3.110}$$

and eq. 3.106 now is:

$$x = \sqrt{\frac{t_o T}{\pi S}}\,(\ln \frac{h_o}{h_x} + \ln C) \tag{3.111}$$

Eq. 3.107, 3.108 and eq. 3.109 remain unchanged. The tidal efficiency can be determined from the straight line graph of x vs. the logarithm of the range ratio, according to:

$$C = (\frac{h_x}{h_o})_{x=o} \tag{3.112}$$

EXERCISE 3.6

The following data is from the Laugarnes hydrothermal system in Reykjavík, Iceland (Thorsteinsson and Elíasson 1970). The range ratio has been measured in different wells in different distances from the shore. The result is given in the following table:

Well No	Range ratio %	Distance m
G6	2.19	1000
G21	3.80	660
G13	4.32	580
G5	4.79	540
G8	5.89	380
G14	10.23	60

The tidal period is 12.3 hours.

1) What is the ratio between the transmissivity and storage coefficient?

2) What is the tidal efficiency?

Solution

1) The data is plotted on Fig. 3.20, and the slope of the straight line is calculated. Eq. 3.107 now gives:

$$\frac{T}{S} = \frac{m^2\pi}{t_o} = \frac{608.01^2 \cdot \pi}{12.3 \cdot 3600} = 26.2\ m^2/s.$$

2) From Fig. 3.20 we find the tidal efficiency according to eq. 3.112:

$$C = \left(\frac{h_x}{h_o}\right)_{x=o} = 11.5\%.$$

Regular semidiurnal fluctuations of small magnitude have been observed in piezometric surfaces of some reservoirs far away from shore. These fluctuations have been attributed to earth tides, resulting from the attraction exerted on the earth's crust by the moon and, to a lesser extent, the sun.

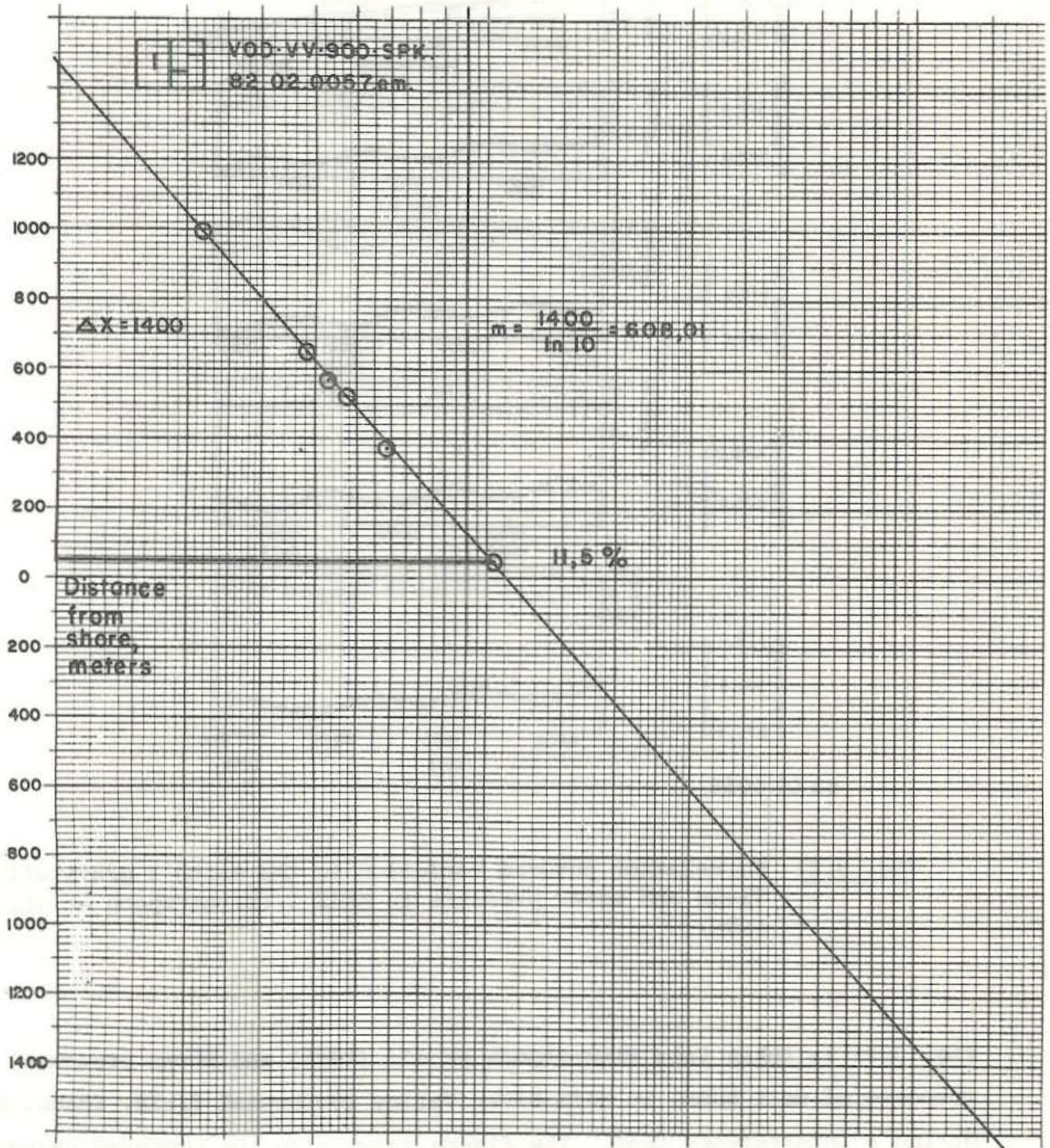

Fig. 3.20 Semilogarithmic plot of range ratios observed in wells at the Laugarnes hydrothermal system against distances from shore (Thorsteinsson and Elíasson 1970)

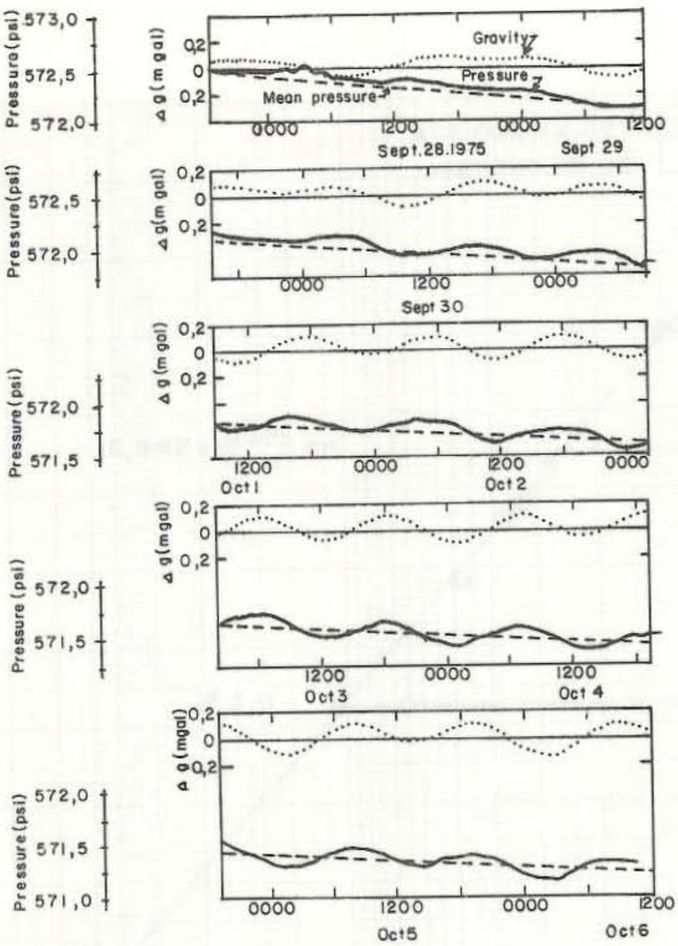

Fig. 3.21 Correlation between variation in the earth's gravitational field and water pressure in RRGE 1. (Witherspoon et al. 1976)

Fig. 3.21 is taken from Witherspoon et al. (1976) and shows pressure response of well RRGE, in Raft River Valley geothermal field, Idaho, U.S.A., during a interference test. The figure shows also the computed changes in the earth's gravitational field for the period September 28 to October 6, 1975. It is clearly seen from this figure that superposed on the overall pressure decline caused by interference due to the producing well are the periodic pressure changes caused by the earth tide effects.

A theoretical study of the response of a well-aquifer system to earth tides has been carried out by Bredehoeft (1975).

3.8 Pressure buildup and Horner methods

One of the most powerful tools at the reservoir engineers disposal in solving complex flow problems is the superposition principle. Let us therefore begin this chapter on pressure buildup by explaining the method. Mathematically the superposition principle states that any sum of individual solutions of a second order linear differential equation is also a solution of the equation. As the differential equation 3.12 is a linear second order differential equation the superposition principle applies. Let us take for an example the case of a well producing at a series of constant rates for the different time periods shown in Fig. 3.22. To determine the wellbore pressure after a total flowing time t_n, when the current mass flow is W_n, the superposition principle is applied to determine the solution in terms of:

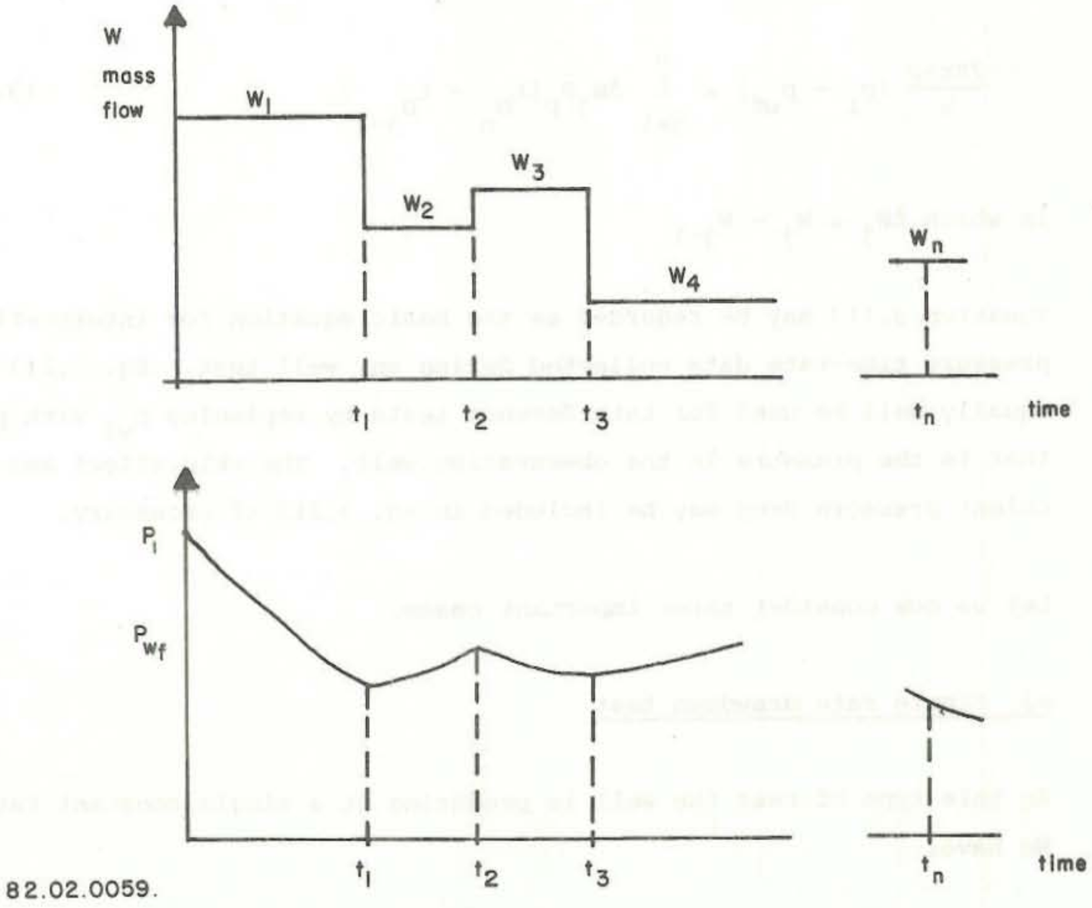

Fig. 3.22 Mass flow history of a well and bottom hole pressure as functions of time

W_1	acting for time	t_n
$+ \ (W_2 - W_1)$	acting for time	$(t_n - t_1)$
$+ \ (W_3 - W_2)$	acting for time	$(t_n - t_2)$
$+ \ (W_i - W_{i-1})$	acting for time	$(t_n - t_{i-1})$
$+ \ (W_n - W_{n-1})$	acting for time	$(t_n - t_{n-1})$

Perhaps the best way to look at the problem is as follows. The initial mass flow W_1, acts over the entire period t_n. At time t_1 a new well is opened to flow at precisely the same location as the original well at a rate $(W_2 - W_1)$ so that the net mass flow after t_1 is W_2. At time t_2 a third well is opened at the same location with mass flow $(W_3 - W_2)$ which reduces the mass flow to W_3 after time t_2 ..... etc.

The complete solution is then:

$$\frac{2\pi kh\rho}{\mu}(p_i - p_{wf}) = \sum_{j=1}^{n} \Delta W_j P_D(t_{D_n} - t_{D_{j-1}}) \qquad (3.113)$$

in which $\Delta W_j = W_j - W_{j-1}$

Equation 3.113 may be regarded as the basic equation for interpreting the pressure time-rate data collected during any well test. Eq. 3.113 may equally well be used for interference tests by replacing p_{wf} with $p(r,t)$ that is the pressure in the observation well. The skin effect and turbulent pressure drop may be included in eq. 3.113 if necessary.

Let us now consider three important cases.

a) Single rate drawdown test

In this type of test the well is producing at a single constant rate. We have:

$$W_1 = W; \quad \Delta W_1 = W; \quad t_{D_n} = t_D$$

And eq. 3.113 reduces to:

$$\frac{2\pi kh\rho}{W\mu}(p_i - p_{wf}) = P_D(t_D) \tag{3.114}$$

which is the equation we have been discussing so far.

b) Pressure buildup testing

This is probably the most common of all well test techniques and the main objective of this chapter. The mass flow and the corresponding pressure response are shown in Fig. 3.23. The well is run at a constant mass flow rate W for a time t and then closed in. During the latter period the closed-in pressure $p_{wf} = p_{ws}$ is recorded as a function of the closed-in time Δt. Eq. 3.113 can again be used but in this case with:

$$W_1 = W; \quad \Delta W_1 = W; \quad t_{D_n} = t_D + \Delta t_D$$
$$W_2 = 0; \quad \Delta W_2 = -W; \quad t_{D_n} - t_D = \Delta t_D$$

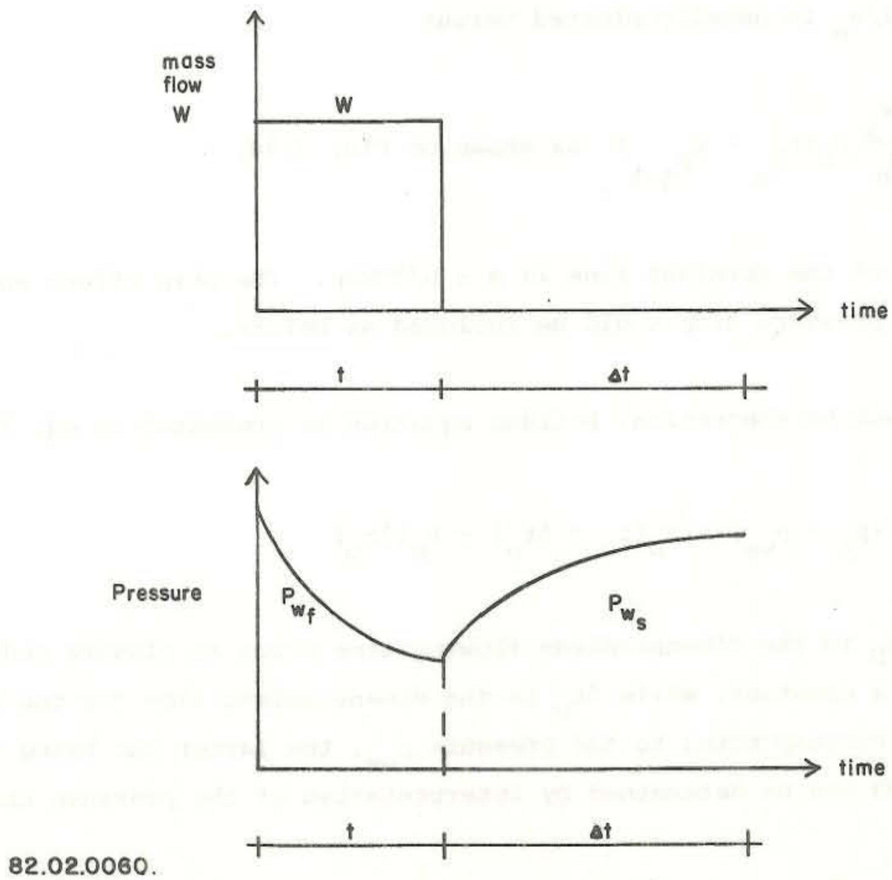

Fig. 3.23 Pressure buildup test a) mass flow b) pressure response

If the skin effect and turbulent pressure drop were included in eq. 3.113 they would disappear by cancellation and the equation reduces to:

$$\frac{2\pi kh\rho}{W\mu}(p_i - p_{ws}) = P_D(t_D + \Delta t_D) - P_D(\Delta t_D) \tag{3.115}$$

Eq. 3.115 is the basic equation for pressure buildup analysis and will be discussed in more detail in the following.

c) Multi-rate drawdown testing

In this form of the well test the mass flow is not constant but varies as a function of time and eq. 3.113 is used directly to analyse the results. Eq. 3.113 is usually written as:

$$\frac{2\pi kh\rho}{W_n\mu}(p_i - p_{wf}) = \sum_{j=1}^{n} \frac{\Delta W_j}{W_n} P_D(t_{D_n} - t_{D_{j-1}}) \tag{3.116}$$

$(p_i - p_{wf})/W_n$ is usually plotted versus

$\sum_{j=1}^{n} \frac{\Delta W_j}{W_n} P_D(t_{D_n} - t_{D_{j-1}})$ as shown on Fig. 3.24.

The slope of the straight line is $m = \mu/2\pi kh\rho$. The skin effect and the turbulent pressure drop could be included as before.

Turning back to theoretical buildup equation as presented in eq. 3.115

$$\frac{2\pi kh\rho}{W\mu}(p_i - p_{ws}) = P_D(t_D + \Delta t_D) - P_D(\Delta t_D)$$

in which t_D is the dimensionless flowing time prior to closure and is therefore a constant, while Δt_D is the dimensionless time for the closed in period corresponding to the pressure p_{ws}, the latter two being variables which can be determined by interpretation of the pressure history.

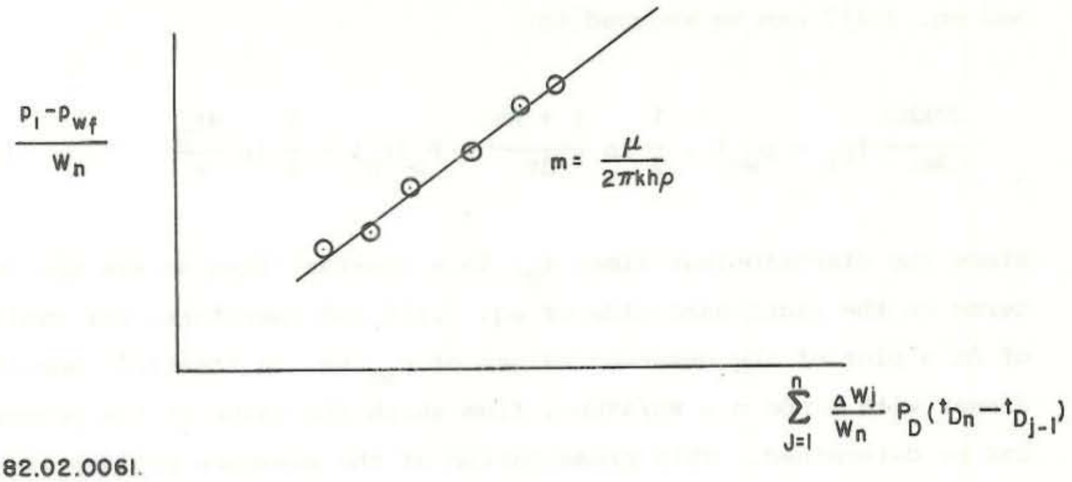

Fig. 3.24 Multirate flow test analysis

By assuming that Δt_D is small enough to allow us to calculate $P_D(t_D)$ in the transient flow regime, but large enough for eq. 3.67 to be valid the above eq. can be approximated as follows:

$$\frac{2\pi kh\rho}{W\mu}(p_i - p_{ws}) = P_D(t_D + \Delta t_D) - \frac{1}{2}\ln\frac{4\Delta t_D}{\kappa} + \frac{1}{2}\ln(t_D + \Delta t_D)$$

$$-\frac{1}{2}\ln(t_D + \Delta t_D)$$

which can alternatively be expressed as:

$$\frac{2\pi kh\rho}{W\mu}(p_i - p_{ws}) = \frac{1}{2}\ln\frac{t + \Delta t}{t} + P_D(t_D + \Delta t_D) - \frac{1}{2}\ln\frac{4(t_D + \Delta t_D)}{\kappa} \tag{3.117}$$

in which dimensionless time has been replaced by real time in the ratio $t+\Delta t/\Delta t$. Again, for small values of the closed-in time Δt:

$$\ln(t_D + \Delta t_D) \simeq \ln(t_D)$$

and $P_D(t_D + \Delta t_D) \simeq P_D(t_D)$

and eq. 3.117 can be reduced to:

$$\frac{2\pi kh\rho}{W\mu}(p_i - p_{ws}) = \frac{1}{2}\ln\frac{t + \Delta t}{\Delta t} + p_D(t_D) - \frac{1}{2}\ln\frac{4t_D}{\kappa} \tag{3.118}$$

Since the dimensionless time, t_D, is a constant then so are the last two terms on the right-hand side of eq. 3.118 and therefore, for small values of Δt a plot of the observed values of p_{ws} vs. $\ln(t+\Delta t)/\Delta t$ should be linear with slope $m = W\mu/4\pi kh\rho$, from which the value of the permeability can be determined. This presentation of the pressure buildup is known as a Horner plot and is illustrated in Fig. 3.25.

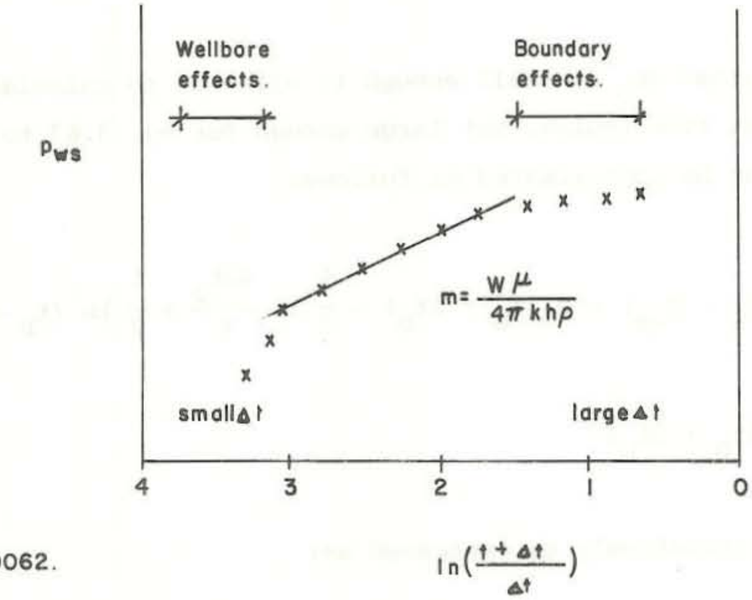

82.02.0062.

Fig. 3.25 Horner pressure buildup plot

Wellbore storage can influence the pressure buildup while Δt is small. Wellbore storage and skin effects must therefore be accounted for.

EXERCISE 3.6

Let the massflow and pressure history be as given by Fig. 3.26.

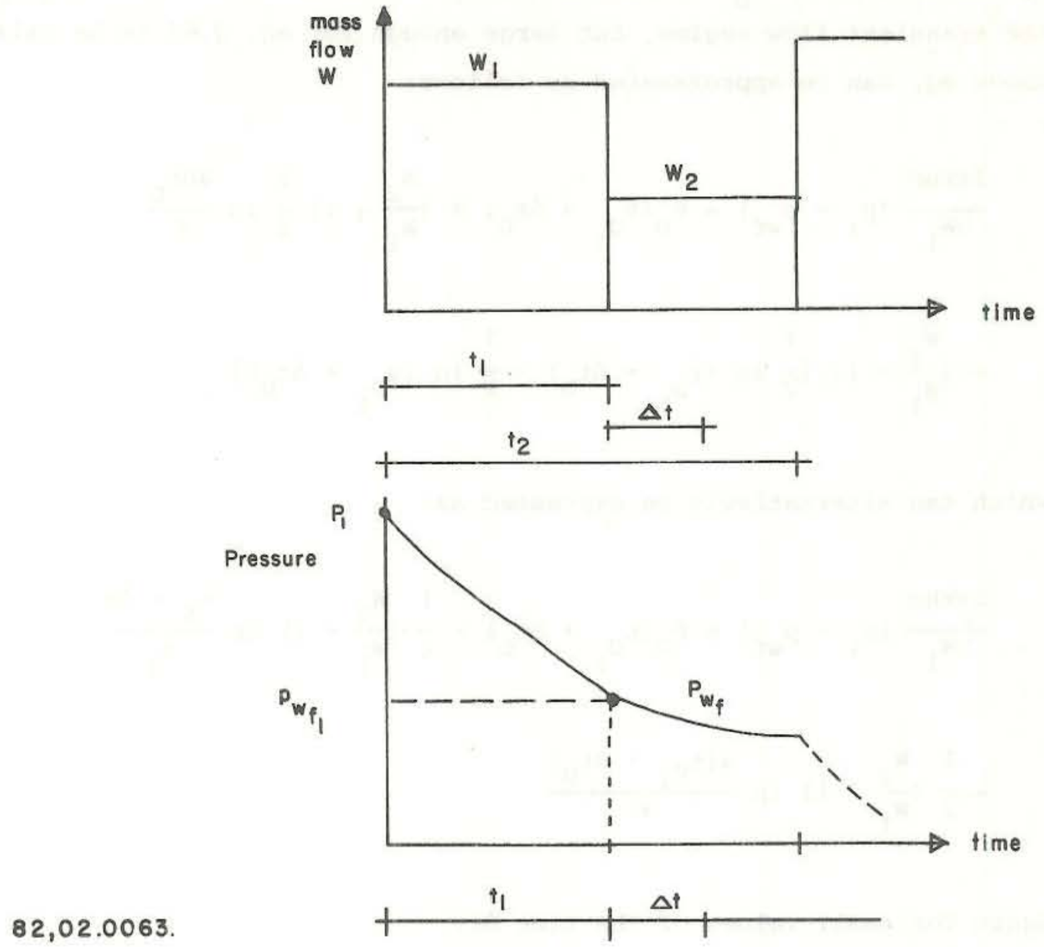

Fig. 3.26 Pressure response test a) mass flow b) pressure response

Calculate the theoretical pressure equation for the time interval $t_1 < t < t_2$.

Solution

We use eq. 3.113 and define:

$$\Delta W_1 = W_1 \qquad t_{D_n} = t_{D_1} + \Delta t_D$$

$$\Delta W_2 = W_2 - W_1$$

$$\frac{2\pi kh\rho}{\mu}(p_i - p_{wf}) = W_1 \, P_D(t_{D_1} + \Delta t_D) + (W_2 - W_1)\, P_D(\Delta t_D)$$

By assuming that Δt_D is small enough to allow us to calculate $P_D(t_D)$ in the transient flow regime, but large enough for eq. 3.67 to be valid the above eq. can be approximated as follows:

$$\frac{2\pi kh\rho}{\mu W_1}(p_i - p_{wf}) = P_D(t_{D_1} + \Delta t_D) + (\frac{W_2}{W_1} - 1)\frac{1}{2}\ln\frac{4\Delta t_D}{\kappa}$$

$$+ (\frac{W_2}{W_1} - 1)\{\frac{1}{2}\ln(t_{D_1} + \Delta t_D) - \frac{1}{2}\ln(t_{D_1} + \Delta t_D)\}$$

which can alternatively be expressed as:

$$\frac{2\pi kh\rho}{\mu W_1}(p_i - p_{wf}) = P_D(t_{D_1} + \Delta t_D) - \frac{1}{2}(\frac{W_2}{W_1} - 1)\ln\frac{t_1 + \Delta t}{t_1}$$

$$+ \frac{1}{2}(\frac{W_2}{W_1} - 1)\ln\frac{4(t_{D_1} + \Delta t_D)}{\kappa}$$

Again for small values of the time Δt:

$$\ln(t_{D_1} + \Delta t_D) \simeq \ln(t_{D_1})$$

and $P_D(t_{D_1} + \Delta t_D) \simeq P_D(t_{D_1})$

and the above eq. can be reduced to:

$$\frac{2\pi kh\rho}{\mu W_1}(p_i - p_{wf}) = \frac{1}{2}(1 - \frac{W_2}{W_1})\ln\frac{t_1 + \Delta t}{t_1} + P_D(t_{D_1})$$

$$- \frac{1}{2}(1 - \frac{W_2}{W_1})\ln\frac{4t_D}{\kappa} \qquad (3.119)$$

Since the dimensionless time, t_{D_1} is a constant then so are the last two terms on the right-hand side of the above eq. and therefore, for small values of Δt a plot of the observed values of p_{wf} vs. $\ln\frac{t_1 + \Delta t}{t_1}$ should be linear with slope $m = \frac{(W_1 - W_2)\mu}{4\pi kh\rho}$, from which the value of the permeability can be determined.

3.9 Response to an instantaneous point injection

Response to an instantaneous point injection is sometimes named slug test in the groundwater well hydrology. Ferris and Knowles (1954) introduced a method for determining the transmissivity of an aquifer from observations of the water level in a well after a known volume of water is suddenly injected into the well.

The pressure response in a point (x,y,z) in a three dimensional space when a mass, M, of water is injected or removed at a point (x', y', z') at time t = o is given by the following expression, see Carslaw and Jaeger (1959)

$$\Delta p = \frac{M}{8\rho\phi c(\pi\frac{k}{\mu c\phi}t)^{3/2}} e^{-\{(x-x')^2 + (y-y')^2 + (z-z')^2\}/\frac{4kt}{\mu c\phi}} \qquad (3.120)$$

In this case the late pressure response would be like $t^{-3/2}$. In case of horizontal flow the pressure response is transmitted in a two dimensional space and the mass, M, is now removed from a line source parallel to the z axis and passing through the point (x', y').

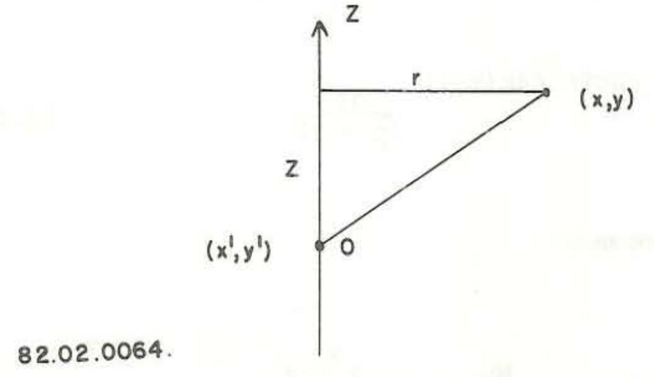

Fig. 3.27 Line source parallel to the z'-axis

Eq. 3.120 can now be written in terms of the notation showed in Fig. 3.27:

$$\Delta p = \frac{M}{8\rho\phi c(\pi\frac{k}{\mu c\phi}t)^{3/2}} e^{-\{r^2 + z^2\}/\frac{4kt}{\mu c\phi}} \tag{3.121}$$

By integrating the point source along the z-axis gives us the line source solution:

$$\Delta p = \frac{M}{8\rho\phi c(\frac{\pi k}{\mu c\phi}t)^{3/2}} \int_{-\infty}^{\infty} e^{-\{r^2 + z^2\}/\frac{4kt}{\mu c\phi}} dz$$

$$\Delta p = \frac{M\mu}{4\rho\pi k} \frac{1}{t} e^{-\mu c\phi r^2/4kt} \tag{3.122}$$

where M is the mass withdrawal per unit length of the line source. If the total mass withdrawal is, m, and the thickness of the aquifer is h eq. 3.122 can be written as:

$$\Delta p = \frac{m\mu}{4\rho\pi kh} \frac{1}{t} e^{-\mu c\phi r^2/4kt} \tag{3.123}$$

In this two dimensional case the late pressure response would be like t^{-1}. Let us now derive the solution for the continuous line source by integrating the fundamental solution, eq. 3.123, in the time domain. Let the mass withdrawal be a function of time, $W = W(t)$

$$\Delta p = \frac{\mu}{4\rho\pi kh} \int_{o}^{t} W(\tau)\, e^{-\mu c\phi r^2/4k(t-\tau)} \frac{d\tau}{(t - \tau)} \tag{3.124}$$

If W(t) is constant this becomes:

$$\Delta p = \frac{W\mu}{4\rho\pi kh} \int_{\frac{r^2\mu c\phi}{4kt}}^{\infty} \frac{e^{-u}}{u} du = - \frac{W\mu}{4\rho\pi kh} Ei(- \frac{r^2\mu c\phi}{4kt}) \tag{3.125}$$

which is the exponential integral solution presented before in eq. 3.60.

EXERCISE 3.7

Fig. 3.28 shows the response of well KG-5 in the Krafla Geothermal field in north east Iceland to an instantaneous increase of volume of water. A curve fitted to the water level data by Grant (1978) is given. The viscosity of the fluid is 10^{-4} Ns/m^2, the density is 865 kg/m^3 and the permeability thickness is 10^{-11} m^3. Estimate the volume of the injected fluid.

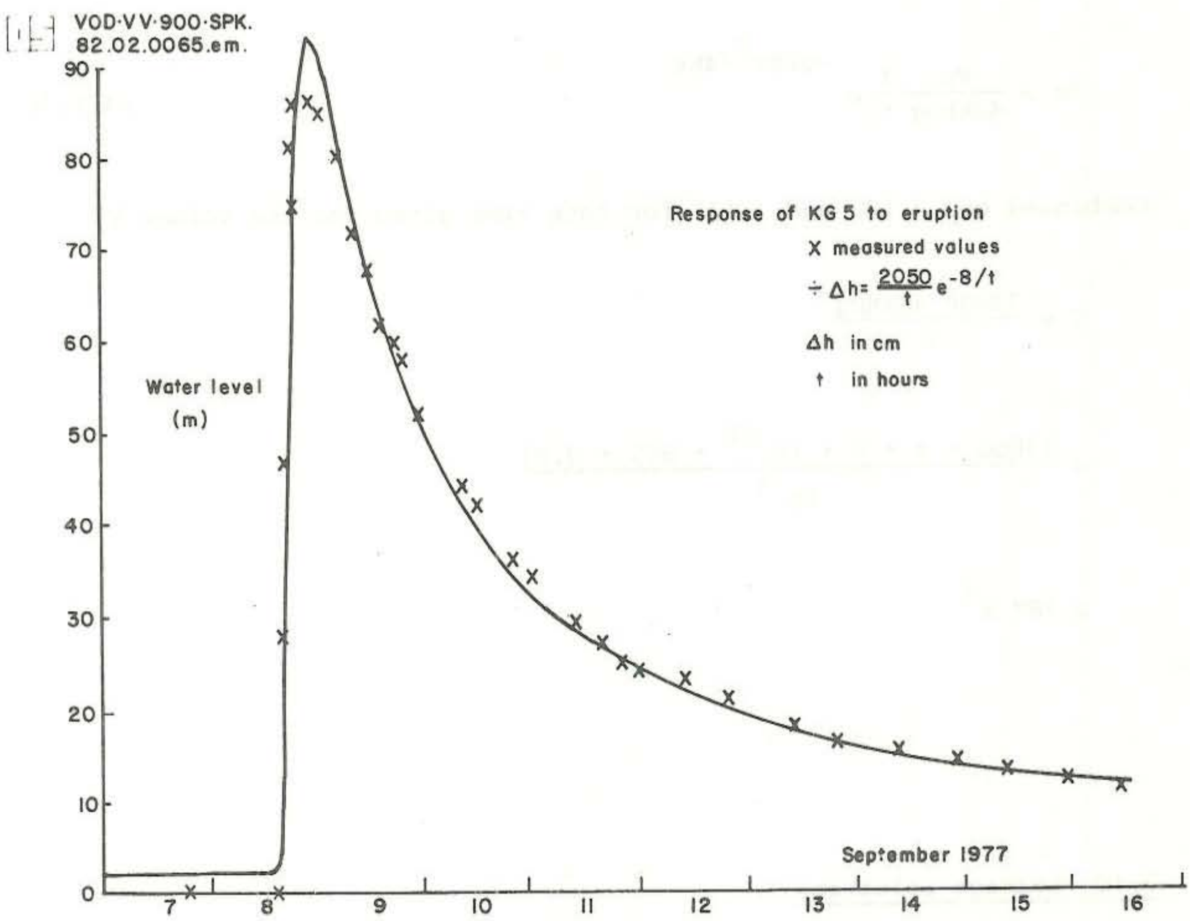

Fig. 3.28 Response of well KG-5 in Krafla to a volcanic eruption situated 5 km from the well (Grant 1978)

Solution

The fitted curve by Grant is given by:

$$\Delta h = \frac{73800}{t} e^{-\frac{28800}{t}} \tag{3.126}$$

where Δh is in meters, and t in sec. According to eq. 3.126 the late response is like t^{-1} and thus the response is in a two dimensional space corresponding to a line source. Physically more correct in this situation we have a point source in a confined aquifer. Because a small distance away from the point source the flow pattern can be treated as horizontal flow, the resulting solution is the same as for a line source.

Eq. 3.123 written in terms of water level and injected volume is given by:

$$\Delta h = \frac{V\mu}{4\pi kh\rho g}\frac{1}{t}e^{-\mu c\phi r^2/4kt} \tag{3.127}$$

Combining eq. 3.126 and 3.127 for late time gives for the volume V:

$$V = \frac{73800\ 4\pi kh\rho g}{\mu}$$

$$= \frac{73800 \cdot 4 \cdot \pi \cdot 10^{-11} \cdot 865 \cdot 9.81}{10^{-4}}$$

$$\cong 787\ m^3$$

3.10 Leakage solutions

Fig. 3.29 shows the situation when there is vertical leakage from an upper aquifer to a lower main aquifer.

Because of the potential difference between the upper aquifer and the main aquifer (the drawdown, s) there can be a leakage through the semipervious layer. The potential difference is s/b, and if the permeability of the semipervious layer is defined as:

$$K = \frac{k\gamma}{\mu} \tag{3.128}$$

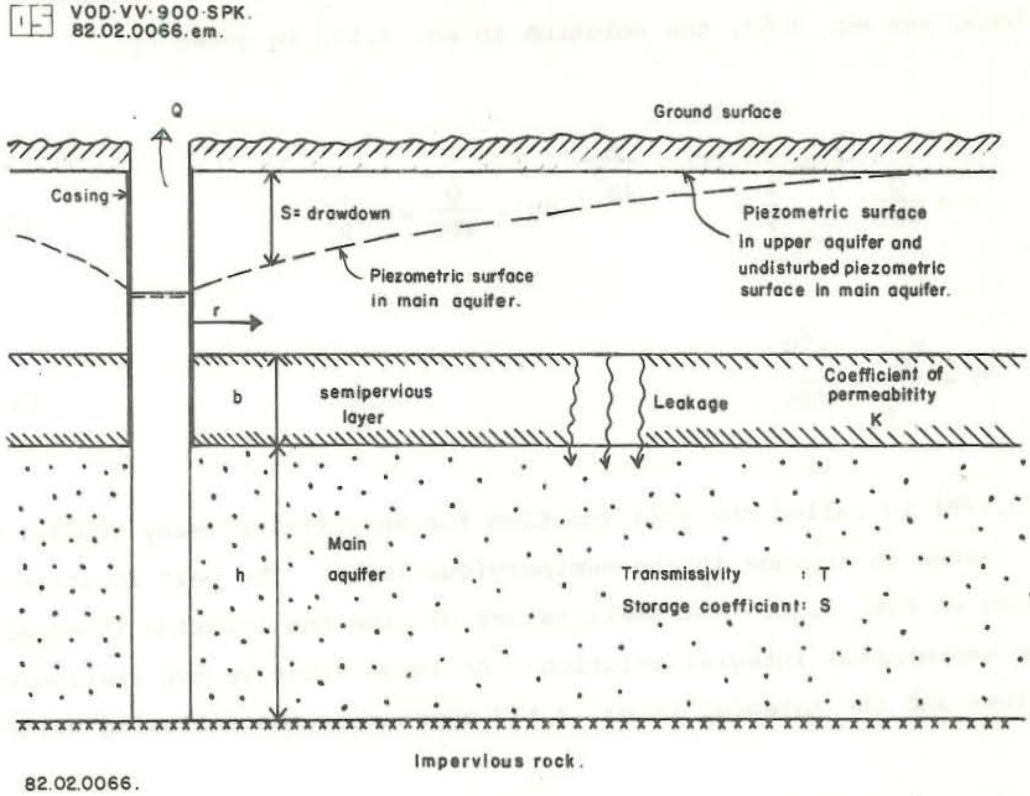

Fig. 3.29 Schematic picture of vertical leakage

The permeability K is called the coefficient of permeability. The total leakage through the semipervious layer is then:

$$\text{Leakage} = \int_0^\infty 2\pi r \frac{s(r)}{b} K \, dr \tag{3.129}$$

By including the leakage in the continuity equation, eq. 3.1, we get the following differential equation in terms of the drawdown, s.

$$\frac{\partial^2 s}{\partial r^2} + \frac{1}{r}\frac{\partial s}{\partial r} - \frac{s}{B^2} = \frac{S}{T}\frac{\partial s}{\partial t} \tag{3.130}$$

where B is defined as:

$$B^2 = \frac{Tb}{K} \tag{3.131}$$

By assuming infinite reservoir case and the line source boundary conditions, see eq. 3.59, the solution to eq. 3.130 is given by:

$$s = \frac{Q}{4\pi T} \int_u^\infty \frac{1}{y} e^{-y - \frac{r^2}{4B^2 y}} dy = \frac{Q}{4\pi T} W(u, \frac{r}{B}) \tag{3.132}$$

$$u = \frac{r_D^2}{4t_D} = \frac{r^2 S}{4Tt} \tag{3.133}$$

$W(u,r/B)$ is called the well function for an infinite leaky aquifer with no change in storage in the semipervious layer. The well function is shown on Fig. 3.30. For small values of time the solution is equal to the exponential integral solution. At large times we get stationary values and the integral in eq. 3.132 approaches the following value:

$$s = \frac{Q}{2\pi T} K_o(r/B) \tag{3.134}$$

Fig. 3.31 shows this steady state type curve. The total steady state leakage can now be calculated according to eq. 3.129:

$$q = \text{steady state leakage} = \frac{QK}{Tb} \int_o^\infty r\, K_o(\frac{r}{B})\, dr$$

$$= \frac{QKB^2}{Tb} \int_o^\infty \frac{r}{B} K_o(\frac{r}{B}) d(\frac{r}{B})$$

Using the definition of B in eq. 3.131 we get:

$$q = Q \int_o^\infty x\, K_o(x) dx = Q \tag{3.135}$$

The steady state leakage is of course equal to the pumping rate.

The three coefficients T, S, and B can be determined by the match point method described in section 3.5 using the type curves in Figs. 3.30-3.31.

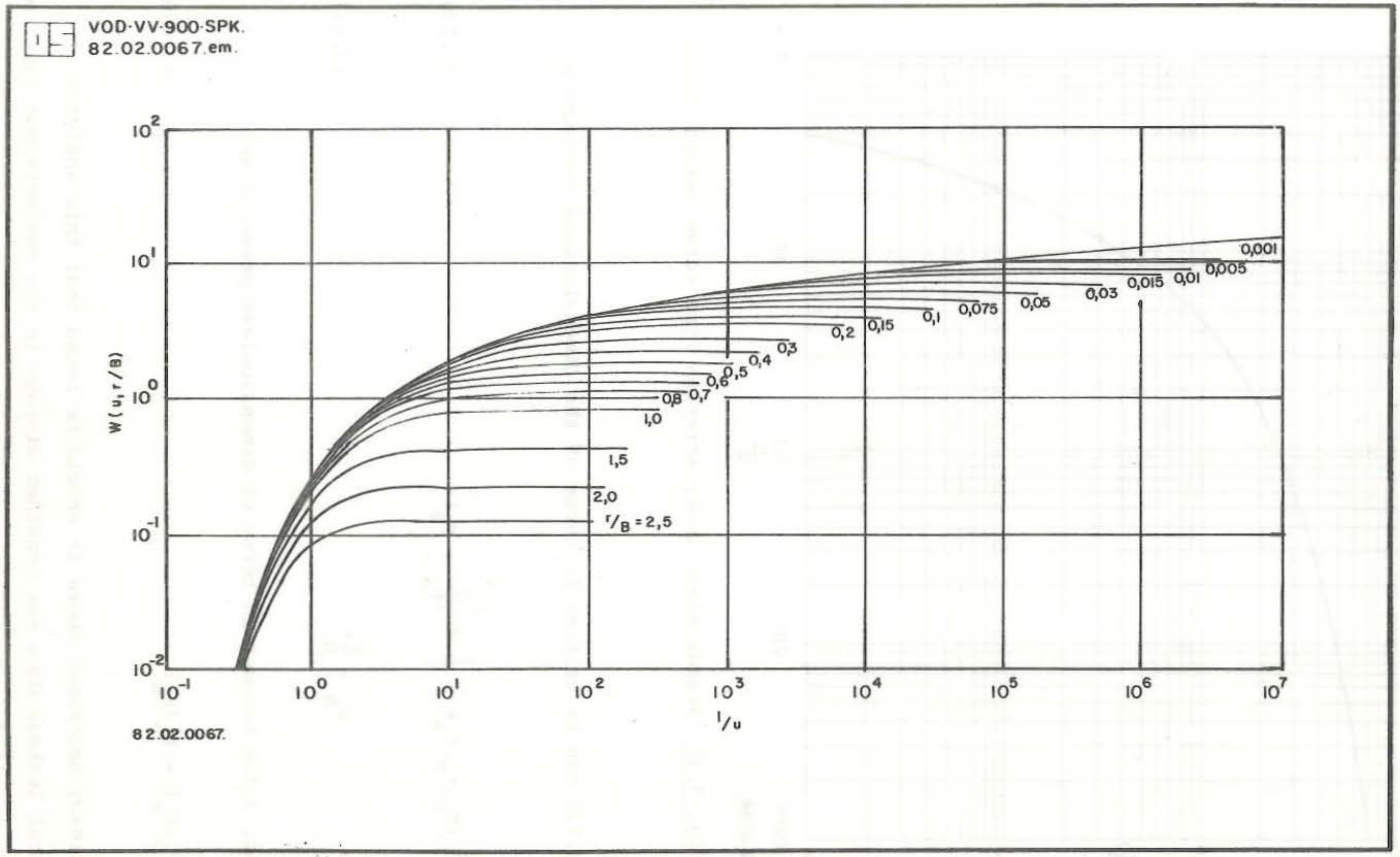

Fig. 3.30 Nonsteady-state leaky artesian type curves (Walton 1970)

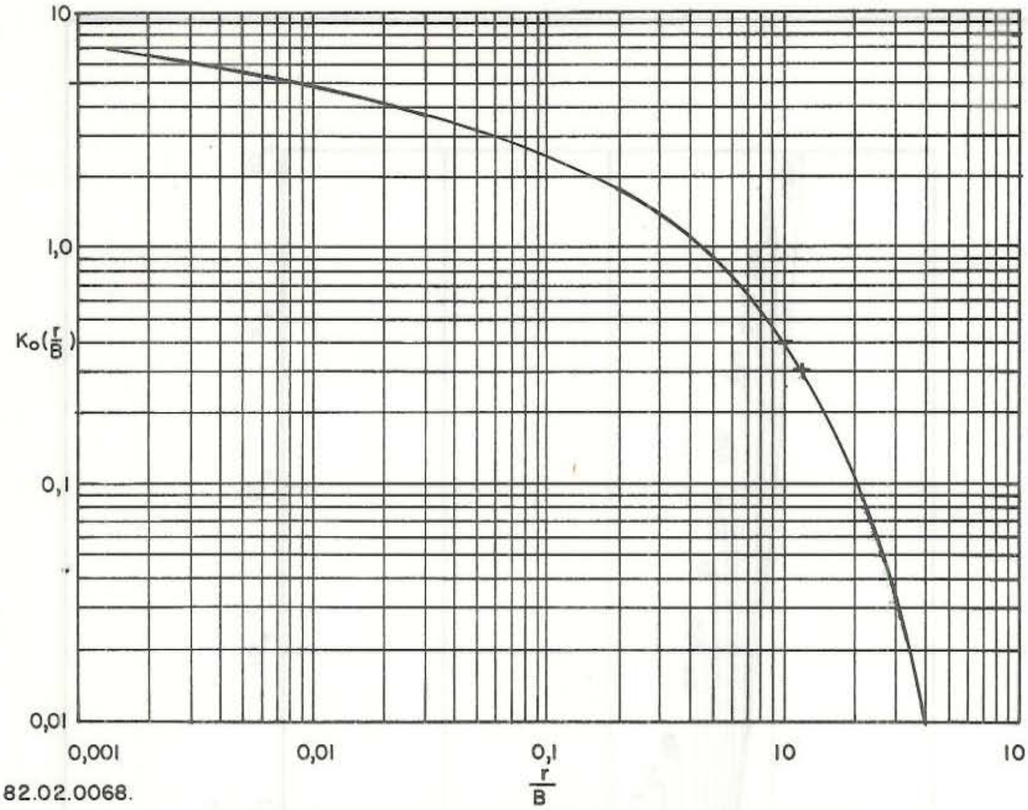

Fig. 3.31 Steady state leaky artesian type curve (Walton 1970)

Eq. 3.132 can be written in terms of the dimensionless pressure as:

$$P_D(t_D, r_D, r_B) = \frac{1}{2} W(\frac{r_D^2}{4t_D}, r_B) \tag{3.136}$$

where $$r_B = \frac{r}{B} \tag{3.137}$$

and eq. 3.134 becomes in terms of dimensionless pressure as:

$$P_D(r_B) = K_o(r_B) \tag{3.138}$$

As already mentioned above it should be noted that this analysis of vertical leakage does not consider storage in the semipervious layer and a more detailed analysis is necessary in that case. See e.g. Engelund (1970).

EXERCISE 3.8

At Selfoss in Southern Iceland there is a low temperature field. The reservoir engineering data is from Halldórsson (1980). The temperature of the field is 86°C. Location map of wells and distances between them is shown in Fig. 3.32. In order to estimate the reservoir parameters S and T an interference test is performed by observing the drawdown in well No. 7, while well No. 10 is pumped at a rate of 45 l/s.

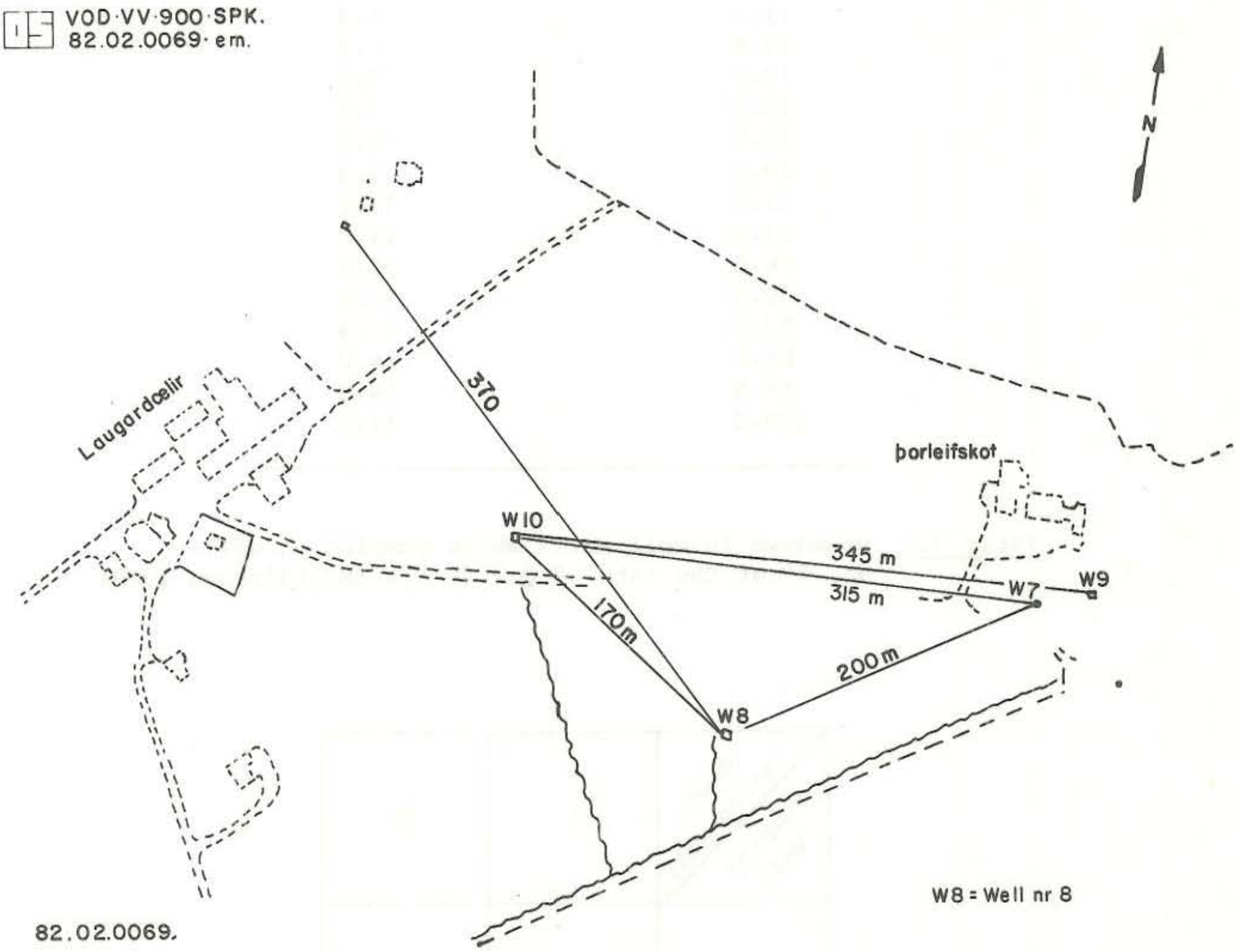

Fig. 3.32 The Selfoss geothermal area (Halldórsson 1980)

The results are given in Table 3.2. After some time the drawdown becomes steady. Table 3.3 shows the flowrate in pumping wells and the corresponding observation wells.

Time hours	Drawdown s meters
0	0
3.5	0.6
5.5	1.4
6.5	2.2
7.7	3.0
9.0	3.8
10.3	4.6
11.3	5.4
12.8	6.2
14.5	7.0
15.5	7.8
17.5	8.6
19.0	9.4
21.0	10.2
23.0	11.0
26.0	11.8
30.0	12.6
53.0	13.4
68.0	14.0
89.5	14.8
170.0	14.8

Table 3.2 Drawdown in well No. 7 while pumping in well No. 10 at the rate of $Q = 45$ l/s (Halldórsson 1980)

Observation well / Pumping well	7	10
8	Q=40 l/s	Q=40 l/s
10	Q=45 l/s	

Table 3.3 Pumping and observation wells

1) Estimate the transmissivity T and the storage coefficient S, using the match point method for the transient data.

2) Estimate the steady state drawdown for the observation wells shown in Table 3.3.

3) If the thickness of semipervious layer is 150 m, estimate its permeability.

4) What thickness of the main aquifer would correspond to this permeability.

The future production of the field is shown in Fig. 3.33.

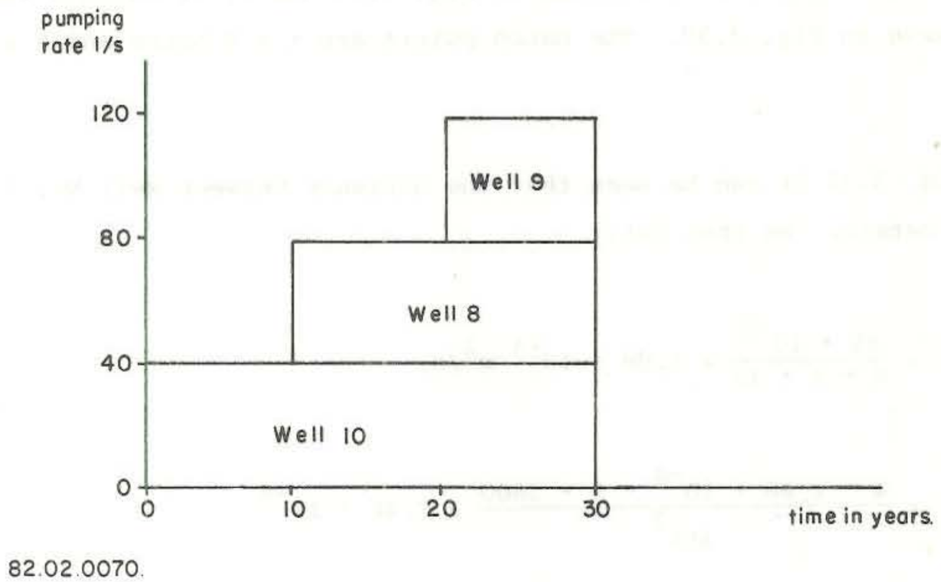

Fig. 3.33 Pumping rate vs. time

The wellbore diameter is equal to 10 in.

5) Calculate the drawdown in well No. 10 as a function of time.

6) If we assume that the distances between the wells are all equal to some average value $\bar{r}$, calculate the drawdown in well No. 10 after 30 years as a function of $\bar{r}$. Assume that the steady state drawdown in the production well itself is 33 m.

7) If the maximum depth of the pumps is 60 m, what should be the minimum distance between wells?

Solution

1) According to the matchpoint method the transmissivity and the storage coefficient is given by:

$$T = \frac{Q}{4\pi s}$$

$$S = \frac{4Tt}{r^2}$$

The data in Table 3.2 is plotted on Fig. 3.34 and it is matched with the type curve in Fig. 3.30. The match points are t = 9 hours and s = 19 meters.

From Fig. 3.32 it can be seen that the distance between well No. 7 and 10 is 315 meters. We then get:

$$T = \frac{45 \cdot 10^{-3}}{4 \cdot \pi \cdot 19} = 1.88 \cdot 10^{-4}\ m^2/s.$$

$$S = \frac{4 \cdot 1.88 \cdot 10^{-4} \cdot 9 \cdot 3600}{315^2} = 2.46 \cdot 10^{-4}$$

2) From Fig. 3.34 we see that r/B = 1.0 was found in the matching. We then have:

$$B = \frac{315}{1.0} = 315\ m$$

Eq. 3.134 together with Fig. 3.31 gives us the steady state drawdown:

$$s_{7.8} = \frac{40 \cdot 10^{-3}}{2 \cdot \pi \cdot 1.88 \cdot 10^{-4}} K_o(\frac{200}{315}) = 23.7\ m$$

$$s_{10.8} = \frac{40 \cdot 10^{-3}}{2 \cdot \pi \cdot 1.88 \cdot 10^{-4}} K_o(\frac{170}{315}) = 28.8 \text{ m}$$

$s_{7.10} = 15.2$ m has already been used, see Fig. 3.34.

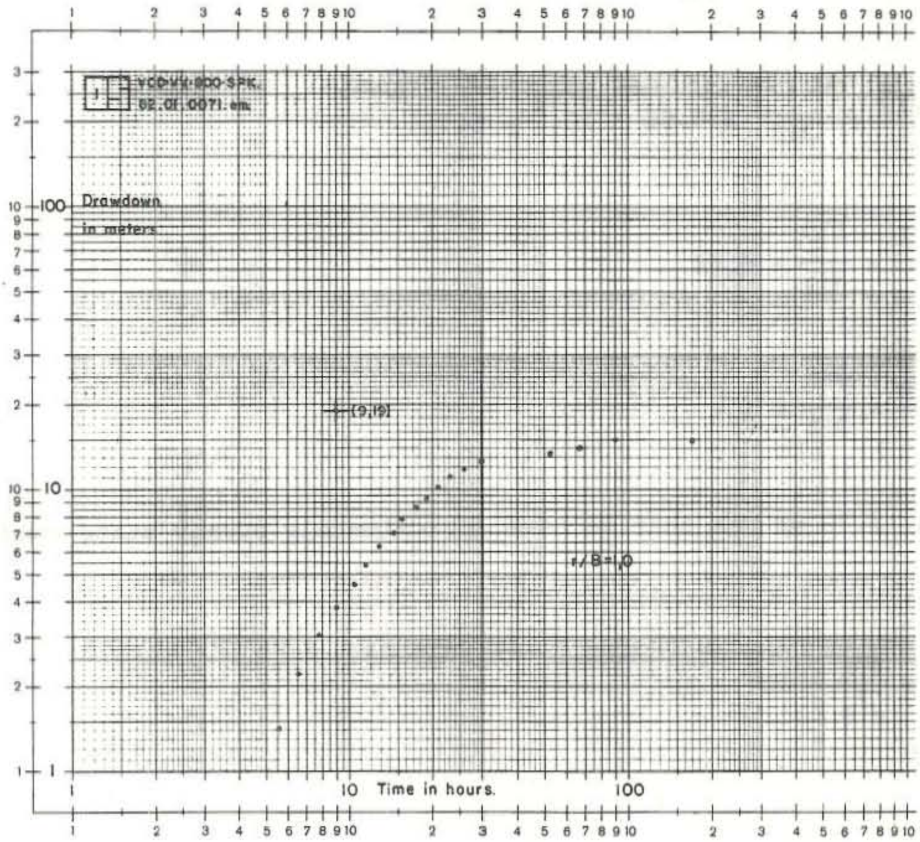

Fig. 3.34 Datacurve for interference test at the Selfoss geothermal field in South Iceland

3) From eq. 3.131 we have:

$$K = \frac{Tb}{B^2} = \frac{1.88 \cdot 10^{-4} \cdot 150}{315^2} = 2.8 \cdot 10^{-7} \text{ m/s}$$

4) The transmissivity is defined as:

$$T = K \cdot h$$

from which we get:

$$h = \frac{T}{K} = \frac{1.88 \cdot 10^{-4}}{2.8 \cdot 10^{-7}} \cong 662 \text{ m}$$

5) We have for the distances between the wells; $r_{10.10} = 0.254$ m, $r_{10.8} = 170$ m, $r_{10.7} = 315$ m from which we get:

$$\frac{r_{10.10}}{B} = \frac{0.254}{315} = 8.06 \cdot 10^{-4} \sim 0.001$$

$$\frac{r_{10.8}}{B} = \frac{170}{315} = 0.54$$

$$\frac{r_{10.9}}{B} = \frac{345}{315} = 1.1$$

From Fig. 3.30 we see that we have approximately steady state conditions after:

$$1/u = \frac{4Tt}{r^2 S} > 10^6$$

that is:

$$t > \frac{10^6 r^2 S}{4T} = \frac{10^6 \cdot 0.254^2 \cdot 2.46 \cdot 10^{-4}}{4 \cdot 1.88 \cdot 10^{-4}} \cong 6 \text{ hours}$$

We have steady state conditions after approximately six hours and therefore it is of no practical interest for the long term behaviour of the field to calculate transient terms. We then have for the drawdown after 10 years:

$$s_{10} = \frac{Q}{2\pi T} K_o(\frac{0.254}{315}) = \frac{Q}{2\pi T} K_o(8.06 \cdot 10^{-4})$$

$$= - \frac{Q}{2\pi T} \ln 8.06 \cdot 10^{-4} = \frac{-40 \cdot 10^{-3}}{2 \cdot \pi \cdot 1.88 \cdot 10^{-4}} \ln 8.06 \cdot 10^{-4}$$

$$= 241 \text{ m}$$

Measured steady state drawdown, was much less than this. This can be explained by a negative skin factor, resulting from a fracture intercepting the well. Calculation of the skin factor from eq. 3.28 gives $s \simeq -6$.

After ten years well 8 starts operating and we now have according to Fig. 3.30 steady state conditions after:

$$t > \frac{10^2 r^2 S}{4T} = \frac{10^2 \cdot 170^2 \cdot 2.46 \cdot 10^{-4}}{4 \cdot 1.88 \cdot 10^{-4}} \simeq 11 \text{ days}$$

and again no practical interest for transient calculations. We then have for the drawdown after 20 years:

$$s_{20} = 241 + \frac{40 \cdot 10^{-3}}{2 \cdot \pi \cdot 1.88 \cdot 10^{-4}} K_o(0.54) = 241 + 28.8 \cong 270 \text{ m}$$

After twenty years well 9 starts operating and we now have according to Fig. 3.30 steady state conditions after:

$$t > \frac{10r^2 s}{4T} = \frac{10 \cdot 345^2 \cdot 2.46 \cdot 10^{-4}}{4 \cdot 1.88 \cdot 10^{-4}} \cong 4.5 \text{ days}$$

and again no practical interest for transient calculations. We then finally have for the drawdown after 30 years:

$$s_{30} = 241 + 28.8 + \frac{40 \cdot 10^{-3}}{2 \cdot \pi \cdot 1.88 \cdot 10^{-4}} K_o(1.1) = 241 + 28.8 + 12.4$$

$$= 282 \text{ m}$$

6) From eq. 3.134 we have:

$$s_{30} = \frac{Q}{2\pi T} K_o(\frac{\bar{r}}{B}) + 33$$

$$s_{30} = \frac{2 \cdot 40 \cdot 10^{-3}}{2 \cdot \pi \cdot 1.88 \cdot 10^{-4}} K_o(\frac{\bar{r}}{315}) + 33$$

$$= 67.7\ K_o(\frac{\bar{r}}{315}) + 33$$

7) From the last problem we have:

$$60 = 67.7\ K_o(\frac{\bar{r}}{315}) + 33$$

which gives:

$$K_o(\frac{\bar{r}}{315}) = \frac{60 - 33}{67.7} \cong 0.40$$

From Fig. 3.31 we then get:

$\frac{\bar{r}}{B} = 1.0$ which gives $\bar{r} = 315$ m

3.11 Jacob's and Rorabaugh's method

Jacob's and Rorabaugh's method is widely used in groundwater hydrology to determine transmissivity and the turbulent pressure drop in the vicinity of the producing well. As will be discussed in this section care must be taken when the method is used for geothermal reservoirs. Eq. 3.46 becomes in terms of drawdown and volumetric rate:

$$s_w = BQ + CQ^2 \qquad (3.139)$$

where s_w is the drawdown in the producing well itself and B and C are some constants, which should be derived by comparison with eq. 3.46. Eq. 3.139 can be written as:

$$\frac{s_w}{Q} = B + CQ \tag{3.140}$$

By pumping the well at different rates and observing the corresponding drawdown, s_w/Q can be plotted against Q and should give a straight line according to eq. 3.140, from which the constants B and C could be determined, see Fig. 3.35.

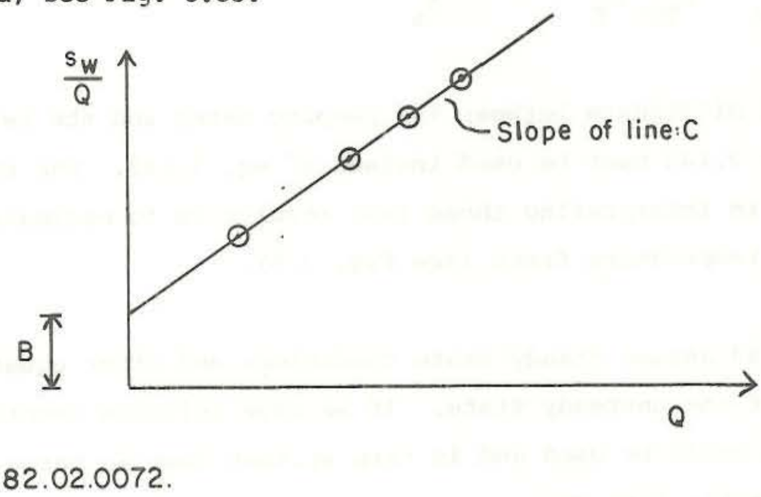

Fig. 3.35 Step-drawdown test

The value of B can be used to determine the formation permeability or transmissivity when there is no skin effect (S = 0). If we have steady state condition eq. 3.46 gives us for B:

$$B = \frac{1}{2\pi T} \ln \frac{r_e}{r_w} \tag{3.141}$$

Eq. 3.141 can be solved for the transmissivity:

$$T = \frac{1}{2\pi B} \ln \frac{r_e}{r_w} \tag{3.142}$$

If $S \neq 0$, T can still be determined by using eq. 3.47 instead of eq. 3.46. The step injection test is to pump cold water into the aquifer. In that case eq. 3.46 is no longer valid and eq. 3.35 from exercise 3.1 must be used. From which we get:

$$B = \frac{1}{2\pi T} (\ln \frac{r_e}{r_w} + (\frac{\mu_T}{\mu_{To}} \frac{\rho_{To}}{\rho_T} - 1) \ln \frac{r_s}{r_w}) \quad (3.143)$$

μ_T and ρ_T are the viscosity and density respectively of the cold pumping water at temperature T and μ_{To} and ρ_{To} is the viscosity and density respectively of the reservoir water at temperature To. Eq. 3.143 solved for T gives:

$$T = \frac{1}{2\pi B} (\ln \frac{r_e}{r_w} + (\frac{\mu_T}{\mu_{To}} \frac{\rho_{To}}{\rho_T} - 1) \ln \frac{r_e}{r_w}) \quad (3.144)$$

If the temperature difference between the pumping water and the reservoir water is great eq. 3.144 must be used instead of eq. 3.142. One of the main difficulties in interpreting these test results is to estimate r_s the radius of the temperature front (see Fig. 3.5).

Eqs. 3.141 and 3.143 assume steady state conditions and other equations must be derived for the unsteady state. If we have infinite reservoir behaviour eq. 3.60 could be used and is here written down in terms of drawdown and volumetric rate as:

$$s = \frac{Q}{4\pi T} W(u) \quad (3.145)$$

By comparing eq. 3.145 with eq. 3.139 it can be seen that:

$$B = \frac{W(u)}{4\pi T} \quad (3.146)$$

which solved for the transmissivity gives:

$$T = \frac{W(u)}{4\pi B} \quad (3.147)$$

For $u<0.01$ eq. 3.145 can be approximated as:

$$s = \frac{Q}{4\pi T} (- \ln u - 0.5772)$$

which then gives for B and T:

$$B = \frac{(-\ln u - 0.5772)}{4\pi T} \tag{3.148}$$

and

$$T = \frac{(-\ln u - 0.5772)}{4\pi B} \tag{3.149}$$

If the temperature difference between the pumping water and the reservoir water is great eqs. 3.147 and 3.149 are no longer valid. Solutions which take the propagation of the temperature front into account must be used. In the case of a sharp temperature front, r_s in eq. 3.144 could be estimated by equating the heat content of the pumping water and the cooled section of the aquifer.

$$Qt\rho_{w,T}c_{w,T} = \pi r_s^2 \, h(\rho_{w,T_o}c_{w,T_o}\phi + \rho_r c_r(1 - \phi)) \tag{3.150}$$

where ρ_w and c_w is the density and heat capacity of the water at temperature T and T_o respectively and ρ_r and c_r is the density and heat capacity of the rock mass and ϕ is the porosity. But because of heat conduction effects and especially dispersion effects there is no sharp temperature front making eq. 3.150 useless in most situations. In the above discussion it has been pointed out that due to great temperature differences between the pumping water and the reservoir water the interpretation of the step injection test is extremely difficult. However for two phase systems injection tests sometimes give the most reliable results for the flow parameters, see Sigurðsson and Stefánsson (1977), and Böðvarsson et al. (1981).

When water is pumped from the well or the well is flowing there is no temperature front to complicate the above method and eq. 3.142 and 3.147 may be used to determine the transmissivity provided the storage coefficient or the effective radius are known.

EXERCISE 3.9

A step drawdown test was perfomed in well MG-8 at the Reykir geothermal field in S.W. Iceland by pumping water from the well (Thorsteinsson 1975). Table 3.4 gives the results of the test.

Drawdown meters	Pumping rate l/s
22.0	26.0
32.0	32.0
44.0	38.0
56.0	44.0

Table 3.4 Step-drawdown test in well MG-8 at Reykir S.W. Iceland

The storage coefficient is $1.5 \cdot 10^{-4}$ and the effective radius of the well is 1000 m. The length of the pumping interval is one hour and the wellbore diameter is 25 cm.

1) Estimate the coefficients for laminar and turbulent pressure drop.

2) Estimate the transmissivity by using eq. 3.142 and 3.147.

Solution

1) The data from Table 3.4 is plotted according to eq. 3.140 on Fig. 3.36. From the figure we get:

$B = 0.19$ m/l/s

$C = 0.025$ m/(l/s)^2

2) Eq. 3.142 gives for the transmissivity:

$$T = \frac{1 \cdot 10^{-3}}{2 \cdot \pi \cdot 0.19} \ln \frac{1000}{0.25} \cong 7 \cdot 10^{-3} \ m^2/s$$

Using this T value gives for u:

$$u = \frac{r_w^2 S}{4Tt} = \frac{0.125^2 \cdot 1.5 \cdot 10^{-4}}{4 \cdot 7 \cdot 10^{-3} \cdot 3600} = 2.3 \cdot 10^{-8} << 0.01$$

and eq. 3.149 can be used.

$$T = \frac{-\ln \dfrac{0.125^2 \cdot 1.5 \cdot 10^{-4}}{4 \cdot 3600 \cdot T} - 0.5772}{4 \cdot \pi \cdot 0.19 \cdot 10^3}$$

$$= 4.19 \cdot 10^{-4} \ln T + 9.2 \cdot 10^{-3}$$

By iteration we get:

$$T \simeq 7.0\ 10^{-3}\ m^2/s$$

82.02.0076.em.

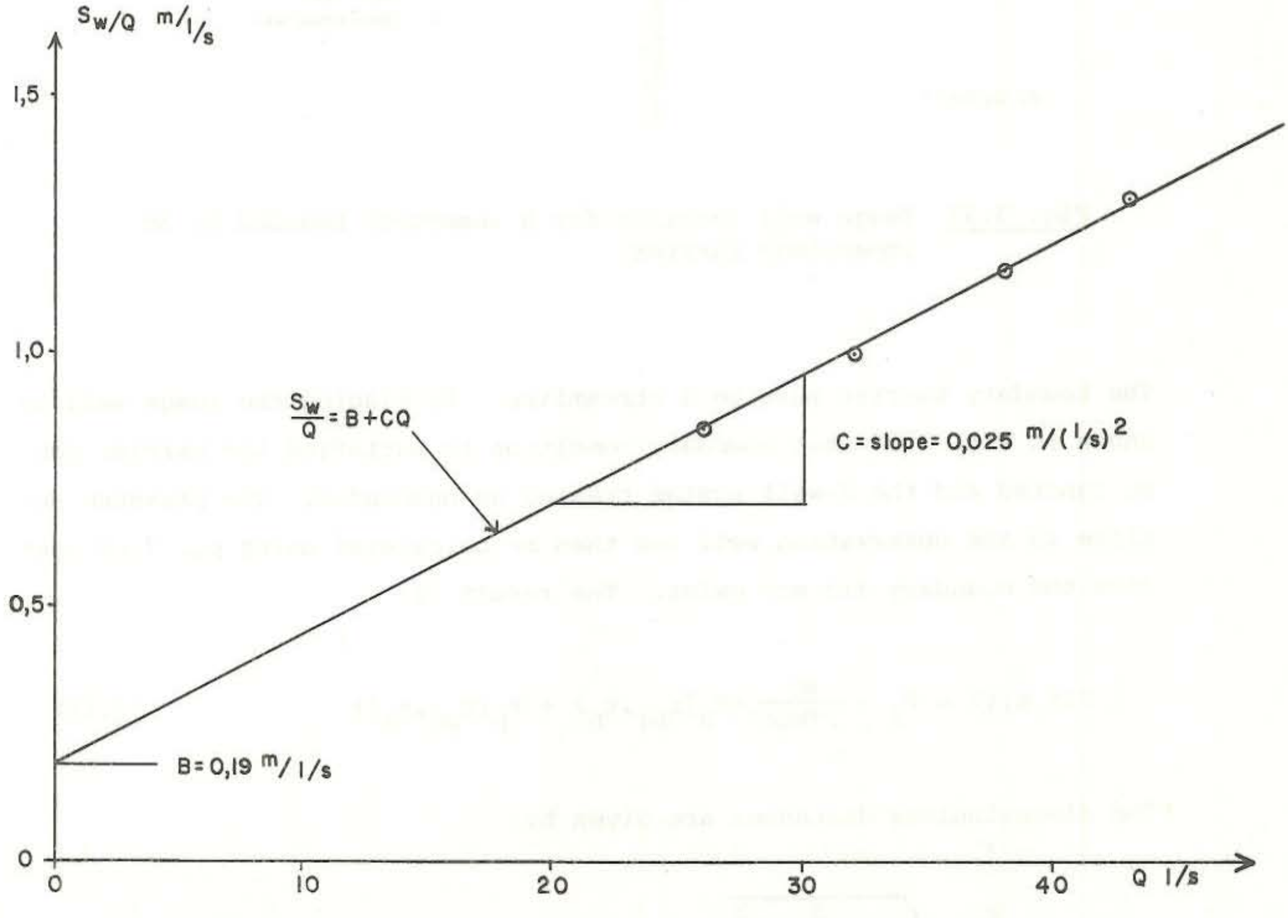

Fig. 3.36 Step-drawdown test in MG-8 at Reykir S.W. Iceland (Thorsteinsson 1975)

3.12 Boundary effects

The boundary effects upon the pressure decline are described qualitatively in section 3.3. In this section the method of images is applied to generate pressure functions in case of bounded reservoir, the impervious boundary case and constant pressure boundary case will be treated. Fig. 3.37 shows an impervious (no flow) boundary and a single well.

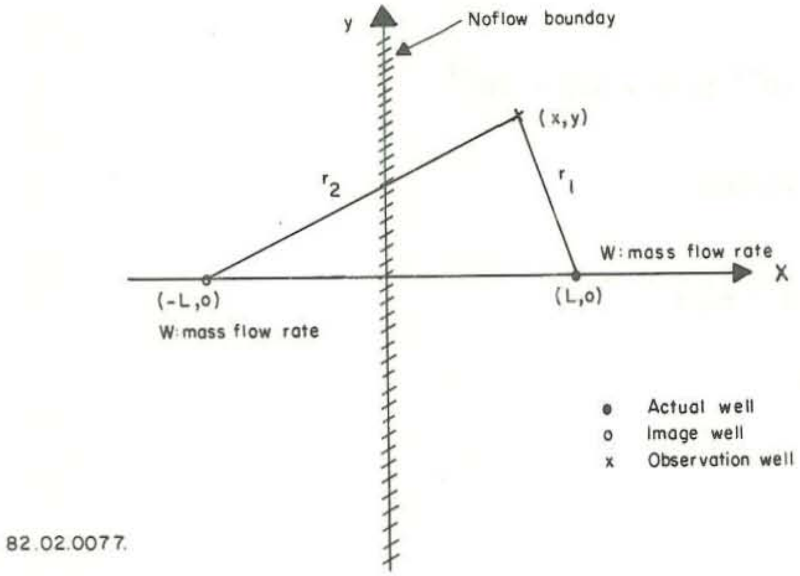

Fig. 3.37 Image well location for a reservoir bounded by an impervious barrier

The boundary barrier must be a streamline. By placing the image well as shown in Fig. 3.37 that boundary condition is satisfied the barrier can be ignored and the 2-well system treated as unbounded. The pressure decline in the observation well can then be calculated using eq. 3.60 just like the boundary did not exist. The result is:

$$P(t,x,y) = P_i - \frac{W\mu}{2\pi kh\rho} (P_D(r_{D1},t_D) + P_D(r_{D2},t_D)) \tag{3.151}$$

The dimensionless distances are given by:

$$r_{D1} = \frac{r_1}{r_w} = \frac{\sqrt{(x-L)^2 + y^2}}{r_w} \tag{3.152}$$

$$r_{D2} = \frac{r_2}{r_w} = \frac{\sqrt{(x+L)^2 + y^2}}{r_w} \tag{3.153}$$

From eq. 3.60 we have:

$$P_D(t_D, r_D) = -\frac{1}{2}\,\mathrm{Ei}\left(-\frac{r_D^2}{4t_D}\right) \tag{3.154}$$

If $t_D/r_D^2 > 25$ we can approximate eq. 3.60 by eq. 3.67. Inserting this in eq. 3.151 we get for the pressure drop:

$$P_i - P(t,x,y) = \frac{W\mu}{2\pi kh\rho}\left(\ln t + \ln \frac{2.246k}{\phi\mu c r_1 r_2}\right) \tag{3.155}$$

which can be written as:

$$P_i - P(t,x,y) = m\left(\ln t + \ln \frac{2.246k}{\phi\mu c r_1 r_2}\right) \tag{3.156}$$

where m is the slope of the straight line for pressure drop vs. the logarithm of time. By comparing eq. 3.156 with eq. 3.74 we see that the slope of the straight line is twice as steep when there is an impervious barrier boundary as if there were no boundary. The reservoir constants can now be estimated by the following equations, which correspond to eq. 3.75-3.78.

$$k = \frac{W\mu}{2\pi h\rho m} \tag{3.157}$$

$$T = \frac{Wg}{2\pi m} \tag{3.158}$$

$$\phi c = \frac{2.246kt_o}{\mu r_1 r_2} \tag{3.159}$$

$$S = \frac{2.246Tt_o}{r_1 r_2} \tag{3.160}$$

From eq. 3.151 we can define a dimensionless pressure function for the reservoir as:

$$P_D(t_D,r_{D1},r_{D2}) = P_D(r_{D1},t_D) + P_D(r_{D2},t_D) \tag{3.161}$$

By using eq. 3.154 we get:

$$P_D(t_D,r_{D1},r_{D2}) = -\frac{1}{2}\left(\mathrm{Ei}\left(\frac{-r_{D1}^2}{4t_D}\right) + \mathrm{Ei}\left(\frac{-r_{D2}^2}{4t_D}\right)\right) \tag{3.162}$$

which can be written as:

$$P_D(t_D,r_D,\beta) = -\frac{1}{2}\left(\mathrm{Ei}\left(-\frac{r_D^2}{4t_D}\right) + \mathrm{Ei}\left(-\beta^2\frac{r_D^2}{4t_D}\right)\right) \tag{3.163}$$

where β is defined as:

$$\beta = \frac{r_{D2}}{r_{D1}} \tag{3.164}$$

The method of images can of course be used in case of more than one boundary. In case of constant head (equipotential) boundary (recharge boundary) the image well must be a recharge well in order to satisfy that constant pressure boundary condition. A system of a discharge well and a corresponding recharge well with the same flowrate is called a dipole system. These are extensively treated in potential theory. Fig. 3.38 shows the image well configuration for different boundary geometry. The method of images transforms the bounded problems into unbounded double infinity problems by using symmetry and antisymmetry. Each line of symmetry is a streamline. Each line of antisymmetry is a potential line. As may be seen from Fig. 3.38 it takes a single infinity of image wells to change single infinity problems into double infinity problems and double infinity and image wells to change completely bounded problems into double infinity problems and in that case the method becomes a little cumbersome. If image wells start falling into the real reservoir area, an infinity of image wells will be created in the vicinity of the reservoir and the method fails.

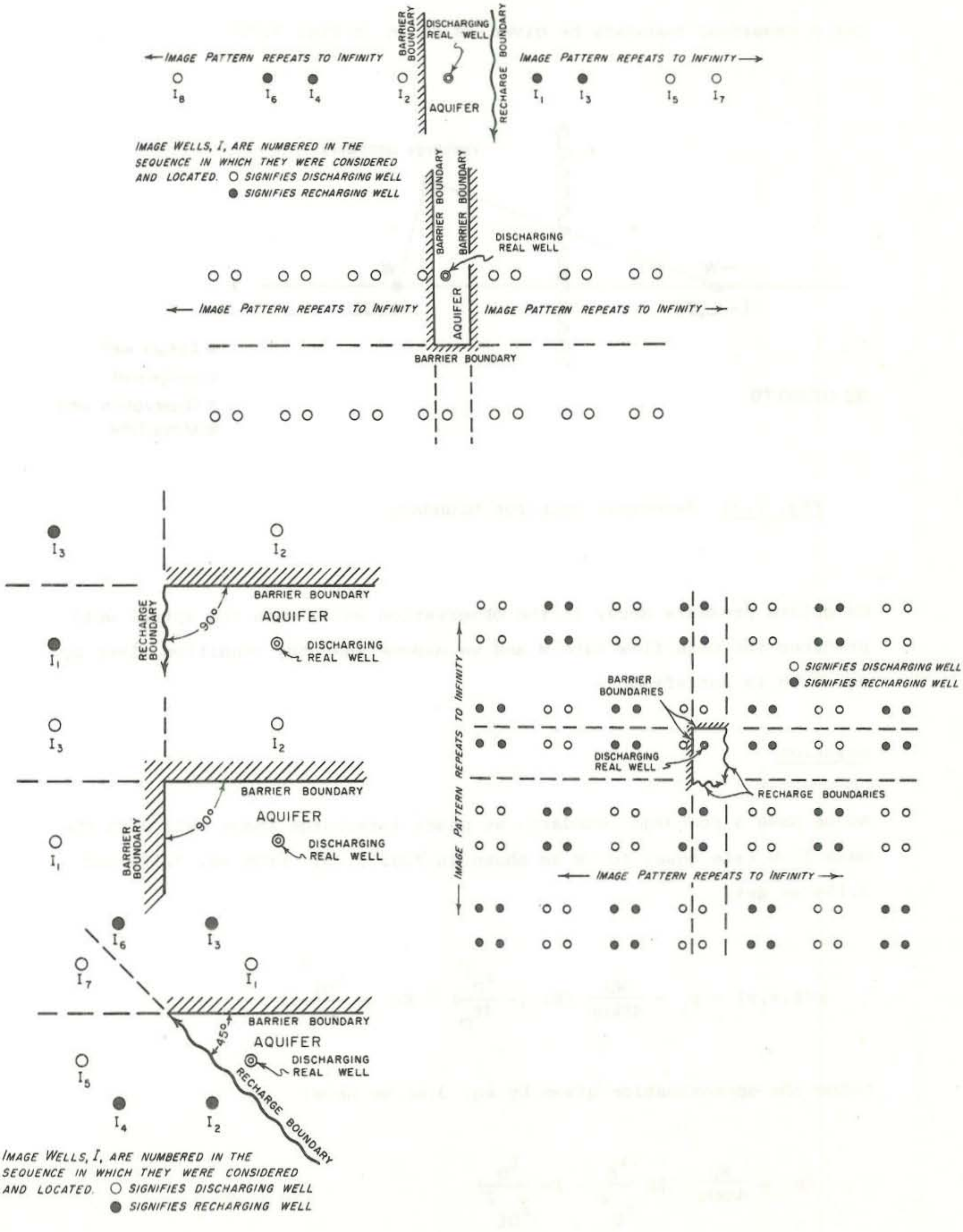

Fig. 3.38 Plans of image well systems for several boundary geometries (Ferris et al. 1962)

EXERCISE 3.10

Let a reservoir boundary be given as shown in Fig. 3.39.

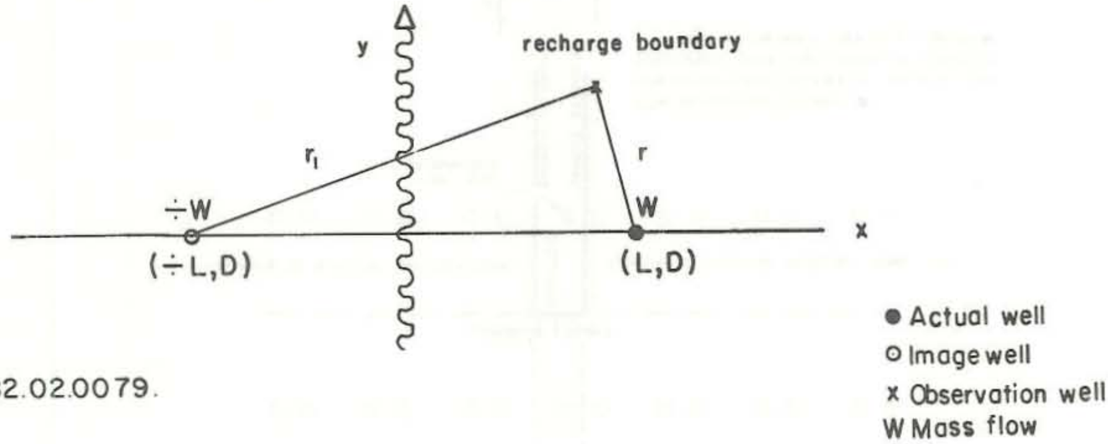

Fig. 3.39 Reservoir recharge boundary

Calculate pressure decay in the observation well, when the actual well produces the mass flow rate W and we assume that the condition given by eq. 3.68 is satisfied?

Solution

As we have a recharge boundary, we place a recharge image well with the mass flow rate equal to -W as shown in Fig. 3.39. From eq. 3.151 and 3.154 we get:

$$p(t,x,y) = p_i - \frac{W\mu}{4\pi kh\rho} \left(\mathrm{Ei}\left(-\frac{r_D^2}{4t_D}\right) - \mathrm{Ei}\left(-\frac{r_{Di}^2}{4t_D}\right)\right)$$

Using the approximation given by eq. 3.66 we have:

$$\Delta p = \frac{W\mu}{4\pi kh\rho} \left(\ln \frac{t_D}{r_D^2} - \ln \frac{t_D}{r_{Di}^2}\right)$$

$$= \frac{W\mu}{2\pi kh\rho} \ln \frac{r_i}{r} \qquad (3.165)$$

which is the formula for the potential field created by a dipole system consisting of one source and a corresponding sink.

The drawdown becomes steady everywhere as could be expected, because eq. 3.165 is only valid for high time values, and the flow must approach steady state with time because of the recharge (constant pressure) boundary condition.

3.13 Wellbore storage effects

In the reservoir engineering literature the liquid flow from the reservoir into the well is sometimes called the sand face flow. The cause of the wellbore storage effect is that the sand face reservoir boundary flow rate does not necessarily have to be equal to the well fluid flow at all times. If a well is suddenly opened, the wellbore pressure will drop, and cause expansion in boiling wells and water level depletion at first in non-boiling wells. If a well is suddenly shut in, fluid continues to pass through the sand face into the hole. Both effects result in changes of the wellbore storage volume. Fig. 3.40 shows a schematic picture of the sand face flowrate vs. dimensionless time for different wellbore storage coefficients. The sand face flowrate can be calculated from the following equation:

$$W_{sf} = W - \rho C \frac{dp_w}{dt} \tag{3.166}$$

where W_{sf} is the sand face mass flow, W is the surface mass flow, C is a wellbore storage coefficient and P_w is the bottomhole pressure. If the well has free liquid level, the wellbore storage coefficient is given by:

$$C = \frac{\pi r_w^2}{\gamma} \tag{3.167}$$

and if the well is completely filled with liquid under pressure the wellbore storage coefficient is given by the following equation:

$$C = V_w C_1 \tag{3.168}$$

where V_w is the volume of the well and C_1 is the compressibility of the liquid in the well. Eq. 3.166 can be nondimenionalized by introducing the dimensionless pressure and time given by eqs. 3.17 and 3.20.

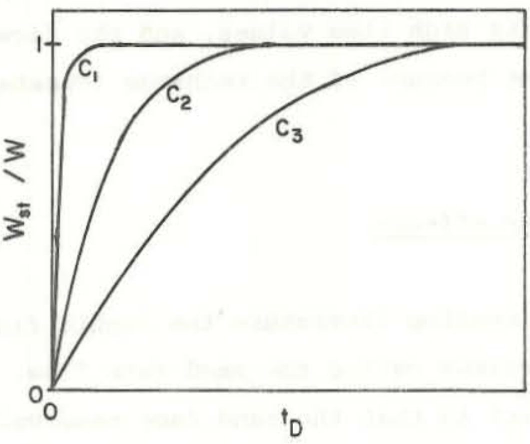

Fig. 3.40 Effect of wellbore storage on a sand face flow rate, $C_3>C_2>C_1$ (Earlougher 1977)

$$\frac{W_{sf}}{W} = 1 - C_D \frac{dP_D}{dt_D} \tag{3.169}$$

where C_D is a dimensionless wellbore storage coefficient defined by:

$$C_D = \frac{C}{2\pi\phi chr_w^2} \tag{3.170}$$

At the beginning of the well test the sand face flow rate is approximately zero in that case eq. 3.169 gives by taking logarithms of both sides:

$$\log \Delta t_D = \log \Delta P_D + \log C_D \tag{3.171}$$

From this eq. we see that from the log-log plot of pressure vs. time we would get a straight line with unit slope. The wellbore storage effect can thus be recognized by unit slope of the early transient pressure data. Fig. 3.41 is an illustration of such a graph. The curves in Fig. 3.42 are determined by solving the usual differential equation and boundary conditions given by eq. 3.59 for the infinite reservoir case by including eq. 3.169 into the third boundary condition getting:

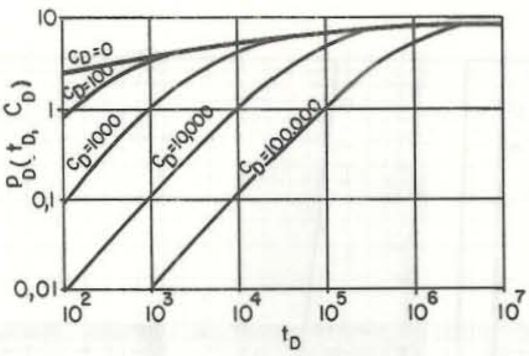

82.02.0081.

Fig. 3.41 Dimensionless pressure including wellbore storage (Wattenbarger and Ramey 1970)

$$\lim_{r_D \to o} r_D \frac{\partial P_D}{\partial r_D} = 1 - C_D \frac{\partial P_D}{\partial t_D} \tag{3.172}$$

This differential eq. was first solved by Everdingen and Hurst (1949) using Laplace transformation techniques. Fig. 3.42 is a full scale picture of such a solution including the skin effect, which will be discussed in section 3.14. Fig. 3.42 can be used for well testing purposes by using the match point method as described in section 3.5.

Once the final portion of the log-log plot is reached (C_D = o line), wellbore storage is no longer important and standard Theis match point method (semilog dataplotting analysis techniques) apply. As a rule of thumb, that time usually occurs about 1 to 1 1/2 cycles in time after the log-log data plot starts deviating significantly from the unit slope. The time may be estimated from (see Earlougher 1977)

$$t_D > (60 + 3.5S)\ C_D \tag{3.173}$$

or approximately:

$$t > \frac{(9.5 + 0.56S)}{kh/\mu} \tag{3.174}$$

Papadopulos and Cooper (1967) took also into account the radius of the wellbore. The boundary conditions in this case are given by eq. 3.69

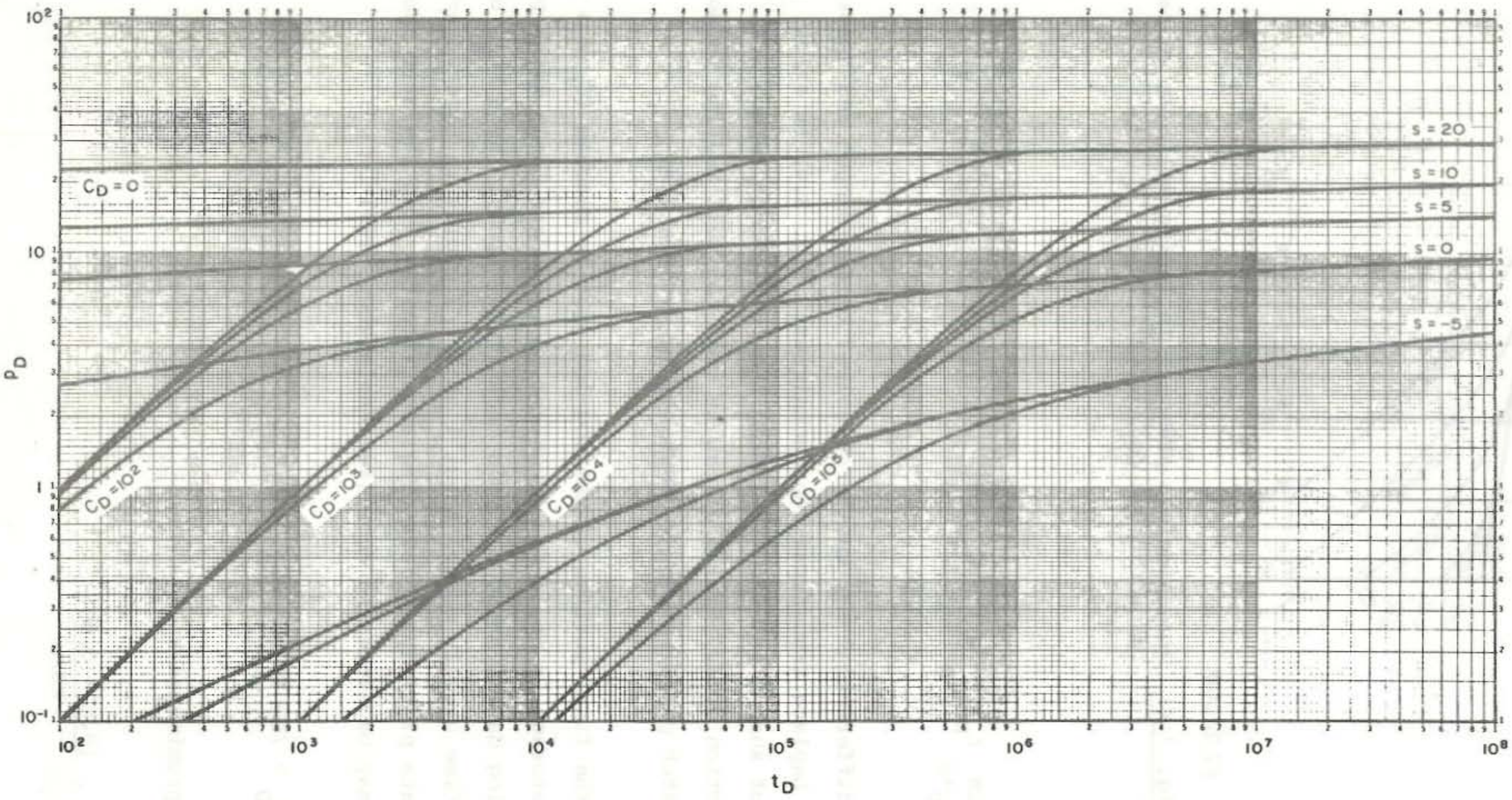

Fig. 3.42 Dimensionless pressure for a single well in an infinite system, wellbore storage and skin included (Agarwal et al. 1970)

except for the third condition which must be altered due to the wellbore storage effect. The altered boundary condition is similar to eq. 3.172 and is given by:

$$\lim_{r_D \to 1} \left(r_D \frac{\partial P_D}{\partial r_D}\right) = 1 - C_D \frac{\partial P_D}{\partial t_D} \tag{3.175}$$

Papadopulos and Cooper gave their solution in the following form written in terms of drawdown and volumetric flow.

$$s_w = \frac{Q}{4\pi T} F(u_w, \alpha) \tag{3.176}$$

where α and u_w are defined in the following way:

$$\alpha = \frac{1}{2C_D} \tag{3.177}$$

$$u_w = \frac{r_w^2 S}{4Tt} \tag{3.178}$$

and the dimensionless drawdown function $F(u_w, \alpha)$ is given in Table 3.5 and shown in Fig. 3.43. Papadopulos and Cooper did not include skin effect in their solution. They give the time corresponding to eq. 3.174 for the Theis equation to apply by:

$$t > 80\gamma\frac{C}{T} \tag{3.179}$$

Including eq. 3.167 gives:

$$t > 80 \frac{\pi r_w^2}{T}$$

For wells of small diameter and/or aquifers of high transmissivity this period is very small. However for wells of large diameter and/or aquifers of low transmissivity this period is considerably larger.

u_w	$\alpha = 10^{-1}$	$\alpha = 10^{-2}$	$\alpha = 10^{-3}$	$\alpha = 10^{-4}$	$\alpha = 10^{-5}$
10	9.755×10^{-3}	9.976×10^{-4}	9.998×10^{-5}	1.000×10^{-5}	1.000×10^{-6}
1	9.192×10^{-2}	9.914×10^{-3}	9.991×10^{-4}	1.000×10^{-4}	1.000×10^{-5}
5×10^{-1}	1.767×10^{-1}	1.974×10^{-2}	1.997×10^{-3}	2.000	2.000
2	4.062	4.890	4.989	4.999	5.000
1	7.336	9.665	9.966	9.997	1.000×10^{-4}
5×10^{-2}	1.260×10^{0}	1.896×10^{-1}	1.989×10^{-2}	1.999×10^{-3}	2.000
2	2.303	4.529	4.949	4.995	5.000
1	3.276	8.520	9.834	9.984	1.000×10^{-3}
5×10^{-3}	4.255	1.540×10^{0}	1.945×10^{-1}	1.994×10^{-2}	2.000
2	5.420	3.043	4.725	4.972	4.998
1	6.212	4.545	9.069	9.901	9.992
5×10^{-4}	6.960	6.031	1.688×10^{0}	1.965×10^{-1}	1.997×10^{-2}
2	7.866	7.557	3.523	4.814	4.982
1	8.572	8.443	5.526	9.340	9.932
5×10^{-5}	9.318	9.229	7.631	1.768×10^{0}	1.975×10^{-1}
2	1.024×10^{1}	1.020×10^{1}	9.676	3.828	4.861
1	1.093	1.087	1.068×10^{1}	6.245	9.493
5×10^{-6}	1.163	1.162	1.150	8.991	1.817×10^{0}
2	1.255	1.254	1.249	1.174×10^{1}	4.033
1	1.324	1.324	1.321	1.291	6.779
5×10^{-7}	1.393	1.393	1.392	1.378	1.013×10^{1}
2	1.485	1.485	1.484	1.479	1.371
1	1.554	1.554	1.554	1.551	1.513
5×10^{-8}	1.623	1.623	1.623	1.622	1.605
2	1.705	1.705	1.705	1.714	1.708
1	1.784	1.784	1.784	1.784	1.781
5×10^{-9}	1.854	1.854	1.854	1.854	1.851
2	1.945	1.945	1.945	1.945	1.940
1	2.015	2.015	2.015	2.015	2.015

Table 3.5 Values of the function $F(u_w,\alpha)$ (Papadopulos and Cooper 1967)

In interference tests the wellbore storage effect and the skin effect can influence the results if the distance between the observation well and the producing well is small. The pressure response at any point in the reservoir will be damped and delayed as a result of the storage effect in the active well, because the main effect of the storage capacity of the flowing well is to cause a time lag for the wellhead flow rate to equal the sand face flow rate. Chu et al. (1980) have presented some type curves for this case.

Miller (1980) has pointed out that additional dimensionless parameter is necessary to describe the wellbore storage due to the time lag between

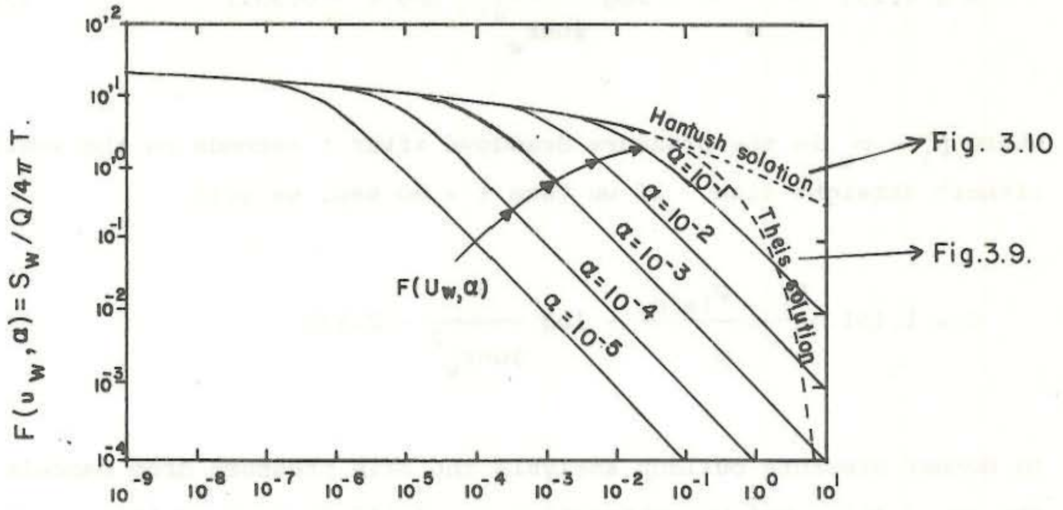

Fig. 3.43 Type curves for the drawdown in a large-diameter well (Papadopulos and Cooper 1967)

the pressure change at the well head and the sand face. That is to say the time it takes for $\frac{dp_w}{dt}$ to become constant in the well. She also demonstrates that temperature effects due to the heating of the well and because of heat losses to the surroundings influence the initial behaviour of the well.

3.14 Partial penetration and skin effect

The skin effect was first introduced in section 3.4 and the skin factor is defined by eq. 3.28. In connection with the wellbore storage effect some dimensionless pressure functions were introduced, which accounted for the skin effect. The skin factor could then be determined by the match point method. We will now demonstrate how the skin factor can be determined by pressure drawdown and pressure buildup testing. In a single rate drawdown test the pressure drawdown according to eq. 3.114 can be written including the skin effect.

$$\frac{2\pi kh\rho}{W\mu}(p_i - p_{wf}) = P_D(t_D) + S \qquad (3.180)$$

and for $\frac{t_D}{r_D^2} > 25$. Eq. 3.180 can be rewritten in terms of the skin factor:

$$S = 1.151 \left(\frac{p_i - p_t}{m} - \log \frac{k}{\phi u c r_w^2} - \log t - 0.351\right) \quad (3.181)$$

where $p_i - p_t$ is the pressure drawdown after t seconds on the semilogarithmic straight line. If we take t = 60 sec. we get:

$$S = 1.151 \left(\frac{p_i - p_{1min.}}{m} - \log \frac{k}{\phi \mu c r_w^2} - 2.13\right) \quad (3.182)$$

In Horner pressure buildup analysis the skin pressure drop cancels out, see eq. 3.115. But by subtracting eq. 3.118 from eq. 3.181 we get by using the same assumptions as above:

$$S = 1.151 \left(\frac{p_{ws} - p_{wf}}{m} - \log \frac{k}{\phi \mu c r_w^2} - \log \Delta t - 0.351\right) \quad (3.183)$$

here $p_{ws} - p_{wf}$ is the pressure buildup after Δt seconds on the semi-logarithmic straight line Horner graph. If we take Δt = 60 sec. we get:

$$S = 1.151 \left(\frac{p_{ws} - p_{wf}}{m} - \log \frac{k}{\phi \mu c r_w^2} - 2.13\right) \quad (3.184)$$

We have so far discussed the skin effect and the turbulent pressure drop which give additional pressure drop in the vicinity of the producing well. The pressure drop is given in terms of the dimensionless pressure.

$$(p_i - p_{wf}) \frac{2\pi k \rho h}{W\mu} = P_D + S + WC \quad (3.185)$$

By comparing this equation with eq. 3.139 we see that the C-coefficient is given by:

$$C = \frac{\text{(Slope of line in Fig. 3.35)} \times 2\pi hkg}{\mu} \quad (3.186)$$

If turbulence affects the pressure response, the constants S and C can only be determined if the well is tested for two different flow rates. For single flow rate test an apparent skin factor is determined, defined as $S' = S + WC$.

So far we have assumed that the producing well is completed across the entire formation thickness thus ensuring horizontal flow. If the well is not fully penetrating, there is a distortion of the radial flow pattern close to the well giving rise to an additional pressure drawdown. This is generally accounted for by using the full formation thickness and including the effect of partial penetration as an additional skin factor. The method of calculating this additional skin is described in the following. Brons and Marting (1961) have shown that the deviation from radial flow due to restricted fluid entry leads to an additional pressure drop close to the wellbore which can be interpreted as an extra skin factor. This is because the deviation from radial flow only occurs in a very limited region around the well and changes in rate, for instance, will lead to an instantaneous perturbation in the wellbore pressure without any associated transient effects. This pseudoskin can be determined as a function of two parameters, the penetration ratio b and the ratio h/r_w where:

$$b = \frac{\text{the total interval open to flow}}{\text{the total thickness of the producing zone}}$$

and

$$\frac{h}{r_w} = \frac{\text{thickness of the producing zone}}{\text{wellbore radius}}$$

Fig. 3.44 gives some examples of the calculation of these parameters.

Fig. 3.45 gives the results of Brons and Marting. Where k_r is the radial permeability and k_z the vertical permeability. Once the pseudoskin has been calculated it must be subtracted from the total skin measured in the well test to give the mechanical skin factor. In case of steady state drawdown in the reservoir Muskat (1946) gives in case of partial penetration for the pressure drop.

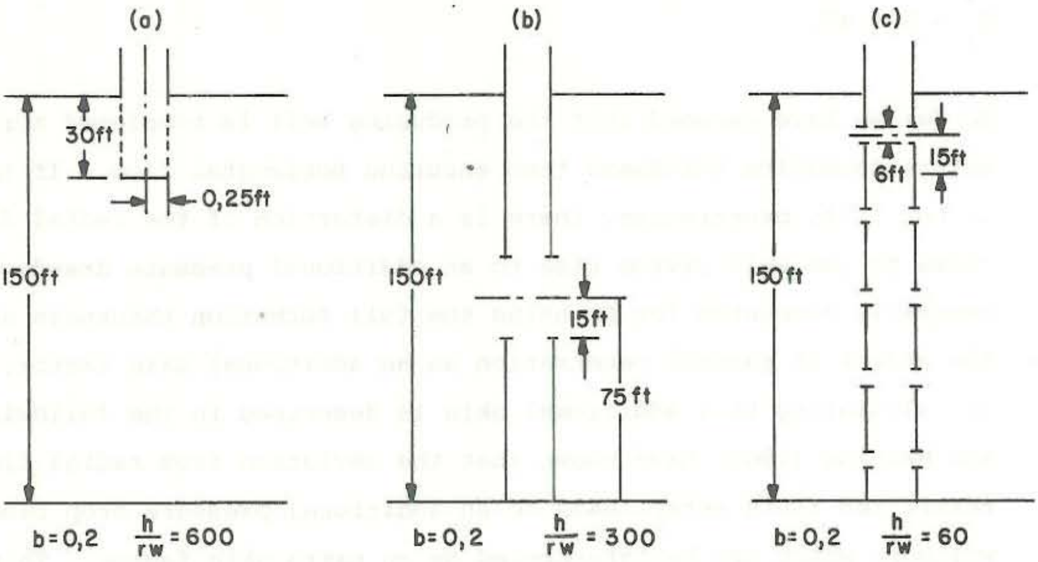

82.01.0084.

Fig. 3.44 Examples of partial well completion showing: (a) well only partially penetrating the formation; (b) well producing from only the central portion of the formation; (c) well with 5 intervals open to production (Brons and Marting 1961)

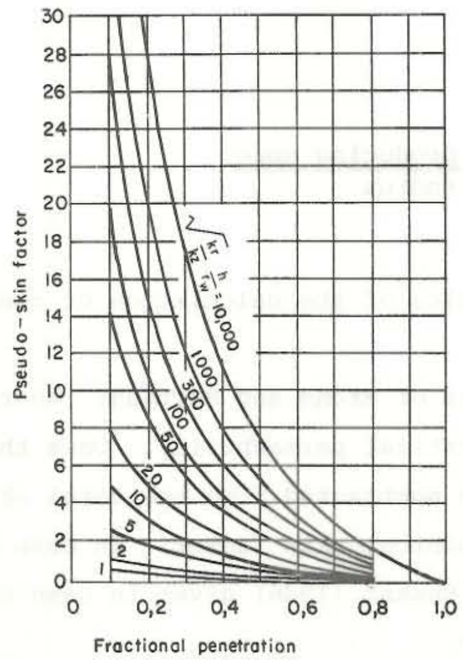

82.02.0085.

Fig. 3.45 Pseudoskin factor for partially penetrating wells (Brons and Marting 1961)

$$\Delta p = \frac{W\mu}{2\pi kh\rho} \ln \left(\frac{r_e}{r_w}\right) \frac{1}{b\left(1 + 7\sqrt{\frac{r_w}{2hb}} \cos \frac{\pi b}{2}\right)} \tag{3.187}$$

By comparing eq. 3.187 and 3.29 we get for the pseudoskin factor:

$$S = \ln \frac{r_e}{r_w} \left(\frac{1}{b\left(1 + 7\sqrt{\frac{r_w}{2hb}} \cos \frac{\pi b}{2}\right)} - 1\right) \tag{3.188}$$

This equation is just valid for equal radial and vertical permeabilities.

Another pseudoskin factor might appear because of slanted wells. Fig. 3.46 schematically shows a well penetrating a formation at an angle θ from the line perpendicular to the formation top and bottom. Fig. 3.47 gives the results by Cinco et al. (1975) for the pseudoskin factor for slanted wells.

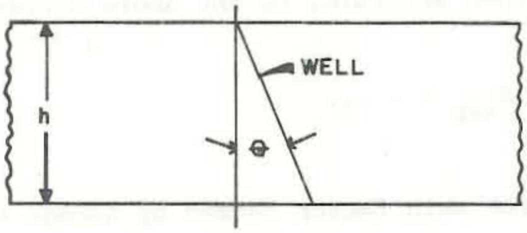

82.02.0049

Fig. 3.46 Definition of terms for slanted wells

The effect of the slanted wells is to provide more wellbore area and, thus, a negative pseudoskin factor.

The productivity index of a well as defined in eq. 3.30 can now be written:

$$PI = \frac{W}{p_e - p_{wf}} = \frac{2\pi hk\rho}{\mu\left(\ln \frac{r_e}{r_w} + S + CW\right)} \tag{3.189}$$

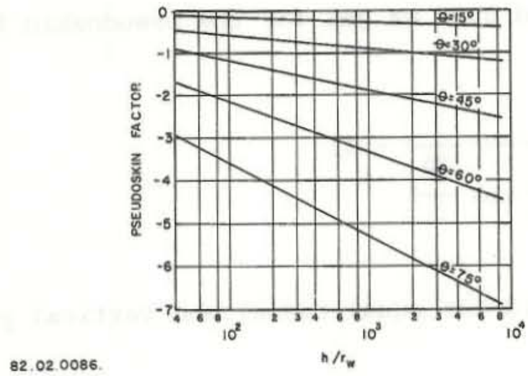

Fig. 3.47 Pseudoskin factor for slanted wells (Cinco et al. 1975)

S is the skin factor and CW is due to the turbulent pressure drop. The skin factor is defined according to the above discussion:

$$S = S_{tr} + S_p + S_{swp} + , \ldots \qquad (3.190)$$

where S_{tr} is the true skin factor caused by damage to the completed portion of the well; S_p is the pseudoskin factor resulting from partial penetration; and S_{swp} is a pseudoskin factor resulting from a slanted well.

3.15 Pressure behaviour of wells intercepting fractures

The principal objective of this section is to provide a summary of the methods used in pressure analysis of wells intercepted by fractures. We will just consider a single fracture existing in a uniform, homogeneous porous formation. Naturally fractured reservoirs consisting of a system of interconnected cracks or failure surfaces coupled to a matrix of different porosity and permeability in a random fashion are not examined. Both vertical and horizontal fractures will be considered. The differential equation is given by eq. 3.13 and the boundary conditions by eq. 3.59 with the difference that boundary condition 3), the wellbore boundary condition is now given by a fracture boundary condition. Two fracture boundary conditions will be considered. The first assumes that the fracture plane is of infinite conductivity. This implies that there is no pressure drop along the fracture plane at any instant in time. The second condition is the uniform-flux fracture, where fluid enters the fracture at a uniform flow rate per unit area of fracture face.

Gringarten et al. (1974) gave the solution for the infinite-conductivity vertical fracture as:

$$p_{w_D}(t_{Dx_f}) = \frac{1}{2}\sqrt{\pi t_{Dx_f}}\left(\mathrm{erf}\,\frac{0.134}{\sqrt{t_{Dx_f}}} + \mathrm{erf}\,\frac{0.866}{\sqrt{t_{Dx_f}}}\right) - 0.067\,\mathrm{Ei}\left(-\frac{0.018}{t_{Dx_f}}\right) - 0.433\,\mathrm{Ei}\left(-\frac{0.750}{t_{Dx_f}}\right) \tag{3.191}$$

where

$$p_{w_D}(t_{Dx_f}) = \frac{2\pi kh\rho}{W\mu}(p_i - p_{wf}) \tag{3.192}$$

and

$$t_{Dx_f} = \frac{kt}{\phi\mu c x_f^{\,2}} \tag{3.193}$$

where erf(x) is the error function of x, $-\mathrm{Ei}(-x)$ is the exponential integral, and x_f is the fracture half length. A plot of eq. 3.191 is shown on Figs. 3.48 and 3.49 on log-log and semi-log paper respectively. At large values of time, $t_{Dx_f} > 3$, eq. 3.191 can be written as:

$$p_{w_D}(t_{Dx_f}) = \frac{1}{2}\ln t_{Dx_f} + 1,100 \tag{3.194}$$

For small values of time ($t_{Dx_f} \leq 0.016$) eq. 3.191 can be approximated as:

$$p_{w_D}(t_{Dx_f}) = \sqrt{\pi t_{Dx_f}} \tag{3.195}$$

This early time period is generally referred to as the linear flow period. As shown in Fig. 3.48 on log-log coordinates this period is characterized by a straight line of slope 0.5. The reason for this may be seen if the logarithm of each side of eq. 3.195 is considered. Taking these logarithms we obtain:

$$\log (P_{w_D}(t_{Dx_f})) = \log \sqrt{\pi} + \frac{1}{2} \log t_{Dx_f} \tag{3.196}$$

Then the reason for the "half slope line" is clear.

For practical well testing purposes eq. 3.191 together with Fig. 3.48 can be used for type-curve matching in order to determine the aquifer parameters. At large values of time eq. 3.194 could be used for traditional semi-log analysis, where the permeability thickness product may be calculated from the slope of the drawdown curve. Once the semi-log straight line has been identified and the permeability thickness product determined the skin factor can be estimated from eq. 3.182 as before.

Gringarten et al. (1974) also arrived at the uniform-flux solution given by:

$$P_{w_D}(t_{Dx_f}) = \sqrt{\pi t_{Dx_f}} \operatorname{erf} \left(\frac{1}{2\sqrt{t_{Dx_f}}}\right) - \frac{1}{2} \operatorname{Ei}\left(-\frac{1}{4t_{Dx_f}}\right) \tag{3.197}$$

This equation is shown on Fig. 3.48 and 3.49. At long times, $t_{Dx_f} \geq 2$ eq. 3.197 may be written as:

$$P_{w_D}(t_{Dx_f}) = \frac{1}{2} (\ln t_{Dx_f} + 2.8091) \tag{3.198}$$

For small times, $t_{Dx_f} \leq 0.16$ eq. 3.195 applies. These eq. can again be used to determine the reservoir parameters. One of the problems in analyzing pressure data by the semi-log approach is that it is difficult to locate the beginning of the pseudo-radial flow period. Inspection of the theoretical solutions, however, indicates that if the one-half slope line can be identified then the correct semi-log line should start approximately two cycles from the time of the end of the one-half slope line for

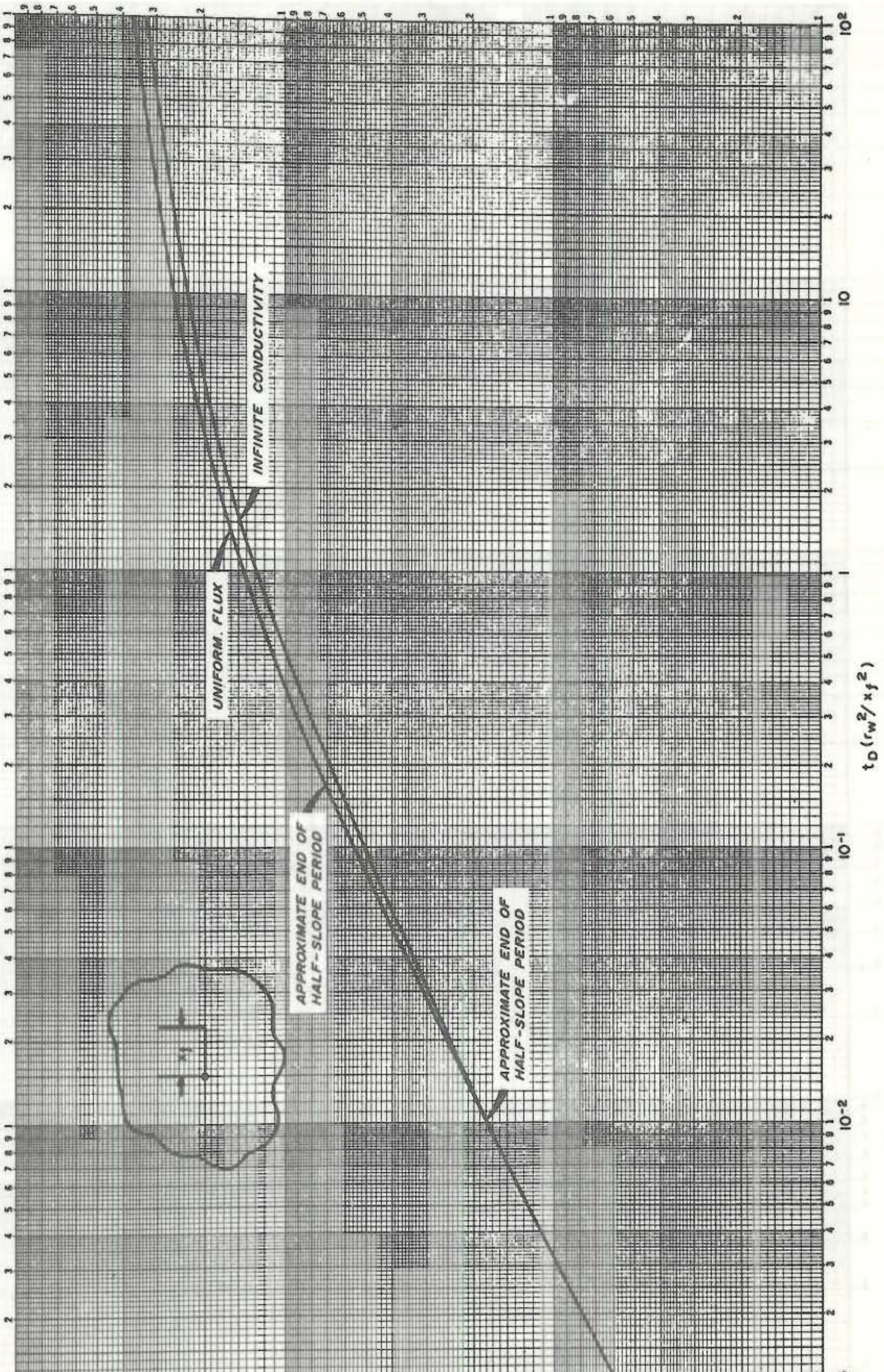

Fig. 3.48 Dimensionless pressure for single, vertically fractured well in an infinite system, no wellbore storage. Log-log plot (Gringarten et al. 1974)

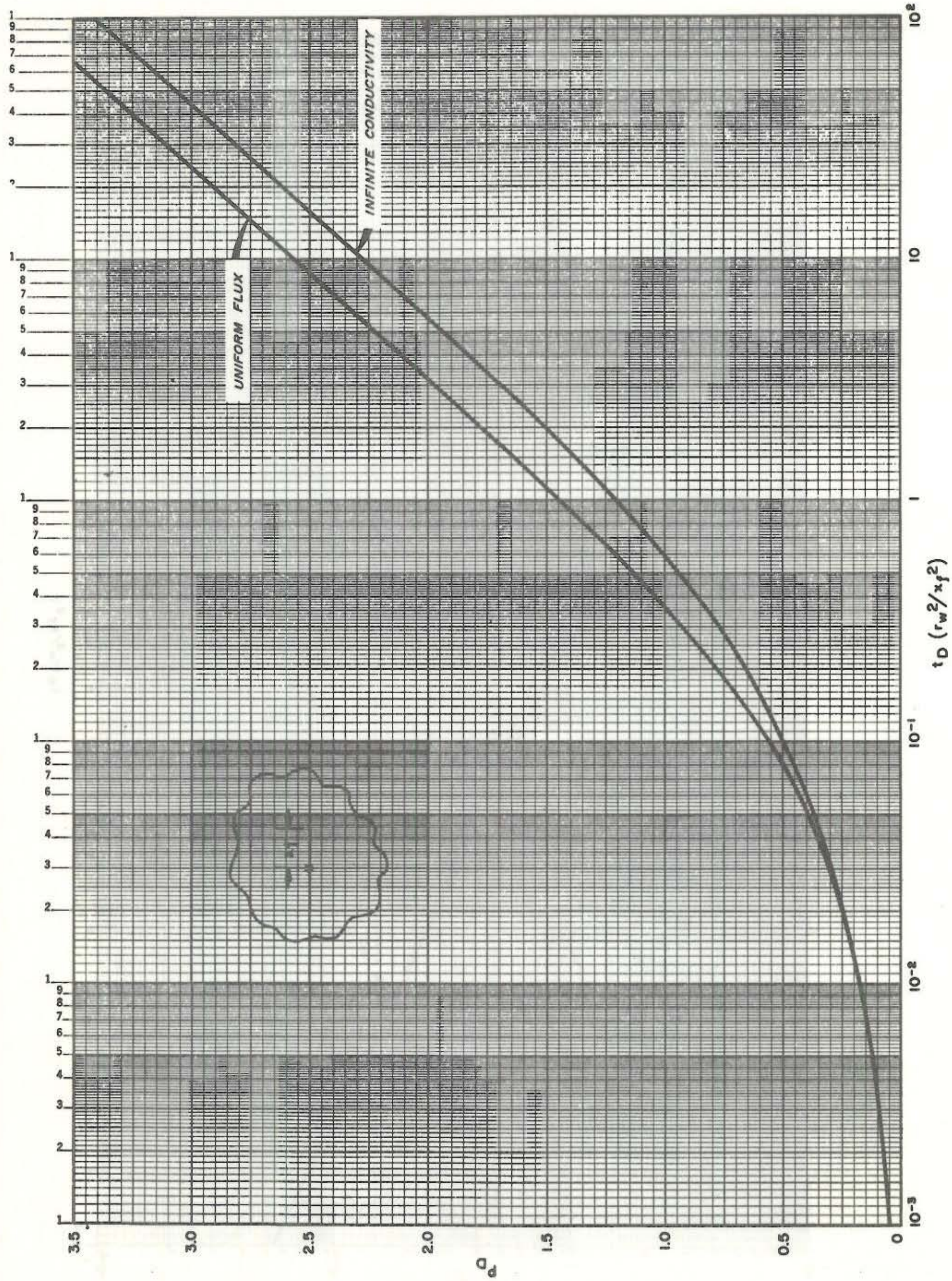

Fig. 3.49 Dimensionless pressure for a single, vertically fractured well in an infinite system, no wellbore storage. Semilog plot (Gringarten et al. 1974)

an infinite-conductivity fracture. For a uniform-flux fracture the time for start of the correct straight line is one cycle from the end of the one-half slope line. A second rule, which is probably more useful than the one stated above, is the "double-ΔP rule". In examining vertically fractured gas wells, Wattenbarger (1967) noticed that the dimensionless pressure drop at the start of the semi-log straight line is twice that of the dimensionless pressure at the end of the one-half slope line. This result, strictly true only for the uniform-flux case, is the "double-ΔP rule". For the infinite-conductivity vertical fracture the pressure change between the end of the one-half slope line and the beginning of the semi-log straight line is approximately 8. In any event it is clear that the ratio of the pressure change must be at least 2. Eq. 3.194 and 3.198 can be written respectively as:

$$P_{w_D}(t_{Dx_f}) = \frac{1}{2}\left(\ln \frac{kt}{\phi\mu c\left(\frac{x_f}{2}\right)^2} + 0.8091\right) \tag{3.199}$$

and

$$P_{w_D}(t_{Dx_f}) = \frac{1}{2}\left(\ln \frac{kt}{\phi\mu c\left(\frac{x_f}{e}\right)^2} + 0.8091\right) \tag{3.200}$$

By comparing these equations with eq. 3.67 it can be seen that by defining the correct effective wellbore radius, the fractured well can be treated as an unfractured well. From eq. 3.199 we see that the correct definition of the effective wellbore radius for an infinite-conductivity vertical fracture is:

$$r_w = \frac{x_f}{2} \tag{3.201}$$

that is one fourth of the fracture length. The correct definition for the uniform-flux fracture can be seen from eq. 3.200 to be:

$$r_w = \frac{x_f}{e} \tag{3.202}$$

In case the fracture has finite capacity, that is the actual finite permeability of the fracture is taken into account, the effective wellbore radius will be different. Fig. 3.50 shows the effect of the finite capacity on the effective wellbore radius. The dimensionless fracture capacity is defined as:

$$F'c_D = \frac{\pi k(2x_f)}{4k_f w} \tag{3.203}$$

where k is the matrix permeability, k_f the fracture permeability and w the fracture width.

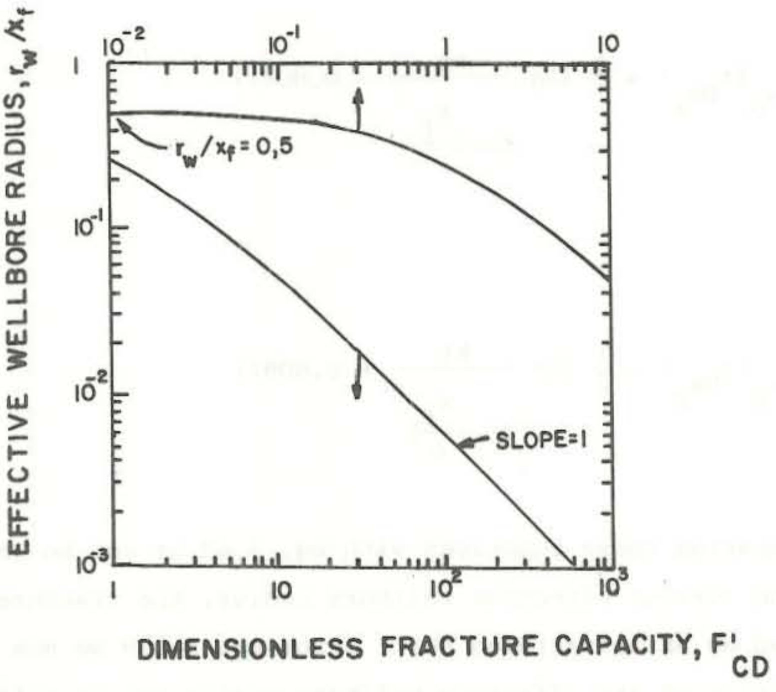

Fig. 3.50 Effective wellbore radius vs. dimensionless fracture capacity (Raghavan 1976)

In many instances there is skin damage associated with the fractured system. Interpretation of data from these wells can be difficult as can be seen from the following. Eq. 3.195 for small times can be written with the skin effect.

$$P_{w_D}(t_{Dx_f}) = \sqrt{\pi t_{Dx_f}} + S \tag{3.204}$$

where S is the skin factor as before. The equation indicates that for small times the first term would be small and thus the one-half slope line would be obscured. Theoretical studies of the wellbore storage effect in fractured wells have been presented by Wattenbarger and Ramey (1968) and Ramey and Gringarten (1975), for the infinite-conductivity vertically fractured well and by Raghavan (1976) for the uniform-flux case.

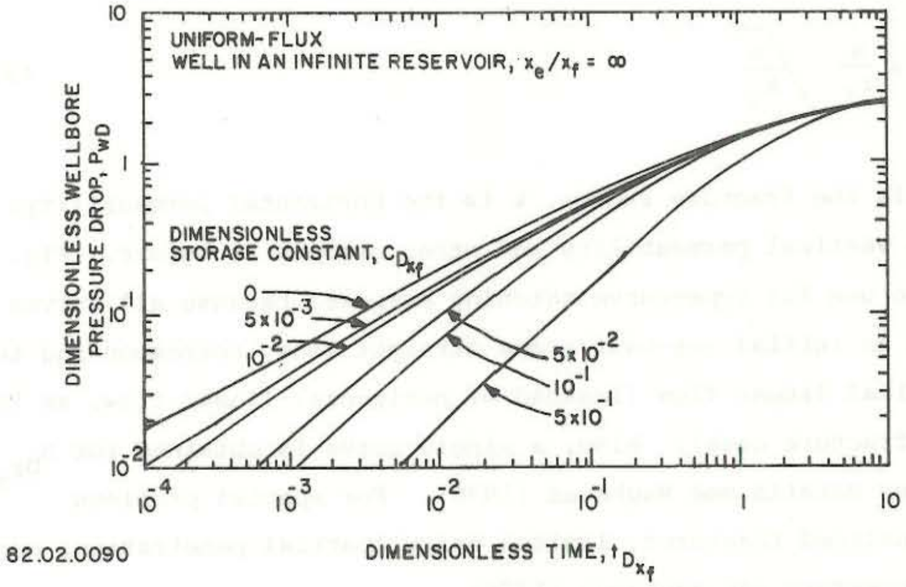

Fig. 3.51 Dimensionless wellbore pressure drop vs. dimensionless time for a uniform-flux vertical fracture with wellbore storage (Raghavan 1976)

Fig. 3.51 is a log-log plot describing the pressure behaviour of a well producing via a uniform-flux fracture which is controlled at early times by wellbore storage. The parameter of interest in Fig. 3.51 is the wellbore storage constant defined as before as:

$$C_{Dx_f} = \frac{C}{2\pi\phi chx_f^2} \tag{3.205}$$

The $C_{Dx_f} = o$ curve corresponds to a fractured well with no wellbore storage. For large values of C_{Dx_f} a line of unit slope similar to that for unfractured systems is obtained, see section 3.13. However for small values of C_{Dx_f} no unit slope line is evident. As time increases, all curves become asymptotic to the $C_{Dx_f} = o$ line. Fig. 3.51 also demonstrates that if wellbore storage is large then the presence of the fracture would be obscured.

The solution for a single horizontal uniform-flux fracture is given in Fig. 3.52. The dimensionless time and thickness are defined as follows:

$$t_{Dr_f} = \frac{kt}{\phi c \mu r_f^{\,2}} \tag{3.206}$$

$$h_{Dr_f} = \frac{h}{r_f} \sqrt{\frac{k}{k_z}} \tag{3.207}$$

where r_f is the fracture radius, k is the horizontal permeability, and k_z is the vertical permeability and other symbols as before. Fig. 3.52 is easy to use for type-curve matching purposes because all curves have in common an initial one-half slope straight line, corresponding to early time vertical linear flow (instead of horizontal linear flow, as for the vertical fracture case). Also, a single curve is obtained for $h_{Dr_f} \geq 100$. For further details see Raghavan (1976). For special problems concerning inclined fractures, limited entry (partial penetration) constant wellbore pressure see Raghavan (1976).

The discussion above has been limited to testing of the production well itself. When performing interference tests the idea of a single vertical fracture might not be correct. In that case the porous medium should be treated as anisotropic. The pressure response caused by a line source well at origin in an anisotropic reservoir is given by:

$$\sqrt{k_{xx}k_{yy} - k_{xy}^{\,2}}\ \frac{2\pi h\rho}{W\mu}\ (p_i - p_{x,y,t})$$

$$= -\frac{1}{2}\,\mathrm{Ei}\left\{\frac{-\phi\mu c}{4t}\left(\frac{k_{xx}y^2 + k_{yy}x^2 - 2k_{xy}xy}{k_{xx}k_{yy} - k_{xy}^{\,2}}\right)\right\} \tag{3.208}$$

where k_{xx}, k_{yy}, k_{xy} are the components of the permeability tensor. By defining the following dimensionless variables:

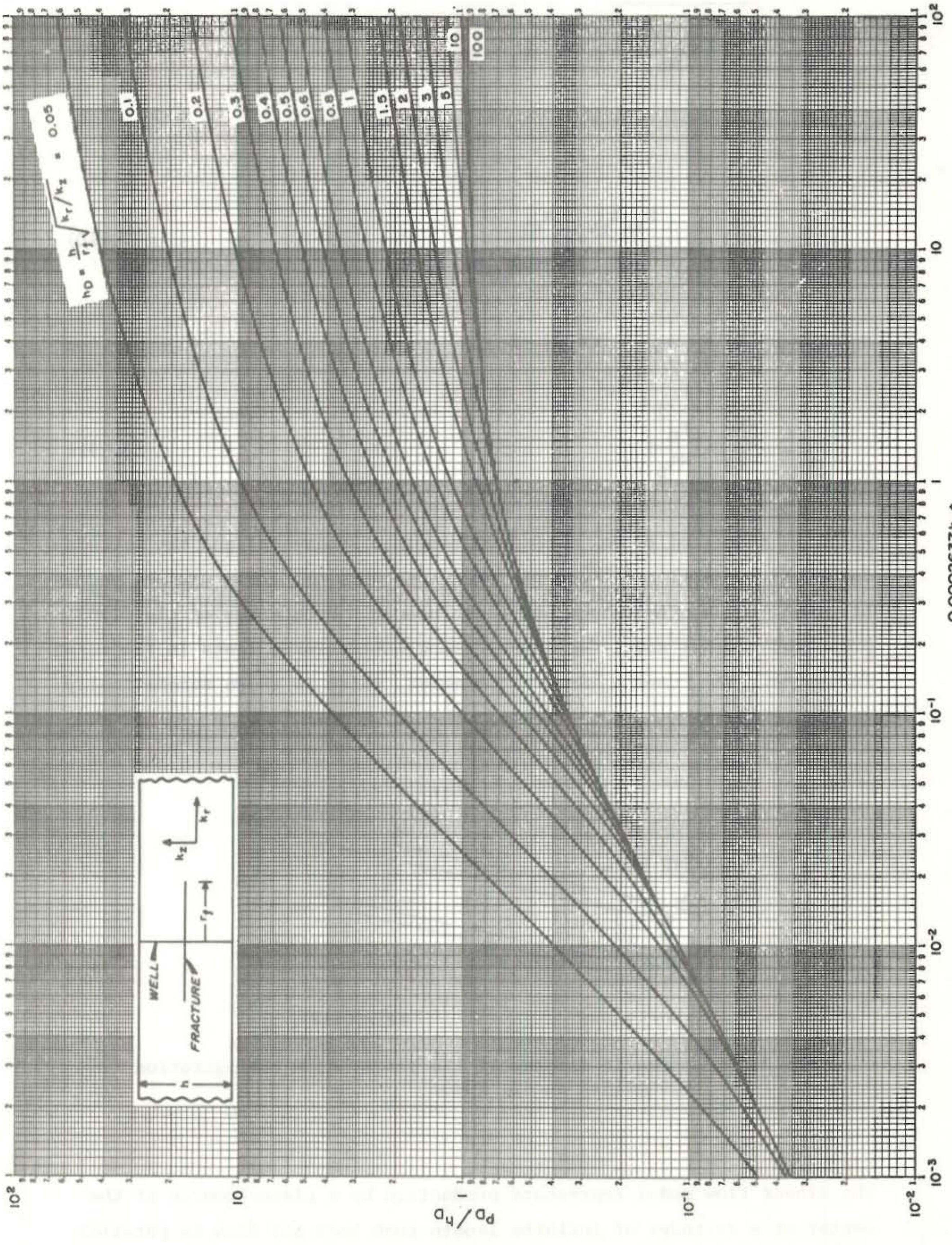

Fig. 3.52 Dimensionless pressure for a single, horizontally fractured (uniform-flux) well in an infinite system, no wellbore storage. Fracture located in the center of the interval (Gringarten et al. 1972)

$$p_D = \frac{\sqrt{k_{xx}k_{yy} - k_{xy}^2}\, 2\pi h\rho}{W\mu} (p_i - p_{x,y,t}) \tag{3.209}$$

and

$$\frac{t_D}{r_D^2} = \frac{t}{\phi\mu c} \frac{k_{xx}k_{yy} - k_{xy}^2}{k_{xx}y^2 + k_{yy}x^2 - 2k_{xy}xy} \tag{3.210}$$

and inserting in eq. 3.208 we obtain:

$$p_D = -\frac{1}{2} \mathrm{Ei}\left(\frac{r_D^2}{4t_D}\right) \tag{3.211}$$

which is identical to eq. 3.60 for isotropic reservoir, and the methods described in section 3.5 can be used. As there are three unknown permeabilities, three observation wells are needed. Economides et al. (1980) presented another model for interpreting interference tests in fractured formation. They used a linear flow model, which is shown schematically in Fig. 3.53.

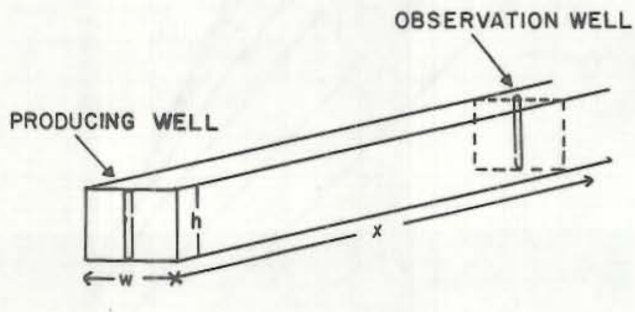

Fig. 3.53 Schematic diagram of the linear flow configuration (Economides et al. 1980)

The linear flow model represents production by a planar source at the center of a cylinder of infinite length such that all flow is parallel to the lateral boundaries. The cross-section of the cylinder is assumed to be a rectangle with height h and width b. This model would be a good approximation in a formation where the faults run parallel and the permeability of the matrix formation is very low. The planar source boundary condition for the linear flow model is analogous to the line source for radial flow. The solution to the problem is given by:

$$\frac{P_D}{x_D} = 2\sqrt{\frac{t_D}{\pi x_D^2}}\exp\left(-\frac{x_D^2}{4t_D}\right) - \mathrm{erfc}\left(\frac{x_D}{2\sqrt{t_D}}\right) \tag{3.212}$$

where

$$t_D = \frac{kt}{\phi\mu c w^2} \tag{3.213}$$

and $x_D = \frac{x}{w}$ (3.214)

A log-log graph of eq. 3.212 is shown in Fig. 3.54. The characteristic half-slope behaviour for log-log graphs of pressure versus time results from small values of x and from large t. The limiting solution for $t_D/x_D^2 \geq 1000$ is:

$$\frac{P_D}{x_D} = 2\sqrt{\frac{t_D}{\pi x_D^2}} \tag{3.215}$$

Values of P_D/x_D vs. t_D/x_D^2 are given in Table 3.6.

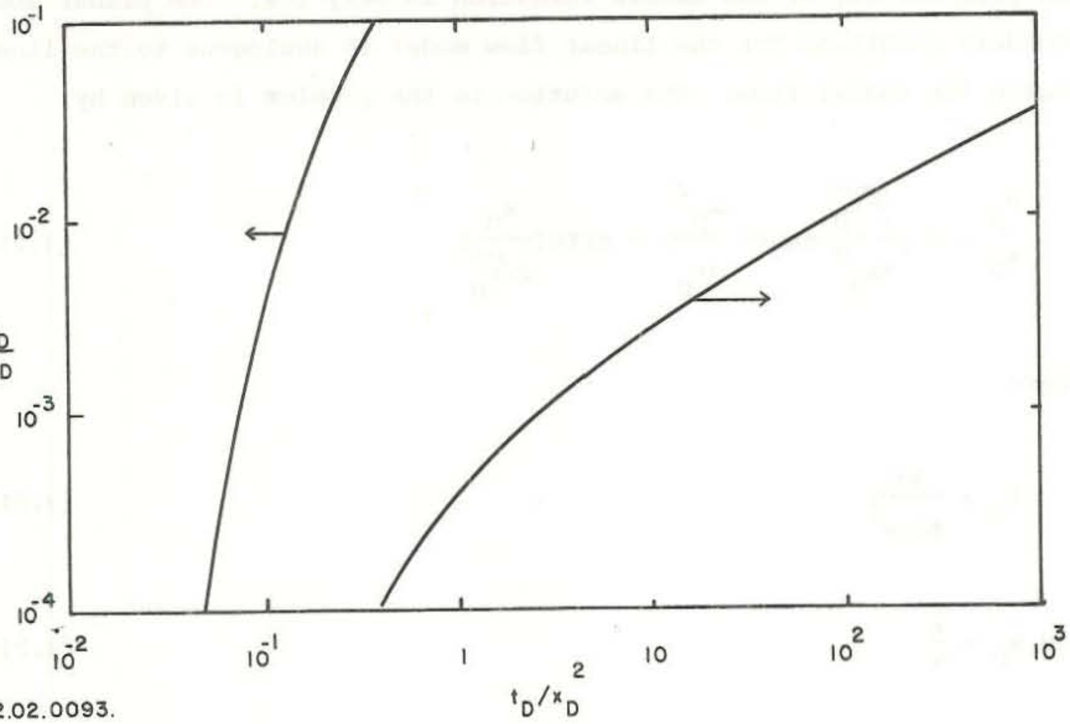

Fig. 3.54 Drawdown interference type-curve for linear flow to a planar source (Economides et al. 1980)

$\frac{t_D}{x_D^2}$	$\frac{p_D}{x_D}$	$\frac{t_D}{x_D^2}$	$\frac{p_D}{x_D}$	$\frac{t_D}{x_D^2}$	$\frac{p_D}{x_D}$
.03	2.204×10^{-6}	2.0	.7912	150.0	12.84
.04	2.850×10^{-5}	3.0	1.115	200.0	14.98
.05	1.347×10^{-4}	4.0	1.396	300.0	18.56
.06	3.930×10^{-4}	5.0	1.648	400.0	21.58
.07	8.676×10^{-4}	6.0	1.878	500.0	24.24
.08	.001603	7.0	2.091	600.0	26.65
.09	.002625	8.0	2.291	700.0	28.86
.10	.003943	9.0	2.479	800.0	30.93
.15	.01465	10.0	2.657	900.0	32.86
.20	.03073	15.0	3.443	1000.0	34.69
.30	.0719	20.0	4.109	1500.0	42.71
.40	.1184	30.0	5.232	2000.0	49.47
.50	.1666	40.0	6.181	3000.0	60.81
.60	.2149	50.0	7.019	4000.0	70.37
.70	.2625	60.0	7.777	5000.0	78.79
.80	.3092	70.0	8.474	6000.0	86.41
.90	.3548	80.0	9.124	8000.0	99.93
1.0	.3993	90.0	9.734	10000.0	111.8
1.5	.6061	100.0	10.31		

Table 3.6 Dimensionless pressure solution for linear flow to a constant rate planar source. (Economides et al. 1980)

Fig. 3.55 shows the combined drawdown buildup interference type-curve for the linear flow model. The buildup part of the type-curve is calculated from eq. 3.115.

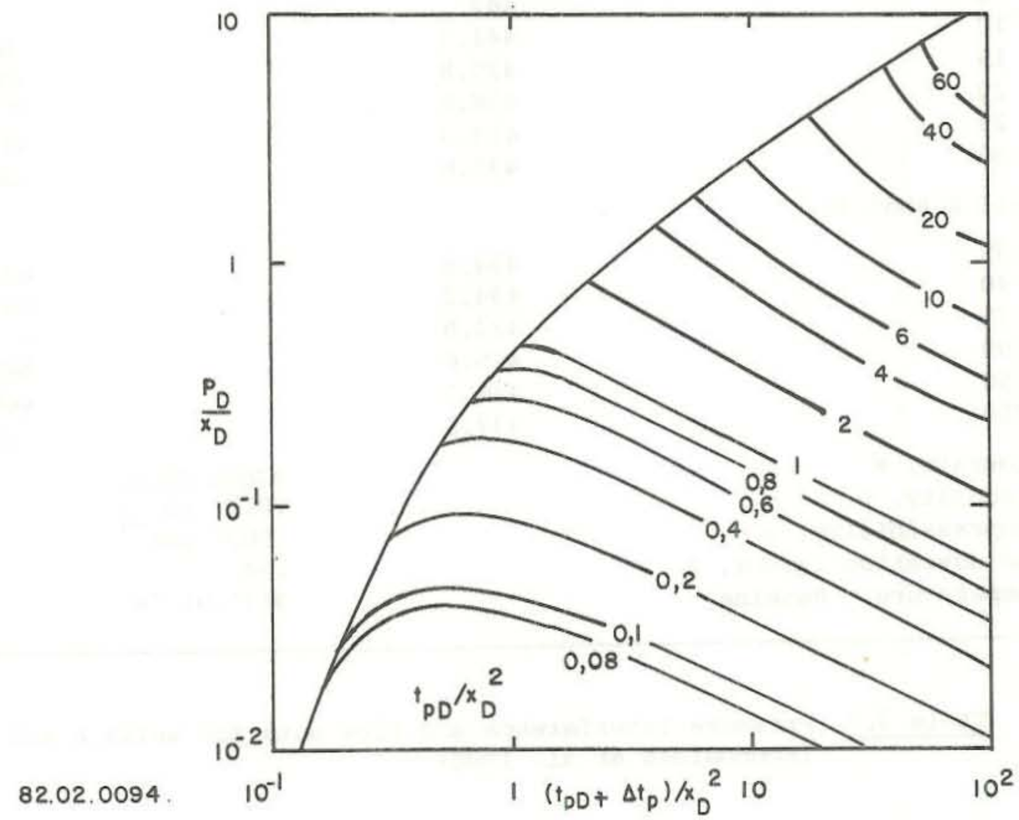

Fig. 3.55 Drawdown-buildup interference type-curve for linear flow to a planar source (Economides et al. 1980)

EXERCISE 3.11

An interference test was run in a new development at the Geysers. Well A was producing for 30 days, while well B, 1800 ft. from well A, was shut in. Pressures recorded at well B and pertinent flow data appears in Table 3.7. Determine the reservoir parameters.

Time (Days)	Bottomhole pressure (psia)	$p_i^2 - p^2$ (psia^2)
0	442	
10	441.3	620
15	439.8	1940
20	438.9	2730
25	437.3	4130
30	435.8	5440
Well A shut in		
35	434.8	6310
40	434.2	6830
75	434.8	6310
100	435.6	5620
150	436.7	4660
250	437.8	3700
Flowrate, W	97000 lb/hr	
Viscosity, μ	.017 cp	
Compressibility, c	.0025 psi^{-1}	
Gas deviation factor, Z	.84	
Temperature, °Rankine	913°-915°R	

Table 3.7 Pressure interference and flow data for wells A and B (Economides et al. 1980)

Solution

The dimensionless variables written in units according to Table 3.6 are as follows:

$$p_D = \frac{kh(p_i^2 - p^2)}{28.62W\mu ZT}$$

$$t_D = \frac{0.000264kt}{\phi\mu cb^2} \tag{3.216}$$

$$x_D = \frac{x}{w}$$

where the units of the constants are:

W in ft., c in psi^{-1}, h in ft., k in md, P in psi, t in hours, temperature T in °R, W in lb/hr, μ in centipoise, x in ft. The dimensionless pressure in eq. 3.216 is defined for compressible steam and will be discussed in section 3.16. The new constants in the dimensionless pressure expression are the temperature, T, and the gas deviation constant, Z. The type-curve in Fig. 3.55 is used and the result is shown in Fig. 3.56.

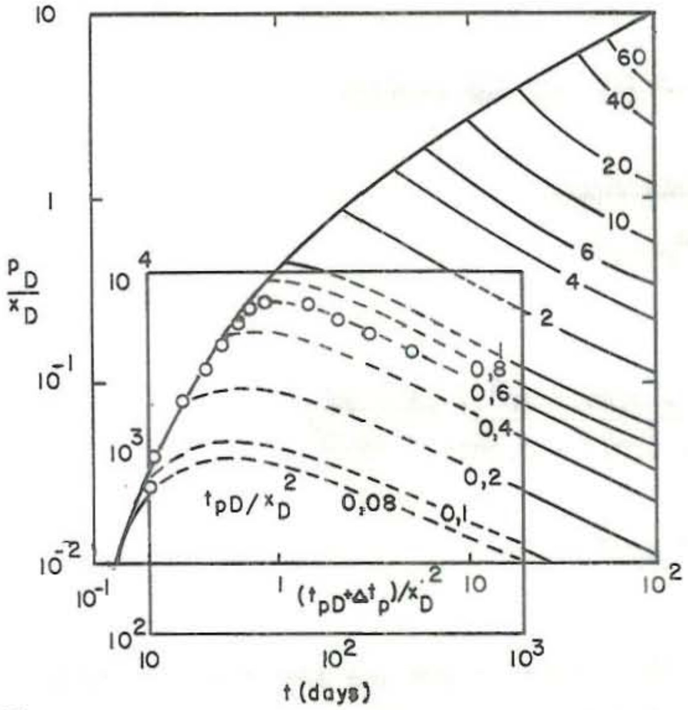

82.02.0095

Fig. 3.56 Type-curve matching for example application-linear flow model (Economides et al. 1980)

The following match points can be obtained:

$$\frac{p_D}{x_D} = 4.1 \cdot 10^{-2} \qquad p_i^2 - p^2 = 1000 \text{ psia}^2$$

$$\frac{t_{pD} + \Delta t_p}{x_D^2} = 2 \cdot 10^{-1} \qquad t = 10 \text{ days}$$

Using eq. 3.216 and solving for the kh product:

$$khW = \frac{p_D}{x_D}\frac{28.62W\mu ZTx}{p_i^2 - p^2}$$

$$= \frac{4.1 \cdot 10^{-2} \cdot 28.62 \cdot 97000 \cdot 0.017 \cdot 0.84 \cdot 914 \cdot 1800}{1000}$$

$$= 2.67 \cdot 10^6 \text{ md ft.}^2$$

Solving eq. 3.216 for the ϕhW product:

$$\phi hW = \frac{0.000264(khW)t}{(\frac{t_D}{x_D^2})\mu c x^2}$$

$$= \frac{0.000264 \cdot 2.67 \cdot 10^6 \cdot 10 \cdot 24}{2 \cdot 10^{-1} \cdot 0.017 \cdot 0.0025 \cdot 1800^2}$$

$$= 6.14 \cdot 10^3 \text{ ft.}^2$$

If we introduce the values of khW and ϕhW obtained above and the value of t_p = 30 days in the dimensionless time equation, we obtain t_{pD}/x_D^2 = = 0.6 which agrees with the type-curve match.

3.16 Well test analysis in two phase flow reservoirs

In a vapour-dominated field we have a two phase flow of water and steam. In a well test lowering of the pressure results in isenthalpic flow towards the well. If the steam becomes dry before it reaches the well, the well will produce superheated steam. Fig. 3.57 shows the pressure-enthalpy diagram for water and steam. The isothermal flow for steam temperature 250°C in the superheated steam region is shown on the figure for a pressure drop of 10 bars. We see from the figure that for isothermal flow of the superheated steam its enthalpy is increased and this extra heat must be delivered by the rock mass. If the steam behaved like ideal gas, then the flow would be isenthalpic as well as isothermal.

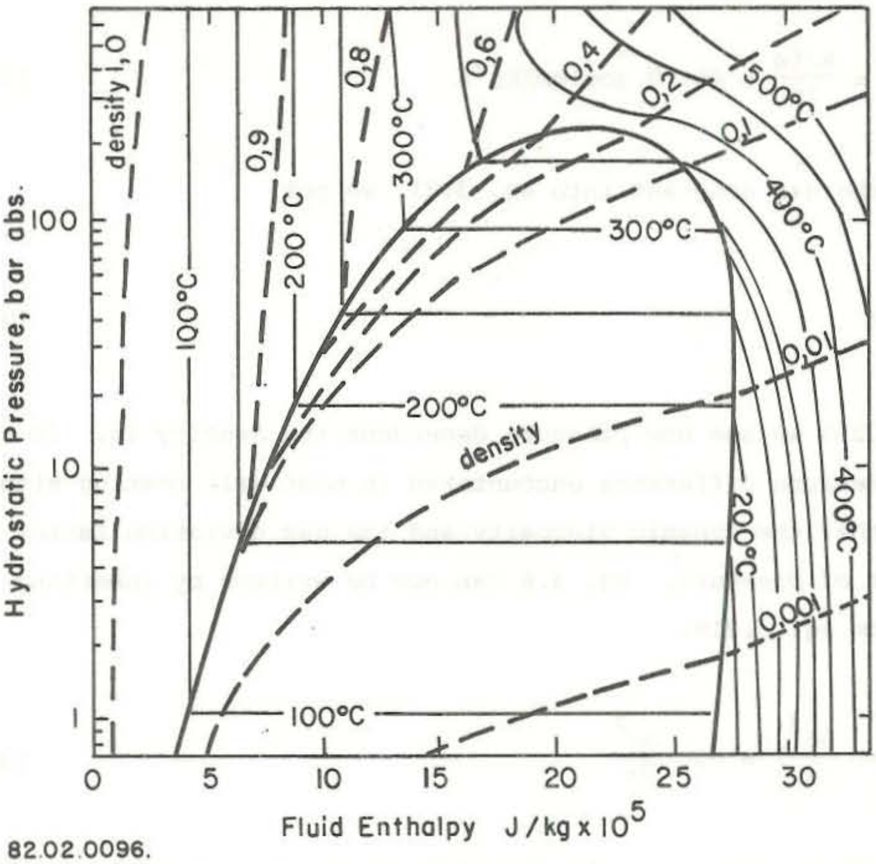

82.02.0096.

Fig. 3.57 Pressure-enthalpy diagram

If we assume that the superheated steam zone around the well dominates in the well test and that the rock delivers enough heat to the steam for it to flow isothermally eq. 3.6 for isothermal, compressible flow can be used:

$$\frac{1}{r} \frac{\partial}{\partial r} \left(\frac{k\rho}{\mu} r \frac{\partial p}{\partial r}\right) = c\rho\phi \frac{\partial p}{\partial t} \tag{3.6}$$

The equation of state for the steam can be written as:

$$p = \frac{\rho R' T}{M} Z \tag{3.217}$$

where R' is the universal gas constant equal to 8314 joules/mole °K, M is the molecular weight of water equal to 18 g/mole, and Z is the gas deviation factor, telling how much the steam deviates from ideal gas.

The gas constant for steam is defined as:

$$R = \frac{R'}{M} = \frac{8314}{18} = 461.9 \text{ joules/kg}^\circ\text{K} \tag{3.218}$$

Inserting the gas constant into eq. 3.217 we get:

$$\frac{p}{\rho RT} = Z \tag{3.219}$$

From eq. 3.219 we see how pressure dependent the density is. In the range of pressure difference encountered in most well testing situations we assume that the dynamic viscosity and the gas deviation factor are independent of pressure. Eq. 3.6 can now be written by inserting the density from eq. 3.219:

$$\frac{1}{r}\frac{\partial}{\partial r}\left(kr\frac{\partial p^2}{\partial r}\right) = c\phi\mu\frac{\partial p^2}{\partial t} \tag{3.220}$$

We now see that we have partly transformed the nonlinearities from eq. 3.6, by using the pressure squared instead of pressure. The compressibility c is still pressure dependent as we see from the following. If we assume that the rock compressibility is small compared with the steam compressibility we get from eq. 3.5:

$$c = \beta \tag{3.221}$$

By combining eq. 3.219 and eq. 3.10 we get:

$$c = \beta = \frac{1}{p} \tag{3.222}$$

showing clearly the pressure dependance of c. The compressibility is a part of the definition of the storage coefficient, see eq. 3.7. The storage coefficient is very different depending on the type of reservoir fluid. Let us define the mass derived from storage per unit decline in pressure per unit area for four different reservoir fluids: 1) water, 2) superheated steam, 3) saturated steam, 4) water in a watertable aquifer.

1) We have from eq. 3.7:

$$\frac{dm}{dp} = \rho_w \beta_w \phi h \tag{3.223}$$

2) We get from eq. 3.7 and 3.222:

$$\frac{dm}{dp} = \rho_s \frac{1}{p} \phi h = \frac{1}{ZRT} \phi h \tag{3.224}$$

3) The pressure and temperature must remain on the saturation curve, see Grant and Sorey (1979), so we have:

$$\Delta T = \Delta p / \frac{dp_s}{dT} \tag{3.225}$$

The Clausius - Clapeyron equation is:

$$\frac{dp_s}{dT} = \frac{\rho_w \rho_s}{\rho_w - \rho_s} \frac{L}{T} \tag{3.226}$$

where L is the latent heat of vapourization. Inserting eq. 3.226 into eq. 3.225 gives:

$$\Delta T = \Delta p \frac{\rho_w \rho_s}{\rho_w - \rho_s} \frac{L}{T} \tag{3.227}$$

With the temperature drop, heat is released from the rock and water, the enthalpy of steam is nearly constant on the saturation line. The amount of heat is given by:

$$\Delta Q = V \{(1 - \phi) \rho_r c_r + \phi S_w \rho_w c_w\} \Delta T \tag{3.228}$$

where V is some reference volume, S_w is water saturation, and the subscripts r,w,s refer to rock, water and steam respectively. This heat is used to evaporate a mass of water given by:

$$\Delta m = \frac{\Delta Q}{L} \tag{3.229}$$

which corresponds to an increase in volume:

$$\Delta V = \Delta m \left(\frac{1}{\rho_s} - \frac{1}{\rho_w}\right) \tag{3.230}$$

The compressibility can now be calculated from the definition by combining eq. 3.227-3.230:

$$\beta_s = \frac{1}{\phi V}\frac{\Delta V}{\Delta p} = \left(\frac{\rho_w - \rho_s}{\rho_w \rho_s L}\right)^2 T \frac{(1-\phi)\rho_r c_r + \phi S_w \rho_w c_w}{\phi} \tag{3.231}$$

T is in degrees Kelvin.

We can now write:

$$\frac{dm}{dp} = \rho_s \beta_s \phi h$$

$$\cong \frac{T}{\rho_s L^2}\{(1-\phi)\rho_r c_r + \phi S_w \rho_w c_w\}\, h \tag{3.232}$$

4) In a watertable reservoir the mass realeased from storage comes from the movement of the watertable. We thus have:

$$dm = \frac{dp}{\gamma}\phi\rho_w \tag{3.233}$$

which results in:

$$\frac{dm}{dp} = \frac{\phi}{g} \tag{3.234}$$

Let us compare these four different cases by inserting numerical values. For example $T = 240^\circ C$, $\phi = 10\%$, $\rho_r = 2500\ kg/m^3$, $c_r = 1000\ J/kg^\circ C$, $S_w = 0.5$, $c_w = 4700\ J/kg^\circ C$, $\beta_w = 1.3 \cdot 10^{-4}\ bar^{-1}$, $\rho_w = 814\ kg/m^3$, $\rho_s = 16.8\ kg/m^3$, $L = 1765\ kJ/kg$, and $h = 1000\ m$.

$$\left(\frac{dm}{dp}\right)_1 = 814 \cdot 1.3 \cdot 10^{-4} \cdot 0.1 \cdot 10^3 = 10.6\ kg/bar\ m^2$$

$$\left(\frac{dm}{dp}\right)_2 = 16.8 \cdot \frac{1}{33.5} \cdot 0.1 \cdot 10^3 = 50.1 \text{ kg/bar m}^2$$

$$\left(\frac{dm}{dp}\right)_3 = \frac{513.15}{16.8 \cdot (1765 \cdot 10^3)^2} (0.9 \cdot 2500 \cdot 1000 +$$

$$+ 0.1 \cdot 0.5 \cdot 814 \cdot 4700) \cdot 10^3$$

$$= 2393.7 \text{ kg/bar m}^2$$

$$\left(\frac{dm}{dp}\right)_4 = \frac{0.1}{9.81} = 1019.4 \text{ kg/bar m}^2$$

From the above figures we can conclude that in two phase reservoirs the vapourization effect dominates the storage behaviour of the reservoir. In watertable reservoirs the free surface effect dominates the storage-behaviour of the reservoir. Eq. 3.7 gives the storage coefficient for a water-dominated reservoir with no watertable. If we have free surface condition in the reservoir the storage coefficient in all the preceeding equations must be replaced by the storage coefficient for a watertable reservoir, which can be derived from eq. 3.7 and 3.234 and is given by:

$$S = \phi \tag{3.235}$$

Let us turn again to eq. 3.220 for superheated steam. As mentioned before the differential equation is nonlinear due to the pressure dependance of the compressibility, which will affect time dependant solutions of the equations, but steady and semi-steady state conditions are given by a linear equation, as we will see in the following. Let us consider the steady condition given in Fig. 3.3. Darcy's law can be expressed as:

$$W = \frac{2\pi rhk\rho}{\mu} \frac{\partial p}{\partial r} \tag{3.236}$$

Inserting ρ from eq. 3.219 gives:

$$W = \frac{2\pi rhkp}{RTZ\mu} \frac{\partial p}{\partial r} \tag{3.237}$$

which can be written as:

$$W = \frac{\pi rhk}{TRZ\mu} \frac{\partial p^2}{\partial r} \tag{3.238}$$

and separating the variables and integrating results in:

$$p^2 - p_{wf}^{\ 2} = \frac{W\mu TRZ}{\pi hk} \ln \frac{r}{r_w} \tag{3.239}$$

which can be compared with eq. 3.25.

If we define a dimensionless pressure as:

$$p_D = \frac{\pi hk}{W\mu TRZ} (p_i^{\ 2} - p^2) \tag{3.240}$$

the solutions for the superheated steam become exactly the same as the solutions given in section 3.4 for the steady state written in terms of dimensionless pressure. Let us now turn to the semi-steady state. Eq. 3.49 for a circular drainage area is:

$$\frac{dp}{dt} = - \frac{W}{c\phi h\rho\pi r_e^{\ 2}} \tag{3.49}$$

By inserting ρ from eq. 3.219 we have:

$$\frac{dp}{dt} = - \frac{WRTZ}{c\phi h\pi r_e^{\ 2} p} \tag{3.241}$$

which can be written as:

$$\frac{dp^2}{dt} = - \frac{2WRTZ}{c\phi h\pi r_e^{\ 2}} \tag{3.242}$$

combining with eq. 3.220 we obtain:

$$\phi h p_i \int_{r_w}^{r_e} c\rho 2\pi r dr - \int_{r_w}^{r_e} c\rho\phi h 2\pi r p_r dr = - Wt$$

According to eq. 3.219 and 3.222, $c\rho$ is constant and can therefore be taken outside the integration above, giving:

$$c\rho\phi h p_i A - c\rho\phi h 2\pi \int_{r_w}^{r_e} p_r r dr = -Wt \qquad (3.246)$$

P_r is taken from eq. 3.244 and the integration must be performed numerically. The result would be quite different from eq. 3.55. If we had assumed that c was independent of pressure in eq. 3.245 we could have arrived at an equation corresponding exactly to eq. 3.55 by using the before mentioned dimensionless pressure functions. But assuming that c is pressure independent is obviously incorrect, because we are in semi-steady state where pressure is falling continuously with time and according to eq. 3.222 c is inversely proportional with pressure. In the case of well testing the situation is different. We are in the infinite reservoir region of the drawdown curve and much smaller pressure drop can be assumed than in the whole period of pseudosteady-state. Let us therefore consider equation 3.220 again, which is, as said before, nonlinear due to the pressure dependance of the compressibility. We assume the well test to last only for a short time so we can consider an infinite reservoir case and we assume the pressure drop to be small so we can linearize the equations by setting the compressibility equal to some average value or its initial value. By defining the dimensionless pressure according to eq. 3.240 and dimensionless radius and time according to eqs. 3.17 and 3.19, eq. 3.220 can be written as:

$$\frac{1}{r_D} \frac{\partial}{\partial r_D} (r_D \frac{\partial P_D}{\partial r_D}) = \frac{\partial P_D}{\partial t} \qquad (3.247)$$

which is exactly the same as the dimensionless differential equation for water, eq. 3.21. The well testing equations for water-dominated reservoirs can thus be used directly with this new definition of the dimensionless pressure, that is to say by using the pressure squared instead of

$$\frac{1}{r}\frac{\partial}{\partial r}\left(kr\frac{\partial p^2}{\partial r}\right) = \frac{-2WRTZ\mu}{h\pi r_e^2} \tag{3.243}$$

which again is a linear equation in pressure squared and can be solved exactly. Integrating once we get:

$$r\frac{\partial p^2}{\partial r} = \frac{-WRTZ\mu}{h\pi r_e^2 k} r^2 + c_1$$

where c_1 is a constant of integration. At the outer no flow boundary $\partial p^2/\partial r = o$ and hence the constant can be evaluated as $c_1 = \frac{WRTZ\mu}{h\pi k}$ which, when substituted in the last equation gives:

$$\frac{\partial p^2}{\partial r} = \frac{WRTZ\mu}{h\pi k}\left(\frac{1}{r} - \frac{r}{r_e^2}\right)$$

Integrating once again:

$$p_r^2 - p_{wf}^2 = \frac{WRTZ\mu}{h\pi k}\left(\ln\frac{r}{r_w} - \frac{r^2}{2r_e^2}\right) \tag{3.244}$$

in which the term r_w^2/r_e^2 is considered negligible.

Eq. 3.244 can be compared with eq. 3.51. If we define the dimensionless pressure for superheated steam according to eq. 3.240 and according to eq. 3.20 in the case of water-dominated reservoir, the solutions in this section and section 3.4 become identical. This is not quite true for the equations in section 3.4 involving time. This can be seen by looking at the derivation leading to the equation corresponding to eq. 3.55. The material balance equation similar to eq. 3.53 is (see Fig. 3.7):

$$\int_{r_w}^{r_e}\int_{p_r}^{p_i} c\rho\phi h 2\pi r\,dp\,dr = -Wt \tag{3.245}$$

which can be integrated to give:

pressure. Let us take Theis solution as an example. To get the same solution as before, the boundary conditions, eq. 3.59, must remain the same.

The two first are straight forward, let us look at number three in some more detail. Darcy's law and the continuity equation require, when $r \to o$:

$$\rho 2\pi r \frac{\partial p}{\partial r} \frac{k}{\mu} h = W \tag{3.248}$$

By using eq. 3.219 we get:

$$\frac{\pi hk}{RTZ\mu} r \frac{\partial p^2}{\partial r} = W \tag{3.249}$$

which can be written as:

$$\frac{r}{r_w} \frac{\partial (\frac{\pi hk}{RTZ\mu W} p^2)}{\partial \frac{r}{r_w}} = 1 \tag{3.250}$$

Inserting from eq. 3.19 and 3.240 we obtain:

$$(r_D \frac{\partial P_D}{\partial r_D})_{r_D \to o} = 1 \tag{3.251}$$

and the boundary conditions become exactly the same as 3.59, and the solution then remains unchanged and we get the exponential integral solution for the new definition of the dimensionless pressure. It is left as an exercise to show that the slope of the semi-log straight line given by eq. 3.74 is now given by:

$$m = \frac{W\mu RTZ}{2\pi kh}, \tag{3.252}$$

Just remember that it is the pressure squared that must be plotted against time.

Before we begin to discuss well testing in two phase reservoirs, it is necessary to introduce the concept of relative permeabilities. Darcy's law has been defined before in section 1 but in case of water and steam flowing together we need modification of Darcy's law. It is generally accepted to write Darcy's law for a two phase flow mixture in the following way for horizontal flow:

$$V_w = - \frac{kk_w(S_w)}{\mu_w} \text{grad } p \tag{3.253}$$

$$V_s = - \frac{kk_s(S_w)}{\mu_s} \text{grad } p \tag{3.254}$$

$k_w(S_w)$ and $k_s(S_w)$ are the relative permeabilities for water and steam respectively, and S_w is the water saturation as before. They are function of water saturation. Typical relative permeability curves are shown in Fig. 3.58. In order to establish the well testing equations we must formulate the conservation of mass and energy.

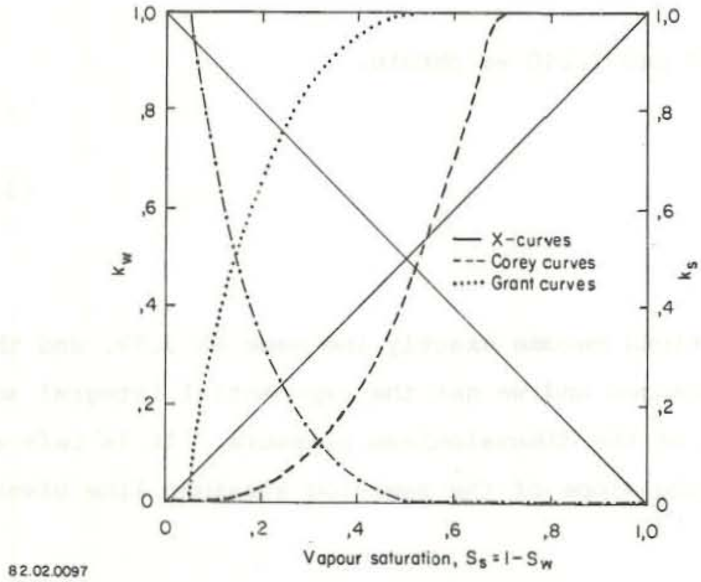

Fig. 3.58 Relative permeability curves

They are given respectively as:

$$\frac{\partial}{\partial t}\,(\phi(\rho_w S_w + (1 - S_w)\rho_s)) + \text{div}\,\{\rho_w V_w + \rho_s V_s\} = o \tag{3.255}$$

$$\frac{\partial}{\partial t}\,\{(1-\phi)\rho_r h_r + \phi S_w \rho_w h_w + \phi(1 - S_w)\rho_s h_s\} + \text{div}\,\{\rho_w h_w V_w + \rho_s h_s V_s\} = o \tag{3.256}$$

where the indices w,s,r mean water, steam and rock respectively. With some approximation, see Sorey et al. (1980) and O'Sullivan (1981), eqs. 3.253 to 3.256 can be simplified to the following equation:

$$\rho_t \beta_s \phi \frac{\partial p}{\partial t} = \frac{1}{r}\frac{\partial}{\partial r}\frac{rk}{\nu_t}\left(\frac{\partial p}{\partial r}\right) + \frac{\rho_t(\rho_w - \rho_s)k}{\rho_w \rho_s (h_s - h_w)\nu_t}\,\text{grad}\,h_t \cdot \text{grad}\,p \tag{3.257}$$

where β_s is defined in eq. 3.231 and ν_t, μ_t, h_t and ρ_t are defined in the following way:

$$\frac{1}{\nu_t} = \frac{k_w}{\nu_w} + \frac{k_s}{\nu_s} \tag{3.258}$$

$$\frac{1}{\mu_t} = \frac{k_w}{\mu_w} + \frac{k_s}{\mu_s} \tag{3.259}$$

$$\frac{h_t}{\nu_t} = \frac{k_w}{\nu_w}h_w + \frac{k_s}{\nu_s}h_s \tag{3.260}$$

$$\rho_t = \frac{\mu_t}{\nu_t} \tag{3.261}$$

and other symbols have been defined before. We will now consider the solution to eq. 3.257 for three different cases.

1) <u>Saturated steam, immobile water phase</u>

Because the steam enthalpy can be considered almost constant eq. 3.257 reduces to:

$$\frac{1}{r}\frac{\partial}{\partial r}\left(\frac{r}{\nu_s}\frac{\partial p}{\partial r}\right) = \frac{\rho_s \beta_s \phi}{k}\frac{\partial p}{\partial t} \tag{3.262}$$

which is nonlinear due to the pressure dependance of the steam kinematic viscosity and density. Grant (1978) has suggested the following transformation in order to remove the nonlinearities from the left hand side.

$$m^* = \int \frac{dp}{\nu_s} \tag{3.263}$$

Inserting eq. 3.263 into eq. 3.262 gives:

$$\frac{1}{r}\frac{\partial}{\partial r}\left(r\frac{\partial m^*}{\partial r}\right) = \frac{\mu_s \beta_s \phi}{k}\frac{\partial m^*}{\partial t} \tag{3.264}$$

which is the ordinary differential equation used in well testing and the methods we have been discussing in this section can be used. Grant (1978) has calculated an approximate formula for m^* given by:

$$m^* = 2.58 \cdot 10^9 \, p^{13/7} \tag{3.265}$$

where p is in bars.

The slope of the semi-log straight line, that is m^* vs. log t, is given by:

$$m = \frac{W}{4\pi kh} \tag{3.266}$$

2) Saturation, immobile steam

In this case we assume that the pressure gradients are small, thus reducing eq. 3.257 to:

$$\frac{1}{r}\frac{\partial}{\partial r}\left(r\frac{\partial p}{\partial r}\right) = \frac{\beta_s \mu_w \phi}{k}\frac{\partial p}{\partial t} \tag{3.267}$$

This is the ordinary well test equation and all the standard well testing procedures can be used. There are small nonlinearities on the right hand side, which can be overcome by using initial values for the parameters on the right hand side.

3) Saturation, both water and steam mobile

It has been shown that the flowing enthalpy, h_t, becomes constant after some time from the starting of the well test, see Sorey et al. (1980). Eq. 3.257 can then be written as:

$$\frac{1}{r}\frac{\partial}{\partial r}\left(r\frac{\partial p}{\partial r}\right) = \frac{\beta_s \mu_t \phi}{k}\frac{\partial p}{\partial t} \tag{3.268}$$

where the left hand side has been linearized by taking ν_t out of the differentiation. Now again the standard well testing methods can be applied. Initial values must be used for the parameters on the right hand side. In this case the differential equation is highly nonlinear and care must be taken when interpreting well tests. It should e.g. be noted when using recovery tests (Horner plot), that although pressure might recover linearly with log (t), that liquid saturation overrecovers. If the pressure rise during recovery is great enough all liquid conditions can be produced around a well that previously discharged under two-phase conditions.

EXERCISE 3.12

The following data are from one well in the Tongonan field in the Philippines, and reported by Paete (1980).

Flowing enthalpy, h_t:	1433 kJ/kg
Fluid temperature, T:	262°C
Well radius, r_w :	10.8 cm

A pressure buildup test was performed, with the massflow rate equal to 26 kg/s prior to closing down the well. The pressure buildup data is given on Fig. 3.59. The well was shut at 1020 hours. The pressure prior to shut in was p_{wf} = 22 bar.

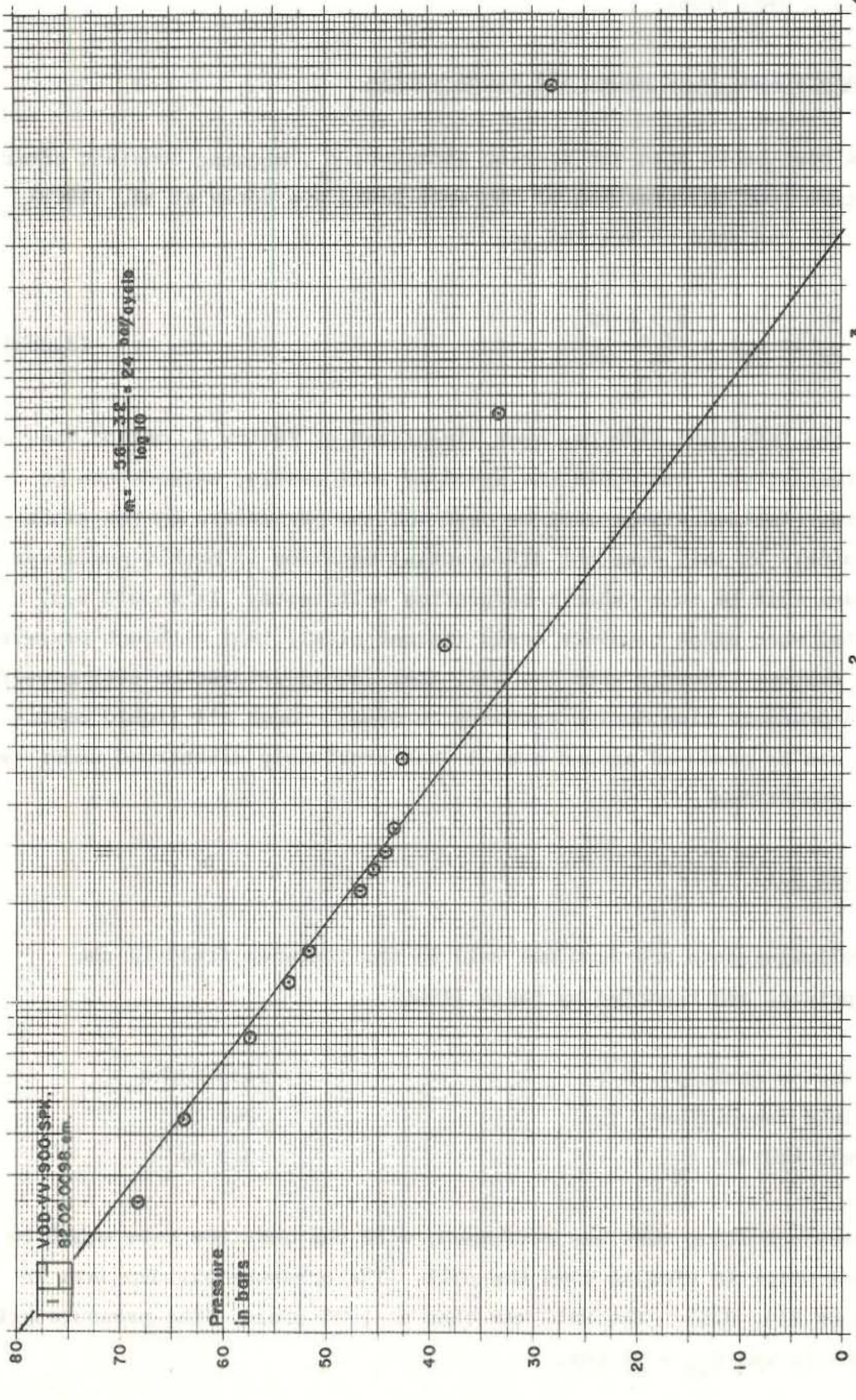

Fig. 3.59 Pressure buildup

Calculate the reservoir parameters and the skin effect.

Solution

From steam tables we get:

$$h_s = 2795 \text{ kJ/kg}$$
$$h_w = 1145 \text{ kJ/kg}$$
$$\rho_s = 24.6 \text{ kg/m}^3$$
$$\rho_w = 780.8 \text{ kg/m}^3$$
$$\mu_s = 18.3 \cdot 10^{-6} \text{ kg/ms}$$
$$\mu_w = 102 \cdot 10^{-6} \text{ kg/ms}$$
$$c_w = 4.983 \text{ kJ/kg°K}$$

Let us take $c_r = 1.0$ kJ/kg°K, $\rho_r = 2500$ kg/m^3, and $\phi = 10\%$. We see that the water enthalpy is less than the flowing enthalpy indicating two phase conditions. By combining eq. 3.258 to eq. 3.260 we get:

$$\frac{k_w}{k_s} = \frac{\mu_w}{\mu_s}\frac{\rho_s}{\rho_w}\frac{(h_s - h_t)}{(h_t - h_w)} \tag{3.269}$$

Inserting numerical values we get:

$$\frac{k_w}{k_s} = \frac{102 \cdot 10^{-6}}{18.3 \cdot 10^{-6}}\frac{24.6}{780.8}\frac{(2795 - 1433)}{(1433 - 1145)} = 0.83$$

Let us assume the Grant relative permeability curves, see Fig. 3.58. We now have:

$$k_w + k_s = 1 \tag{3.270}$$

Inserting the above value we get for the relative permeabilities:

$$k_s = 0.55$$

$$k_w = 0.45$$

Fig. 3.58 gives with the above relative permeabilities $S_w = 0.84$, again showing two phase conditions. We can now use eq. 3.231 to calculate the two phase compressibility:

$$\phi\beta_s = \left(\frac{780.8 - 24.6}{780.8 \cdot 24.6 \cdot (2795 - 1145) \cdot 10^3}\right)^2 \cdot 535 \cdot \{0.9 \cdot 1000 \cdot$$

$$\cdot\, 2500 + 0.1 \cdot 0.84 \cdot 780.8 \cdot 4983\}$$

$$\cong 7.8 \cdot 10^{-7}\ \mathrm{Pa}^{-1}$$

Eq. 3.258 and eq. 3.259 give for the flowing kinematic viscosity and dynamic viscosity:

$$\frac{1}{\nu_t} = \frac{0.45 \cdot 780.8}{102 \cdot 10^{-6}} + \frac{0.55 \cdot 24.6}{18.3 \cdot 10^{-6}}$$

$$\nu_t = 2.4 \cdot 10^{-7}\ \mathrm{m}^2/\mathrm{s}$$

$$\frac{1}{\mu_t} = \frac{0.45}{102 \cdot 10^{-6}} + \frac{0.55}{18.3 \cdot 10^{-6}}$$

$$\mu_t = 2.9 \cdot 10^{-5}\ \mathrm{kg/ms}$$

The analysis of the pressure buildup data is given on Fig. 3.59. We now get for the permeability thickness (see Fig. 3.25):

$$kh = \frac{W\nu_t}{4\pi m} = \frac{26 \cdot 2.4 \cdot 10^{-7}}{4 \cdot \pi \cdot \frac{24}{\ln 10} \cdot 10^5} = 0.5\ \mathrm{dm}$$

We can now calculate the skin effect according to eq. 3.184 with $\Delta t = 60{,}000$ sec. and $P_{ws} = 37$ bar, by assuming the aquifer thickness to be 10 m.

$$S = 1.151\ \left(\frac{(37 - 22)}{24} - \log \frac{0.5 \cdot 10^{-12} \cdot 10}{7.8 \cdot 10^{-7} \cdot 0.108^2 \cdot 2.9 \cdot 10^{-5}}\right.$$

$$\left. - \log 1{,}000 - 2.13\right)$$

$$= 1.151\ (0.63 - 1.3 - 3.0 - 2.13) \cong - 7.2$$

Let us finally describe a situation that might occur in a well test in a water-dominated reservoir. By applying the standard well testing methods we determine the parameters for the water-dominated reservoir. As pressure drops a flash front propogates into the reservoir away from the wellbore. To begin with the water zone dominates the two phase zone and the parameters determined would be the same as before. In the long term the two phase zone becomes dominant and the parameters determined would be representative for that zone. See Horne et al. (1980) and Garg (1980) for discussion on phase boundaries. Finally a dry steam zone might become the controlling zone. The above description shows clearly the complications involved in a two phase flow test analysis.

4 RESERVOIR MECHANICS

4.1 Introduction

This section on reservoir mechanism describes how the geothermal reservoir behaves under natural conditions and exploitation. General equations for the flow in geothermal reservoirs will be formulated. Hydrothermal convection will be discussed as a part of the natural state of the reservoir. For the engineer developing a geothermal reservoir, the question of energy capacity of the reservoir is very important. Equally important are the rate, at which this energy can be exploited, and for how long it is possible to extract the energy at this rate. In order to understand and try to answer these questions we discuss reservoir response and capacity, heat extraction from geothermal reservoirs and reinjection. Due to the non-linearity of the equations describing flow in geothermal reservoirs, no analytical solutions exist and numerical methods have to be used. A small section on numerical models is therefore included.

4.2 General equations for the flow in geothermal reservoirs

The equations for the flow in a porous medium are presented. They are the ordinary conservation equations in fluid mechanics. That is the conservation of mass, momentum and energy together with the necessary constitutive relationship and equations of state. In order to shorten the presentation, the equations will not be derived microscopically, but the reader is referred to Pinder (1979). The conservation equations are the following:

Conservation of mass:

$$\frac{\partial}{\partial t}\left(\phi S_w \rho_w + \phi(1 - S_w)\rho_s\right) + \mathrm{div}\,\{\rho_w V_w + \rho_s V_s\} = 0 \tag{4.1}$$

Conservation of momentum:

$$V_w = -\frac{k k_w(S_w)}{\mu_w}\,\mathrm{grad}\,P \tag{4.2}$$

$$V_s = - \frac{kk_s(S_w)}{\mu_s} \text{ grad } P \tag{4.3}$$

Conservation of energy:

$$\frac{\partial}{\partial t}((1-\phi)\rho_r h_r + \phi S_w \rho_w h_w + \phi(1-S_w)\rho_s h_s) + \text{div}(\rho_w h_w V_w + \rho_s h_s V_s) = \text{div}(\lambda_e \text{ grad } T) \tag{4.4}$$

all the above symbols have been defined before. Eqs. 4.2 and 4.3 are the Darcy equations for two phase flow defined in section 3, see eqs. 3.253 and 3.254. In writing down these equations we have used the enthalpy (h), as a variable in the energy equation and we have neglected viscous dissipation and pressure work, see Garg and Pritchett (1977) and Pinder (1979) for detailed derivation.

In well test analysis we can neglect the heat conduction term on the right hand side of eq. 4.4 and eq. 3.257 in section 3 can then be derived. The differential equation 3.12 for a horizontal isothermal flow in a single phase water reservoir of constant thickness can be derived from the above equation by volume averaging. If we use vertical averaging, neglect the transient terms in the energy equation and introduce circular symmetry, the above equations read in cylindrical coordinates:

Mass:

$$\frac{\partial}{\partial t}(\rho_w \phi h) = - \frac{1}{r} \frac{\partial (r \rho_w V_w h)}{\partial r} \tag{4.5}$$

Momentum:

$$V_w = - \frac{k}{\mu_w} \frac{\partial p}{\partial r} \tag{4.6}$$

Energy:

$$T = \text{constant} \tag{4.7}$$

Combining we get:

$$\frac{1}{r}\frac{\partial}{\partial r}\left(\frac{k\rho_w h}{\mu_w} r \frac{\partial p}{\partial r}\right) = \frac{\partial}{\partial t}(\rho_w \phi h) \tag{4.8}$$

or

$$\frac{1}{r}\frac{\partial}{\partial r}\left(\frac{k\rho_w}{\mu_w} r \frac{\partial p}{\partial r}\right) = \frac{1}{h}\frac{\partial}{\partial t}(\rho_w \phi h) \tag{4.9}$$

Eq. 4.9 is identical to eq. 3.2 and the rest of derivation of eq. 3.12 now follows section 3.1.

The equations 4.1-4.4 are highly nonlinear and in most cases no analytical solution exists and therefore numerical methods must be applied. The differential equations must be solved with the appropriate boundary conditions and one set of boundary conditions gives e.g. the solution for hydrothermal convection discussed in section 4.4.

4.3 Reservoir capacity, response and heat extraction from geothermal reservoirs

Let us start this section by introducing a schematic simplified model of a geothermal reservoir as described in Fig. 4.1.

The geothermal reservoir has a surface area, A and a thickness, h. Overlying the geothermal reservoir is a cold water zone sealed from the reservoir by a caprock. In the reservoir we have a water and steam zone and a hot water zone. Their relative magnitude is dependent on if the reservoir is water-dominated or vapour-dominated. The general flow picture is shown in the figure. If fluid is withdrawn from the reservoir at the rate W_w, an internal pressure drop will occur. It stimulates a recharge flow from the sides, W_r, and may change the base inflow, W_b, and the steamflow, W_s, and the natural discharge flow, W_d. The mass balance is given by the following equation:

$$W_b + W_r = W_w + W_s + W_d \tag{4.10}$$

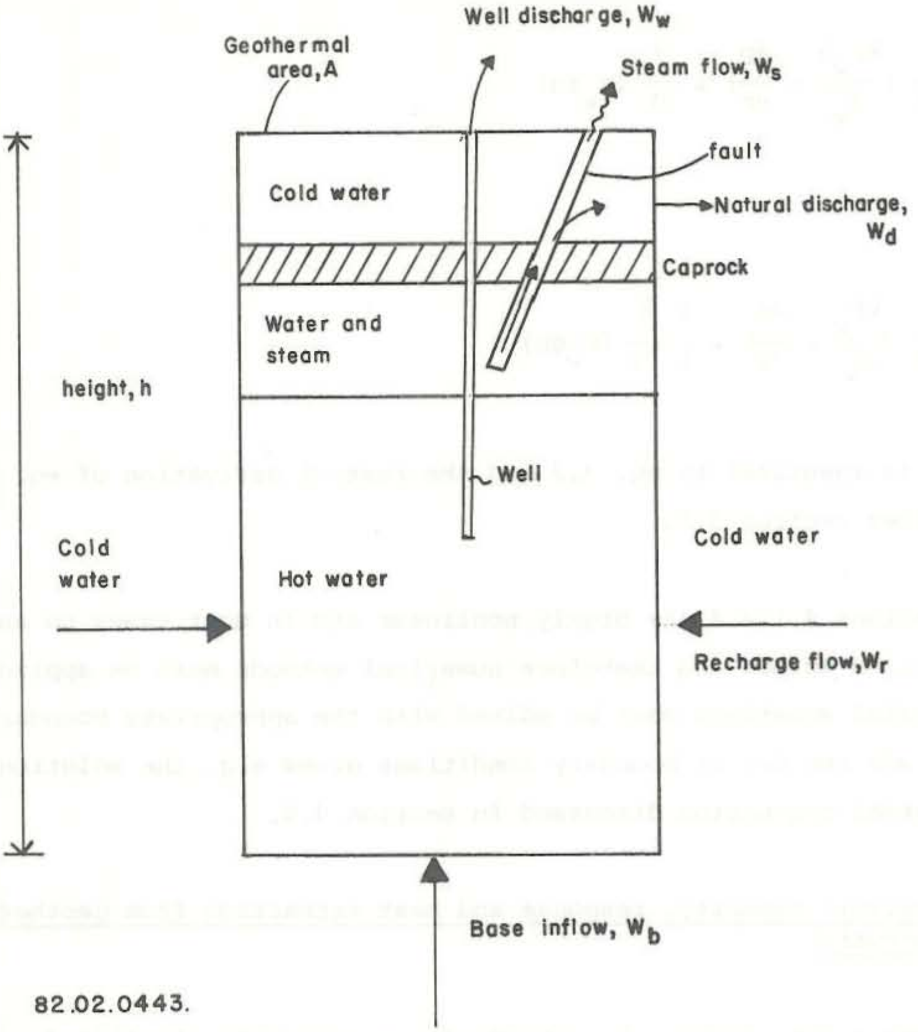

Fig. 4.1 A schematic model of a geothermal reservoir (Adapted from McNabb 1975)

Let us look at each of these flows in eq. 4.10.

1) The base inflow, W_b. In most models of geothermal systems it is assumed that cold meteoric water percolates down to some considerable depth where it is heated and driven, due to the density difference, back up to the surface. The flow path involved is so long that the pressure changes due to exploitation do not change the flow very much. The baseflow will therefore be treated as a constant under exploitation.

2) The recharge flow, W_r. The recharge inflow is created by the pressure difference between the inside and outside of the geothermal reservoir.

This inflow will increase with increasing drawdown due to exploitation. This recharge water will have the effect of moving in the cold side boundaries of the reservoir. The cold water percolates into the reservoir and gets heated by the heat stored in the rock and hot water already resident in the pores. When exploitation of a field starts, the pressure starts declining thus increasing the pressure difference between the inside and the outside of the reservoir. But very long time may elapse before any effect of the recharge is observed, due to low permeability zones near the boundary. When considering possible recharge due to exploitation it must be kept in mind that in the natural state of the reservoir there may exist great pressure differences between the inside and outside of the geothermal reservoir due to the higher temperature of the reservoir. In the Svartsengi geothermal field in Iceland there was a 16 bar pressure difference at 1000 m depth between the inside and outside of the reservoir in the natural state of the reservoir.

As a result of the recharge flow the reservoir properties will change by time. These changes can be observed in reservoir pressure, chemistry and enthalpy.

3) <u>The well discharge, W_w.</u> The total well discharge will be controlled by several factors, mainly well head pressure. The well discharge will be discussed in more detail in section 5.

4) <u>Natural discharge, W_d, and steam flow, W_s.</u> If we increase the well discharge sufficiently to decrease the reservoir pressure, the natural discharge might reverse in sign because the pressure difference which maintains the flow becomes reversed. We then have a recharge of cold water from above and the steam flow stops.

In view of the simplified model we have been discussing let us now return to the main topic of this section, that is reservoir capacity, the response and heat extraction from geothermal reservoirs. The energy stored in the water zone of the geothermal reservoir in Fig. 4.1 is:

$$q_h = (c_r\rho_r(1 - \phi) + \phi c_w\rho_w)\Delta ThA \qquad (4.11)$$

where ΔT is the temperature difference between the reservoir and the surroundings and A is the reservoir area. Let us take an example of a reservoir with the following data: $\Delta T = 200^\circ C$, $h = 1000$ m, $\rho_r = 2500$ kg/m^3, $c_r = 1000$ J/kg$^\circ$C, $\rho_w = 812$ kg/m^3, $\phi = 0.1$, $c_w = 4200$ J/kg$^\circ$C, we can then calculate the heat energy:

$$q_h = (1000 \cdot 2500 \cdot 0.9 + 0.1 \cdot 4200 \cdot 812) \cdot 200 \cdot 1000 \cdot 10^6$$

$$= (4.5 + 0.68) \cdot 10^{17} = 5.18 \cdot 10^{17} \text{ joules} \simeq 16488 \text{ MW year/km}^2 \text{ thermal}$$

87% of the energy is in the rock and only 13% is in the water. 16488 MW year/km^2 corresponds to a 330 MW/km^2 for fifty years. If the area of the geothermal field is e.g. 4 km^2 this figure corresponds to 1320 MW for fifty years. If the heat extraction process just consisted of taking the fluid in the reservoir, we would only get about 13% of the total heat content. The heat extraction must therefore aim at mining the heat from the rock and we will turn to that later on. The heat energy calculated above is not all available for power production due to the efficiency in the mining operation and in the power plant, which is less than one. It is customary to multiply this energy with a factor, recovery factor, in order to calculate the energy presumably available for power production. The recovery factor is poorly defined. Many authors have discussed the appropriate magnitude of the recovery factor, r, it seems that it can range up to ~ 25% for hot-water reservoirs. If we take e.g. r = 0.1 in the example above we would get for the recoverable energy:

$$Q_h = rq_h = 0.1 \cdot 16488 = 1649 \text{ MW year/km}^2 \text{ thermal}$$

which again corresponds to 132 MW for fifty years in a geothermal area of 4 km^2. This method to estimate reservoir capacity is known as the volume method, see Muffler and Cataldi (1978) and is accepted as a method for geothermal assessment. The uncertainty of the method lies in the estimation of the recovery factor, which depends on many factors such as, the nature of the reservoir, its degree of fracturing, its temperature variation; the nature of the fluid, noncondensable gas; and the way in which the field is operated, the reinjection strategy, the rate of withdrawal. The main drawbacks of this method is perhaps that it is very difficult to include available information on the performance of individual wells into the estimation of r.

In the exploitation of a reservoir we may at some time exceed reservoir capacity, which means that we do not get the sufficient discharge from the wells. The reservoir drawdown can at any time be stopped and the wells operated at constant pressure, but then the discharge will decrease logarithmically with time. This corresponds to the constant pressure solution given in section 3.6. Let us however estimate the discharge decline with the following:

$$W = W_1 \cdot e^{-t/K} \tag{4.12}$$

where t is the time elapsed since we started operating the wells at constant pressure and mass flow equal to W_1. K is some time constant for the geothermal reservoir which can be estimated if we have constant pressure data for mass flow vs. time, see Zais and Böðvarsson (1980) for analysis of production decline in geothermal reservoirs. Let us assume that we have to stop due to economical reasons the exploitation of the field at time t_o, and then the discharge has decreased to W_o.

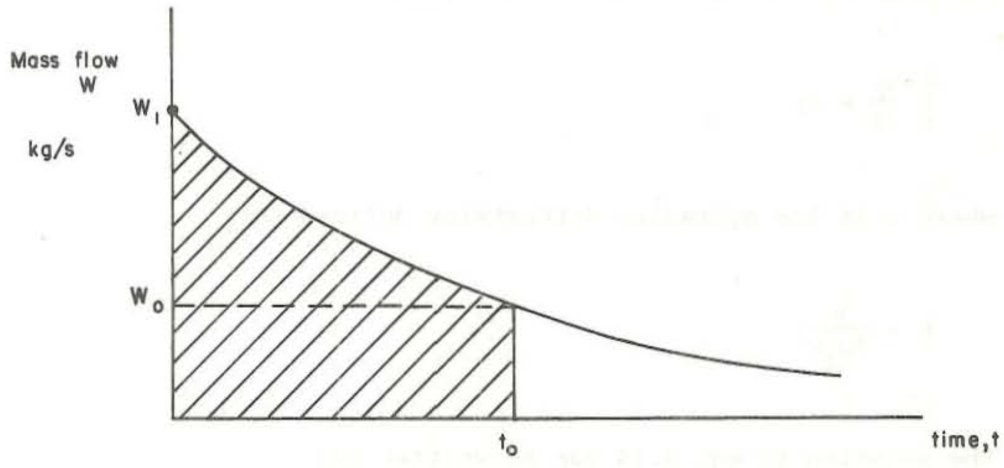

82.02.0445.

Fig. 4.2 Production decline in geothermal reservoirs

The area in Fig. 4.2 shows the total amount of fluid that can be withdrawn until we reach the capacity limits and is therefore the present state capacity. We have for this capacity, U:

$$U = \int_{o}^{t_o} W_1 \, e^{-t/K} dt = K(W_1 - W_o) \tag{4.13}$$

From U it is now possible to calculate the total thermal energy available to power production. This figure is, for all practical purposes the present state capacity of our geothermal field. Now compare eq. 4.13 to eq. 4.11 and the following calculations that include an estimate of the recovery factor r. It is quite clear that the present state capacity should be equal to the recoverable energy minus already produced energy. But in practice it will be almost impossible to estimate the recovery factor so accurately as to make these two estimates of the present state capacity equal.

Let us now turn to the second topic of this section, which is reservoir response. The reservoir response was discussed in detail in section 3 so let us just draw some general conclusions from that discussion. In section 3 we saw that the differential-equation for pressure for some pressure transformation could be linearized to give an equation of the same type as the heat conduction equation:

$$\frac{1}{\kappa}\frac{\partial p}{\partial t} = \Delta p \tag{4.14}$$

where κ is the hydraulic diffusivity defined as:

$$\kappa = \frac{k}{\phi \mu_t c} \tag{4.15}$$

The solution to eq. 4.14 can be written as:

$$p - p_o = \int_{o}^{\infty} f(t - \tau) W(\tau) d\tau \tag{4.16}$$

where f is the instantaneous unit response function of the reservoir. Another unit response function can be defined as:

$$F(t) = \int_{o}^{t} f(\tau) d\tau \tag{4.17}$$

Eq. 4.16 can then be written in terms of F as:

$$p - p_o = \int_o^{\infty} W(\tau) \frac{dF(t - \tau)}{d\tau} d\tau \qquad (4.18)$$

If we have field data for pressure decline and mass flow rate eq. 4.18 can be solved numerically, by using the least square procedure, in order to determine the unit response function. (See Barelli and Palama 1980 and Zais and Böðvarsson 1980). The unit response function is just the reservoir response to unit mass flow rate. It is therefore very convenient to use for well testing purposes. If it is not possible due to some practical considerations to maintain constant mass flow rate in a well test, the method above can be used to determine the unit response function, which then can be analysed by the standard methods described in section 3, which require constant flowrate. Fig. 4.3 gives a result of such calculations for the Svartsengi geothermal field in Iceland.

For the calculations shown in Fig. 4.3 there were available 2000 days of drawdown and mass flow rate records. The unit response function was determined for that period. The response function is then extrapolated by a fitted theoretical model into the future. The unit response function can then be used to calculate future pressure drop, provided that all existing boundaries of the system have shown up in the historical pressure record.

The unit response function for the infinite reservoir case is given by:

$$F(t) = \frac{\nu_t}{4\pi kh} (-Ei(- \frac{r^2}{\kappa t})) \qquad (4.19)$$

as may be seen from eqs. 3.60 and 3.22.

We can now use eq. 4.18 to solve eq. 4.14 for the case of constant pumping (W = constant):

$$p - p_o = \frac{W\nu_t}{4\pi kh} (-Ei(- \frac{r^2}{\kappa t})) \qquad (4.20)$$

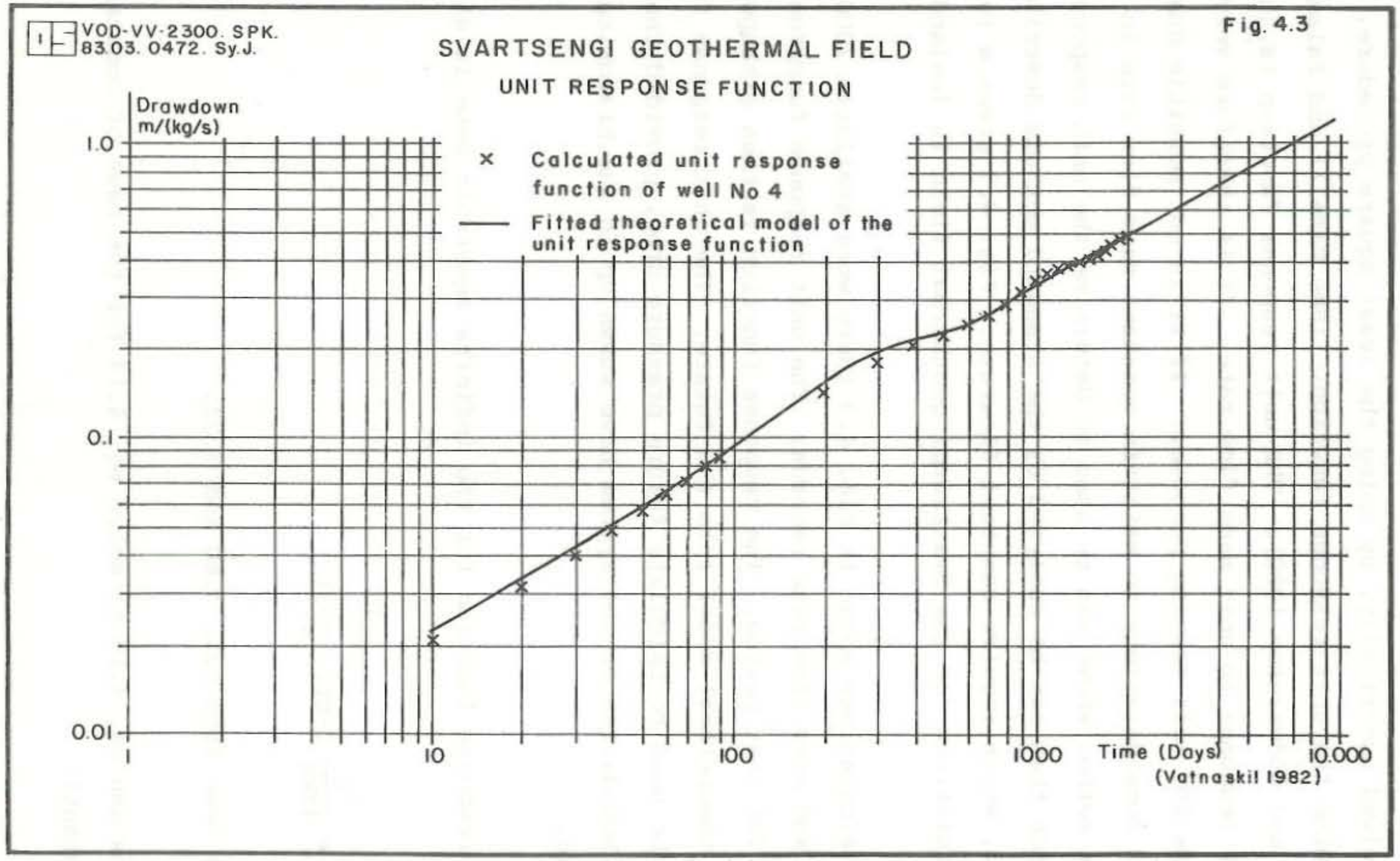

Fig. 4.3 Unit response function. The Svartsengi geothermal field (Vatnaskil 1982).

From the equation above we see that constant pressure drop $p - p_o$ corresponds to a constant argument of the unit response function that is $\frac{r^2}{\kappa t}$ = constant. The pressure drop has therefore diffused out a distance on the order of $\sqrt{\kappa t}$ at time t. Let us define the diffusion radius:

$$r_d = \sqrt{\kappa t} = \sqrt{\frac{kt}{\phi\mu_t c}} \tag{4.21}$$

The diffusion radius for a two phase system is much smaller than for water-dominated systems due to the much greater compressibility of the two phase mixture, see section 3.16. The ratio of two phase compressibility to water compressibility can be as great as 10^4. The ratio between the diffusion radia is given approximately by:

$$\frac{r_d^{\text{two phase}}}{r_d^{\text{water}}} = \sqrt{\frac{c^{\text{water}}}{c^{\text{two phase}}}} = \sqrt{\frac{1}{10^4}} \simeq 0.01 \tag{4.22}$$

We see that the diffusion front travels two orders of magnitude faster in water reservoirs than in two phase reservoirs. This explains why interference tests are difficult to perform in a two phase reservoir, because of the relatively long time for the pressure front to diffuse out to the observation well. Because the speed of the diffusion front spreading through compressed liquid is high it only takes a relatively short time for the pressure pulse to cross a liquid-dominated geothermal field. It takes the pressure pulse a short time to reach the boundaries of the system and thus creating cold recharge from the side boundaries. This cold pressure front sweeps through the reservoir and mines heat from the formation, which contains most of the heat content in the reservoir as we saw in the preceeding example. This is a very desirable mode of exploitation, because it means that the wells can have a long lifetime, as their region of exploitation is the entire field. Let us calculate the speed of the temperature front. Eq. 4.4 can be written for compressed liquid and we neglect heat conduction effects:

$$\{(1 - \phi)\rho_r c_r + \phi\rho_w c_w\} \frac{\partial T}{\partial t} = - \rho_w c_w V \cdot \text{grad } T \tag{4.23}$$

If we define:

$$\alpha = \frac{\rho_w c_w}{(1 - \phi)\rho_r c_r + \phi\rho_w c_w} \tag{4.24}$$

and assume for simplicity the flow field is uniform and horizontal eq. 4.23 becomes:

$$\frac{\partial T}{\partial t} = - \alpha V \frac{\partial T}{\partial x} \tag{4.25}$$

Solution to eq. 4.25 is given by:

$$T = f(x - \alpha V t) \tag{4.26}$$

From this solution we see that the speed of the temperature front is given by αV. V is the Darcy velocity, the actual velocity is then given by:

$$V_o = \frac{V}{\phi} \tag{4.27}$$

and the speed of the temperature front can then be written as:

$$V_T = \alpha\phi V_o \tag{4.28}$$

The heat front is thus delayed relatively to the hydraulic front by the factor $\alpha\phi$. Let us as an example calculate this factor for the following values. $\rho_w = 812\ kg/m^3$, $c_w = 4200\ J/kg°C$, $\rho_r = 2500\ kg/m^3$, $c_r = 1000\ J/kg°C$, $\phi = 0.1$, we have:

$$\alpha\phi = \frac{1}{1 + \frac{1 - \phi}{\phi}\frac{\rho_r}{\rho_w}\frac{c_r}{c_w}} = \frac{1}{1 + \frac{0.9}{0.1} \cdot \frac{2500}{812}\frac{1000}{4200}} \simeq 0.13$$

The speed of the heat front is in this case seven to eight times smaller than the hydraulic front. If the boundary recharge is small due to low permeability zones at the boundaries, very small heat mining from the rock is then possible. As most of the reservoir heat content is in the rock, it is very important to be able to exploit that too. For that purpose reinjection of cold water might be necessary.

We have seen that the compressibility of the two phase mixture is much greater than for a single phase fluid. We have also seen that it takes much longer time for the pressure pulse to diffuse out to the boundaries in a two phase fluid. Each well then just exploits the reservoir in its immediate vicinity. Very little recharge is now induced from the boundaries and the heat must now be mined from the rock differently than for the compressed water reservoir. This is also what really takes place in two phase mixtures. In two phase reservoirs, pressure drop is accompanied by a temperature drop, energy is mined from the rock thus cooled.

4.4 Natural convection in geothermal reservoirs

A hydrothermal system may be looked upon as a thermodynamical engine that pumps energy from the interior of the earth by means of free or forced convection. In free convection the flow is driven by the density gradients and there is a close non-linear relationship between the temperature distribution and the flow field. In forced convection the flow is driven by external pressure gradients and more or less independent of the temperature. Flow within geothermal reservoir is often of a mixed type where both external pressure gradients and internal density gradients drive the fluid flow. In a reservoir we have often the situation that internal flow is of the free convection type, but flow towards wells is almost entirely forced convection type.

Free convection flow in homogeneous thin layers of single phase fluids at moderate flow velocities takes place in regular hexagonal flow-cells (Benard-cells).

The flow is upwards in the middle of the cell when the fluid is liquid, down when it is gas (Palm 1960). The flow characteristics are functions of the Rayleigh number:

$$Ra = g \frac{\beta \rho_w c_w}{\nu_w} \frac{k}{\lambda_e} \Delta T h \qquad (4.29)$$

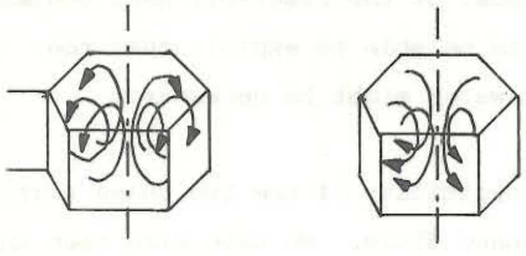

82.02.0447.

Fig. 4.4 Flow in Benard-cells

β is the volume coefficient of thermal expansion defined in eq. 2.8 and ΔT is the maximum temperature difference, and other symbols have been defined before. The Rayleigh number relates buoyancy forces to viscous forces.

When there is no convection (low temperature differences) the heat flux is constant everywhere and the temperature distribution is linear (constant temperature gradient). When $Ra > 4\pi^2 \simeq 40$ convection starts and the temperature gradient is disturbed.

Fig. 4.5 shows the temperature distribution in a porous medium heated from below. We see that the "hot area" gradient has a great resemblance to what we find in geothermal areas. The heat flux caused by such convection is measured by the Nusselt's number (Nu):

$$Nu = \frac{\text{Heat flux with convection}}{\text{Heat flux without convection}} \text{ (same temperature difference)} \tag{4.30}$$

Fig. 4.6 shows some experimental results for the relation between the Nusselt's number and the Rayleigh number for liquid water.

Elíasson (1973) gave the following equation for the solid line in Fig. 4.6:

$$Nu = \frac{2}{3\pi} \sqrt{Ra} \tag{4.31}$$

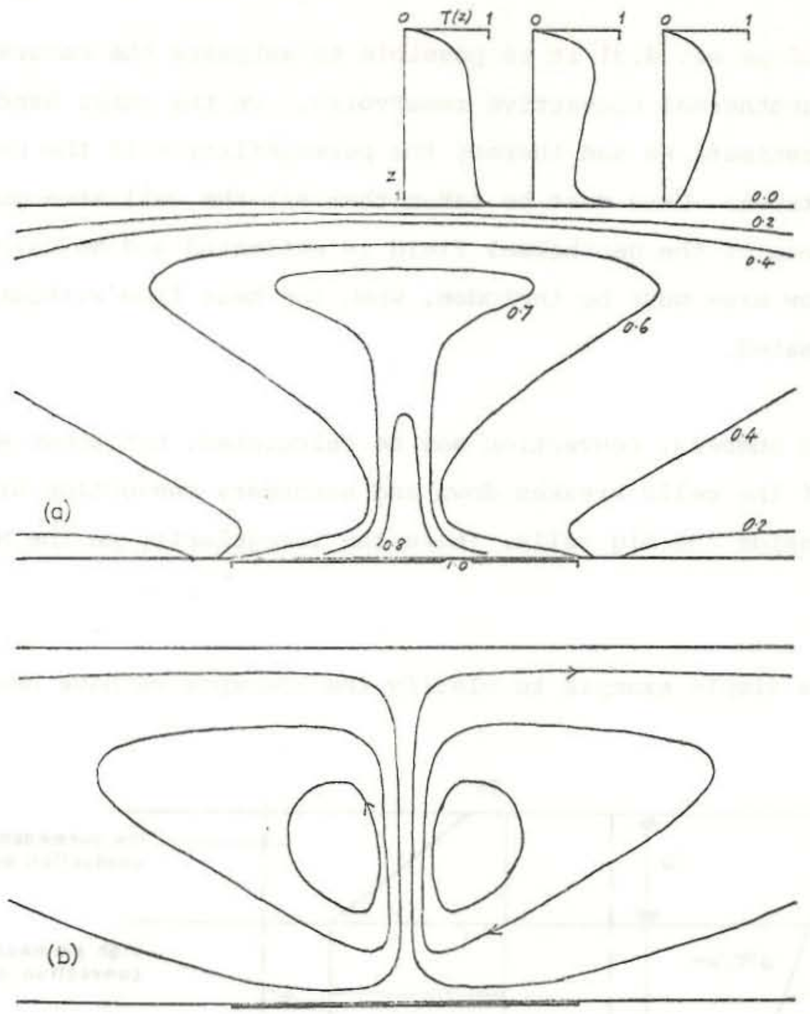

Fig. 4.5 Two-dimensional temperature, velocity distribution for free convection in a porous medium; a) isotherms and temperature distribution with depth; b) streamlines. (Elder 1965)

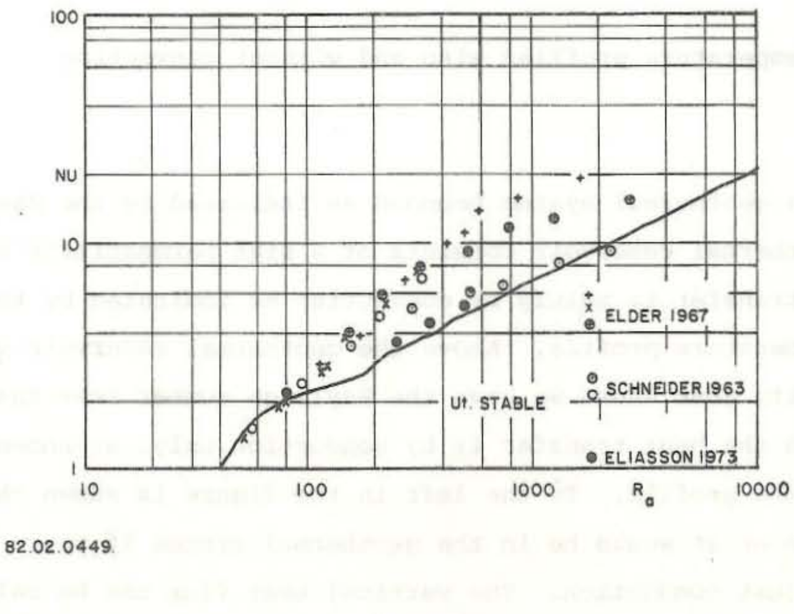

Fig. 4.6 Nu-Ra experimental results (Elíasson 1973)

By using Fig. 4.6 or eq. 4.31 it is possible to estimate the natural heat output of geothermal convective reservoirs. On the other hand it is possible to estimate Ra and thereby the permeability k if the natural heat output is known. Care must be taken that all the cell area must be included when area of the geothermal field is estimated and Nu calculated, i.e. the downflow area must be included, when the heat flow without convection is estimated.

For low Rayleigh numbers, convection may be calculated, but above Ra = 250 the stability of the cells breakes down and secondary convection starts in smaller cells inside the big cells, (note the irregularity on the Nu-Ra graph).

Let us look at a simple example to clarify the concepts we have been defining:

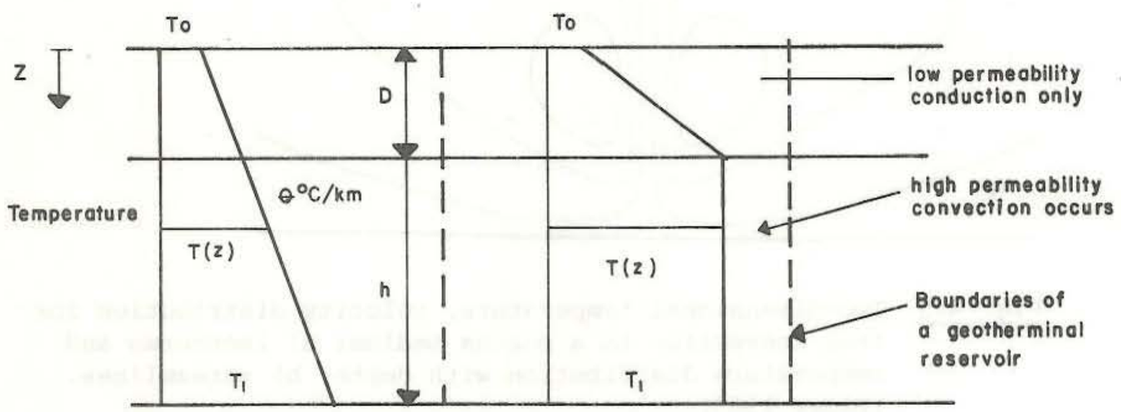

82.02.0450

Fig. 4.7 Temperature profiles with and without convection

Fig. 4.7 shows a geothermal system bounded as indicated by the dashed lines. The geothermal reservoir consists of a high permeability zone where the heat transfer is mainly by convection as indicated by the nearly constant temperature profile. Above the geothermal reservoir we have a low permeability zone where we have the Rayleigh number less than the critical one and the heat transfer is by conduction only, as shown by the linear temperature profile. To the left in the figure is shown the temperature profile as it would be in the geothermal system if there were no convection but just conduction. The vertical heat flux can be calculated as the heat flux by conduction in the low permeability zone. We have:

$$q_{convection} = \frac{T_1 - T_o}{D} \lambda \tag{4.32}$$

If there were no convection the heat flux is given by:

$$q_{conduction} = \frac{(T_1 - T_o)}{(h + D)} \lambda \tag{4.33}$$

The Nusselt number is then given by:

$$Nu = \frac{q_{convection}}{q_{conduction}} = 1 + \frac{h}{D} \tag{4.34}$$

Let us take the following numerical values for an example: $h = 1000$ m, $D = 100$ m, $\beta = 1.7 \cdot 10^{-3} \,{}^{\circ}C^{-1}$, $\rho_w = 812$ kg/m^3, $c_w = 4200$ J/kg, $\nu_w = 1.4 \cdot 10^{-7}$ m^2/s, $\lambda_e = 1.7$ watt/m°C, $T_o = 10$°C, $T_1 = 240$°C. The Nusselt number is according to eq. 4.34:

$$Nu = 1 + \frac{1000}{100} = 11$$

Eq. 4.31 then gives for the Rayleigh number:

$$Ra = (\frac{3\pi}{2} Nu)^2 = 2687 >> 4\pi^2$$

ΔT in eq. 4.29 is given by:

$$\Delta T = (T_1 - T_o) \frac{h}{h + D} = 230 \cdot \frac{1000}{1100} = 209^{\circ}C$$

Eq. 4.29 then gives for the permeability:

$$k = \frac{Ra\nu_w\lambda_e}{g\beta\rho_w c_w \Delta Th} \tag{4.35}$$

Inserting numerical values we get:

$$k = \frac{2687 \cdot 1.4 \cdot 10^{-7} \cdot 1.7}{9.81 \cdot 1.7 \cdot 10^{-3} \cdot 812 \cdot 4200 \cdot 209 \cdot 1000} \cong 54 \text{ md.}$$

Let us now calculate the necessary permeability to maintain convection in a high temperature geothermal reservoir. From eq. 4.29 and the necessary condition that Ra > $4\pi^2$ we get:

$$k > \frac{4\pi^2 \nu_w \lambda_e}{g\beta \rho_w c_w \Delta T h} \tag{4.36}$$

Inserting the same numerical values as above gives:

$$k > \frac{4 \cdot \pi^2 \cdot 1.4 \cdot 10^{-7} \cdot 1.7}{9.81 \cdot 1.7 \cdot 10^{-3} \cdot 812 \cdot 4200 \cdot 209 \cdot 1000} \cong 0.8 \text{ md.}$$

This is a very low permeability indicating that we would have convection in most high temperature geothermal reservoirs.

Let us now derive the differential equations describing the single phase convection of water. In case of single phase water eqs. 4.1-4.4 reduce to the following equations, if we neglect the transient term in the equation of continuity, add the gravity term to the momentum equation and apply Boussinesq assumption, which consists of neglecting the variation in the density everywhere in the equations except in the buoyancy term:

$$\text{div } V = 0 \tag{4.37}$$

$$V = - \frac{K}{\mu_w} (\text{grad } p + \rho_w g) \tag{4.38}$$

$$\frac{\partial T}{\partial t} = \text{div } (\kappa_e \text{ grad } T) - \alpha V \cdot \text{grad } T \tag{4.39}$$

where α is defined in eq. 4.24 and κ_e is the effective diffusivity defined as:

$$\kappa_e = \frac{\lambda_e}{(1 - \phi)\rho_r c_r + \phi\rho_w c_w} \tag{4.40}$$

These equations have been treated by many authors with various boundary conditions and with respect to geothermal reservoirs. See e.g. Elíasson (1973), Combarnous and Boris (1975), Witherspoon et al. (1975), Garg and Kassoy (1981), Lapwood (1948), Caltagirone (1975), Wooding (1963). A linear stability analysis of the above equations shows that thermal convection in a liquid-saturated porous layer is initiated when a critical value of the Rayleigh number, Ra, is exceeded. In a horizontal layer of constant thickness and a constant temperature difference across, the critical Rayleigh number is $4\pi^2$, as originally proved by Lapwood.

In the above we have just considered the relative simple single phase convection of water with constant fluid properties. Straus and Schubert (1977) determined the critical Rayleigh number for variable fluid properties. They also investigated the basic physical processes involved in three-dimensional medium convection with phase transition. They found that the phase change instability mechanism induces convection prior to the onset of ordinary buoyancy driven thermal convection. Finally we mention that Straus and Schubert (1979) showed that the buoyancy of the geothermal fluid depends heavily on the presence of CO_2 because of the large volume changes that occur when CO_2 enters or leaves solution and forces water to simultaneously change phase.

4.5 Lumped and distributed reservoir models

The simplest type of a geothermal reservoir model is the "lumped parameter" model. In this case, the entire geothermal system is described in terms of only a few major parameters. Instead of considering the internal distribution of mass and energy, attention is restricted to the total amounts within the system and what crosses the boundaries. In these models, time is the only independent variable, and the system can therefore be characterized mathematically by a set of ordinary differential equations or an equivalent set of algebraic expressions representing total mass and energy balance. Lumped parameter models are appealing for their simplicity, generality and ease of application. A model in which the properties of the rock and the fluid are allowed to vary in space is called a distributed parameter model. Unlike the lumped parameter models, which are relatively simple mathematically and for which the use of numerical computing methods is not a dominant feature, distributed parameter models are often so complicated that large computers are needed to obtain numerical solutions to the partial differential equations describing the heat and fluid flow processes. By taking into account spatial variations of these properties the resulting problem may become too complex to be treated analytically. An alternative approach is to replace the governing partial differential equations by an equivalent set of algebraic equations and then solve the problem numerically with the aid of a computer. In order to explain the difference between these two model approaches and to show their use in reservoir engineering some examples will be given in the following.

Let us first take an example of a lumped parameter convection model. The following model was used for the Svartsengi geothermal reservoir in Iceland (see Kjaran et al. 1980). Fig. 4.8 explains the mechanism of the model.

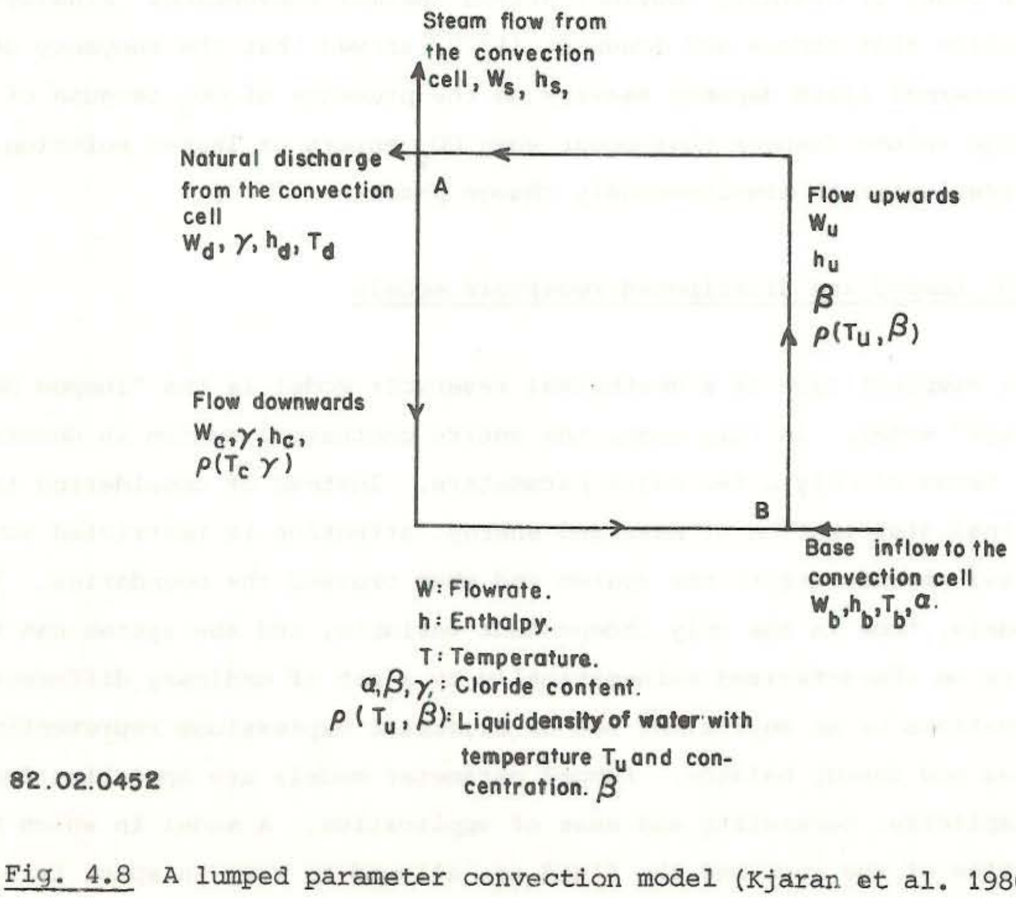

Fig. 4.8 A lumped parameter convection model (Kjaran et al. 1980)

A base inflow flows into the geothermal reservoir and due to buoyancy effects it is convected upwards, a part of it flows away as a natural discharge and steam flow, but the rest flows down again to mix with the base inflow. Due to the vapourization the chloride content in the Svartsengi geothermal water is different in the different flowpaths in the convection cell. The conservation equations for mass, energy and chloride concentration can be written in points A and B as:

Point A:

Mass: $$W_u = W_c + W_d + W_s \tag{4.41}$$

Energy: $$W_u h_u = W_s h_s + W_d h_d + W_c h_c \tag{4.42}$$

Concentration: $$W_u \beta = W_d \gamma + W_c \gamma \tag{4.43}$$

Point B:

Mass: $$W_u = W_c + W_b \tag{4.44}$$

Energy: $$W_u h_u = W_c h_c + W_b h_b \tag{4.45}$$

Concentration: $$W_u \beta = W_c \gamma + W_b \alpha \tag{4.46}$$

Eqs. 4.41-4.46 can be arranged to give the following equations:

$$W_c = W_u \frac{\beta - \alpha}{\gamma - \alpha} \tag{4.47}$$

$$W_b = W_u \frac{\gamma - \beta}{\gamma - \alpha} \tag{4.48}$$

$$W_d = W_u \frac{\alpha}{\gamma} \frac{\gamma - \beta}{\gamma - \alpha} \tag{4.49}$$

$$W_s = W_u \frac{\gamma - \beta}{\gamma} \tag{4.50}$$

$$h_c = h_u - L\,\frac{\gamma - \beta}{\gamma} \tag{4.51}$$

$$h_b = h_u + L\,\frac{\beta - \alpha}{\gamma} \tag{4.52}$$

where L is the latent heat of vapourization. If we assume that the chloride concentration is known we have here 6 equations with seven unknowns. In order to determine W_u, so the equations above can be solved, let us look at Fig. 4.9, which shows a vertical section through the convection cell. Darcy's law for the flow in the convection cell can be written as:

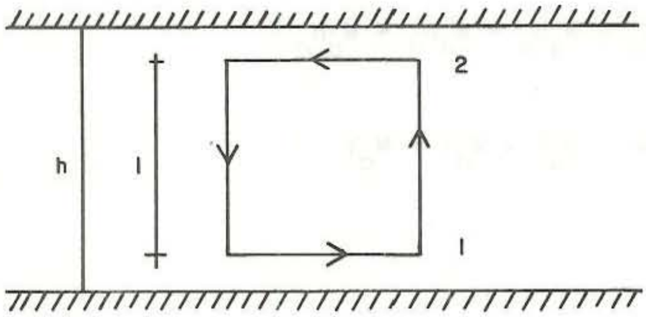

Fig. 4.9 Vertical section through the convection cell

$$\frac{g}{K}\,U_i + \rho g_i + \frac{\partial p}{\partial x_i} = 0 \tag{4.53}$$

where the symbols are defined in the following way:

U_i: massflux vector, $kg/s/m^2$
K : coefficient of permeability, m/s
g_i: acceleration of gravity (o,g), m/s^2
ρ : density, kg/m^3
p : pressure, N/m^2
x_i: coordinates, i = 1.2, m

Integrating eq. 4.53 around the convection cell gives:

$$\oint \frac{g}{K} U_i ds + \oint \rho g_i \cdot ds + \oint \frac{\partial p}{\partial x_i} ds = 0 \qquad (4.54)$$

The first term in eq. 4.54 is due to the energy dissipation in the flow, the second term is the buoyancy effect in the convection and is in fact the density difference between the upflow and downflow. The third and last term is the integration of the pressure gradient and must equal zero for the closed integration path. The second term in eq. 4.54 can be approximated as:

$$\oint \rho g_i ds = gl\Delta\rho \qquad (4.55)$$

where $\Delta\rho$ is the density difference between the downflow and the upflow. The upflow in the convection cell occurs over much smaller area than the downflow, the energy dissipation is therefore greatest in the upflow area. The first term in eq. 4.54 can therefore be approximated in the following way:

$$\oint \frac{g}{K} U_i ds = \frac{g}{K} \frac{\overline{u}}{1 - \varepsilon} l \qquad (4.56)$$

where $\overline{u}$ is the massflux in the upflow and ε is the part of the energy dissipation, which occurs in the downflow and must be much smaller than 0.5. Equating equations 4.55 and 4.56 we get:

$$\overline{u} = - K(1 - \varepsilon)\Delta\rho = K(1 - \varepsilon)(\rho(T_c,\gamma) - \rho(T_u,\beta)) \qquad (4.57)$$

If the area of the upflow is A, the upflow can be written as:

$$W_u = KA(1 - \varepsilon)(\rho(T_c,\gamma) - \rho(T_u,\beta)) \qquad (4.58)$$

If the coefficient of permeability, K, the upflow area A and the energy dissipation factor, ε, can be estimated, the upflow can be calculated from eq. 4.58. This upflow value can then be used to solve eqs. 4.47-4.52.

The result of these calculations has been used for the Svartsengi geothermal reservoir to calculate the natural heat flow from the reservoir, which is given by:

$$q_{natural} = W_u h_u - W_c h_c \tag{4.59}$$

The next example is a distributed parameter model just around a discharging well. The example given is for a geothermal field with low gas concentration. The following example is from the Kawah Kamojang geothermal reservoir in Jawa presented by Grant (1979). The steam discharging from vapour-dominated fields usually contains some gases. Carbon dioxide and hydrogen sulphide are the most common. As these gases are soluble in water, the reservoir's stock of gas partitions itself between the liquid and vapour phases. When the pressure and saturation vary, there is a transfer of mass from one phase to another, and this usually implies a change in the gas concentration in each phase. Large quantities of gas markedly affect field behaviour (Grant 1977), in two phase systems with both phases mobile. A simpler case is when the gas content is small. Then the gas has little effect on the equations for conservation of mass and energy. The small gas concentration functions only as a tracer, without otherwise affecting field behaviour. Let us first consider a distributed model for the reservoir response to the discharging well. According to Grant (1979) the geothermal reservoir contains immobile water and mobile steam. There is also a small amount of gas present, mixed with the steam and dissolved in the water. Changing the flow rate at the wellhead causes a response in the reservoir pressure and gas content.

The pressure response is given by eqs. 3.263 and 3.264. The changes in gas content are determined by the equation for conservation of gas:

$$\frac{\partial}{\partial t}\{\phi S_w \rho_w n_w + \phi(1 - S_w)\rho_s n_s\} = -\operatorname{div}\{\rho_w n_w V_w + \rho_s n_s V_s\} \tag{4.60}$$

where n_w and n_s is the mass fraction of gas in water and steam respectively. Now using that the water is immobile, $V_w = 0$ and inserting Darcy's law into eq. 4.60 we get:

$$\frac{\partial}{\partial t}\{\phi S_w \rho_w n_w + \phi(1 - S_w)\rho_s n_s\} = k \operatorname{div}\{\frac{n_s}{\nu_s}\operatorname{grad} P\} \tag{4.61}$$

We now introduce the following definition:

$$\gamma = (1 - S_w)\rho_s + \frac{n_w}{n_s} S_w \rho_w \tag{4.62}$$

Grant (1979) assumes that the variations in γ with saturation and temperature can be ignored, and it can be evaluated at undisturbed reservoir conditions. By inserting the definition of γ into eq. 4.61 we get by using cylindrical coordinates:

$$\phi\gamma \frac{\partial n_s}{\partial t} = \frac{k}{r}\frac{\partial}{\partial r}\{r \frac{n_s}{\nu_s}\frac{\partial p}{\partial r}\} \tag{4.63}$$

By using the pressure solution from eq. 3.264 and inserting into eq. 4.63 for $\partial p/\partial r$ we get:

$$\gamma\phi \frac{\partial n_s}{\partial t} = \frac{W}{4\pi h}\frac{2}{r}\frac{\partial}{\partial r}\{n_s e^{-r^2/4\kappa t}\} \tag{4.64}$$

where W is the mass flow rate from the discharging well as before. Grant (1979) has shown, that by introducing the similarity variable defined by:

$$\xi = r^2/4\kappa t \tag{4.65}$$

eq. 4.64 can be reduced to:

$$- \gamma\phi\xi \frac{dn_s}{d\xi} = \frac{W}{4\pi\kappa h}\frac{d}{d\xi}(n_s e^{-\xi}) \tag{4.66}$$

which can be integrated to give:

$$\ln \frac{n_s}{n_{so}} = - \int_{\frac{r_w^2}{4\kappa t}}^{\infty} \frac{we^{-\xi}d\xi}{\xi + we^{-\xi}} \tag{4.67}$$

where n_{so} is the initial mass fraction of gas in steam, before the well was switched on and w is defined by:

$$w = \frac{W}{4\pi\gamma\phi\kappa h} = \frac{W}{4\pi k h}\frac{\mu_s c}{\gamma} \tag{4.68}$$

Let us now use a lumped-parameter model for the change in gas content according to Grant (1979). Let us model the geothermal reservoir as a confined box, from which fluid is withdrawn. Let the volume of the box be V, and the mass withdrawal W. Then conservation of gas is:

$$\frac{d}{dt}\{V\phi[S_w\rho_w n_w + (1 - S_w)\rho_s n_s]\} = - n_s W \tag{4.69}$$

remembering that we have just steam flow, because the water was immobile. Using the same definitions and approximations as before we get:

$$\frac{d}{dt}(V\phi\gamma n_s) = V\phi\gamma\frac{dn_s}{dt} = - n_s W \tag{4.70}$$

Integrating the above equation results in:

$$\ln\left(\frac{n_s}{n_{so}}\right) = -\frac{\int W dt}{V\phi\gamma} \tag{4.71}$$

In case of constant mass flow rate we have:

$$\ln\left(\frac{n_s}{n_{so}}\right) = -\frac{Wt}{V\phi\gamma} \tag{4.72}$$

where t is the total flowing time. Comparing eqs. 4.72 and 4.67 we see that now the gas concentration is dependent on cumulative mass flow rate instead of directly on the mass flow rate in eq. 4.67. This is a direct consequence of the confined reservoir in the lumped parameter model above, contrary to the infinite reservoir we used in the distributed parameter model leading to eq. 4.67. Let us now assume we have two different gases with different concentrations. Eq. 4.72 now gives for the two gases denoted by subscribts 1 and 2:

$$\frac{d(\ln n_{s1})}{d(\ln n_{s2})} = \frac{\gamma_2}{\gamma_1} \tag{4.73}$$

Integrating yields:

$$\ln n_{s1} = \frac{\gamma_2}{\gamma_1} \ln n_{s2} + C \tag{4.74}$$

If the concentration of gas 1 is plotted against the concentration of gas 2, on log-log paper, the result should be a straight line. The slope of the straight line is given by:

$$\eta = \frac{\gamma_2}{\gamma_1} = \frac{(1 - S_w)\rho_s + \frac{n_{w2}}{n_{s2}} S_w \rho_w}{(1 - S_w)\rho_s + \frac{n_{w1}}{n_{s1}} S_w \rho_w} \tag{4.75}$$

In this expression for the slope, all the variables are known functions of temperature, except the saturation S_w. Thus from the slope, the water saturation of the rock can be immediately obtained, independent of other physical parameters such as permeability of porosity. The following example is given by Grant (1979) for the Kawah Kamojang, geothermal field, Java.

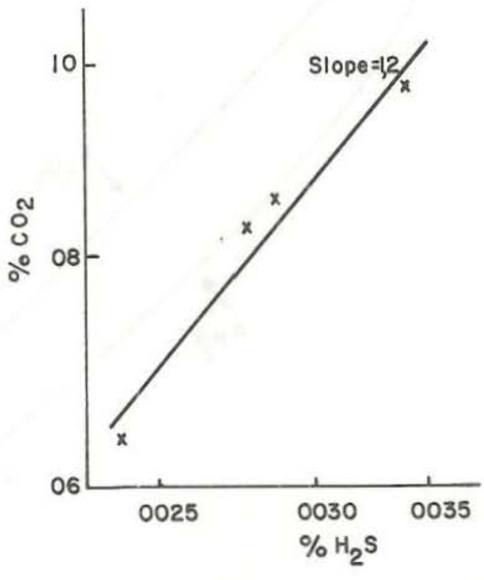

82.02.0454.

Fig. 4.10 Log-log plot of CO_2-H_2S concentrations for KMJ11 (Grant 1979)

Log-log plot of CO_2-H_2S concentrations is given in Fig. 4.10 for one well.

The reservoir temperature is 240°C. For low gas concentrations the mass fraction can be approximated by the mole fraction, that is:

$$\frac{n_w}{n_s} = A = \frac{N^w/N^w_{H_2O}}{N^s/N^s_{H_2O}}$$ where $N^w_{H_2O}$ and $N^s_{H_2O}$ is the number of moles of water in water phase and steam phase respectively and N^w and N^s is the number of moles of the noncondensable gas in water phase and steam phase respectively. According to Fig. 4.11 we have:

$$A_{CO_2} \cong \frac{n_{wCO_2}}{n_{sCO_2}} = 0.007, \quad A_{H_2S} \cong \frac{n_{wH_2S}}{n_{sH_2S}} = 0.0216.$$

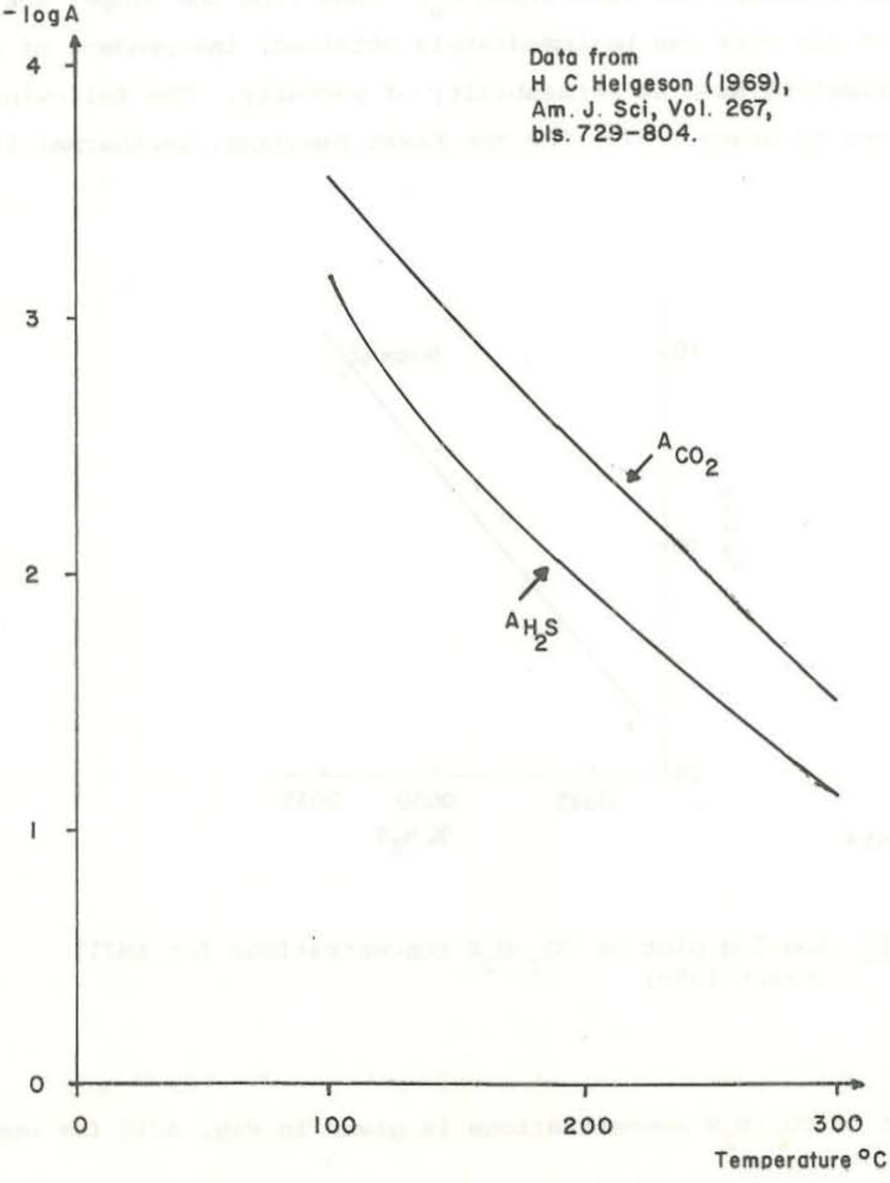

Fig. 4.11 A_{H_2S} and A_{CO_2} vs. temperature (Arnórsson 1973)

From steam tables we have, $\rho_w = 814\ kg/m^3$ and $\rho_s = 16.8\ kg/m^3$. We can now write according to eq. 4.62:

$$\gamma_{H_2S} = 16.8 + 0.78\ S_w \tag{4.76}$$

$$\gamma_{CO_2} = 16.8 - 11.1\ S_w \tag{4.77}$$

From eq. 4.74 and the slope of the line in Fig. 4.10 we get:

$$\eta = 1.2 = \frac{16.8 + 0.785\ S_w}{16.8 - 11.1\ S_w}$$

which gives for the water saturation:

$$S_w = 0.24.$$

Thus with the assumptions made the water saturation of the undisturbed reservoir is found to be 24%. Even a small mass fraction of noncondensable gas changes the behaviour of the geothermal reservoir, and we finally show an example of a distributed parameter model of such a gas dominated field. In its natural state, the partial pressure of the noncondensable gas causes the reservoir to boil at a lower temperature than does a pure water field. Under exploitation the presence of CO_2 or H_2S, which are the most common gases in geothermal fields, dominate the transport and thermodynamical characteristics of the flow. The Broadlands (Ohaki) geothermal field in New Zealand is an example of a gas-dominated field, (Grant 1977 and Zyvoloski and Sullivan 1980). The initial pressure response to exploitation at Broadlands is dominated by changes in gas pressure. The differential equations describing the distributed parameter model are the conventional equations for the conservation of mass, momentum, energy and carbon dioxide. The equations for the conservation of mass, momentum and energy are the same as before given by eqs. 4.1-4.4 if we replace the water phase with liquid phase and the steam phase with a vapour phase, denoted by the subscripts ℓ and v instead of w and s. The equation for carbon dioxide is given by:

$$\frac{\partial}{\partial t}\{\phi S_\ell \rho_\ell n_\ell + \phi(1 - S_\ell)\rho_v n_v\} = -\text{ div }\{\rho_\ell n_\ell V_\ell + \rho_v n_v V_v\} \tag{4.78}$$

Together with these equations we need some thermodynamical relationships:

1) Density:

The vapour phase density is given according to Gibbs-Dalton law by:

$$\rho_v = \rho_s + \rho_c \tag{4.79}$$

where ρ_s is the density of steam and ρ_c is the density of CO_2. The density of steam can be taken from steam tables and similar tables for the density of carbon dioxide exist (see Sutton 1976). The amount of CO_2 in the liquid phase is small and neglected in the liquid density, that is:

$$\rho_\ell = \rho_w \tag{4.80}$$

2) Carbon dioxide content:

From the definitions of gas densities and mass fraction of CO_2 we have:

$$n_v = \frac{\rho_c}{\rho_v} \tag{4.81}$$

For the liquid phase Sutton (1976) gives the empirical formula:

$$n_\ell = \alpha(T)p_c \tag{4.82}$$

3) Enthalpy:

$$h_\ell = n_\ell h_{\ell c} + (1 - n_\ell)h_w \tag{4.83}$$

$$h_v = n_v h_{vc} + (1 - n_v)\ (U_s + \frac{p}{\rho_v})$$

$$= n_v h_{vc} + (1 - n_v)\ U_s + \frac{p}{\rho_s}) \qquad (4.84)$$

$$= n_v h_{vc} + h_s - n_v U_s$$

where $h_{\ell c}$ and h_{vc} are the specific enthalpies of dissolved and gaseous carbon dioxide respectively and U stands for internal energy.

4) Viscosity:

The carbon dioxide is assumed to have no effect upon the viscosities. That is:

$$\mu_v = \mu_s \qquad (4.85)$$

$$\mu_\ell = \mu_w \qquad (4.86)$$

5) The total pressure can be calculated as the sum of steam pressure and partial pressure of carbon dioxide as:

$$p = p_s + p_c \qquad (4.87)$$

These equations are too complicated to be solved analytically and numerical methods must be used. Zyvoloski and Sullivan (1980) have solved these equations numerically. Their conclusion is that the reservoir response to exploitation is initially governed by changes in partial pressure of the CO_2. Another effect demonstrated by their results is that the presence of CO_2 leads to a reduced compressibility of the fluid and, therefore, a faster propagation of pressure transients. Let us look at these effects in more detail. The two phase compressibility was defined in eq. 3.231 and can be defined in relation to relative volume changes as:

$$\frac{\Delta V}{V} = \beta_s \Delta p_s \qquad (4.88)$$

At reservoir temperature 260°C, water saturation equal to 0.5, and 10% porosity the two phase compressibility is approximately 1 bar^{-1}. The compressibility resulting from the carbon dioxide can be written similarly to eq. 4.88 as:

$$\frac{\Delta V}{V} = \beta_c \Delta p_c \tag{4.89}$$

In order to calculate β_c we note that the volume changes when CO_2 leaves the water solution can be calculated from eq. 4.82 and written as:

$$\frac{\Delta V}{V} = \frac{\Delta n_\ell}{\rho_c} \rho_w \cong \frac{\alpha(T)\Delta p_c}{\rho_c} \rho_w \tag{4.90}$$

By using eqs. 4.79, 4.81 and 4.89 we can write for the compressibility:

$$\beta_c = \frac{\alpha(T)\rho_w(1 - n_v)}{n_v \rho_s} \tag{4.91}$$

According to Sutton (1976) $\alpha(T)$ is given by the following formula:

$$\alpha(T) = \{5.4 - 3.5 \frac{T}{100} + 1.2 (\frac{T}{100})^2 \} 10^{-9} \text{ Pa}^{-1} \tag{4.92}$$

and n_v can be calculated from:

$$n_v = p_c/p \tag{4.93}$$

Let us calculate β_c with typical data from the Broadlands: $T = 260°C$, from steam tables we get: $\rho_w = 784 \text{ kg/m}^3$, $\rho_s = 23.7 \text{ kg/m}^3$. α is calculated from eq. 4.92:

$$\alpha(260°C) = \{5.4 - 3.5 \frac{260}{100} + 1.2 (\frac{260}{100})^2 \} \cdot 10^{-9} = 4.4 \cdot 10^{-9} \text{ Pa}^{-1}$$

Table 4.1 given by Sutton and McNabb (1977) gives the partial pressure of CO_2 for the Broadlands geothermal field, which gives $p_c = 12.42$ bar for $T = 260°C$. n_v can now be calculated from eq. 4.93:

$$n_v = \frac{12.42}{59.33} = 0.209$$

T deg	P bars	P_c bars	n_w %	n_s %	h_l MJ/kg	h_v MJ/kg
180	11.47	1.44	0.04	12.58	0.762	2.449
190	14.46	1.91	0.06	13.19	0.807	2.441
200	18.04	2.50	0.08	13.85	0.851	2.431
210	22.33	3.26	0.11	14.61	0.897	2.417
220	27.44	4.25	0.15	15.47	0.942	2.399
230	33.50	5.53	0.20	16.51	0.989	2.374
240	40.66	7.20	0.28	17.70	1.035	2.345
250	49.17	9.42	0.39	19.15	1.082	2.309
260	59.33	12.42	0.55	20.94	1.131	2.261
270	71.66	16.65	0.78	23.24	1.179	2.200
280	87.16	23.03	1.15	26.42	1.229	2.114
290	107.77	33.38	1.78	30.97	1.279	1.993
295	121.87	41.86	2.31	34.35	1.303	1.905
296	125.17	44.01	2.44	35.16	1.308	1.884
297	128.71	46.37	2.59	36.02	1.313	1.862
298	132.47	48.96	2.75	36.96	1.317	1.838
299	136.58	51.86	2.94	37.97	1.322	1.812
300	141.05	55.12	3.14	39.08	1.326	1.783
301	146.21	59.06	3.39	40.39	1.331	1.750
302	152.06	63.67	3.68	41.87	1.335	1.712
303	158.87	69.23	4.02	43.58	1.339	1.669
304	167.07	76.18	4.46	45.60	1.342	1.618

Table 4.1 Values of temperature, total pressure, partial pressure of CO_2, mass ratios n_l, n_v of CO_2 in the liquid and vapour phases, and the specific enthalpy h_l, h_v of each phase on the theoretical boiling curve for the Broadlands (Sutton and McNabb, 1977)

Eq. 4.91 now gives for the compressibility:

$$\beta_c = \frac{4.4 \cdot 10^{-9} \cdot 784 \cdot (1 - 0.209)}{0.209 \cdot 23.7} \cong 0.06 \text{ bar}^{-1}$$

which can be compared with the two phase compressibility 1 bar^{-1}. From eqs. 4.88 and 4.89 we see, because $\beta_c < \beta_s$ that for the same volume change the drop in partial pressure for carbon dioxide is much greater than the drop in steam pressure. Let us now define the total compressibility resulting from the two phase compressibility and carbon dioxide compressibility in the usual way according to the following equation:

$$\frac{\Delta V}{V} = \beta \Delta p \qquad (4.94)$$

where Δp is the total pressure drop defined from eq. 4.87 as:

$$\Delta p = \Delta p_c + \Delta p_s \qquad (4.95)$$

By combining eqs. 4.88, 4.89, 4.94 and 4.95 for the same volume change we get:

$$\frac{1}{\beta} = \frac{1}{\beta_c} + \frac{1}{\beta_s} \qquad (4.96)$$

Because $\beta_c << \beta_s$ we have that:

$$\beta \simeq \beta_c \qquad (4.97)$$

We see that the compressibility now becomes less than the compressibility for a pure two phase mixture without carbon dioxide. As we have noted before this changes the pressure transmission significantly.

4.6 Reinjection into geothermal reservoirs

Reinjection of geothermal wastewater is gradually becoming a preferred means of waste disposal. At present continuous reinjection is practiced at the Geysers, California (Chasteen 1975 and Kruger and Otte 1973), Ahuachapan, El Salvador (Einarsson et al. 1975 and Cuellar et al. 1981), Mak Ban, Phillippines (Horne 1981), and at five Japanese geothermal fields (Otake, Onuma, Onikobe, Hatchobaru, and Kakkonda) (Horne 1981, Kubota and Aosaki 1975 and Hayaski et al. 1978). Small-scale reinjection tests have been reported at a number of geothermal fields, e.g. Baca, New Mexico (Chasteen 1975); East Mesa, California (Mathias 1975); Larderello, Italy (Giovannoni 1981); Cerro Prieto, Mexico (Vides 1975); Broadlands, New Zealand (Brixley and Grant 1979); and Tongonan, Phillippines (Studt 1980).

Reinjection of water into geothermal reservoirs during utilization is intended to serve threefold purposes. 1) waste water disposal 2) pressure maintenance 3) improved energy extraction.

Geothermal power plants producing electricity produce often waste water, which creates disposal problems. Maintaining pressure is important in many geothermal reservoirs. In the Svartsengi high temperature field in Iceland pressure must be maintained in order to keep calcite precipitation inside the cemented casings of the wells (Kjaran et al. 1981). Maintaining pressure is also important in order to reduce subsidence. In section 4.3 we discussed natural recharge into geothermal reservoirs. When the natural recharge is small reinjection can be used to improve the heat extraction process by mining heat from the rock. The danger in employing reinjection is the possibility that the colder water will prematurely break through from the zones around the injection well into the production region, thus drastically reducing the efficiency of the operation. Production wells are sited to produce at high flow rates of geothermal steam, and are drilled to the depth at which production occurs. Reinjection wells, on the other hand, may be sited with greater degree of choice, since their major superficial requirement is only the intersection of some permeable formation. In view of the greater freedom of choice, there is correspondingly greater controversy as to where to best locate reinjection wells in a given system. Horne (1981) defines the following location of reinjection wells: a) injection into one side of a system and production from the other, referred to by Horne (1981) as side by side, and b) an intermixed arrangement of reinjection wells and production wells, referred to as intermixed. Other than the choice of lateral position, reinjection wells may be drilled to intersect formations at shallower, equal, or greater depths than the producing formation. These are referred to by Horne as above, equal and below. There is disagreement as to which arrangement is best suited to reservoir preservation criteria. In many cases, geologic, environmental, or economic factors may more greatly influence the choice. Table 4.2 gives a summary of production and reinjection data in Japan as reported by Horne (1981).

Station		Onikobe	Kakkonda	Onuma	Hatchobaru	Otake
Capacity		25 Mw	50 Mw	10 Mw	55 Mw	12 Mw
1980 Production		7.5 Mw	~40 Mw	7 Mw	55 Mw	12 Mw
Production	No. of wells	12	11	5	8	4
	Av. depth	300 m	1000 m	1600 m	1000 m	500 m
	Total steam	75 t/hr	380 t/hr	91 t/hr	400 t/hr	120 t/hr
	WHP *)	200 kPa	686 kPa	300 kPa	481 kPa	304 kPa
Reinjection	No. of wells	1	15	4	14	8
	Av. depth	1000 m	700 m	800 m	1000 m	500 m
	Total flow	115 t/hr	2700 t/hr	360 t/hr	400 t/hr	680 t/hr
	Temperature	95°C	~160°C	95°C	60/95°C	95°C
	Pressure	0	540 kPa	0	0	0
	Configuration	side/below	mixed/above	side/above	side/equal	side/equal
Tracer flow rate		--	n.a.	up to 4 m/hr	up to 80 m/hr	~0.3 m/hr
Comments		Gas interference	-	-	Silica Scaling	Accepts water from Hatchobaru 175 t/hr

Table 4.2 Summary of production and reinjection in Japan, September 1980 (Horne 1981)

*) WHP: Well head pressure

According to Horne (1981) the following conclusions can be drawn from the Japanese experience.

(1) In many cases, reinjected water moves through the reservoir through fractures or fissures of extremely high permeability. It is therefore of great importance to determine inter-well connectivities in the designing of a reinjection-scheme.

(2) In cases where inter-well flows do occur, the resulting thermal interference can be greatly detrimental to the performance of the producing well. On the other hand, the hydraulic interference may be beneficial in providing pressure support. The problem is one of removing the reinjection well to such a safe distance that the cooled reinjected water is reheated before arriving at the producing well.

(3) In view of the "safe distance" requirement, the "side-by-side" reinjection configuration would seem preferable to the "intermixed arrangement. Experience in Japan however, shows that either configuration can cause thermal interference if inter-well spacing is insufficient.

(4) Maintenance of reservoir pressure by reinjection may indeed be beneficial; however, in practice, only a single example of performance improvement has been observed (at Otake). On the other hand, three examples of reduction in performance by thermal interference have been observed (Hatchobaru, Kakkonda, and Onuma). If priorities are to be allocated, it appears to be expedient to avoid thermal interaction even at the cost of losing hydraulic support.

Finally Horne (1981) summarizes the above experience in the following two statements:

a) Reinjection wells and production wells should be as hydraulically far apart as possible.

b) Underground flow paths need to be fully understood before embarking on a reinjection scheme.

The above example by Horne (1981) is an actual experience from five japanese geothermal fields. Theoretical analysis can also give valuable answers and insight into the physical nature of the injection process, but they can never replace actual field experiments. One of the answers we can get from theoretical analysis is e.g. the advancement of the thermal front. The equation governing the advancement of the cold water front in a porous medium for a hot water reservoir is obtained from eq. 3.150:

$$r = \sqrt{\frac{\alpha Q t}{\pi h}} \tag{4.98}$$

where α is defined in eq. 4.24.

If the advancement of the thermal front for a hot water reservoir is in a single fracture the equation for the diffusion radius becomes different and is now given by according to Böðvarsson and Tsang (1981).

1) Early-time behaviour:

$$r = \sqrt{\frac{Q t \rho_w c_w}{\pi w \rho_f c_f}} \tag{4.99}$$

where w is the fracture aperture, and ρ_f and c_f are the density and specific heat of the fracture material respectively.

2) Intermediate-time behaviour:

$$r = \left(\frac{Q^2 t (\rho_w c_w)^2}{4.396 \lambda \rho_r c_r \pi^2}\right)^{1/4} \tag{4.100}$$

where λ is the thermal conductivity of the rock matrix and other symbols have been defined before.

3) Late-time behaviour:

$$r = \sqrt{\frac{Q t \rho_w c_w}{\pi (2 \rho_r c_r D + \rho_f c_f w}} \tag{4.101}$$

where D is the thickness of the rock matrix per fracture.

The transition between the early-time behaviour and intermediate-time behaviour occurs at the following time and distance according to Böðvarsson and Tsang (1981).

$$t = \frac{w^2}{4.396} \frac{(\rho_f c_f)^2}{\lambda \rho_r c_r} \tag{4.102}$$

$$r = \sqrt{\frac{Q_w}{4.396\pi} \frac{\rho_w c_w \rho_f c_f}{\rho_r c_r \lambda}} \tag{4.103}$$

and the transition from the intermediate-time solution to the long-time solution is given by:

$$t = \frac{\rho_r c_r D^2}{4.396\lambda} \left(2 + \frac{\rho_f c_f w}{\rho_r c_r D}\right)^2 \tag{4.104}$$

$$r = \sqrt{\frac{\rho_w c_w Q D}{4.396\pi\lambda} \left(2 + \frac{\rho_f c_f w}{\rho_r c_r D}\right)} \tag{4.105}$$

The results above apply for the injection of cold water into a hot water reservoir. In that case the fluid remains single phase, but for the injection of cold water into a two phase or dry steam reservoir the spreading cold water heats up by extracting thermal energy from the rock and as it advances, the reservoir fluid condenses. Theoretical analysis is much more difficult in this case (see O'Sullivan and Pruess 1980). As mentioned before field experiments should always be conducted in order to choose reinjection strategy. One of these experiments is to use tracer tests in order to be able to understand the underground flow paths. Because the flow situation is influenced by dispersion effects, theoretical analysis of the tracer test results are difficult. But without much theoretical calculations the time for the tracer to reach production wells can be measured, as shown in Table 4.2. A comprehensive evaluation of well-to-well tracers for geothermal reservoirs is given by Vetter and Zinnov (1981).

4.7 Numerical modelling of geothermal reservoirs

In section 4.2 the general equations for the flow in geothermal reservoirs were formulated. Having generated this set of governing equations, one is faced with the task of solving a set of highly non-linear partial-differential equations. In nearly all cases, this is approached numerically. There are several difficulties encountered in the numerical solution of the geothermal reservoir equations. The first task is to select a set of independent variables since several possibilities exist. One must then decide upon a method of approximation. Currently, finite difference and finite element schemes are employed. One is now confronted with the problems associated with the simulation of convection dominated transport, namely numerical dispersion (oscillations) and diffusion (smearing of a sharp front). Possibly the most difficult task, however, remains; the efficient and accurate treatment of the highly non-linear coefficients.

From the reservoir engineering point of view, there are two additional factors to be considered. The field application of a geothermal code requires a proper representation of the wellbore dynamics and thermodynamics. This is particularly important in the case of simulations in the immediate vicinity of the well. A second practical problem involves the reduction of the general three-dimensional system to an areal two-dimensional representation. This requires, of course, formal integration over the vertical direction. This integration should be carried out carefully so that essential elements of the reservoir physics are salvaged.

Further description of the numerical methods and codes will not be given here but the reader is referred to Pinder (1979).

Finally it should be mentioned that at the sixth Stanford Worshop on Geothermal Reservoir Engineering held at Stanford University December 16-18, 1980 one session was devoted to geothermal reservoir engineering computer code comparison (see Kruger and Ramey 1980). Most of the computer codes available in USA were compared and no significant difference in the results were observed between the existing computer methods and codes.

5 WELL PERFORMANCE

5.1 Introduction

The well is a part of the system exploited and it is through the well we get our fluid to operate the power plant. It is therefore of importance to be able to understand the reservoir well interaction. The flow in the wellbore is either a two phase flow of water and steam or saturated steam. Well logging methods and their interpretation will not be treated here, but the reader is referred to Stefánsson and Steingrímsson (1980) and Grant (1979).

5.2 Pressure discharge relation

Fig. 5.1 is a schematic picture of the pressure in a discharging well and its immediate vicinity. Far away from the well we have undisturbed reservoir pressure, p_e. As we have seen in section 3 the pressure declines towards the well resulting in well pressure, p_w. In section 3.11 we saw that the pressure decline in the well can be written as:

$$p_e - p_w = BW + CW^2 \tag{5.1}$$

where the first term on the right hand side is due to the pressure drop in the reservoir as well as skin effect around the well, and the second term is due to turbulent pressure drop. If the second term is small in relation to the first term, eq. 5.1 becomes:

$$W = \text{constant} \cdot (p_e - p_w) \tag{5.2}$$

and if the first term is small in relation to the second term eq. 5.1 now becomes:

$$W = \text{constant} \cdot \sqrt{p_e - p_w} \tag{5.3}$$

In section 3.16 we saw that if the fluid in the vicinity of the well is superheated steam, the same equations apply if we replace the pressure term in the equations with the pressure squared. Eq. 5.1 then becomes for a

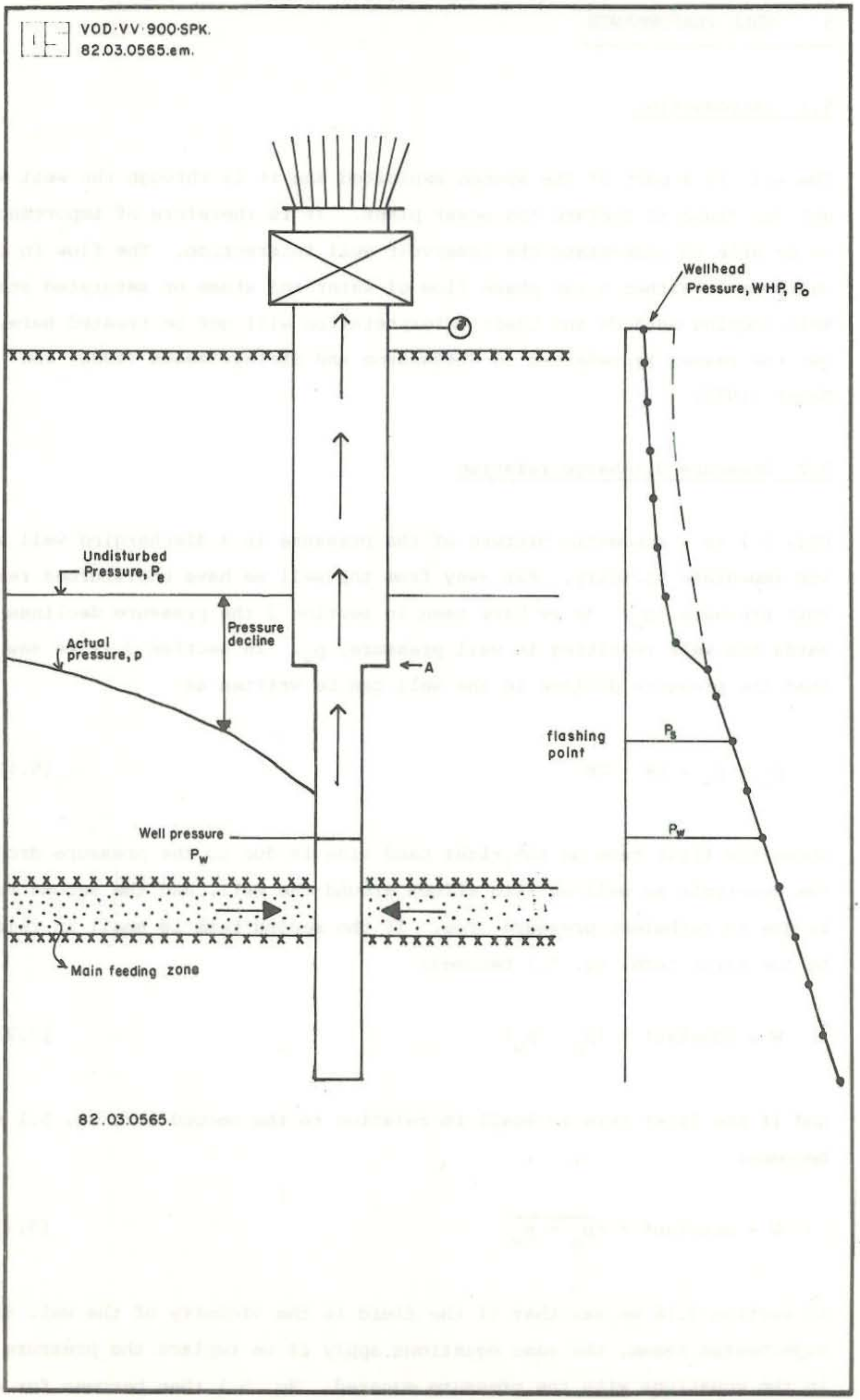

Fig. 5.1 Characteristics of a flowing well

superheated steam reservoir:

$$p_e^{\ 2} - p_w^{\ 2} = BW + CW^2 \tag{5.4}$$

If we now assume that $BW >> CW^2$ eq. 5.4 becomes:

$$W = \text{constant} \cdot (p_e^{\ 2} - p_w^{\ 2}) \tag{5.5}$$

and in case of $CW^2 >> BW$ eq. 5.4 becomes:

$$W = \text{constant} \cdot \sqrt{p_e^{\ 2} - p_w^{\ 2}} \tag{5.6}$$

Eqs. 5.1-5.6 are the socalled discharge pressure relations, where the reference pressure is the well pressure, p_w, at the feeding point in the well. If we ignore frictional pressure drop in the well and assume the well to have zero length, which also includes that we neglect the weight of the fluid overlying the feeding zone in the well, the feeding point pressure, p_w, becomes equal to the well head pressure, p_o. p_w can then be replaced by p_o in eqs. 5.1-5.6. We then get what commonly is known as theoretical pressure discharge relation, where the reference pressure in the wellbore is the well head pressure. Theoretical pressure discharge curves are shown in Figs. 5.2 and 5.3. The wellbore is of course not of zero length and we must take into account the frictional pressure drop, acceleration of the fluid in the wellbore and the gravity term, we then get the actual pressure discharge relations. These effects are called wellbore effects. These are shown on Figs. 5.2 and 5.3 for different well depths and well diameters for steam wells at the Geysers in California. Fig. 5.4 shows typical pressure-discharge relation for a liquid-dominated reservoir in Svartsengi, Iceland. We see on Figs. 5.2, 5.3 and 5.4 that the wellbore effect is greater for narrow holes than for wide holes, it is also greater for deep wells than for shallow wells as was to be expected as the wellbore effect is essentially flow-resistance.

If the liquid does not flash in the wellbore or in the reservoir we can use eq. 5.1 to calculate pressure decline for various pumping rates, when the constants B and C have been determined according to the methods in section 3.11, and a suitable pump arrangement can be designed.

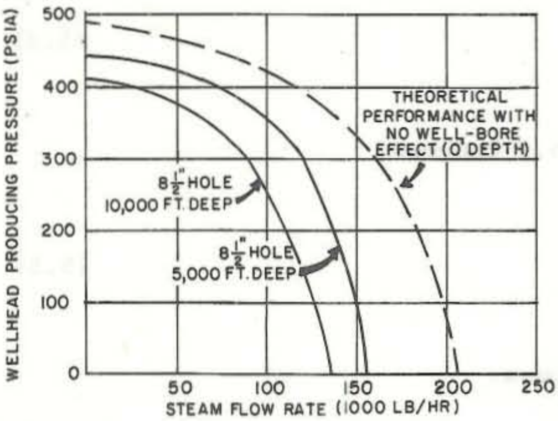

82.03.0560.

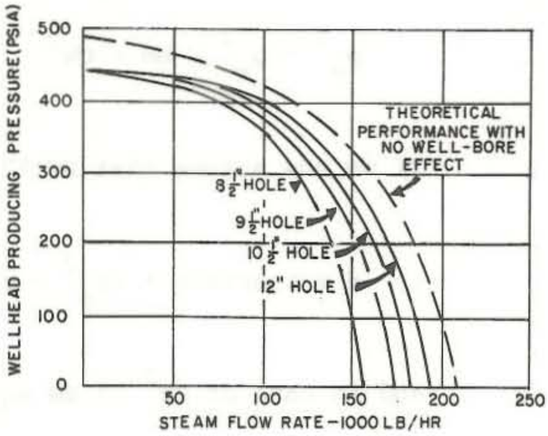

82.03.0561.

Fig. 5.2 Steam-flow rate vs. well head pressure for two well depths for a typical steam well at the Geysers (Kruger and Otte 1973)

Fig. 5.3 Steam-flow rate vs. well head pressure for various equivalent pipe diameters for a typical 5,000-ft steam well at the Geysers (Kruger and Otte 1973)

Let us now calculate the actual pressure-discharge relations for steam wells. The momentum equation for the flow in the well is given by:

$$-\frac{dp}{dz} = \frac{f}{D}\frac{\rho V^2}{2} + \rho V \frac{dV}{dz} \tag{5.7}$$

where f is the friction factor, D the well diameter, V the steam velocity and z is a vertical coordinate, positive in the upwards direction.

The equation of state is:

$$\rho = \frac{p}{ZRT} \tag{5.8}$$

and if we assume isothermal flow eq. 5.8 becomes:

$$\rho = C_1 p \tag{5.9}$$

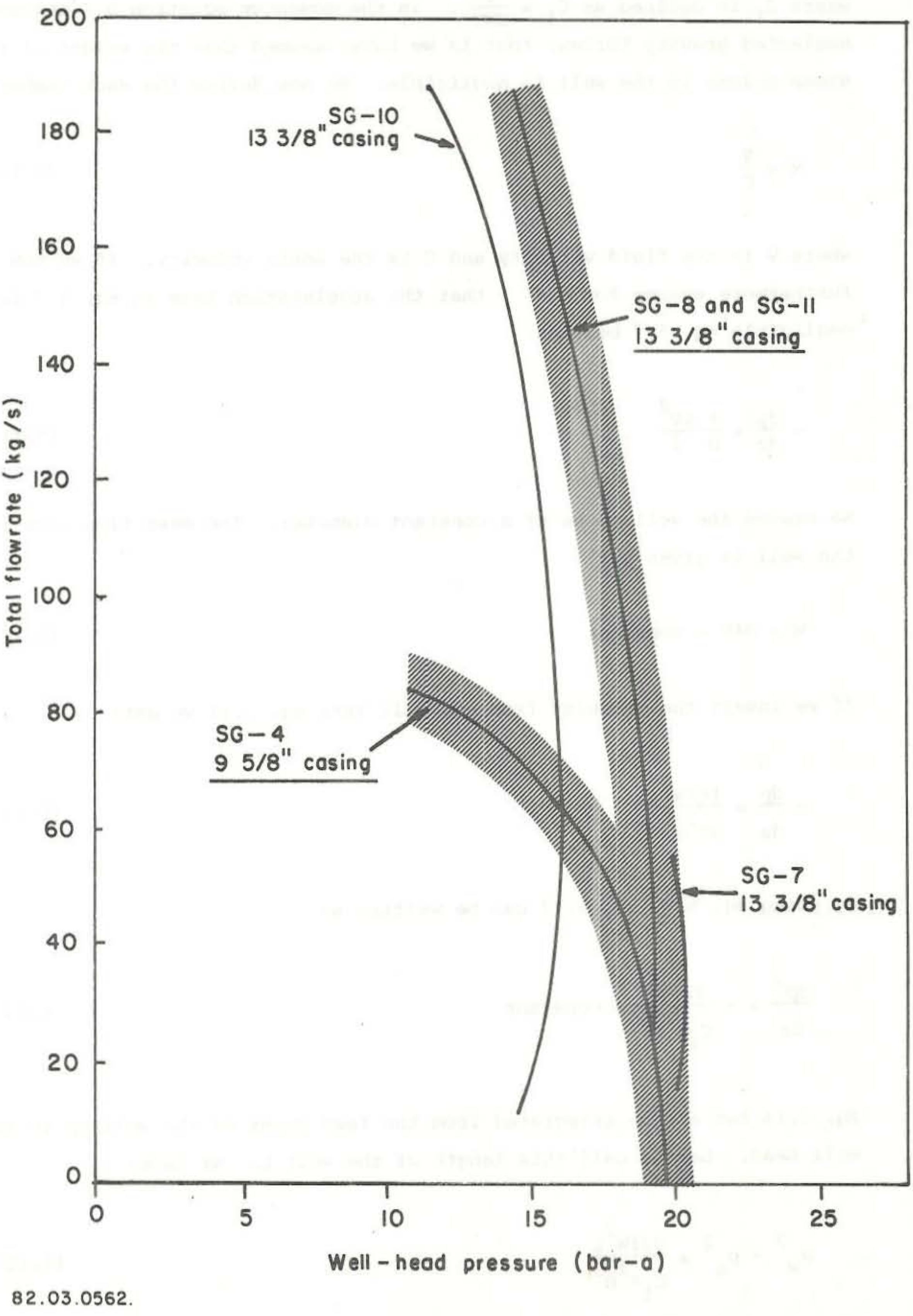

Fig. 5.4 Typical bore output characteristic of Svartsengi wells (Regalado 1981)

where C_1 is defined as $C_1 = \frac{1}{ZRT}$. In the momentum equation 5.7 we have neglected gravity forces, that is we have assumed that the weight of the steam column in the well is negligible. We now define the Mach number as:

$$M = \frac{V}{C} \tag{5.10}$$

where V is the fluid velocity and C is the sonic velocity. If we now furthermore assume for $M << 1$ that the acceleration term in eq. 5.7 is negligible eq. 5.7 becomes:

$$-\frac{dp}{dz} = \frac{f}{D}\frac{\rho V^2}{2} \tag{5.11}$$

We assume the well to be of a constant diameter. The mass flow rate in the well is given by:

$$W = \rho AV = \text{constant} \tag{5.12}$$

If we insert the velocity from eq. 5.12 into eq. 5.11 we get:

$$-\frac{dp}{dz} = \frac{16fW^2}{\rho\pi^2 D^5} \tag{5.13}$$

By using eq. 5.9, eq. 5.13 can be written as:

$$\frac{dp^2}{dz} = -\frac{32fW^2}{C_1\pi^2 D^5} = \text{constant} \tag{5.14}$$

Eq. 5.14 can now be integrated from the feed point of the well up to the well head. Let us call this length of the well L. We have:

$$p_w^{\ 2} - p_o^{\ 2} = \frac{32fW^2 L}{C_1\pi^2 D^5} \tag{5.15}$$

Eq. 5.15 can be written as:

$$\left(\frac{p_o}{p_w}\right)^2 + \left(\frac{W}{bp_w}\right)^2 = 1 \tag{5.16}$$

where b is defined as:

$$b = \sqrt{\frac{C_1 \pi^2 D^5}{32fL}} \tag{5.17}$$

Eq. 5.16 is the equation of an ellipse and a schematic plot of the equation is given in Fig. 5.5 with p_w as a parameter.

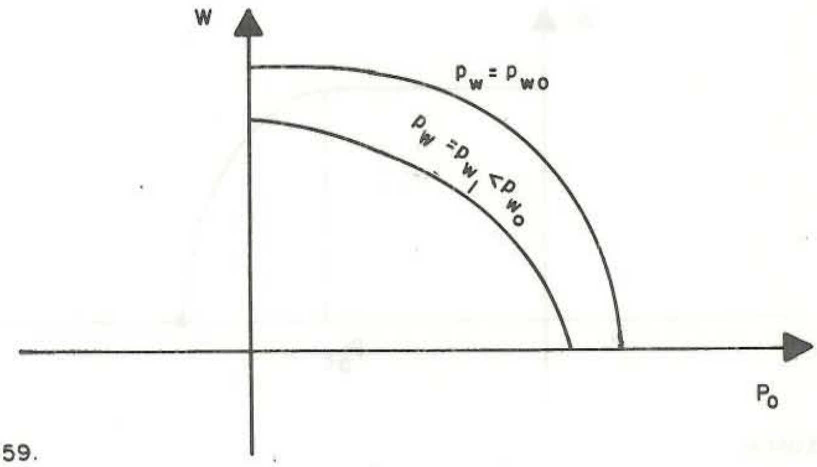

82.03.0559.

Fig. 5.5 Schematic picture of eq. 5.16

p_{wo} is the initial pressure in the reservoir, as pressure declines with time the pressure-discharge relation changes according to eq. 5.16 as shown in Fig. 5.5. We also see that eq. 5.16 is in accordance with Figs. 5.2 and 5.3. The effect of well depth and well diameter is also described by eq. 5.16 as indicated in Figs. 5.2 and 5.3.

When the Mach number becomes larger the assumption of neglecting the acceleration term is no longer valid and the full momentum equation, eq. 5.7, must be applied. The energy equation for the isothermal well flow can be written as:

$$dq = - 2VdV \tag{5.18}$$

where q is the heat flow to the well. For large velocities and Mach numbers this heat flow can become unrealistically high and the isothermal flow assumption will no longer be valid. Adiabatic flow assumption is therefore more realistic. The reader is referred to standard textbooks in fluid mechanics for these large Mach number flows. For increasing velocity we might end up with choked flow or critical flow, that is the steamflow in the well or in the formation becomes sonic. After we get critical flow in the well or in the formation we can lower the WHP without increasing the massflow rate. When this happens at a WHP, p_{oc}, say, the pressure discharge graph will be a straight line with constant flow rate for decreasing WHP, as shown in Fig. 5.6:

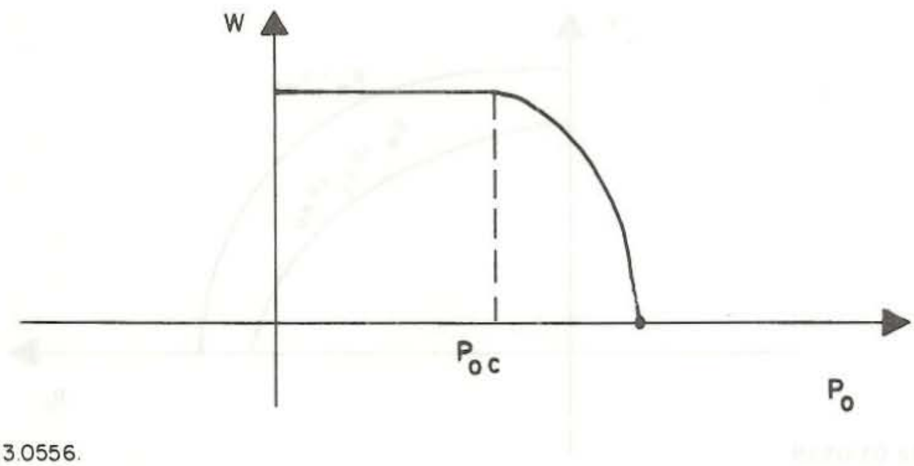

Fig. 5.6 A schematic picture of a pressure-discharge relation with choked flow

Such critical flow has tendency to happen where two phase flow enters the wellbore and in widening flow sections, where we have a change in well diameter, but scale deposits will do the same.

Calculation of the pressure-discharge relation when flashing occurs in the well is more complicated, because of the two phase flow situation. Next section describes two phase flow calculation.

5.3 Two phase flow calculations

Let us start this section on two phase flow by calculating the location of the flash level in the well. Let us call the height of the flash level above the feeding zone in the well z^*, see Fig. 5.1. Now using the energy equation in the single phase water from the feeding point up to the flash level, where the pressure is denoted p_s, we get:

$$\frac{p_w}{\gamma_w} = \frac{p_s}{\gamma_w} + z^* + f\,\frac{8W^2 z^*}{\rho_w^2 \pi^2 D^5 g} \tag{5.19}$$

where f is the friction factor in the single phase water zone. Eq. 5.19 solved for z^* gives:

$$z^* = \frac{(p_w - p_s)}{(\gamma_w + \frac{8fW^2}{\pi^2 D^5 \rho_w})} \tag{5.20}$$

If we insert p_w from eq. 5.1 into eq. 5.20 we get:

$$z^* = \frac{p_e - BW - CW^2 - p_s}{(\gamma_w + \frac{8fW^2}{\pi^2 D^5 \rho_w})} \tag{5.21}$$

The saturation pressure p_s is just a function of temperature, C is constant but B is a function of time as we have seen in section 3. Eq. 5.21 shows then how the flash level drops with time as the pressure drops in the reservoir. Sometimes it is accurate enough to neglect the frictional pressure drop when calculating the flash level, in that case eq. 5.21 becomes:

$$z^* = \frac{p_e - BW - CW^2 - p_s}{\gamma_w} \tag{5.22}$$

The two phase flow situation will just be discussed briefly in the following, but the reader is referred to Wallis (1969), Ryley (1980) and Kütükcüoglu (1969). Fig. 5.7 shows the flow pattern in a vertical two phase flow and Fig. 5.8 shows the flow pattern boundaries.

82.03.0558

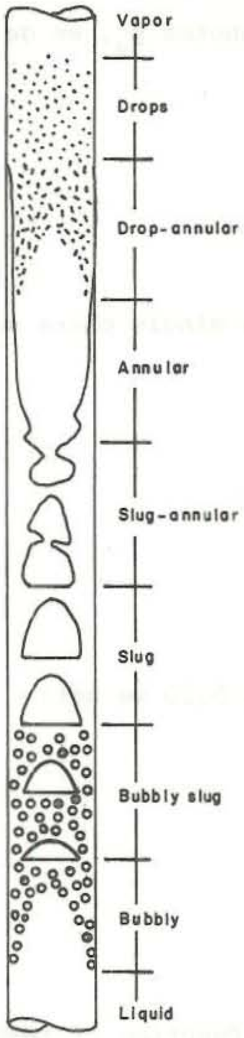

Fig. 5.7 Flow pattern in a vertical two phase flow

Basically it is possible to distinguish three fundamental physical models. The HOMOGENEOUS flow model is the simplest. This assumes that the liquid and the gas or vapour are uniformly distributed over the flow cross section and in the flow direction so that the mixture can be regarded as a single phase flow with suitably defined mean values of the thermodynamic and hydrodynamic properties of the two phases. However, the meaningful definition of mean physical properties, particularly viscosity, of the two phase mixture leads to difficulty. The homogeneous flow model is frequently used as a reference.

In the SEPARATED flow model, or slip model, it is assumed that the gas

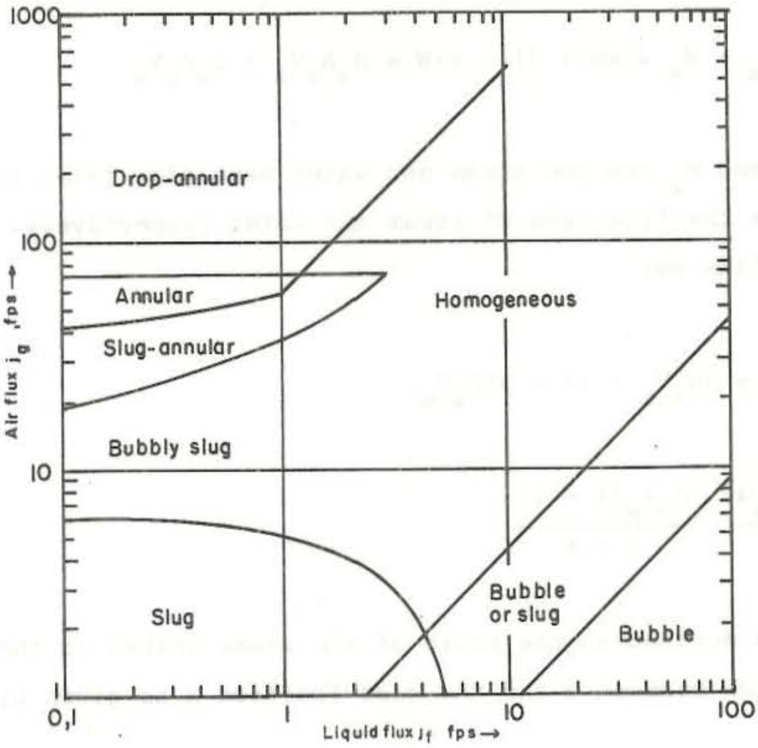

82.03.0557.

Fig. 5.8 Flow-pattern boundaries for vertical upflow of air and water (Wallis, 1981)

and the liquid flow separately as continuous phases with distinct mean velocities within different parts of the flow cross section. A set of basic equations is formulated for each phase, the solution is closed by expressions detailing the interaction of the two phases and the interaction of the two phases with the channel walls. These are obtained from empirical equations which give the mean void fraction, defined as the mean proportion of a pipe's cross sectional area containing the gaseous phase, or the ratio of the mean velocities (slip) and the wall shear stress as functions of the primary parameters of flow. This model represents the other limiting case; the actual flow behaviour lies somewhere between the homogeneous and separated flow models.

Below the separated flow model is used, as it represents the more general case with water and steam having different velocities. The equations for conservation of mass, momentum and energy are presented without giving detailed derivations. Only steady state conditions are considered.

Conservation of mass:

$$W = W_s + W_w = xW + (1 - x)W = \rho_s A_s V_s + \rho_w A_w V_w \tag{5.23}$$

where W_s and W_w are the steam and water mass flow rates respectively. A_s and A_w are the flow area of steam and water respectively. We now define the mass flux as:

$$G = \frac{W}{A} = \alpha\rho_s V_s + (1 - \alpha)\rho_w V_w$$

$$= \frac{\rho_s V_s \alpha}{x} = \frac{\rho_w V_w (1 - \alpha)}{1 - x} \tag{5.24}$$

where α is defined as the ratio of the steam volume to the total volume. The relation between α and the mass fraction x is given by:

$$\alpha = \frac{x\rho_w}{(1 - x)\rho_s S + x\rho_w} \tag{5.25}$$

where S is the slip factor defined by:

$$S = \frac{V_s}{V_w} \tag{5.26}$$

Conservation of momentum:

$$-\frac{dp}{dz} = \rho_m g + A \frac{d}{dz} (W_s V_s + W_w V_w) - (\frac{dp}{dz})_F \tag{5.27}$$

The first term on the right hand side is the hydrostatic pressure drop with the average density:

$$\rho_m = \alpha\rho_s + (1 - \alpha)\rho_w \tag{5.28}$$

The second term is the acceleration and can be rewritten as:

$$\frac{1}{A}\frac{d}{dz}(W_s V_s + W_w V_w) = G^2 \frac{d}{dz}\left(\frac{x^2}{\rho_s \alpha} + \frac{(1-x)^2}{\rho_w(1-\alpha)}\right) \tag{5.29}$$

In order to be able to calculate α according to eq. 5.25 we have to know the slip factor in eq. 5.26. Many empirical equations exist and one of them is the Moody slip factor defined as (see Kütükcüoglu 1969).

$$S = \frac{V_s}{V_w} = \left(\frac{\rho_w}{\rho_s}\right)^{1/3} \tag{5.30}$$

The last term on the right hand side of eq. 5.27 is the frictional pressure drop. Many methods are available to calculate this pressure drop and one of them is the method of Martinelli and Nelson (1948) where the frictional pressure drop is written as:

$$\left(\frac{dp}{dz}\right)_F = \phi_{fo}^2 \left(\frac{dp}{dz}\right)_{fo} \tag{5.31}$$

$\left(\frac{dp}{dz}\right)_{fo}$ is the single phase pressure drop, resulting from if the total mass flow in the well flowed as water. This term can be easily calculated by standard methods. ϕ_{fo} is called two phase flow multiplier given e.g. by Martinelli and Nelson (1948) as a function of x. See also Kütükcüoglu (1969) for various methods to calculate the two phase frictional pressure drop.

Conservation of energy:

$$q = \frac{d}{dz}\left(\frac{1}{2} x V_s^2 + \frac{1}{2}(1-x)V_w^2 + x h_s + (1-x)h_w + g_z\right) \tag{5.32}$$

where q is the heat flow into the well from the surroundings per unit length, per unit massflow rate. These conservation equations together with steam table data give the necessary equations for the solution of the two phase flow problem. The equations are too complicated to be solved analytically and must be integrated numerical vertically up the well, from the flash point up to the well head. Fig. 5.9 shows an example of the result of such calculation. Eq. 5.21 showed us that the flash level

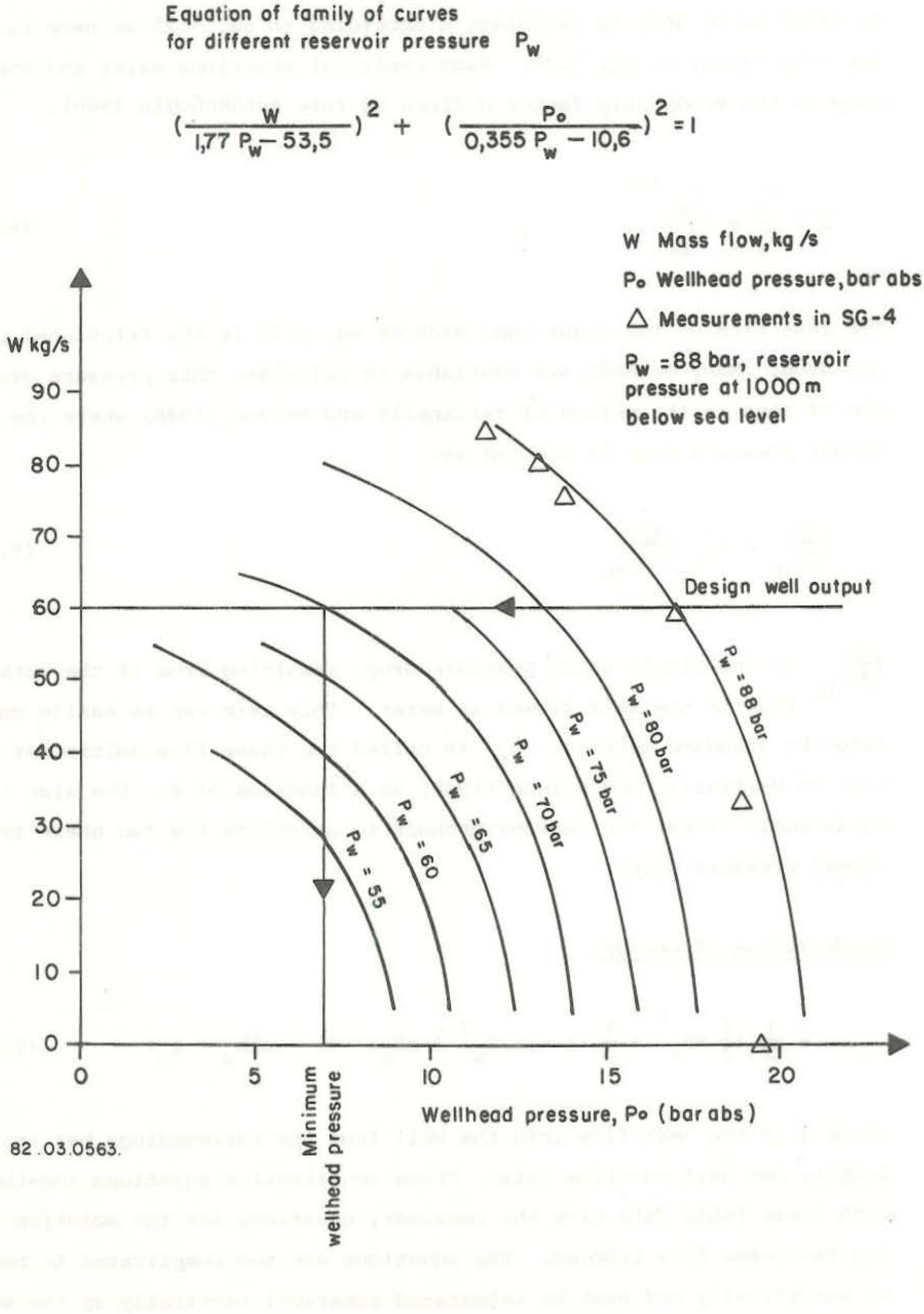

Fig. 5.9 Results of numerical two phase flow calculations for wells for different reservoir pressures at 1000 m depth (Kjaran et al. 1980)

dropped for declining reservoir pressure. The family of curves in Fig. 5.9 shows us the result of the two phase flow calculations for declining reservoir pressure and the figure can be compared with Fig. 5.5 which schematically shows the same for a steam well. The following equation has been fitted to the family of curves in Fig. 5.9.

$$\left(\frac{W}{b_1 p_w - C_1}\right)^2 + \left(\frac{p_o}{b_2 p_w - C_2}\right)^2 = 1 \qquad (5.33)$$

with the numerical values of the constants given in Fig. 5.9. If eq. 5.33 is compared with eq. 5.16 for the steam well, we see that they are quite similar. We also see from Fig. 5.9 that if the well is operated at constant flow rate equal to the designed well output 60 kg/s, the WHP drops as the reservoir pressure drops, finally when a minimum WHP pressure is reached the well must be operated at that constant WHP, and the mass flow rate declines as indicated by the arrow in Fig. 5.9. Fig. 5.6 shows a schematic picture of a pressure-discharge relation with choked flow in a steam well. Choked flow also occurs in the two phase well. Fig. 5.10 shows a pressure-discharge graph for well KJ-7 in the Krafla geothermal field. We see that the massflow rate does not change with different well head pressure. It seems likely that there is choked flow (in the well). Theoretical calculations of critical flow in the two phase flow well are complicated and will not be given here. Let us instead look at the following simple calculations. Choking conditions are characterized with sonic fluid velocity. The velocity of sound is given by:

$$C = \sqrt{K/\rho} \qquad (5.34)$$

where K is the bulk modulus of the fluid equal to the reciproc of the fluid compressibility. If we assume that steam behaves like a perfect gas we have for the sound velocity in steam, as the sound is transmitted isentropically:

$$C_s = \sqrt{kRT} \qquad (5.35)$$

where k is the ratio of the heat capacities at constant pressure and volume. If we have a mixture of water and steam bubbles the speed of sound

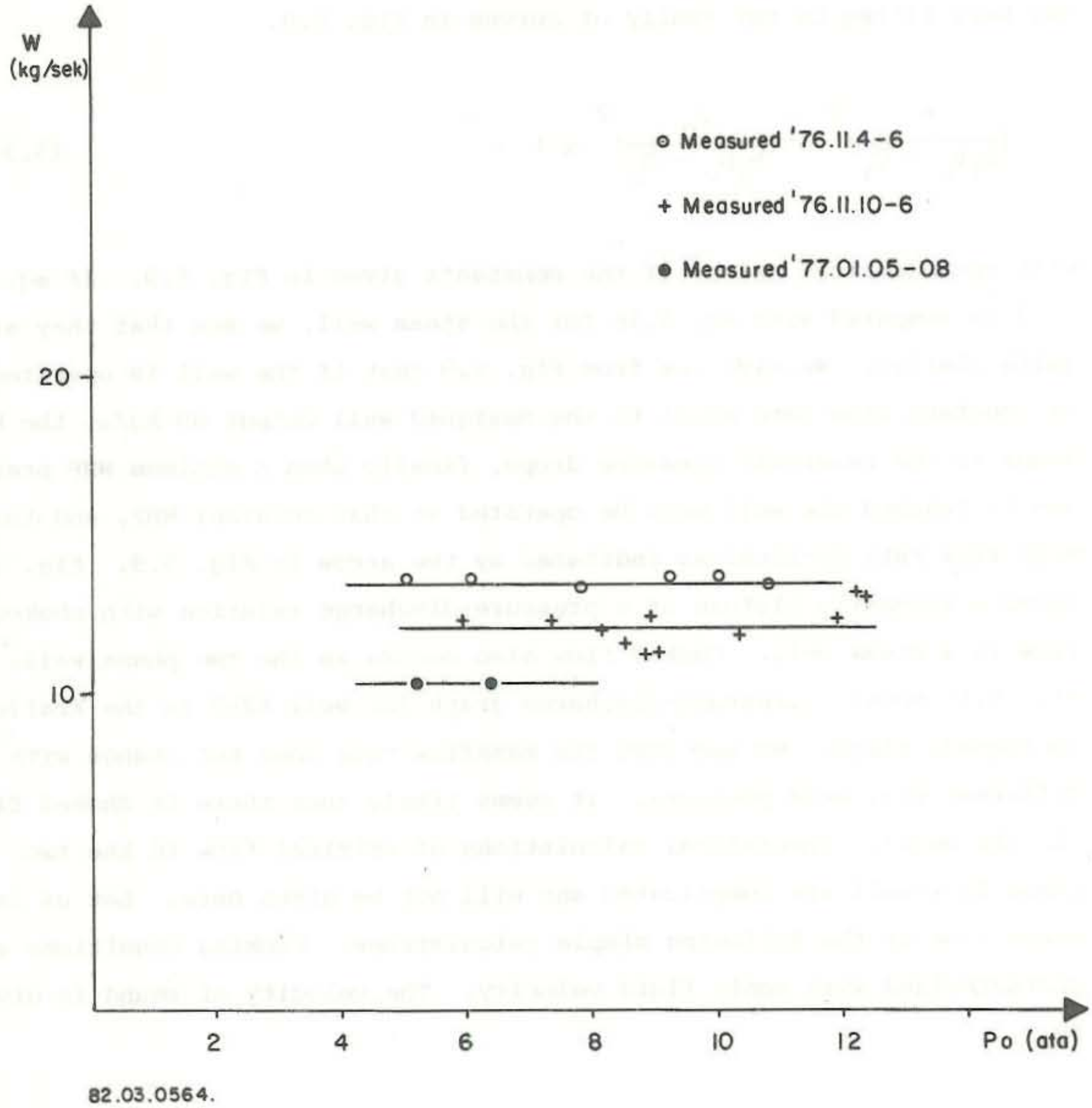

Fig. 5.10 Pressure-discharge relation for well KJ-7, Krafla geothermal field, Iceland (Steingrímsson and Gíslason 1978)

in that mixture is given by 5.34 as:

$$C_m = \sqrt{K_m/\rho_m} \tag{5.36}$$

If α is the proportion of steam by volume, the density of the mixture is:

$$\rho_m = \alpha\rho_s + (1 - \alpha)\rho_w \tag{5.37}$$

The bulk modulus for the mixture is given by:

$$\frac{1}{K_m} = \frac{\alpha}{K_s} + \frac{1 - \alpha}{K_w} \tag{5.38}$$

At low steam concentrations the sound is transmitted nearly at constant temperature and the bulk modulus for steam is then given by eq. 3.222. We now have for the sound velocity:

$$C_m = \sqrt{\frac{p_s K_w}{(\alpha K_w + (1 - \alpha)p_s)\ (\alpha\rho_s + (1 - \alpha)\rho_w)}} \tag{5.39}$$

Let us insert numerical values as an example to calculate sound velocity in water, steam and a steam-water mixture. We use the following values. $T = 240°C$, $K_w = 10^4$ bar, $p_s = 33.5$ bar, $\alpha = 0.3$, $\rho_w = 812\ kg/m^3$, $\rho_s = 16.8\ kg/m^3$, $R = 461.9$, $k = 1.3$. The velocity of sound in water is now given by:

$$C_w = \sqrt{\frac{K_w}{\rho_w}} = \sqrt{\frac{10^9}{812}} = 1110\ m/s$$

and the sound velocity in steam:

$$C_s = \sqrt{kRT} = \sqrt{1.3 \cdot 461.9\ (240 + 273.15)} = 555\ m/s$$

and for the steam water mixture:

$$C_m = \sqrt{\frac{10^5 \cdot 33.5 \cdot 10^9}{(0.3 \cdot 10^9 + 0.7 \cdot 33.5 \cdot 10^5)\ (0.3 \cdot 16.8 + 0.7 \cdot 812)}} \cong 140\ m/s$$

We see that the velocity of sound is drastically reduced to the velocity in either water or steam. Choking condition in a two phase well are therefore possible at relatively low fluid velocities. For water with a small concentration of steam bubbles the elastic modulus of the mixture is reduced with no appreciable reduction in density, and thus the acoustic velocity is reduced. For steam with minute water droplets, the density of the mixture is increased, with no appreciable change in elastic modulus, and again the accoustic velocity is reduced.

6 REFERENCES

Agarwal, R., Al-Hussainy, R., Ramey, H.J., Jr., 1970: An Investigation of Wellbore Storage and Skin Effect in Unsteady Liquid Flow, I. Analytical Treatment Soc. Pet. Eng. J., 279-290, Trans., AIME, 249.

Arnórsson, S., 1973: Uppleyst efni í heitu vatni. National Energy Authority. OSJHD-7317 Iceland. (Dissolved solids in hot water, report in Icelandic).

Barelli, A., Palama, A., 1980: On some Computation Methods of Unit Response Functions from Varying-Rate Data. Geothermics, Vol. 9, 261-269, Pergamon Press.

Bear, J., 1972: Dynamics of fluids in porous media. American Elsevier publishing Company. N.Y.

Benedikt Steingrímsson, Gestur Gíslason, 1978: see Steingrímsson, B., Gíslason, G., 1978.

Bredehoeft, J.D., 1975: Response of Well-Aquifer System to Earth Tides. Journal of Geophysical Research, 72, No. 12, 3075.

Brixley, P.F., Grant, M.A., 1979: Reinjection testing at Broadlands in Proceedings of 4th Workshop on Geothermal Reservoir Engineering, Stanford University.

Brons, F., Marting, V.E., 1961: The Effect of Restricted Fluid Entry on Well Productivity. J. Pet. Tech., February, 172-174, Trans. AIME.

Böðvarsson, G., 1961: Physical characteristics of natural heat resources in Iceland. U.N. Conf. New Sources Energy, Rome, G/24.

Böðvarsson, G.S., Tsang, C.F., 1981: Injection and thermal breakthrough in fractured geothermal reservoirs. Lawrence Berkeley Laboratory, University of California, Berkeley, LBL-12698.

Böðvarsson, G.S., Benson, S., Sigurðsson, Ó., Halldórsson, G.K., Stefánsson, V., 1981: Analysis of Well Data From the Krafla Geothermal Field in Iceland. Proceedings Seventh Workshop ; Geothermal Reservoir Engineering, Dec. 15-17, 1981 Stanford University, Stanford, California.

Caltagirone, J.P., 1975: Thermoconvective instabilities in a Horizontal Porous Layer. J. Fluid Mech., 72, 269-287.

Carslaw, H.S., Jaeger, J.G., 1959: Conduction of Heat in Solids. Oxford, Clarendon Press, 2. Ed.

Chasteen, A.J., 1975: Geothermal Steam condensate reinjection, in Proceedings Second United Nations Symposium, Vol. 2, San Francisco, California.

Chu, Chun Wei, Garcia-Rivera, J., Raghavan, R., 1980: Analysis of Interference Test Data Influenced by Wellbore Storage and Skin at the Flowing Well. J. Pet. Tech., Jan. 1980.

Cinco, H., Miller, F.G., Ramey, H.J., Jr., 1975: Unsteady-State Pressure Distribution Created by a Directionally Drilled Well. J. Pet. Tech. Nov, 1392-1400, Trans., AIME, 259.

Combarnous, M.A., Bories, S.A., 1975: Hydrothermal convection in saturated porous media, Advances in Hydroscience, 10, 231-307.

Cuellar, G., 1975: Behaviour of silica in geothermal wast waters, in Proceedings Second United Nations Symposium, Vol. 2, San Francisco, California.

Dietz, D.N., 1965: Determination of Average Reservoir Pressure from Build-Up Surveys J. Pet. Tech. Aug. 955-959.

Donaldsson, I.G., 1970: The Simulation of Geothermal Systems with a Simple Convection model. Geothermics (1970). Special issue 2, Vol. 2, 649-654.

Donaldsson, I.G., Grant, M.A., 1981: Heat Extraction from Geothermal Reservoirs, in Geothermal Systems: Principles and Case Histories. Edited by L. Rybach and L.J.P. Muffler; 145-180. John Wiley and Sons, Ltd.

Earlougher, R.C., Jr., 1977: Advances in Well Test Analysis. Monograph Volume 5, SPE.

Economides, E.C., Economides, M.J., Miller, F.G., 1980: Interference Between Wells in a Fractured Formation. Geothermal Resources Council, Transactions Vol. 4. Sept.

Einarsson, S.S., Vides, A.R., and Cuellar, G., 1975: Disposal of geothermal waste water by reinjection, in Proceedings Second United Nations Symposium, Vol. 2, San Francisco, California.

Elder, J.W., 1965: Physical Processes in Geothermal Areas, in Terrestrial Heat Flow, Ed. W.H.K. Lee, American Geophysical Union, Publ. No. 1288, 211-239.

Eliasson, J., 1973: Convective Ground Water Flow. Institute of Hydrodynamics and Hydraulic Engineering. Technical University of Denmark. Series Paper 3.

Eliasson, J., Arnalds, S. St., Kjaran, S.P., 1977: Svartsengi, Straumfræðileg rannsókn á jarðhitasvæði. National Energy Authority, Reykjavík, Iceland. OS ROD 7718, OS SFS 7702. (Svartsengi, Reservoir Engineering aspects of the geothermal field, report in Icelandic).

Engelund, F., 1953: On the laminar and turbulent flows of ground water through homogeneous sand. Transactions of the Danish Academy of Technical Sciences. ATs. No. 3.

Engelund, F., 1970: Pumping from leaky artesian aquifers. Nordic Hydrology. Vol. 1. 1970.

van Everdingen, A.F., Hurst, W., 1949: The Application of the Laplace Transformation to Flow Problems in Reservoirs. Trans. AIME 186, 305-324.

van Everdingen, A.F., 1953: The Skin Effect and its Impedient to Fluid Flow into a Wellbore. Trans. AIME, 198, 171-176.

Ferris, J.G., Knowles, D.B., 1954: The slug test for estimating transmissibility, U.S. Geol. Surv. Ground Water Note 26, 1-7.

Ferris, J.G., Knowles, D.B., Brown, R.H., Stallman, R.W., 1962: Theory of Aquifer Tests, U.S. Geol. Surv. Water Supply Paper 1536-E.

Garg, S.K., Pritchett, J.W., 1977: On Pressure-Work, Viscous Dissipation and the Energy Balance Relation for Geothermal Reservoirs. Advances in Water Resources, Vol. 1, No. 1.

Garg, S.K., 1980: Pressure Transient Analysis for Two-Phase (Water/Steam) Geothermal Reservoirs. SPEJ, June, 206-214.

Garg, S.K., Kassoy, D.R., 1981: Convective Heat and Mass Transfer in Hydrothermal Systems, in Geothermal Systems: Principles and Case Histories. Edited by L. Rybach and L.J.P. Muffler, 37-76, John Wiley and Sons Ltd.

Giovannoni, A., Allegrini, G., Cappetti, G., 1981: First results of a reinjection experiment at Larderello, in Proceedings of 6th Workshop on Geothermal Reservoir Engineering, Stanford University, California.

Gísli K. Halldórsson, 1980: See Halldórsson, G.K., 1980.

Grant, M.A., 1977: Broadlands - A Gas-Dominated Geothermal Field. Geothermics, Vol. 6, 9-29. Pergamon Press.

Grant, M.A., 1978: The Pseudopressure of Saturated Steam. Proceedings 4th Workshop on Geothermal Reservoir Engineering, Stanford Geothermal Program, SGP-TR-50, Stanford University, Stanford, California.

Grant, M.A., 1978: A personal letter to Dr. Valgarður Stefánsson, National Energy Authority, Reykjavík, Iceland.

Grant, M.A., Sorey, M.L., 1979: The Compressibility and Hydraulic Diffusivity of a Water-Steam Flow. Water Resources Research, June, Vol. 15., No. 3.

Grant, M.A., 1979: Interpretation of downhole measurements in geothermal wells. Applied Mathematics Division, Report No. 88. Department of Scientific and Industrial Research, Wellington, New Zealand.

Grant, M.A., 1979: Water Content of the Kawah Kamojang Geothermal Reservoir. Geothermics, Vol. 8, 21-30, Pergamon Press.

Gringarten, A.C., Ramey, H.J.J., Jr., Raghavan, R., 1972: Pressure Analysis for Fractured Wells. Paper SPE 4051 presented at the SPE-AIME 47th Annual Fall Meeting, San Antonio, Texas, Oct. 8-11.

Gringarten, A.C., Ramey, H.J., Jr., Raghavan, R., 1974: Unsteady-State Pressure Distributions Created by a Well with a Single Infinite-Conductivity Vertical Fracture. SPEJ, Aug.

Gunnar Böðvarsson, 1961: see Böðvarsson, G., 1961.

Halldórsson, G.K., 1980: Niðurstöður dopluprófana á vinnslusvæði Hitaveitu Selfoss. National Energy Authority Internal report (Some results of step-drawdown tests at the Selfoss geothermal field, in Icelandic).

Hayashi, M., Mimura, T., Yamasaki, T., 1978: Geological setting of reinjection wells in the Otake and the Hatchobaru geothermal fields, Japan. Transactions, Geothermal Resources Council, Vol. 2, 263-266.

Horne, R., Satman, A., Grant, M.A., 1980: Pressure Transient Analysis of Geothermal Wells with Phase Boundaries. Paper presented at the 55th Annual Fall Technical Conference and Exhibition of the Society of Petroleum Engineers, held in Dallas, Texas, Sept. 21-24.

Horne, R., 1981: Geothermal reinjection experience in Japan. Paper presented at the California Regional SPE meeting, Bakersfield, California, SPE-9925.

Jacob, C.E., 1946: Radial Flow in a Leaky Artesian Aquifer. Transaction American Geophysical Union, Vol. 27, 198-205.

Jacob, C.E., Lohman, S.W., 1952: Non-steady Flow to a Well of Constant Drawdown in an Extensive Aquifer. Trans., AGU, Aug., 559-569.

Jónas Elíasson, 1973: see Elíasson, J., 1973.

Jónas Elíasson, Sigurður St. Arnalds, Snorri P. Kjaran, 1977: see Elíasson, J., Arnalds, S.St., Kjaran, S.P., 1977.

Kappelmeyer, O., Haenel, R., 1974: Geothermics with Special Reference to Application. Gebrüder Borntraeger - Berlin.

Kjaran, S.P., Elíasson, J., Halldórsson, G.K., 1980: Svartsengi, Athugun á vinnslu jarðhita. National Energy Authority, Reykjavík, Iceland, OS80021/ROD10-JHD17. (Svartsengi, Reservoir Engineering study, report in Icelandic).

Kruger, P., Otte, C., 1973: Geothermal Energy, Stanford University Press, Stanford, California.

Kruger, P., Ramey, H.J., Jr., 1978: Stimulation and Reservoir Engineering of Geothermal Resources. First Annual Report to U.S. Department of Energy. Stanford Geothermal Program, SGP-TR-28.

Kruger, P., Ramey, H.J., Jr., 1980: Summaries Sixth Workshop on Geothermal Reservoir Engineering. Stanford Geothermal Program, Stanford University, Stanford, California.

Kubota, K., Aosaki, K., 1975: Reinjection of geothermal hot water at the Otake geothermal field, in Proceedings Second United Nations Symposium, Vol. 2, San Francisco, California.

Kütükcüoglu, A., 1969: Strömungsform, Dampfvolumenanteil und Druckabfall bei Zweiphasenströmung von Wasser-Wasserdampf in Rohren. VDI-VERLAG, Reihe 7, Nr. 18. Düsseldorf.

Lapwood, E.R., 1948: Convection of a Fluid in a Porous Medium, Proceedings Cambridge Philosophical Society, 44, 508-521.

Martinelli, R.C., Nelson, D.B., 1948: Prediction of pressure drop during forced circulation boiling of water. Trans. Am. Soc. Mech. Engis. 70(6), 695-702.

Mathias, K.E., 1975: The Mesa geothermal field - a preliminary evaluation of five geothermal wells, in Proceedings Second United Nations Symposium, Vol. 2, San Francisco, California.

Miller, C.W., 1980: Wellbore Storage Effects in Geothermal Wells. SPE, Dec. 1980.

McNabb, A., 1975: A model of the Wairakei geothermal field, Unpublished report, Applied Mathematics Division, Department of Scientific and Industrial Research, Wellington, New Zealand.

Mueller, T.D., Witherspoon, P.A., 1965: Pressure Interference Effects within Reservoirs and Aquifers. J. Pet. Tech. April, 471-474, Trans., AIME, 234.

Muffler, P., Cataldi, R., 1978: Methods for Regional Assessment of Geothermal Resources. Geothermics, Vol. 7, 53-89, Pergamon Press.

Muskat, M., 1946: The Flow of Homogeneous Fluids through Porous Media, McGraw-Hill, New York; 2nd printing by Edwards, Ann. Arbor, Mich.

Ómar Sigurðsson, Valgarður Stefánsson, 1977: see Sigurðsson, Ó., Stefánsson, V., 1977.

Paete, M.G., 1980: A Model for Well 108. Production Section Tonganan Geothermal Project. PNOC-Energy Development Corporation, Geothermal Division, internal report.

Palm, E., 1960: On the Tendency towards Hexagonal Cells in Steady Convections, J. Fluid Mech., Vol. 8, No. 2, 183-192.

Pálmason, G., Sæmundsson, K., 1979: Summary of conductive heat flow in Iceland. In Terrestrial Heat Flow in Europe. ed. Cernák and Rybach, 218-220, Springer 1979.

Papadopulos, I.S., Cooper, H.H., Jr., 1967: Drawdown in a Well of Large Diameter. Water Resources Research. Vol. 3., No. 1.

Pinder, G.F., 1979: State-of-the-Art Review of Geothermal Reservoir Modelling. Geothermal Subsidence Research Management Program. Earth Sciences Division, Lawrence Berkeley Laboratory. University of California.

Raghavan, R., 1976: Pressure Behaviour of Wells Intercepting Fractures. Proceedings, Invitational Well-Testing Symposium, LBL-7027, March 1978, 117-160.

Ramey, H.J., Jr., Gringarten, A.C., 1975: Effect of High Volume Vertical Fractures on Geothermal Steam Well Behaviour, paper presented at the second United Nations symposium on the use and Development of Geothermal Energy, San Francisco May 20-29.

Regalado, J.R., 1981: A study of the Response to Exploitation of the Svartsengi Geothermal Field SW-Iceland. National Energy Authority, The United Nations University, UNU Geothermal Training Programme, Iceland. Report 1981-7.

Ryley, D.J., 1980: Analysis of the flow in the reservoir-well system, in the Sourcebook on the Production of Electricity from Geothermal Energy, Joseph Kestin, editor in chief. United States Department of Energy, Division of Geothermal Energy. Brown University, Providence Rhode Island.

Schubert, G., Strauss, J.M., 1977: Two-phase convection in a porous medium. J. Geophys. Res. 82, 3411-3421.

Sigurðsson, Ó., Stefánsson, V., 1977: Lekt í borholum í Kröflu. National Energy Authority, Reykjavík, Iceland, OS JHD 7727 (Well permeabilities in the Krafla geothermal field, report in Icelandic).

Snorri P. Kjaran, Jónas Elíasson, Gísli K. Halldórsson, 1980: see Kjaran, S.P., Elíasson, J., Halldórsson, G.K., 1980.

Sorey, M., 1976: Numerical Analysis of the Hydrothermal System of Long Valley Caldera, Second Workshop Geothermal Reservoir Engineering. Stanford University, Stanford, California.

Sorey, M.L., Grant, M.A., Bradford, E., 1980: Nonlinear Effects in Two-Phase Flow to Wells in Geothermal Reservoirs. Water Resources Research, Vol. 16, No. 4, Aug., 767-777.

Stefán Arnórsson, 1973: see Arnórsson, S., 1973.

Stefánsson, V., Steingrímsson, B., 1980: Geothermal Logging I, An Introduction to techniques and interpretation. National Energy Authority, Reykjavík, Iceland, OS-80017/JHD09.

Stefánsson, V., Björnsson, S.: Physical Aspects of Hydrothermal Systems, in Geodynamics series, Vol. 8, AGU, Washington D.C. (in press).

Steingrímsson, B., Gíslason, G., 1978: Krafla, aflmælingar á borholum, National Energy Authority, Reykjavík, Iceland, OS JHD 7804 (Pressure-discharge measurements in wells at the Krafla geothermal field, report in Icelandic).

Straus, J.M., Schubert, G., 1977: Thermal Convection of Water in a Porous Medium: Effects of Temperature- and Pressure-Dependent Thermodynamic and Transport Properties. J. Geophys. Res. 82, 325-333.

Straus, J.M., Schubert, G., 1979: Effect of CO_2 on the buoyancy of geothermal fluids. Geophys. Res. Lett. 6, 5-8.

Studt, F.E., 1980: Geothermal fluid injection-experience in New-Zealand and Philippines, paper presented at the NATO CCMS Geothermal Conference, Paris, France.

O'Sullivan, M., Pruess, K., 1980: Analysis of injection testing of Geothermal reservoirs. Geothermal Resources Council, Transactions, Vol. 4.

O'Sullivan, M.J., 1981: A Similarity Method for Geothermal Well Test Analysis. Water Resources Research, Vol. 17, No. 2, 390-398, April.

Sutton, F.M., 1976: Pressure-temperature curves for a two-phase mixture of water and carbon dioxide. N.Z. Journal of Science, 19, 297-301.

Sutton, F.M., McNabb, A., 1977: Boiling Curves at Broadlands geothermal field, New Zealand. N.Z. Journal of Science, Vol. 20, 333-337.

Sveco and Virkir, 1976: Feasibility Report for the Olkaria Geothermal Project. United Nations and Government of Kenya.

Theis, C.V., 1935: The Relation Between the Lowering of Piezometric Surface and the Rate and Duration of Discharge of a Well Using Groundwater Storage. Transactions, American Geophysical Union, Vol. 16, 519-524.

Thorsteinsson, Th., 1969: Vatnsstöðumælingar í borholum á Seltjarnarnesi 1966-1969. National Energy Authority, Reykjavík, Iceland, Internal report, Sept. 1969. (Water level measurements in wells in Seltjarnarnes 1966-1969, report in Icelandic).

Thorsteinsson, Th., Elíasson, J., 1970: Geohydrology of the Laugarnes Hydrothermal System in Reykjavík, Iceland. U.N. Symposium on the Development and Utilization of Geothermal Resources, Pisa 1970, Vol. 2, Part. 2.

Thorsteinsson, Th., 1975: The Redevelopment of the Reykir Hydrothermal System in S.W. Iceland. Second United Nations Symposium on the Development and use of Geothermal Resources, San Francisco, California, May 20-29.

Vatnaskil, 1982: Svartsengi, Vatnsborðslækkun með vinnslu. Unnið fyrir Hitaveitu Suðurnesja. (Water table drawdown in the Svartsengi geothermal field with production, report in Icelandic).

Vetter, O.J., Zinnov, K.P., 1981: Evaluation of Well-to-Well Tracers for Geothermal Reservoirs. Part 1: Literature Survey, Part 2: Laboratory Work. Geothermal Reservoir Engineering Management Program, Earth Science Division, Lawrence Berkeley Laboratory, University of California, Berkeley.

Vides, A., 1975: Recent studies of the Ahuachapan geothermal field, in Proceedings Second United Nations Symposium, Vol. 2, San Francisco, California.

Wallis, G.B., 1969: One-dimensional Two-phase Flow. McGraw-Hill Book Company, N.Y.

Walton, W.C., 1970: Groundwater Resource Evaluation. McGraw Hill Book Company, N.Y.

Wattenbarger, R.A., 1967: Effects of Turbulence, Wellbore Damage, Wellbore Storage and Vertical Fractures on Gas Well Testing. Ph.D. Dissertation, Stanford University, Stanford, California.

Wattenbarger, R.A., Ramey, H.J., Jr., 1968: Gas Well Testing with Turbulence, Damage and Wellbore Storage, J. Pet. Tech. Aug. 877-887.

Wattenbarger, R.A., Ramey, H.J., Jr., 1970: An Investigation of Wellbore Storage and Skin Effect in Unsteady Liquid Flow II. Finite Difference Treatment. Soc. Pet. Eng. J. 291-297, Trans., AIME 249.

Witherspoon, P.A., Neuman, S.P., Sorey, M.L., Lippmann, M.J., 1975: Modelling Geothermal Systems, paper presented at the International Meeting on Geothermal Phenomena and its Applications, Academia Nazionale dei Lincei, Rome, Italy, March 3-5, 1975, LBL-3263, May 1975, 68 pp.

Witherspoon, P.A., Narasimhan, T.N., McEdwards, D.G., 1976: Results of Interference Tests from two Geothermal Reservoirs. 51st Annual Fall Meeting of the Society of Petroleum Engineers of AIME, New Orleans, La., Oct. 3-6.

Wooding, R.A., 1963: Convection in a Saturated Porous Medium at Large Rayleigh Number of Peclet Number. J. Fluid Mech., 15, 527-544.

Zais, E.J., Böðvarsson, G., 1980: Analysis of Production Decline in Geothermal Reservoirs. Geothermal Reservoir Engineering Management Program. Earth Science Division. Lawrence Berkeley Laboratory, University of California, Berkeley.

Zyvoloski, G.A., O'Sullivan, M.J., 1980: Simulation of a Gas-Dominated, Two-Phase Geothermal Reservoir. Society of Petroleum Engineers Journal, Feb., 52-58.

Þorsteinn Thorsteinsson, 1969: see Thorsteinsson, Th., 1969.

Þorsteinn Thorsteinsson, 1970: see Thorsteinsson, Th., 1970.

Þorsteinn Thorsteinsson, 1975: see Thorsteinsson, Th., 1975.